VOLUME 13 (1959) No. 3

NUCLEAR PHYSICS

JOURNAL DEVOTED TO THE EXPERIMENTAL AND THEORETICAL STUDY OF THE FUNDAMENTAL CONSTITUENTS OF MATTER AND THEIR INTERACTIONS

EDITOR: L. ROSENFELD · COPENHAGEN

W. BRENIG, Two particle approximations of the many body problem (II). . 333

J. SAWICKI, Spin-orbit splittings in nuclei (II) 350

J. M. ARAÚJO, Collective vibrations of closed-shell nuclei 360

A. C. DOUGLAS and N. MACDONALD, Compound nucleus processes in medium mass nuclei. 382

R. BEURTEY, P. CATILLON, R. CHAMINADE, H. FARAGGI, A. PAPINEAU et J. THIRION Diffusions élastiques et inélastiques de protons de 11 MeV sur les isotopes ^{64}Zn, ^{66}Zn, ^{68}Zn 397

K. F. RILEY, $C^{12}(p, 2p)B^{11}$ in the impulse approximation 407

A. G. SITENKO and V. K. TARTAKOVSKY, On diffractional disintegration of deuterons. 420

SAUL BARSHAY, Low-type integral equations for the absorption and production of K mesons 435

A. M. BRODSKY and D. D. IVANENKO, On a possible connection between isobaric spin and strangeness and inversion properties of spinors 447

M. L. MEHTA and C. S. WARKE, $Cl^{35}(d, p)Cl^{36}$ in the unified model 451

FERNANDO E. PRIETO, Parity non-conservation in hyperon decays 456

NORTH-HOLLAND PUBLISHING COMPANY-AMSTERDAM

November (1) 1959

EDITORIAL BOARD

AUSTRALIA & NEW ZEALAND:	H. Messel (Sydney), M. L. Oliphant (Canberra)
AUSTRIA:	B. Karlik, (Vienna), H. Thirring (Vienna)
BELGIUM:	M. de Hemptinne (Louvain), J. Verhaeghe (Ghent)
CANADA:	G. Volkoff (Vancouver)
DENMARK:	C. Møller (Copenhagen), S. Rozental (Copenhagen)
FINLAND:	L. Simons (Helsinki)
FRANCE:	A. Berthelot (Saclay), S. Gorodetzky (Strasbourg)
GERMANY (DEM. REP.):	G. Hertz (Leipzig)
GERMANY (FED. REP.):	W. Gentner (Freiburg i. B.), J. H. D. Jensen (Heidelberg)
GREAT BRITAIN:	S. Devons (Manchester), T. H. R. Skyrme (Harwell)
HUNGARY:	L. Janossy (Budapest)
INDIA:	H. Bhabha (Bombay), R. Ramanna (Trombay)
IRISH REPUBLIC:	J. McConnell (Maynooth)
ISRAEL:	G. Racah (Jerusalem)
ITALY:	E. Amaldi (Rome)
JAPAN:	S. Kikuchi (Tokyo), S. Tomonaga (Tokyo)
MEXICO:	M. Moshinsky (Mexico)
NETHERLANDS:	H. Brinkman (Groningen), S. R. de Groot (Leiden)
NORWAY:	E. Hylleraas (Oslo), A. Lundby (Oslo), H. Wergeland (Trondheim)
POLAND:	L. Infeld (Warsaw)
PORTUGAL:	J. M. Araújo (Porto), J. R. de Almeida Santos (Coimbra)
SOUTH AMERICA:	G. Beck (Saõ Paulo), J. Leite Lopes (Rio de Janeiro)
SPAIN:	J. M. Otero (Madrid), C. Sanchez del Rio (Madrid)
SWEDEN:	O. Klein (Stockholm), K. Siegbahn (Uppsala), I. Waller (Uppsala)
SWITZERLAND:	P. Huber (Basel), P. Scherrer (Zürich)
U.A.R. & ARAB COUNTRIES:	F. El Bedewi (Alexandria), M. G. Nooh (Cairo)
U.S.A.	H. H. Barschall (Madison, Wisconsin), V. Weisskopf (Cambridge, Mass.)
U.S.S.R.:	M. A. Markov (Moscow), I. S. Shapiro (Moscow), D. V. Skobeltzyn (Moscow)
YUGOSLAVIA:	I. Supek (Zagreb)

CONTRIBUTIONS may be sent to the Editor, Professor L. Rosenfeld, NORDITA, Blegdamsvej 17, Copenhagen Ø, either directly, or preferably through the intermediary of one of the members of the Editorial Board of the country or region in which the author is working. They may be written in English, French or German.

NUCLEAR PHYSICS is published in fortnightly issues. The subscription price per volume of 700 pages is fl 57.00; 114s; $ 15.00. Post-free.

SUBSCRIPTIONS should be sent to the publishers, NORTH-HOLLAND PUBLISHING COMPANY, P.O.Box 103, Amsterdam or to any subscription-agent.

BOOKS FOR REVIEW should be sent to Professor Rosenfeld.

No part of this issue may be reproduced in any form, by print, photoprint, microfilm or any other means without written permission from the publisher. Reprints, photoprints or microfilms are obtainable at cost from the publisher.

Printed in the Netherlands

1.C | *Nuclear Physics* **13** (1959) 333—349; © *North-Holland Publishing Co., Amsterdam*
Not to be reproduced by photoprint or microfilm without written permission from the publisher

TWO PARTICLE APPROXIMATIONS OF THE MANY BODY PROBLEM (II)

W. BRENIG

Max-Planck-Institut für Physik und Astrophysik, München

Received 29 May 1959

Abstract: A formulation of the theory of nuclear reactions is presented which exhibits very explicitly the connection between the shell model and the compound nucleus model. A Breit-Wigner formula is derived in which the hard sphere scattering is replaced by the shell model scattering. Although the compound states are in general complicated many-body excitations, the two-particle approximation of Brueckner *et al.* can be shown to be sufficient for the calculation of the *average* properties contained in the optical model. Furthermore it is proved that the S-matrix, analogously to the ground state energy, could be calculated in a 'model approach' in which the correlations of the target nucleons are taken into account, but nevertheless the final result is expressed in terms of the momentum distribution of uncorrelated nucleons as in the original Goldberger method. The real and imaginary parts of the optical potential are calculated and the energy dependence of the so-called rearrangement energy is estimated, resulting in a slight increase of the effective mass.

1. Introduction

In a preceding paper [1]) a method was developed equivalent to Brueckner's approximation [2]) of the many-body problem for the ground state energy of a system of fermions interacting with strong short-range two-body forces. We now consider the extension of this method to the treatment of scattering problems.

As an application we shall give a justification of the optical model in the low energy (resonance) region and derive expressions for the volume parts of the optical potential (well depth of the real part and volume absorption constant).

There exist already several papers [3–9]) dealing with similar problems. In part the conclusions of these papers are confirmed by the following considerations. In addition we shall omit or clarify some of the usual approximations:

a) There is at first the disregard of the application of the Pauli principle to the scattered particle and the target nucleons. The difficulty of the complete antisymmetrisation is mainly a consequence of the fact that in the usual scattering formalism the target nucleons and the scattered particle are treated on a different footing. In zeroth order the interaction of the target

nucleons is completely taken into account, whereas the effect of the interaction of the scattered particle with the target nucleons has to be calculated by solving the scattering problem. Since this interaction is not symmetrical with respect to all particles, it is obvious that the Pauli principle leads to difficulties, even if it may be considered formally [7, 9]). Therefore, we shall develop a generalisation of the scattering formalism in which all particles occur symmetrically, so that the Pauli principle will present no difficulty.

b) This generalisation also sheds new light on a question raised by Brueckner [5]), namely the influence of deviations of the momentum distribution of the target nucleus from the ideal Fermi gas on the imaginary part of the optical potential. This appears already to be included in the usual Brueckner method, so that there is no need of introducing additionally the momentum distribution of the target nucleus. We shall consider this point in more detail below.

c) A third question concerns the neglection of the excitation of two and more particles of the target nucleus in comparison with the compound nucleus description of nuclear reactions, according to which in general many particles are assumed to be excited. In this connection we shall show that as long as direct three-body collisions may be neglected (which is the usual Brueckner approximation) the optical potential may be calculated from the one-particle excitations alone, although the compound nucleus states are in general complicated many-body excitations.

2. Scattering Formalism in Terms of Shell Model Functions

In the following we consider the special case of the scattering of one particle by a complex nucleus with an energy below the lowest reaction threshold. The inclusion of reactions, however, presents no difficulties [10]). We introduce the following notation:

$$(T_1+v_1)|0\rangle = E_0|0\rangle, \quad \langle 0|0\rangle = 1, \tag{1}$$

is the Schrödinger equation for the internal motion of the target nucleus, T_1 being the kinetic energy of the internal motion;

$$T_r|\mathbf{k}\rangle = \varepsilon|\mathbf{k}\rangle, \quad \langle \mathbf{k}|\mathbf{k}'\rangle = \delta(\mathbf{k}-\mathbf{k}') \tag{2}$$

is the equation for the free relative motion of the scattered particle with respect to the target nucleus.

The eigenstates $\psi^+_{0\mathbf{k}}$ (and $\psi^-_{0\mathbf{k}}$) with incoming (and outgoing) scattered waves of the total system

$$(T_1+T_r+v_1+v_r)\psi^\pm_{0\mathbf{k}} = (T+v)\psi^\pm_{0\mathbf{k}} = H\psi^\pm_{0\mathbf{k}} = (E_0+\varepsilon)\psi^\pm_{0\mathbf{k}} = E\psi^\pm_{0\mathbf{k}} \tag{3}$$

are usually defined by the limit for $\eta \to +0$ of

$$\psi^{\pm}_{0\mathbf{k}} = \frac{\pm i\eta}{H-E\pm i\eta}|0\mathbf{k}\rangle, \tag{3a}$$

where $|0\mathbf{k}\rangle$ is the antisymmetrised product of $|0\rangle$ and $|\mathbf{k}\rangle$. Since this leads to the antisymmetrisation difficulties mentioned above we shall define $\psi^{\pm}_{0\mathbf{k}}$ more symmetrically as solutions of the integral equations

$$\psi^{\pm}_{0\mathbf{k}} = \varphi^{\pm}_{0\mathbf{k}} - \frac{1}{H_0-\mathscr{E}\pm i\eta} w\psi^{\pm}_{0\mathbf{k}} \tag{4}$$

where

$$w = v-V-E_0+\mathscr{E}_0;$$

$H_0 = T+V$ is a suitable model Hamiltonian, (fixed later on by self-consistency conditions); $\varphi^{\pm}_{0\mathbf{k}}$ the corresponding scattering state of the model, $\mathscr{E} = \mathscr{E}_0+\varepsilon$ the energy of this state and $\mathscr{E}_0$ the model energy of the target nucleus. With inclusion of the Pauli principle eq. (4) is only correct if the model Hamiltonian is symmetrical with respect to all particles, otherwise $\varphi^{\pm}_{0\mathbf{k}}$ has to be replaced by a more complicated expression (see Appendix).

We now write down an expression for the S-matrix which follows from eq. (4):

$$S_{\mathbf{k}\mathbf{k}'} = s_{\mathbf{k}\mathbf{k}'} - 2\pi i\langle\varphi^{+}_{0\mathbf{k}}|w|\varphi^{-}_{0\mathbf{k}'}\rangle\delta(\varepsilon-\varepsilon') \tag{5}$$

where

$$s_{\mathbf{k}\mathbf{k}'} = \langle\varphi^{+}_{0\mathbf{k}}|\varphi^{-}_{0\mathbf{k}'}\rangle$$

is the S-matrix of the model. In the usual formalism following from (3a) it is easy to see that (apart from antisymmetrisation) $\psi^{-}_{0\mathbf{k}}$, in coordinate space, behaves asymptotically as

$$\psi_{0\mathbf{k}} \sim |0\rangle(e^{i\mathbf{k}\cdot\mathbf{r}} + t(\mathbf{k}, k\mathbf{r}/r)e^{ikr}/r) \tag{6}$$

where $t(\mathbf{k}, \mathbf{k}')$ is connected with the S-matrix by

$$S_{\mathbf{k}\mathbf{k}'} = \delta(\mathbf{k}-\mathbf{k}') - 2\pi i t(\mathbf{k}, \mathbf{k}')\delta(\varepsilon-\varepsilon').$$

It is also easy to see that, according to (4), $\psi^{-}_{0\mathbf{k}}$ contains asymptotically a factor

$$\varphi_0(e^{i\mathbf{k}\cdot\mathbf{r}} + t(\mathbf{k}, k\cdot\mathbf{r}/r)e^{ikr}/r),$$

where φ_0 is the model target ground state, but it is more difficult to prove that the complete asymptotical behaviour is exactly the same as in (6), and that accordingly (3a) and (4) are equivalent and (5) is the correct S-matrix (see Appendix).

To give a rough idea of the content of eq. (4) we neglect hard core potentials and write down the second order perturbation terms, i.e.

$$\psi^{+}_{0\mathbf{k}} = \varphi^{+}_{0\mathbf{k}} - \frac{1}{H_0-\mathscr{E}+i\eta} w\varphi^{+}_{0\mathbf{k}}. \tag{7}$$

If we now assume that H_0 is a shell model type Hamiltonian, i.e. V is a sum of one-particle potentials, and that v is a sum of two-body potentials, then $\varphi^+_{0\mathbf{k}}$ is a determinant of one-particle functions and the perturbative term is a sum of determinants which differ from $\varphi^+_{0\mathbf{k}}$ by no more than two quantum numbers.

The shell model energy $\mathscr{E}_0$ and potential V may now be defined by the condition that all contributions from determinants differing from $\varphi^+_{0\mathbf{k}}$ in less than two quantum numbers should vanish. This leads to †

$$\begin{aligned} V_{\mu\nu} &= \sum_\rho v_{\rho\mu,\,\rho\nu}, \\ V_{\mu\mathbf{k}} &= \sum_\rho v_{\rho\mu,\,\rho\mathbf{k}}, \\ V_{\mathbf{k}'\mathbf{k}} &= \sum_\rho v_{\rho\mathbf{k}',\,\rho\mathbf{k}}, \end{aligned} \tag{8}$$

where the sum runs over the states of the target nucleons, exchange terms being included in this definition (greek letters denote discrete states, latin letters continuum one-particle states). This means that the scattered particle moves in the same potential as the target nucleons without having any influence on their motion, since the scattering state $\mathbf{k}$ does not occur in the sum over ρ.

After this definition of the model by the conditions (8), only two-particle excitations occur as perturbations. They may be labelled by four quantum numbers, namely those of the two states which are empty in $\varphi^+_{0\mathbf{k}}$ and of the two states which are occupied instead of them. All these contributions are of the form

$$-\frac{v_{\mu\nu,\,\kappa\lambda}}{\varepsilon_\mu+\varepsilon_\nu-\varepsilon_\kappa-\varepsilon_\lambda+i\eta}\,\varphi^{(\kappa\lambda)}_{\mu\nu}, \tag{9}$$

where the ε_μ are the one-particle energies of the shell model. One of the empty states κ, λ may be replaced by the continuum state $\mathbf{k}$, and one or both of the occupied states μ, ν may be an arbitrary continuum state ($\mathbf{p}$ or $\mathbf{q}$).

The contributions (9) correspond to various virtual excitations which may occur by means of two-body collisions. In some cases, however, there appear vanishing energy denominators corresponding to real physical processes. These are always connected with a de-excitation of the state $\mathbf{k}$ and may be summarized by the following scheme:

$$\mathbf{k},\lambda \rightarrow \begin{cases} \mu,\,\nu\text{: resonance scattering,} \\ \mathbf{p},\,\nu\text{: inelastic scattering,} \\ \mathbf{p},\,\mathbf{q}\text{: 'ionisation'.} \end{cases} \tag{10}$$

The 'ionisation' can only happen above the reaction threshold and can be

† This is equivalent to a Hartree-Fock type condition and may be obtained from the Hulthèn-Kohn variational principle if one chooses for $\psi^+_{0\mathbf{k}}$ a determinant as trial function.

excluded according to our restriction to sufficiently low energies. The inelastic scattering leads to a discrete excited target state (which later on decays, for instance by the emission of gamma rays) and corresponds to non-unitarity of the $S_{\mathbf{kk}'}$ defined in (5). We shall not discuss these possibilities further, although of course they have to be considered in calculating the imaginary part of the optical potential. The transition to the discrete states μ, ν corresponds to resonance scattering in finite nuclei, as we shall show in more detail. This is coherent with the shell model scattering as long as one deals with stationary states, but the coherence is destroyed if one considers the scattering of wave-packets with a sufficiently small coherence length, or the averaged cross-sections of stationary states. The same may be achieved if one considers the limiting case of an infinite target nucleus, when the sums over intermediate states may be replaced by integrals. Then the resonance scattering goes over into 'sideway scattering', which is known to be incoherent with the forward scattering. These types of incoherence together with the above-mentioned inelastic scattering is the cause of the absorption i.e. of the imaginary part of the optical potential for low energies.

3. Resonances

The singularity which occurs in second order perturbation theory if $\varepsilon_\mu+\varepsilon_\nu = \varepsilon+\varepsilon_\lambda$ may be treated like the degenerate case in the perturbation theory of discrete states by projecting the degenerate state out of the Green's function in (4) and adding it to the inhomogeneous part:

$$\psi^+_{0\mathbf{k}} = \varphi^+_{0\mathbf{k}}+c^+(\mathbf{k})\varphi_1-\frac{P}{H_0-\mathscr{E}+i\eta}w\psi^+_{0\mathbf{k}} \tag{11}$$

where $P = 1-|\varphi_1\rangle\langle\varphi_1|$; ($\varphi_1$ is the discrete state degenerate with $\varphi^+_{0\mathbf{k}}$). Formally the solution of (11) may be written as

$$\psi^+_{0\mathbf{k}} = \Omega(\mathscr{E})\varphi^+_{0\mathbf{k}}+c^+(\mathbf{k})\Omega(\mathscr{E})\varphi_1 \tag{12}$$

where

$$\Omega(\mathscr{E}) = \left(1+\frac{P}{H_0-\mathscr{E}+i\eta}w\right)^{-1}, \quad \langle\varphi_1|\Omega|\varphi^+_{0\mathbf{k}}\rangle = 0, \quad \langle\varphi_1|\Omega|\varphi_1\rangle = 1.$$

Since the coefficient of $\varphi^+_{0\mathbf{k}}$ and the energy are already fixed by (11) there is no secular equation, as in the degenerate case of a pure discrete spectrum, but only an inhomogeneous linear equation. This follows from the Schrödinger equation, which may be written in the form

$$(\mathscr{E}-H_0-w)(\Omega\varphi^+_{0\mathbf{k}}+c^+\Omega\varphi_1) = 0. \tag{13}$$

Multiplying from the left side by $\langle\varphi_1|$ we obtain

$$c^+(\mathbf{k}) = \frac{\langle\varphi_1|w\Omega|\varphi^+_{0\mathbf{k}}\rangle}{\mathscr{E}-\mathscr{E}_1-\langle\varphi_1|w\Omega|\varphi_1\rangle}. \tag{14}$$

If we now again write down all terms up to the lowest non-vanishing order of perturbation theory, the result is

$$c^+(\mathbf{k}) = \frac{v^+_{\mu\nu,\,\kappa\mathbf{k}}}{\varepsilon+\varepsilon_\kappa-\varepsilon_\mu-\varepsilon_\nu-\Delta-i\gamma}, \tag{15}$$

where †

$$v^\pm_{\mu\nu,\,\kappa\mathbf{k}} = \langle\varphi_1|v|\varphi^\pm_{0\mathbf{k}}\rangle = \int\varphi_\mu^*(1)\varphi_\nu^*(2)v_{12}\varphi_\kappa(1)\varphi_{\mathbf{k}}^{\pm}(2)\mathrm{d}(12)-(\text{exchange}),$$

$$\gamma = \pi\int|v^+_{\mu\nu,\,\kappa\mathbf{k}'}|^2\delta(\varepsilon-\varepsilon')\mathrm{d}\mathbf{k}', \tag{16}$$

$$\Delta = v_{\mu\nu,\,\mu\nu}-v_{\mu\kappa,\,\mu\kappa}-v_{\nu\kappa,\,\nu\kappa}.$$

As can be seen from (15), the coefficient $c(\mathbf{k})$ shows a resonance behaviour. The width γ of the resonance which occurs in (15) instead of the infinitesimal η in (9) is a function of the energy ε. But since most of the contributions in the integral $v^+_{\mu\nu,\,\kappa\mathbf{k}}$ occurring in (16) come from inside the nucleus, where the one-particle scattering states $\varphi_{\mathbf{k}}{}^+(\mathbf{r})$ are only slowly varying with ε, this variation is small (giant resonances!).

The consequence of this resonance effect is a maximum of the cross-section as a function of ε. To show this, we have to consider the S-matrix, which, after insertion of (12) and (15) into (5), is of the form

$$S_{\mathbf{k}\mathbf{k}'} = s_{\mathbf{k}\mathbf{k}'}-2\pi i\frac{v^+_{\kappa\mathbf{k},\,\mu\nu}v^-_{\mu\nu,\,\kappa\mathbf{k}}}{\varepsilon-\varepsilon_{\mathrm{r}}+i\gamma},\ \varepsilon_{\mathrm{r}} = \varepsilon_\mu+\varepsilon_\nu-\varepsilon_\kappa+\Delta. \tag{17}$$

This is the well known Breit-Wigner formula, in which the hard sphere scattering is replaced by the shell model scattering.

On the other hand, if one looks for the scattering of a wave packet $\psi(t) = \int a(\mathbf{k})\psi^+_{0\mathbf{k}}\mathrm{e}^{-i\mathscr{E}t}\mathrm{d}\mathbf{k}$ with an average energy in the neighbourhood of ε_{r} and an energy spread large compared to γ, the probability $|\langle\varphi_1|\psi(t)\rangle|^2$ of finding the state φ_1 in the wave packet according to (12), (15) is approximately given by $\approx\mathrm{e}^{-2\gamma t}$ for $t>0$. This means that the stable shell model state φ_1 corresponds to a metastable state in the exact solution. The fact that usually the lifetime $\frac{1}{2}\gamma$ is small compared to ε_{r} shows that the coupling of the two shell model states φ_1 and $\varphi^+_{0\mathbf{k}}$ is small, i.e. the shell model in this sense is a good approximation.

At this point we should add a few remarks on the ambiguity coming from the arbitrariness of the choice of the model H_0 in (4). At first sight one has the impression that by using different H_0's one may produce resonances of arbitrary position and width. But this is not the case. In the derivation of (17) essential use is made of the self-consistency conditions (8). If instead of this an arbitrary H_0 is used, the energy shift Δ and the width γ become large in general. Especially γ might be so large that for $|\varepsilon-\varepsilon_{\mathrm{r}}|$ comparable to

† There is also a second order contribution to the energy shift Δ, which we have neglected, since there is already a first order term.

γ there is another eigenstate of H_0 degenerate with $\varphi^+_{0\mathbf{k}}$, which means that our approximations for the derivation of (17) are no longer valid.

On the other hand, if one uses a perturbation expansion (or Brueckner approximation) for the treatment of (4) there occur in lowest orders only those resonances which have a simple connection with shell model excitations, i.e., for instance, no collective resonance states.

Mainly, there are two improvements to be considered in our simplified treatment of (4):

a) In general there is more than one state φ_1 degenerate or almost degenerate (i.e. $|\varepsilon_1-\varepsilon| \lesssim \gamma$) with $\varphi^+_{0\mathbf{k}}$. Let us call these states φ_n; then, instead of (11) one has to write

$$\psi^+_{0\mathbf{k}} = \varphi^+_{0\mathbf{k}} + \sum_n c_n{}^+ \varphi_n - \frac{P}{H_0-\mathscr{E}+i\eta} w\psi^+_{0\mathbf{k}}, \quad P = 1 - \sum_n |\varphi_n\rangle\langle\varphi_n|, \tag{18}$$

and instead of the simple linear relation (14) one obtains the equation

$$\sum_n \{(\mathscr{E}-\mathscr{E}_m)\delta_{mn} - \langle\varphi_m|w\Omega|\varphi_n\rangle\} c_n{}^+ = \langle\varphi_m|w\Omega|\varphi^+_{0\mathbf{k}}\rangle. \tag{19}$$

Then c_n contain not only one resonance denominator but as many as there are degenerate states. The resonance energies $\mathscr{E}_\lambda$ and their widths γ_λ may be found by solving the secular equation

$$\sum_n \{(\mathscr{E}-\mathscr{E}_m)\delta_{mn} - \langle\varphi_m|w\Omega|\varphi_n\rangle\} c_{n\lambda} = (\mathscr{E}_\lambda - i\gamma_\lambda) c_{m\lambda}, \tag{20}$$

and the corresponding resonance part of the S-matrix is of the form

$$S^{(r)}_{\mathbf{k}\mathbf{k}'} = \sum_\lambda \frac{\langle\varphi^+_{0\mathbf{k}}|\Omega w|\varphi_\lambda\rangle\langle\varphi_\lambda|w\Omega|\varphi^-_{0\mathbf{k}'}\rangle}{\mathscr{E}-\mathscr{E}_\lambda+i\gamma_\lambda}, \tag{21}$$

where

$$\varphi_\lambda = \sum_n c_{n\lambda}\varphi_n.$$

This equation is in general complicated, but we can draw from it a conclusion, which is important in connection with the simultaneous validity of the two-particle approximation and the compound nucleus description.

In the two-particle approximation as well as in second order perturbation theory there is no direct coupling of two-particle excitations of the target nucleus to the entrance channel $\varphi^+_{0\mathbf{k}}$. More explicitly:

$$\gamma_m = \mathrm{Im}\,\langle\varphi_m|w\Omega|\varphi_m\rangle \approx \pi \int |\langle\varphi_m|v|\varphi^+_{0\mathbf{k}'}\rangle|^2 \delta(\varepsilon-\varepsilon')\mathrm{d}\mathbf{k}' = 0 \tag{22}$$

for two-particle excitations φ_m. This means that in zeroth order (i.e. neglecting non-diagonal terms in (20)) one obtains the width zero for the two particle excitations. But actually there are non-vanishing non-diagonal elements connecting single with twofold excitations, and these with higher excitations. Therefore, the resulting resonance states are superpositions of

many different excitations and each of them has a non-vanishing width. This means that the compound states are in general complicated, and only if there are no two-particle excitations degenerate with a single excitation (a case which may occur only at low energies for not too large nuclei) the formation of the compound system consists of a single collision of the incoming particle with a target nucleon. Nevertheless, the imaginary part of the optical potential can be calculated from these simple collisions, since it contains only the average values of the widths which may be calculated easily by taking the trace of the secular matrix

$$\sum_{\lambda}(\mathscr{E}_{\lambda}-i\gamma_{\lambda}) = \sum_{m}(\mathscr{E}_{m}+\langle\varphi_{m}|w\Omega|\varphi_{m}\rangle).$$

Now, in second order perturbation theory, using (22), or more generally in the two-particle approximation, we have

$$\sum_{\lambda}\gamma_{\lambda} = \sum_{m}\gamma_{m} \approx \sum_{\text{single excitations}}\gamma_{m}. \tag{22a}$$

According to this 'sum rule' the strength function and the optical potential may be calculated from the two-particle collisions alone, in so far as *direct* three-body collisions may be neglected, as is done in the two-particle approximation.

b) A second improvement concerns the correlations among the nucleons introduced by the hard core. In second order perturbation theory they are contained in the non-singular terms (9) and may be taken into account by a redefinition of the shell model. In the presence of a hard core the matrix elements occurring in (9) are infinite, and finite results can only be obtained after summing at least all contributions of the repeated virtual scattering of two particles, or more directly by starting from (12) in which all these contributions are summed and using methods similar to those of ref.[1]).

The result may be expressed by introducing the appropriate t-matrices instead of v in (8), (9), (15), (16) and (17). We shall consider this in more detail for infinite nuclear matter below. At first sight the validity of the two-particle approximation might be doubtful for scattering problems, since the solutions of the so-called Bethe-Goldstone equation for the scattering of the incoming particle inside nuclear matter do not approach the unperturbed states asymptotically. There is real, not only virtual, scattering and a corresponding phase shift in contrast to the behaviour of the ground-state Bethe-Goldstone solutions.

But the Pauli principle still acts to diminish the real scattering at least for low energies. Actually, the phase shift of the Bethe-Goldstone solutions tends to zero if the relative momentum of the two particles approaches the Fermi momentum. A measure of the ratio of real to virtual scattering is the ratio of the imaginary to the real part of the optical potential. So far as this ratio is small one might expect the two-particle approximation to be valid.

4. The Optical Model

In spite of the complex resonance behaviour of the cross section its average properties can be well described in terms of a suitable complex one particle potential [11]), depending only upon a small number of parameters, mainly a real well depth (independent of mass number), a radius, a surface thickness, and coefficients of volume and surface absorption.

So far as one is not interested in surface effects, one may consider the limiting case of infinitely extended nuclear matter. This has been done in great detail for the ground state [2, 12]).

In nuclear matter it is no longer necessary to project out the resonance states in (4), since they are continuously distributed and therefore produce no singularities. But we may split up (4) into

$$\psi^+_{0\mathbf{k}} = \varphi^+_{0\mathbf{k}} - \frac{\mathscr{P}}{H_0-\mathscr{E}} w\psi^+_{0\mathbf{k}} + i\pi\delta(H_0-\mathscr{E})w\psi^+_{0\mathbf{k}}, \tag{22}$$

where $\mathscr{P}$ means principal value, and treat the imaginary term on the right hand side as a small perturbation. To define the optical potential it is convenient to use another expression than (5) for the S-matrix, namely (see Appendix)

$$S_{\mathbf{k}\mathbf{k}'} = \delta(\mathbf{k}-\mathbf{k}') - 2\pi i\langle\psi^+_{0\mathbf{k}}|\varepsilon - T_\mathbf{r}|\varphi_{0\mathbf{k}'}\rangle\delta(\varepsilon-\varepsilon'),\ \varphi_{0\mathbf{k}'} = \varphi_0|\mathbf{k}'\rangle. \tag{24}$$

This means that one has to find a one-particle operator $W = W_\mathbf{r} + iW_\mathbf{i}$ obeying

$$(\varepsilon - T_\mathbf{r})\psi_\mathbf{k}{}^+ = W\psi_\mathbf{k}{}^+, \quad \psi_\mathbf{k}{}^+ = \langle\varphi_0|\psi^+_{0\mathbf{k}}\rangle, \tag{25}$$

which then by definition is the optical potential †. The main difference between (24), (25) and the corresponding formulas cited above[3–9]) is the occurrence of φ_0 instead of $|0\rangle$. The freedom in the choice of φ_0 is in complete analogy to the ground state calculations. Here one may also write

$$E_0 = \langle 0|H_\mathbf{i}|0\rangle = \langle\varphi_0|H_\mathbf{i}|\psi_0\rangle \tag{26}$$

where

$$\psi_0 = |0\rangle/\langle\varphi_0|0\rangle,$$

although (26) is much more obvious than (24).

Therefore, the S-matrix or the optical potential may be calculated from the same type of t-matrices as in the ground state, the summation running over the momentum distribution of the model state φ_0, and *not* of the true target state $|0\rangle$.

If in zeroth order we neglect the absorption, i.e. the imaginary part in (23),

† This is only true for nuclear matter. For finite nuclei the definition (25) yields a W varying very rapidly with the energy, since it has to reproduce the resonances. The usual optical potential is not the average value of W, but that potential which yields the averaged S-matrix.

then, because of the homogeneity of nuclear matter, $\psi_{\mathbf{k}}^{+}$ is represented by a plane wave. Its wave number inside nuclear matter may be called $\mathbf{q}$, so that $T\psi_{\mathbf{k}}^{+} = (q^2/2m)\psi_{\mathbf{k}}^{+}$. This means that in order to determine W one has only to find the wave number of $\psi_{\mathbf{k}}^{+}$ for a given energy $E_0+\varepsilon$ of the total system.

In the two-particle approximation one obtains, in complete analogy to the ground state,

$$E = E_0+\varepsilon = \sum_{\mathbf{k}} \frac{k^2}{2m} + \frac{q^2}{2m} + \tfrac{1}{2}\sum_{\mathbf{k},\mathbf{k}'} K_{\mathbf{kk}',\mathbf{kk}'} + \sum_{\mathbf{k}} K_{\mathbf{kq},\mathbf{kq}}. \tag{27}$$

The sums include spins and isospins and should be replaced by integrals in the final results. The t-matrices are replaced by corresponding K-matrices (according to the use of the principal value in (23)), which are defined by

$$K_{\mathbf{qq}',\mathbf{kk}'} = \langle \varphi_{\mathbf{qq}'} | v_{12} | \psi_{\mathbf{kk}'} \rangle \tag{28}$$

in terms of the solutions $\psi_{\mathbf{kk}'}$ of the Bethe-Goldstone equation

$$\psi_{\mathbf{kk}'} = \varphi_{\mathbf{kk}'} - \frac{P}{H_{12}-\varepsilon_{\mathbf{k}}-\varepsilon_{\mathbf{k}'}} v_{12}\psi_{\mathbf{kk}'}. \tag{29}$$

Here $\varphi_{\mathbf{kk}'}$ is the antisymmetrised product of plane waves, spin and isospin states, H_{12} is the one particle shell model Hamiltonian, and

$$\varepsilon_{\mathbf{k}} = \frac{k^2}{2m} + V(k), \quad V(k) = \sum_{\mathbf{k}'} K_{\mathbf{kk}',\mathbf{kk}'}; \tag{30}$$

P is a projection operator which excludes all intermediate states occupied by the target nucleons and the one state $\mathbf{q}$.

If we treat the effect of the exclusion of this one state as a small perturbation †, one has in zeroth order $W = V = W_{\mathrm{r}}$. In first order one has to take into account the perturbation of the double sum in (27) because of the change in P:

$$W_{\mathrm{r}}(q) = V(q) + \tfrac{1}{2}\sum_{\mathbf{k},\mathbf{k}'} \delta K_{\mathbf{kk}',\mathbf{kk}'} = V(q) + \Delta(q). \tag{31}$$

Using the formal solution of (29) we obtain, with $e = H_{12}-\varepsilon_{\mathbf{k}}-\varepsilon_{\mathbf{k}'}$,

$$\delta K = \delta v \frac{1}{1+\dfrac{P}{e}v} = K\frac{\delta P}{e}K. \tag{32}$$

Thus, the final result for $\Delta(q)$ is

$$\Delta(q) = \tfrac{1}{2}\sum_{\substack{k,k'\le k_{\mathrm{f}} \\ q'>k_{\mathrm{f}}}} \frac{|K_{\mathbf{qq}',\mathbf{kk}'}|^2}{\varepsilon_{\mathbf{q}}+\varepsilon_{\mathbf{q}'}-\varepsilon_{\mathbf{k}}-\varepsilon_{\mathbf{k}'}}. \tag{33}$$

† Recently [13–15]), there have appeared several papers on this effect for $q = k_{\mathrm{f}}$[2], the so-called rearrangement energy. The fact that it is not negligible was first brought to the author's attention by Dr. F. Beck in 1957.

Since this first order correction turns out to be rather large, one should also take into account the second order term, i.e. the perturbation of $V(k)$ because of the first order change in K. As we do not intend to calculate the value but only the derivative of $\Delta(q)$, we shall not consider this term in more detail. It is easy to see that it has approximately the same q dependence as the first order term (33).

To determine $W_r(q) = V(q)+\Delta(q)$ as a function of ε from (31), we assume the effective mass approximation for $W(q)$ as well as for $V(q)$:

$$\begin{aligned} \frac{q^2}{2m} + W_r(q) &= \varepsilon_0 + \frac{q^2}{2\hat{m}} = \varepsilon, \\ \frac{q^2}{2m} + V(q) &= \varepsilon_1 + \frac{q^2}{2m^*}; \end{aligned} \tag{34}$$

ε_1 and m^* may be taken from Brueckner and Gammel [2]) (this together with (31) and $k_f^2/2m)+W_r(k_f) = -16$ MeV yields value of $\Delta(k_f) \approx 15$ MeV); ε_0 is fixed by the saturation condition $\varepsilon_0+k_f^2/(2\hat{m}) = -\varepsilon_b = -16$ MeV (ε_b is the average binding energy) and $\hat{m}$, which has to be calculated from the derivative $\Delta'(q)$ of the rearrangement energy $\Delta(q)$:

$$\frac{k_f}{\hat{m}} = \frac{k_f}{m^*} + \Delta'(k_f). \tag{35}$$

From (34) we obtain for $W_r(\varepsilon)$

$$W_r(\varepsilon) = -\frac{\hat{m}}{m}\varepsilon_b - \frac{k_f^2}{2m} - \varepsilon\left(1 - \frac{\hat{m}}{m}\right). \tag{36}$$

Now the derivative of Δ, according to (33), consists of two parts, one coming from the derivative of the K-matrix and one from the denominator. Because of momentum conservation, and the condition that $\mathbf{k}$ and $\mathbf{k}'$ should be inside the Fermi sphere, the values of K entering into (33) are of the order of

$$K(\langle\tfrac{1}{2}|\mathbf{q}-\mathbf{q}'|\rangle_{av},\ \langle\tfrac{1}{2}|\mathbf{k}-\mathbf{k}'|\rangle_{av})\delta_{\mathbf{q}+\mathbf{q}',\,\mathbf{k}+\mathbf{k}'}$$

(neglecting the dependence of K on the total momentum and higher than s-waves), where $\frac{1}{2}\langle|\mathbf{k}-\mathbf{k}'|\rangle_{av} \approx \sqrt{\frac{3}{10}}\mathbf{k}_f$, the average relative momentum in the Fermi sphere, and $\frac{1}{2}\langle|\mathbf{q}-\mathbf{q}'|\rangle_{av} \approx q$.

Since the main contribution in (33) comes from the hard core † the average q-dependence is of the form $k \approx \sin qa/qa$, which is roughly constant for $q \approx k_f$ because of the smallness of $k_f a$ (a being the core radius).

This means that the main contribution to (33) comes from the denominator and implies a relationship between $\Delta(q)$ and the momentum distribution $n(k)$ of the target nucleus in Brueckner's approximation (ref. [5]), eq. (25)), namely

† See for instance refs. [14, 15]).

$$\Delta'(k_f) \approx -\frac{k_f}{m^*} n_f, \qquad (37)$$
$$n_f = \lim_{k \to k_f} n(k), \; k > k_f.$$

Inserting this into the expression (35) for $\hat{m}$ we obtain, for small values of n_f,

$$\hat{m} \approx m^*(1+n_f). \qquad (38)$$

The value of n_f may be estimated by calculating

$$\frac{k_f \Delta'(k_f)}{\Delta(k_f)} = 2k_f^2 \langle (k_f^2+q'^2-k^2-k'^2)^{-2} \rangle_{\mathrm{av}} \cdot \langle (k_f^2+q^2-k^2-k'^2)^{-1} \rangle_{\mathrm{av}}^{-1},$$

where the averaging has to be done in the sense of the integration in (33) including momentum conservation. This gives, roughly,

$$\frac{k_f \Delta'(k_f)}{\Delta(k_f)} = \tfrac{1}{2} k_f^2 [\langle \tfrac{1}{4}(\mathbf{q}-\mathbf{q}')^2 \rangle_{\mathrm{av}} - \tfrac{1}{4} \langle (\mathbf{k}-\mathbf{k}')^2 \rangle_{\mathrm{av}}]^{-1}_{q'=k_f} \approx k_f^2 (k_f^2 - \tfrac{3}{10} k_f^2) = \tfrac{5}{7}.$$

Since in the integral for Δ' the lower values of the energy denominator, because of their quadratical appearence, are a little more preferred than in Δ, this value is underestimated, but we expect roughly $k_f \Delta'(k_f) \approx \Delta(k_f)$. This yields, with Brueckner and Gammel's value of $\Delta(k_f) \approx 15$ MeV, a value $n_f \approx \frac{1}{10}$ which agrees with Brueckner's calculations [5]).

Combining this with (38) and Brueckner's value $m^* = 0.75\, m$ we obtain $\hat{m} \approx 0.85\, m$ and $W(0) = -52$ MeV in good agreement with the experimental value [16]) $-$ 50 MeV.

We should mention that the main uncertainty in the theoretical value of $W(0)$ comes not from the value of $\hat{m}$ (which justifies our rough approximations above) but from the uncertainty of k_f^2. A more sensible test for the correctness of $\hat{m}$ is the energy dependence of $W(\varepsilon)$ which is not yet known experimentally with great accuracy †.

Let us now consider the imaginary part of W. If we take the imaginary part of (23) into account in first order, we obtain the well known formula [4])

$$W_1(q) = \pi \sum_{\substack{k<k_f \\ q',\, p>k_f}} |K_{\mathbf{q'p},\mathbf{qk}}|^2 \delta(\varepsilon_{\mathbf{q}'}+\varepsilon_{\mathbf{p}}-\varepsilon_{\mathbf{q}}-\varepsilon_{\mathbf{k}}). \qquad (39)$$

We should emphasize that although the correlations of the target nucleons have been taken into account the summation in (39) runs over the *unperturbed* momentum distribution. This is in complete analogy to the summations in eq. (27) for the energy. Of course one can choose the model state φ_0 equal to the true state $|0\rangle$. Then in (39) the momentum distribution of the true ground state would appear. But simultaneously one would have to calculate

† The giant resonance in the nuclear photoeffect seems to indicate a somewhat lower value of $\hat{m}$; cf. for instance ref. [17]).

the K-matrix according to the true approach (cf. for instance ref. [18])) and no longer from eqs. (28), (29). Since, because of (24), the final result of the model approach and the true approach is the same, it is much easier to use consistently the model approach and to start from (39).

If we neglect the **k**-dependence of K, the final result is on account of energy and momentum conservation,

$$W_1(q) = 2\pi m^* q \langle K^2(\tfrac{1}{2}q)\rangle_{\mathrm{av}} \rho f(q), \tag{40}$$

where ρ is the nuclear density,

$$K(k) = \frac{1}{k^2}\int \sin krv(r)\psi_k(r)\mathrm{d}r, \tag{41}$$

and ψ_k is the solution of the Bethe-Goldstone equation normalised as $\psi_k(r) \sim \sin kr$ for $r \to \infty$ (higher than s-waves being again neglected). The average is taken over the spin and isospin indices. In free space $\langle K^2\rangle$ is connected with the average total cross section $\bar{\sigma}$ by $\langle K^2\rangle = \bar{\sigma}/4\pi m^2$.

The function $f(q)$ expresses the effect of the Pauli principle; it approaches 1 for large values of q/k_f:

$$f(q) = 1 - 7k_f^2/5q^2, \quad q^2 \geqq 2k_f^2,$$

and zero for $q = k_f$:

$$\begin{aligned} f(q) &= 1 - 7k_f^2/5q^2 + 2k_f^2(2 - q^2/k_f^2)^{\frac{5}{2}}/5q^2, \quad q^2 \leqq 2k_f^2 \\ &= 3(q^2 - k_f^2)^2/4k_f^4, \qquad\qquad\qquad\qquad q \approx k_f. \end{aligned}$$

If it is expressed in terms of ε,

$$f(\varepsilon) = \left(\frac{\varepsilon + \varepsilon_b}{k_f^2/2m}\right)^2 \left(\frac{\hat{m}}{m}\right)^2, \qquad \varepsilon \approx 0,$$

it contains a factor $(\hat{m}/m)^2$ in comparison to the usual Goldberger value [19]), which gave rough agreement with experimental data. This means that, together with the m^* in (40), W_1 contains a factor $m^*\hat{m}^2/m^3 \approx 0.55$, which yields a value of W_1 too small in comparison with experiment if one disregards the enhancement of the absorption on the surface.

For the theoretical explanation of the surface absorption one has to consider at least the following effects:

1) The Pauli principle is less effective in the surface region because of the lower density. One may estimate this effect in a kind of Thomas Fermi approximation: if one assumes a reasonable decrease of W_r in (34) on the nuclear surface, one can calculate the local wave number q from (34) and the local Fermi momentum k_f from $\varepsilon_f = -\varepsilon_b = \varepsilon_0 + k_f^2/2\hat{m}$ (assuming constant ε_b). The local density is then given by $\rho = 2k_f^3/3\pi^2$. Inserting these values into (40) one finds only a very slight increase of W_1 (less than 10 %) if one neglects the variation of m^* and $\langle K^2\rangle$. This is a consequence of the approximate compensation of the increase in $f(q)$ by the decrease in ρ.

2) The variation of m^* and $\langle K^2 \rangle$ may be estimated by simply interpolating m between the value $m^* = 0.7\ m$ inside and $m^* = m$ outside (i.e. for $\rho = 0$) the nucleus, and by assuming an energy dependence $\langle K^2 \rangle = c/q^2$ which is known to be good for the experimental cross section. Then according to (40) W_1 is proportional to $m^*(k_f/q)^3 f(q)$. This function is plotted below for $\varepsilon = 0$ and shows a maximum on the surface. For a comparison with experimental data one should use the actual separation energy of the special nucleus (instead of the value 16 MeV of nuclear matter) which yields a larger maximum.

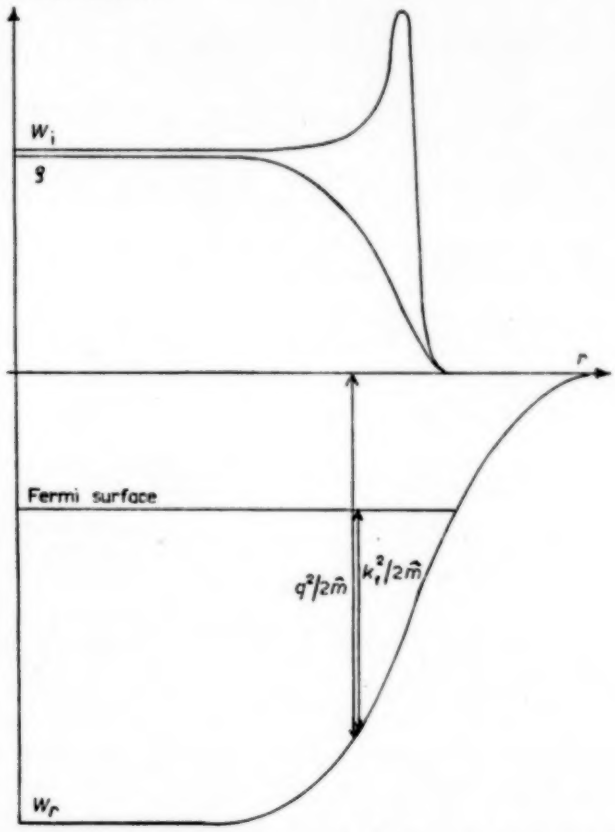

Fig. 1. Real and imaginary part of the optical potential for $\varepsilon = 0$ (arbitrary units).

This was done by K. Harada and N. Oda [20]), also ref. [27]), and ref. [21]) unfortunately with $m^* = m$, which yields a much too large total absorption cross section.

3) For finite nuclei eq. (39) is replaced by a more complicated expression in which the plane wave states are replaced by shell model wave functions. Because of the Pauli principle only the outer shells come into play for low energies. Now, the density of the outer shells increases on the surface because of the appearance of a classical turning point. This corresponds to an increase of the 'effective' K to be used in (39). A rough estimate of this effect yields an additional enhancement of the absorption in the surface of about fourty percent.

4) The non-hermiticity of the shell model potential ($V_{\mu\nu} \neq V^*_{\nu\mu}$) which was found in ref.[1]) also gives a contribution to W_1. If one uses the definition (19) of ref.[1]) one finds an increase of the non-hermitian part of V in the surface large enough to produce the total experimental value of the surface absorption. But this contribution is overestimated since the approximation (23a) and the simple extension of (24) to $\mu, \nu > N$ of ref.[1]) are too rough for this purpose. One has to define V so as to compensate as well as possible the higher order terms of the two-particle approximation, which is a complex condition †.

5) The estimates on the basis of the Thomas-Fermi model are of course only very rough for nuclear problems because of the rapid change of all properties in the surface region. In principle one should solve the Bethe-Goldstone equation at least for a semi-infinite region of nuclear matter. But even this is very difficult.

I am indebted to Prof. Heisenberg for an interesting discussion concerning the connection between the shell model and the compound nucleus model and Dr. G. Lüders for many critical comments.

Appendix

We shall now give a derivation (this does not mean a mathematical rigorous proof) of the eq. (5) and (24). The starting point is the general asymptotic condition [10]) for wave packets, which we write using the notation of (1), (2), (3), (3a):

$$\psi^+_{0\varphi} = \lim_{t\to\pm\infty} e^{iHt} \int e^{-iEt} \varphi(\mathbf{k}) |0\mathbf{k}\rangle d\mathbf{k}. \qquad (A.1)$$

This defines the scattering states $\psi^{\pm}_{0\varphi}$ by a strong limit. Because of the Pauli principle there exists in general no (hermitian) operator obeying $H_0|0\mathbf{k}\rangle = E|0\mathbf{k}\rangle$. We demonstrated above that this does not raise any objection in principle, but leads to serious practical difficulties. These difficulties can be overcome by a more symmetrical definition of the scattering states which are obtained by a suitable generalisation of (A.1).

The most general form of (A.1) is obtained if one replaces the $|0\rangle$ state by *any* localized state φ_0 of the target nucleus (with $\langle\varphi_0|0\rangle = 1$) and the $|\mathbf{k}\rangle$ state by *any* scattering state $|\mathbf{k}^{\pm}\rangle$ of the scattered particle which approaches $|\mathbf{k}\rangle$ for large positive and negative times, respectively.

One can verify that all these definitions yield the same $\psi^+_{0\varphi}$ by expanding

† If one uses the addition of an average energy shift in the energy denominator of the t-matrix as Goldstone proposes [22]) the non-hermitian part of V is smaller than above. Bethe's [23]) V is hermitian but the higher order terms introduce a larger non-hermiticity, and one should expect the higher order terms to be much more important on the surface because of the smaller effect of the Pauli principle.

$|0\rangle$ into the eigenstates of the target nucleus. Then the discrete states produce contributions oscillating asymptotically $\sim e^{i(E_n-E_0)t}$ (E_n denoting the energies of the excited states) and the continuum states corresponding to the various disintegration possibilities of the target nucleus yield terms vanishing asymptotically in the sense of weak convergence †. Thus, it is only necessary to take a mathematically reasonable limiting process which makes the oscillating terms vanish, for instance the Abelian limit

$$\lim_{t\to\infty} f(t) \to \lim_{\eta\to 0} \eta \int_0^\infty f(t) e^{-\eta t} dt.$$

After inserting all this into (A.1) we obtain, for the special case $\varphi(\mathbf{k}) \to \delta(\mathbf{k}-\mathbf{k}')$, and with $\varphi^+_{0\mathbf{k}}$ = antisymmetrised product of φ_0 and $|k^+\rangle$,

$$\psi^+_{0\mathbf{k}'} = \frac{i\eta}{H-E'+i\eta} \frac{\varphi^+_{0\mathbf{k}'}}{|\langle\varphi_0|0\rangle|^2}, \tag{A.2a}$$

$$\psi^-_{0\mathbf{k}} = \frac{-i\eta}{H-E-i\eta} \frac{\varphi^-_{0\mathbf{k}}}{|\langle\varphi_0|0\rangle|^2}. \tag{A.2b}$$

Here we have assumed $\langle\varphi_0|\varphi_0\rangle = 1$ so that the normalisation of $\psi^+_{0\mathbf{k}}$ is given by $\langle\psi^+_{0\mathbf{k}}|\psi^+_{0\mathbf{k}'}\rangle = \delta(\mathbf{k}-\mathbf{k}')/|\langle\varphi_0|0\rangle|^2$. The normalisation factors $|\langle\varphi_0|0\rangle|^2$ are included here in order to avoid them in the expression for $S_{\mathbf{k},\mathbf{k}'}$. This expression is obtained by multiplying (A.2a) by $s_{\mathbf{k},\mathbf{k}'} = \langle\varphi^+_{0\mathbf{k}}|\varphi^-_{0\mathbf{k}'}\rangle$ and integrating over $\mathbf{k}'$. After subtraction of (A.2b) one has

$$\psi^-_{0\mathbf{k}} = \int s_{\mathbf{k}\mathbf{k}'} \psi^+_{0\mathbf{k}'} d\mathbf{k}' - \frac{2i\eta}{(H-E)^2+\eta^2} (H-E) \frac{\varphi^-_{0\mathbf{k}}}{|\langle\varphi_0|0\rangle|^2}. \tag{A.3}$$

Scalar multiplication with $\psi^+_{0\mathbf{k}'}$ yields (5).

The other form (24) is obtained very similarly if one replaces $\varphi^+_{0\mathbf{k}}$ by the antisymmetrized product $\varphi_{0\mathbf{k}}$ of φ_0 and $|\mathbf{k}\rangle$.

If we now assume that $\varphi^+_{0\mathbf{k}}$ is the eigenstate of a model Hamiltonian H_0, we can derive an integral equation for $\psi^+_{0\mathbf{k}}$ by using the asymptotic condition (A.2a) in the reversed direction:

$$\varphi^+_{0\mathbf{k}} = \frac{i\eta}{H_0-\mathscr{E}+i\eta} \psi^+_{0\mathbf{k}} = \psi^+_{0\mathbf{k}} - \frac{1}{H_0-\mathscr{E}+i\eta} w\psi^+_{0\mathbf{k}}, \tag{A.4}$$

which is eq. (4). Note that the normalization of $\psi^+_{0\mathbf{k}}$ defined by (A.2a) and (A.4) is identical if $\langle\varphi^+_{0\mathbf{k}}|\varphi^+_{0\mathbf{k}'}\rangle = \delta(k-k')$.

† This weak convergence condition also forms the basis of a very general treatment of bound states in the scattering formalism of field theory. (Cf. for instance ref. [24]).)

References

1) W. Brenig, Nuclear Physics **4** (1957) 363
2) K. A. Brueckner and J. L. Gammel, Phys. Rev. **109** (1958) 1023; further references may be found in this paper

3) N. C. Francis and K. M. Watson, Phys. Rev. **92** (1953) 291
4) K. A. Brueckner, R. J. Eden and N. C. Francis, Phys. Rev. **100** (1955) 891
5) K. A. Brueckner, Phys. Rev. **103** (1956) 172
6) A. M. Lane, R. G. Thomas and E. P. Wigner, Phys. Rev. **98** (1955) 18
7) F. N. Medina, Thesis, Göttingen (1958)
8) H. Feshbach, Ann. Rev. of Nucl. Science **8** (1958) 49
9) F. Coester and H. Kümmel, Nuclear Physics **9** (1958/59) 225
10) H. Ekstein, Phys. Rev. **101** (1956) 880;
W. Brenig and R. Haag, Fortschr. d. Phys. (in print)
11) H. Feshbach, C. E. Porter and V. F. Weisskopf, Phys. Rev. **96** (1954) 448
12) L. J. Gomes, J. D. Walecka and V. F. Weisskopf, Ann. of Phys. **3** (1958) 241
13) K. A. Brueckner, Phys. Rev. **110** (1958) 597
14) P. Mittelstaedt, Nuclear Physics **9** (1958/59) 116
15) D. J. Thouless, Phys. Rev. **112** (1958) 906
16) P. Mittelstaedt, Nuclear Physics **8** (1958) 171
17) V. F. Weisskopf, Nuclear Physics **3** (1957) 423
18) A. Klein and R. Prange, Phys. Rev. **112** (1958) 994
19) M. L. Goldberger, Phys. Rev. **74** (1948) 1269
20) K. Harada and N. Oda, Progr. theor. Phys. **21** (1959) 260
21) L. Verlet and F. Gavoret, Nuovo Cimento **10** (1958) 505
22) J. Goldstone, Proc. Roy. Soc. **239** (1957) 267
23) H. A. Bethe, Phys. Rev. **103** (1956) 1353
24) W. Zimmerman, Nuovo Cimento **10** (1958) 597

1.C *Nuclear Physics* **13** (1959) 350—359; © *North-Holland Publishing Co., Amsterdam*
Not to be reproduced by photoprint or microfilm without written permission from the publisher

SPIN-ORBIT SPLITTINGS IN NUCLEI (II)

J. SAWICKI
Palmer Physical Laboratory, Princeton University, Princeton, New Jersey
and
University of Washington, Seattle, Washington †

Received 26 July 1959

Abstract: The j-doublet splittings of single-particle nuclear levels are calculated in terms of the effective two-body spin-orbit interaction operator — the reaction matrix. The recent result of Brueckner *et al.* is used for the odd-state K^-_{LS}-operator corresponding to Gammel-Thaler potentials. On the same basis the even-state K^+_{LS} is neglected. The exchange amplitudes of the K^-_{LS}-operator are taken into account and also the "higher derivative" terms. The self-consistent nuclear density of the Ca^{40}-nucleus and other forms of this density are used to calculate the doublet splittings of Ca^{41}. Satisfactory results are obtained. The doublet splittings of the nuclei Pb^{209}, Bi^{209}, O^{17} and He^5 are discussed. A discussion is presented of the spin-orbit splittings in spheroidally deformed nuclei.

1. Introduction

In a previous paper [1]) (further referred to as I) a discussion was presented of the j-doublet splittings of the single-particle levels in nuclei containing a spin-saturated core and one extra core nucleon ††. The effective two-body spin-orbit interaction between the extra core nucleon and each of the core nucleons was taken in the form of the spin-orbit part of the reaction matrix K. This operator was applied in the usual phase shift approximation corresponding to the Gammel-Thaler and Signell-Marshak potentials and also in a simplified approximate form taken in part from the paper by Brueckner, Gammel and Weitzner [2]).

The core density function was taken in a form corresponding to generally correlated core ground state wave functions and a particular application was made to the $1d_{\frac{5}{2}}-1d_{\frac{3}{2}}$ splitting in the O^{17}-nucleons with the use of

† Supported in part by the U. S. Atomic Energy Commission and the Higgins Scientific Trust Fund.

†† Through an unfortunate oversight a factor 2 is missing in eq. (24) of I; consequently all the final numbers $\Delta(\Delta E)_{LS}$ of I should be doubled. A factor 4 is missing in eq. ($A_1$1) of appendix I and also $\int_0^\infty k^2 dk\, j_1(2kr) = \frac{1}{16}\pi[-\delta'(r)/r^2+\delta''(r)/r]$, but the final eq. ($A_1$3) is correct). The numbers $\alpha^{\text{Born}}_{\text{S}-\text{M}}$ and $\delta^{\text{Born}}_{\text{S}-\text{M}}$ of the first "Note added in proof" are based on misunderstood parameters of Signell, Zinn and Marshak; the appropriate numbers would be $\alpha^{\text{Born}}_{\text{S}-\text{M}} = 26.76\ f^5$ MeV and $\delta^{\text{Born}}_{\text{S}-\text{M}} = -13.82\ f^7$ MeV, if the "flat" cut-off were used. However, as the modified Gartenhaus triplet odd potential contains a hard core, the "flat" cut-off procedure is completely arbitrary. Some further criticism of certain other points of section 2 of I is given in the text.

Dąbrowski's wave function which is a solution of the O^{16} saturation problem[3]).

In general, given the "exact" core wave function it is not easy to solve the even approximate integral equation for the reaction matrix of the extra core particle (compare a footnote in I, p. 371). The best approach to the problem seems to be that of Brueckner, Gammel and Weitzner (B-G-W) who solve the Hartree-Fock problem with their self-consistent reaction matrix K. In fact, if one uses their K-matrix in our problem, one should compute also the appropriate core density using their self-consistent wave functions, solutions of the Hartree-Fock problem.

Such a density has been already available for the Ca^{40}-nucleus [4]), but not yet for O^{16} for which the density corresponding to Dąbrowski's function should be a fair assumption, as the density function, after all, is not critically sensitive to the details of the reaction matrix, provided it is a reasonable solution of the core saturation problem.

Since the time when part I was submitted for publication, the new results of Brueckner, Lockett and Rotenberg [4–6]) became available, enabling not only to compute the Ca^{41} doublet splittings, but also providing new information on the spin-orbit part of the K-matrix.

According to these results the even-state K^+_{LS}-matrix of ref. [2]) which was used in sction 2 of I was found to be much smaller than estimated previously and probably negligible [6]). In fact K^+_{LS} was finally assumed to be zero. On the other hand the odd-state K^-_{LS} was found to be large and important. This is consistent with the result of the phase shift approximation of the K_{LS}-matrix (compare section 3 of I). The odd-state K^-_{LS} corresponding to the modified Gammel-Thaler potentials was found to be approximately equal to the regular part of the local potential V^-_{LS} of Gammel-Thaler [7]), i.e.

$$K^+_{LS} \approx 0, \qquad K^-_{LS}(r_{12}) \approx \begin{cases} 0 \text{ for } r_{12} < r_c = 0.5\, f \\ V^-_{LS}(r_{12}) \text{ for } r_{12} > r_c. \end{cases} \tag{1}$$

The latter relationship between the K-matrix and V is consistent with the general qualitative analysis by Moszkowski [8]).

In section 2 we shall present expressions for the spin-orbit splittings in core-plus one-particle nuclei obtained with the use of eq. (1). In section 3 numerical estimates will be presented for the Ca^{41} (Sc^{41}) j-splittings and also for other nuclei. In section 4 the case of spheroidally deformed nuclei is considered.

The case of Ca^{41} is particularly interesting as new experimental results have now become available [9]), contradicting some of the previous data [10–11]).

Recently two interesting papers appeared on the problem of the doublet splittings. Skyrme [12]) presented a discussion of a simplified phase shift approximation of the K_{LS}-matrix for the Gammel-Thaler and Signell-Marshak potentials. This approximation was found not to be consistent with

all the data. Clark [13]) avoided the use of K-matrix by assuming a Jastrow type wave function for the whole nucleus rather than only for the "core". He used the Gammel-Thaler and Signell-Zinn-Marshak potentials in the approximation of the first moment, i.e. the higher derivative terms of the density were neglected. He also neglected all the exchange amplitudes. His numerical results for heavy nuclei seem to be of the right order of magnitude. The isobaric spin dependence of the two-body potentials was considered and also the possible difference between the proton and neutron densities.

2. Calculation of the Doublet Splitting

Let the extra core particle in question be a neutron and let the core contain $A-1 = 2Z$ particles. As the even states K^+_{LS} is zero according to eq. (1) we have only contributions from K^-_{LS} i.e. from the isobaric spin triplet states ($I = 1$). There are contributions from the $\frac{1}{2}(A-1)$ neutrons and one-half of the contributions from the $\frac{1}{2}(A-1)$ protons ($T = 1, T_3 = 0$). First let us write the energy shift corresponding to the non-local $\langle \mathbf{r}_{12}|K|\mathbf{r}'_{12}\rangle_{LS,\,\mathrm{odd}}\,\mathbf{L}\cdot\mathbf{S} = -\langle \mathbf{r}_{12}|K|-\mathbf{r}'_{12}\rangle_{LS,\,\mathrm{odd}}\,\mathbf{L}\cdot\mathbf{S}$ in the notation of ref.[2]) and coming from the neutron-neutron pairs only:

$$(\Delta E)^{\mathrm{n-n}}_{LS} = \tfrac{1}{2}\tfrac{3}{4}\sum_j \int \mathrm{d}(1)\mathrm{d}(2)\mathrm{d}(1')\mathrm{d}(2')\psi_0^*(1)\phi_j^*(2)\langle \mathbf{r}_{12}|K|\mathbf{r}'_{12}\rangle_{LS,\,\mathrm{odd}}\,\mathbf{L}\cdot\mathbf{S} \times[\psi_0(1')\phi_j(2')-\psi_0(2')\phi_j(1')]. \quad (2)$$

The factor $\frac{1}{2}$ in front stands for the fact that only the neutrons 2 are to be taken out of the sum $\sum_j$ over all the core single particle states $\phi_j(2)$, and the factor $\frac{3}{4}$ means that only the triplet spin states are to be taken into account. The extra core particle state $\psi_0(1)$ we shall assume in the following to be the (unperturbed) shell model wave function satisfying the Schrödinger equation with a central spin independent single particle potential. In view of the above-mentioned property of the non-local odd-state K-matrix, eq. (2) may be written in the form

$$(\Delta E)^{\mathrm{n-n}}_{LS} = \tfrac{3}{4}\sum_j \int \mathrm{d}(1)\mathrm{d}(2)\mathrm{d}(1')\mathrm{d}(2')\psi_0^*(1)\phi_j^*(2)\langle \mathbf{r}_{12}|K|\mathbf{r}'_{12}\rangle_{LS} \times\mathbf{L}\cdot\mathbf{S}\psi_0(1')\phi_j(2'). \quad (3)$$

In obtaining eq. (3) use was made also of the fact that 1 and 2 are dummy variables of integration and can be exchanged with $\mathbf{r}'_{12}\to-\mathbf{r}'_{12}$.

The approximation is now used, following the results of Brueckner *et al.*[4-6]),

$$\langle \mathbf{r}_{12}|K|\mathbf{r}_{12}\rangle_{LS,\,\mathrm{odd}} \approx K^-_{LS}(r_{12})\tfrac{1}{2}(1-P^r_{1'2'})\delta(\mathbf{r}_{12}-\mathbf{r}'_{12})\delta(\mathbf{R}_{12}-\mathbf{R}'_{12}) \quad (4)$$

† If there existed $a\langle \mathbf{r}_{12}|K|\mathbf{r}_{12}\rangle_{LS,\,\mathrm{even}}$, it would probably be equal approximately to $K^+_{LS}(r_{12})\tfrac{1}{2}\big(1+P^r_{1'2'}\big)\delta(\mathbf{r}_{12}-\mathbf{r}'_{12})\delta(\mathbf{R}_{12}-\mathbf{R}'_{12})$.

where $\mathbf{R}_{12}$, $\mathbf{R}'_{12}$ are the centre of mass vectors. It follows immediately that we can write

$$(\Delta E)_{LS}^{n-n} \approx \tfrac{1}{2}\tfrac{3}{4}\sum_j \int \mathrm{d}(1)\mathrm{d}(2)\psi_0^*(1)\phi_j^*(2)K_{LS}^-(r_{12})\mathbf{L}\cdot\mathbf{S}[\psi_0(1)\phi_j(2) - \psi_0(2)\phi_j(1)] = (\Delta E)_{\mathrm{d}}^{n-n} + (\Delta E)_{\mathrm{ex}}^{n-n}, \quad (5)$$

the sum of the direct and the exchange terms. It is easy to show that the corresponding energy shift from the neutron-proton pairs $(\Delta E)_{LS}^{n-p}$ is equal to one-half of $(\Delta E)_{LS}^{n-n}$ in the approximation of the neutron density equal to the proton density, $\rho_n(r_2) \approx \rho_p(r_2) \approx \frac{1}{2}\rho(r_2)$, provided the K-matrix of eq. (4) is used. The total energy shift is then

$$(\Delta E)_{LS} = \tfrac{3}{4}\tfrac{3}{4}\sum_j \int \mathrm{d}(1)\mathrm{d}(2)\psi_0^*(1)\phi_j^*(2)K_{LS}^-(r_{12})\mathbf{L}\cdot\mathbf{S}[\psi_0(1)\phi_j(2) - \psi_0(2)\phi_j(1)] = (\Delta E)_{\mathrm{d}} + (\Delta E)_{\mathrm{ex}}. \quad (6)$$

Let us introduce the mixed density function

$$\rho(\mathbf{r}_2, \mathbf{r}_2'') = \rho(\mathbf{R}, \mathbf{r}) \equiv \sum_j \phi_j(2)\phi_j(2'') \quad (7)$$

where $\mathbf{R} = \frac{1}{2}(\mathbf{r}_2 + \mathbf{r}_2'')$, $\mathbf{r} = \mathbf{r}_2 - \mathbf{r}_2''$.

The direct term was calculated in I. The higher derivative terms simplify if $\nabla_{\mathbf{r}}\rho|_{r=0} = 0$ (e.g. ρ corresponding to harmonic oscillator wave functions). Using the result of eq. (15) of I we can write

$$(\Delta E)_{\mathrm{d}} \approx \tfrac{3}{2}\tfrac{\pi}{8}\int \mathrm{d}^3\mathbf{R}\psi_0^*(\mathbf{R})\left[\frac{I_1}{R}\frac{\mathrm{d}\rho(R)}{\mathrm{d}R} + \frac{I_2}{10R}\frac{\mathrm{d}}{\mathrm{d}R}(\nabla^2\rho(R))\right] \times(\boldsymbol{\sigma}_1\cdot\mathbf{L})\psi_0(\mathbf{R}) = \langle V_{LS}^{\mathrm{d}}(R)\boldsymbol{\sigma}_1\cdot\mathbf{L}\rangle \quad (8)$$

where I_1 and I_2 are the moments of $(-K_{LS}^-(r))$, defined as

$$I_1 = -\int_0^\infty K_{LS}^-(s)\times s^4\mathrm{d}s, \qquad I_2 = -\int_0^\infty K_{LS}^-(s)s^6\mathrm{d}s.$$

The term $(\Delta E)_{\mathrm{ex}}$ is more complicated. Using the method of Nigam and Sundaresan [14]) † and of I one can show that

$$(\Delta E)_{\mathrm{ex}} = -(\tfrac{3}{4})^2 4\frac{4\pi}{(2\pi)^6} i\int \mathrm{d}^3\mathbf{k}_1\mathrm{d}^3\mathbf{k}'_1\int \mathrm{d}^3\mathbf{R}\mathrm{d}^3\mathbf{r}\psi_0^*(\mathbf{k}'_1)\mathrm{e}^{i\mathbf{p}\cdot\mathbf{R}} \times \mathrm{e}^{-i(\mathbf{k}_1-\frac{1}{2}\mathbf{p})\cdot\mathbf{r}}(\mathbf{p}\times\boldsymbol{\sigma}_1)\mathbf{r}/r\rho(\mathbf{R},\mathbf{r})F(r)\psi_0(\mathbf{k}_1), \quad (9)$$

$$F(r) = \int_0^\infty k^3\mathrm{d}k j_1(2kr)f_{\mathrm{X}}(2k),$$

$$f_{\mathrm{X}}(u) = \frac{4\pi i}{u}\frac{\mathrm{d}}{\mathrm{d}u}\int_0^\infty r'^2\mathrm{d}r' j_0(ur')K_{LS}^-(r') = \frac{4\pi i}{u}\frac{\mathrm{d}}{\mathrm{d}u}\varphi(u)$$

where $\psi_0(\mathbf{k})$ is the Fourier transform of $\psi_0(\mathbf{R})$ and $\mathbf{p} = \mathbf{k}'_1 - \mathbf{k}_1$. If now $\rho(\mathbf{R}, \mathbf{r})$ does not strongly depend on the direction of $\mathbf{r}$, i.e. $\rho(\mathbf{R}, \mathbf{r}) \approx \rho(\mathbf{R}, r)$, and if we use the approximation of ref. [14]) and of I: $(\mathbf{k}_1 - \frac{1}{2}\mathbf{p})\cdot\mathbf{r} \approx \mathbf{k}_1\cdot\mathbf{r}$, it

† A factor (−4) is missing in eqs. (5), (10) and (11) and in table 1 of this reference, in addition to the mistakes pointed out in I (private communication from Dr. Nigam).

follows from eq. (9) that

$$(\Delta E)_{ex} \approx -(\tfrac{3}{4})^2 4 \frac{(4\pi)^2}{(2\pi)^6} \int d^3\mathbf{k}_1 d^3\mathbf{k}'_1 \int d^3\mathbf{R} \psi_0^*(\mathbf{k}'_1) e^{i\mathbf{p}\cdot\mathbf{R}} \boldsymbol{\sigma}_1 \cdot (\mathbf{k}_1 \times \mathbf{k}'_1) \times \int_0^\infty r^2 dr \rho(\mathbf{R}, r) [j_1(k_1 r)/k_1] F(r) \psi_0(\mathbf{k}_1) \quad (10)$$

which corresponds to eq. (A_1 1) of I. The crudest approximation of appendix 1 of I is obtained when we replace $f_X(2k)$ by $4\pi i(-\frac{1}{3}I_1)$ which implies $F(r) \propto d/dr(\delta(r)/r)$. Provided $\varphi(0) = \varphi(\infty) = 0$, which holds e.g. for $K_{LS}^-(r)$ of Brueckner *et al.*[4-6]), of it can be shown that $F(r) = -\frac{1}{8} i\pi^2 r K_{LS}^-(r)$.

We shall now expand $j_1(k_1 r)$ in its power series and retain the first two terms:

$$j_1(k_1 r)/k_1 \approx \tfrac{1}{3} r(1 - \tfrac{1}{5} k_1^2 r^2). \quad (11)$$

The higher powers would correspond to the higher "derivative terms" of $(\Delta E)_{ex}$. It can be shown that the next term of this series would produce a small contribution to $(\Delta E)_{ex}$.

It follows that

$$L(k_1, \mathbf{R}) = k_1^{-1} \int_0^\infty r^2 dr \rho(\mathbf{R}, \mathbf{r}) j_1(k_1 r) F(r)$$

$$\approx -\tfrac{1}{8} i\pi^2 \tfrac{1}{3} \int_0^\infty r^4 dr (1 - \tfrac{1}{5} k_1^2 r^2) \rho(\mathbf{R}, r) K_{LS}^-(r) \equiv iL_0(\mathbf{R}) + ik_1^2 L_1(R). \quad (12)$$

If now $\rho(\mathbf{R}, r) \equiv \rho(R, r)$, it is easy to show that

$$(\Delta E)_{ex} = (\tfrac{3}{4})^2 4 \frac{(4\pi)^2}{(2\pi)^3} \int d^3\mathbf{R} \psi_0^*(\mathbf{R}) \left[\frac{1}{R} \frac{d}{dR} L_0(R) - \frac{1}{R} \frac{d}{dR} L_1(R) \nabla^2 \right] \times (\boldsymbol{\sigma}_1 \cdot \mathbf{L}) \psi_0(\mathbf{R}). \quad (13)$$

Finally, let us assume that the r-dependence of ρ can be separated off as $\rho(R, r) = \rho(R) f(r)$. It then follows that

$$(\Delta E)_{ex} = \tfrac{3}{2} \tfrac{\pi}{8} \int d^3\mathbf{R} \psi_0^*(\mathbf{R}) \left[\frac{I_1}{R} \frac{d}{dR} \rho(R) + \frac{I_2}{5R} \frac{d}{dR} \rho(R) \nabla^2 \right] \times (\boldsymbol{\sigma}_1 \cdot \mathbf{L}) \psi_0(\mathbf{R}) = \langle V_{LS}^{ex} \boldsymbol{\sigma}_1 \cdot \mathbf{L} \rangle \quad (14)$$

where

$$I_1 = -\int_0^\infty K_{LS}^-(s) f(s) s^4 ds, \qquad I_2 = -\int_0^\infty K_{LS}^-(s) f(s) s^6 ds.$$

3. Numerical Calculations and Discussion

Throughout the numerical calculations $K_{LS}^-(r)$ of eq. (1) was used with $V_{LS}^-(r)$ of Gammel-Thaler [7]) equal to $-V_{LS}^- e^{-\mu r}/\mu r$ for $r > 0.5$ *f*; $V_{LS}^- = 7317.5$ MeV, $\mu = 3.7\ f^{-1}$. Consequently, $I_1 = 55.9\ f^5$ MeV, $I_2 = 91.4\ f^7$ MeV.

A form of $f(r) = e^{-\gamma r^2}$, $\gamma = 4.61/R_0^2$, $R_0 = 1.18\ A^{\frac{1}{3}}$ *f* was used by several

authors [15-14]). This assumption corresponding to Swiatecki's modified Fermi model appropriate to final nuclei is probably not very unrealistic and any more realistic r-dependence of $\rho(R, r)$ should not change $(\Delta E)_{ex}$ critically as only the small values of r are of importance for $L_0(r)$ and $L_1(R)$. With this assumption we find $\bar{I}_1 = 35.9\ f^5$ MeV, $\bar{I}_2 = 39.6\ f^7$ MeV.

Let us first consider the density $\rho(R)$ of the Ca^{40}-nucleus obtained from the self-consistent solutions of the Hartree-Fock equations by Brueckner *et al.*, published in ref. [4]). As it is seen from slide 6, p. 152 of ref. [4]), the neutron and the proton densities differ from each other rather little; consequently we shall neglect this difference.

A reasonable approximation to $\rho(R)$ with the normalization $\int d^3\mathbf{R}\rho(R) = A-1 = 40$ turns out to be of the parabolic form †;

$$\rho(R) \approx \begin{cases} 0.35-0.0211\ R^2 & \text{for} \quad R < 4f \\ 0 & \text{for} \quad R > 4f. \end{cases} \tag{15}$$

With this form of the density the term proportional to I_2 is zero. $\Psi_0(\mathbf{R})$ is assumed to be a harmonic oscillator wave function; the radial functions are

$$\text{state 1f:} \quad R_{13}(R) = N_3 e^{-\frac{1}{2}\nu' R^2} R^3, \qquad N_3^2 = \frac{\sqrt{\nu'}\,\nu'^4\,32}{\sqrt{\pi}7!!} \tag{16a}$$

$$\text{state 2p:} \quad R_{21}(R) = N_{21} e^{-\frac{1}{2}\nu' R^2} R(1-\tfrac{2}{5}\nu' R^2), \qquad N_{21}^2 = \frac{\sqrt{\nu'}\,\nu'\,20}{\sqrt{\pi}3!!}\,. \tag{16b}$$

The value of the parameter $\nu' = 0.2378\ f^{-2}$ was taken from Kurath [17]) and Levinson and Ford [18]).

The doublet splittings are then computed from

$$\Delta_{nl} = -(2l+1)\langle V_{LS}^{d}(R) + V_{LS}^{ex}(R)\rangle. \tag{17}$$

It follows that $\Delta_{1f} \approx 6.5$ MeV and $\Delta_{2p} \approx 2.5$ MeV, their ratio being $\mathscr{R} = \Delta_{1f}/\Delta_{2p} = 2.6$. The exchange term $(\Delta E)_{ex}$ is equal to 48 % of $(\Delta E)_d$ and the term proportional to $\bar{I}_2$ is almost -10 % of Δ_{1f}—a negative contribution. To illustrate the overlap of $|\Psi_0(\mathbf{R})|^2$ and $V_{LS}(R)$ let us mention that, if there were no cut off of $\rho(R)$ at $R = 4f$, we would have $\Delta_{1f} = 14.83$ MeV, $\Delta_{2p} = 6.35$ MeV, $\mathscr{R} = 2.33$.

The quantities Δ_{1f} and Δ_{2p} were recently measured for Sc^{41} by precision scattering of protons from Ca^{40} by Class *et al.*[9]). They were found to be $\Delta_{1f} = 6.4$ MeV, $\Delta_{2p} = 2.2$ MeV ($\mathscr{R} = 2.91$). The latter number 2.2 differs much from $\Delta_{2p} = 0.52$ MeV, earlier in use by Kisslinger [15]) and in ref.[14]), suggested by the experimental results of refs.[10]) and [11]). Nussbaum [19]) gives $\Delta_{2p} \approx 2$ MeV for Ca^{41}.

† However, the RMS radius here is equal about $3f$, whereas the "experimental" value should be about $3.5\ f$ according to Hofstaedter [16]). An advantage of this form of $\rho(R)$ is that the j-doublet splittings are not very sensitive to the form of $\psi_0(\mathbf{R})$.

Another form of $\rho(R)$ was taken from the charge density obtained from high energy electron scattering experiments:

$$\rho(R) = \frac{A\rho_1}{Ze} \Big/ (e^{(R-c)/z_1} - 1) \tag{18}$$

with $\rho_1 = 1.28 \times 10^{19}$ Cb/cm^3, $c = 3.64\, f$, $z_1 = 0.5682\, f$, as given by Hofstaedter [16]). If we disregard the higher derivative terms (i.e. those proportional to I_2 and $\tilde{I}_2$), we obtain in this case $\Delta_{1f} = 4.37$ MeV and $\Delta_{2p} = 1.04$ MeV, the latter number being too small by a factor of about 2.

Finally, the "shell model" harmonic oscillator density of Ca^{40} given in Heisenberg's book [20]) was used:

$$\rho(R) = \frac{4}{(r_0\sqrt{2\pi})^3} \frac{1}{2} \left(5 + \frac{R^4}{r_0^4}\right) e^{-\frac{R^2}{2r_0^2}} \tag{19}$$

with $r_0 = 1.7975\, f$, resulting from $\hbar\omega(Ca^{40}) = 5.84$ MeV. The doublet splittings for this case, computed without the $I_2(\tilde{I}_2)$-terms, are far too large: $\Delta_{1f} = 22.25$ MeV, $\Delta_{2p} = 11.45$ MeV ($\mathscr{R} = 1.94$).

We conclude that with our choice of $\psi_0(\mathbf{R})$ the density $\rho(R)$ of eq. (15) provides the best agreement with the data.

Let us now discuss some of the doublet splittings in the $A = 209$ nuclei. Blin-Stoyle [21]) calculated the j-splittings Δ_{2g}, Δ_{3d} and Δ_{1i} of the 2g, 3d, and 1i levels of the odd neutron in Pb^{209} outside the doubly-closed core of Pb^{208}. He neglected $(\Delta E)_{ex}$ and the higher derivative terms. He used a trapezoidal form of $\rho(R)$, and $\psi_0(\mathbf{R})$ of the same form as that of a particle in a square well of infinite depth. Under these assumptions $I_1 = (\frac{3}{4})^{-1} \times 54.6\, f^5$ MeV, the value of the nuclear radius $R_0 = 1.2\, A^{\frac{1}{3}} f$ and his density parameter $t = 0.2$ are consistent with all the data.

Our $\frac{3}{4}I_1 = \frac{3}{4}55.9\, f^5$ MeV is close to I_1 mentioned above. However, if we include the $\tilde{I}_1$-part of the exchange term, we have to use for comparison $\frac{3}{4}(I_1 + \tilde{I}_1) = 68.88\, f^5$ MeV which is $\frac{3}{4} \times 1.2615$ times the number required by Blin-Stoyle.

If $\rho(R)$ of the form of eq. (18), is used with Hofstaedter's parameters [16]) $\rho_1 = 1.07 \times 10^{19}$ Cb/cm^3, $c = 6.47\, f$ and $z_1 = 0.6136$, and the functions $\psi_0(\mathbf{R})$ are the usual harmonic oscillator wave functions with the parameter $\nu' = 0.1842\, f^{-2}$ taken from True and Ford [22]) (ν' for $A = 207$, 206), we find $\Delta_{2g} = 2.52$ MeV, provided the I_2 and $\tilde{I}_2$ terms are neglected. The experimental $\Delta_{2g} = 2.03$ MeV. However, Δ_{3d} equal 14 MeV disagrees badly with the suggested experimental $\Delta_{3d} = 0.98$ MeV, which seems to show that our choice of $\psi_0(\mathbf{R})$ is quite inconsistent with $\rho(R)$ for this case. The splitting Δ_{2f} of Bi^{209} was also computed and found to be 2 MeV, as compared with Blin-Stoyle's [21]) 0.66 MeV.

The 1d-doublet splitting in O^{17} was calculated in I for several cases with

different assumptions concerning $\rho(R)$ and K_{LS}. If we again disregard the I_2 and $\bar{I}_2$ terms and use Dąbrowski's $\rho(R)$ with $\lambda' = 0.678$ of I and K_{LS}^{-} of eq. (1), we find $\Delta_{1d} = 14.6$ MeV against the experimental 5.08 MeV. Although the higher derivative terms decrease the calculated value, Δ_{1d} is too large anyway, which indicates that the gradient of Dąbrowski's $\rho(R)$ is too steep. Another shortcoming of that perturbation calculation is that $\psi_0(\mathbf{R})$ is assumed to be the harmonic oscillator wave function of the $1d_{\frac{5}{2}}$-ground state, while the $1d_{\frac{3}{2}}$-state is not bound.

Although $K_{LS}^{-}(r)$ of eq. (1) can hardly be expected to be realistic for the He^5-nucleus, it seems interesting to see how much one would have to change the moments $I_1, I_2, \bar{I}_1, \bar{I}_2$ to account for the experimental $1p_{\frac{3}{2}}-1p_{\frac{1}{2}}$ doublet splitting in He^5 equal to $\Delta_{1p} = 2.5$ MeV. It seems reasonable to assume after Feingold [23]) the He^4 ground state wave function to be of the form

$$\phi(1, 2, 3, 4) = \left(\frac{\nu}{\pi}\right)^3 \chi_0^0(\sigma_1\sigma_2)\chi_0^0(\sigma_3, \sigma_4) e^{-\frac{1}{2}\nu \sum_{i=1}^{4} r_i^2} \tag{20}$$

where $\chi_0^0(\sigma_i, \sigma_j)$ is the singlet spin function and $\nu' = 0.36213\, f^{-2}$. The computed mixed density is

$$\rho(R, r) = 4\left(\frac{\nu}{\pi}\right)^{\frac{3}{2}} e^{-\nu R^2} e^{-\frac{1}{4}\nu r^2}. \tag{31}$$

Next, we assume after Hughes and Le Couteur [24]) $\psi_0(\mathbf{R})$ to be a solution of the wave equation with the square well of radius $a = 3f$ corresponding to the zero binding energy of the odd neutron. In fact the energy of the virtual level $1p_{\frac{3}{2}}$ being the ground state of the He^5 nucleus equals only about 90 keV. Consequently, the radial wave function of $\psi_0(\mathbf{R})$ is

$$R_{11}(R) = \begin{cases} \sqrt{\frac{2}{3}}\,\frac{\pi}{a^{\frac{3}{2}}}\, j_1\left(\frac{\pi}{a} R\right) & \text{for} \quad R \leqq a \\ \sqrt{\frac{2a}{3}}\, R^{-2} & \text{for} \quad R > a. \end{cases} \tag{22}$$

The final expression we find for $(\Delta E)_d$ is

$$(\Delta E)_d = \frac{9}{2\sqrt{\pi}} \nu^2 \sqrt{\nu} \left\{ \frac{2\pi^2}{3} \int_0^1 y^2 dy e^{-\nu a^2 y^2} [I_1 - \nu I_2 + \tfrac{2}{5} I_2 \nu^2 a^2 y^2] j_1(\pi y)^2 \right.$$
$$\left. + \tfrac{2}{3} [e^{-\nu a^2}(I_1 - \nu I_2) - \sqrt{\pi}\sqrt{\nu}\, a(1 - \phi(\sqrt{\nu}\, a))(I_1 - \tfrac{6}{5}\nu I_2)\right\} \tag{23}$$

where $\phi(x)$ is the usual probability integral. Similarly the exchange term is found to be

$$(\Delta E)_{ex} = \frac{9}{2\sqrt{\pi}} \nu^2 \sqrt{\nu} \left\{ \frac{2\pi^2}{3} (\bar{I}_1 - \tfrac{1}{5}(\pi/a)^2 \bar{I}_2) \int_0^1 y^2 dy e^{-\nu a^2 y^2} j_1(\pi y)^2 \right.$$
$$\left. + \tfrac{2}{3} \bar{I}_1 [e^{-\nu a^2} - \sqrt{\pi}\sqrt{\nu} a (1 - \phi(\sqrt{\nu} a))] \right\}. \tag{24}$$

The numerical results are $(\Delta E)_{\mathrm{d}} = 0.622$ MeV and $(\Delta E)_{\mathrm{ex}} = 0.419$ MeV, so that $\Delta_{1\mathrm{p}} \approx 1.04$ MeV, which is too little by a factor of about 2.5. The relative contribution of the terms proportional to I_2 in $(\Delta E)_{\mathrm{d}}$ is equal to about $-40\,\%$ of the I_1 terms, and that of the term proportional to $\tilde{I}_2$ in $(\Delta E)_{\mathrm{ex}}$ is less than $-24\,\%$ of the $\tilde{I}_1$ term.

In conclusion we can say that K_{LS}^{-} of eq. (1) corresponding to the Gammel-Thaler potentials produced doublet splittings of the right sign and of the correct order of magnitude. In particular, rather good agreement with the data is obtained for $\Delta_{1\mathrm{f}}$ and $\Delta_{2\mathrm{p}}$ in Ca^{41} if the self-consistent Hartree-Fock density is used. The exchange terms and the lowest order "higher derivative" terms are not negligible in general. The greatest uncertainty in our calculations presents the choice of $\Psi_0(\mathbf{R})$, the extra core nucleon wave function. As soon as the self-consistent Hartree-Fock solutions for $\Psi_0(\mathbf{R})$ become available, realistic values of doublet splittings should be easily obtained.

4. Spin-Orbit Coupling in Spheroidally Deformed Nuclei

In the case of deformed nuclei the single particle orbital angular momentum is not a good quantum number of the intrinsic motion of this particle. In the asymptotic case of no spin-orbit coupling the l-projection on the symmetry axis Λ is a good quantum number (cf. ref. [25])). The single particle wave functions can be written in this case as

$$|N\Lambda\Sigma\rangle = \sum_{l} a_{l\Lambda} |Nl\Lambda\Sigma\rangle \tag{25}$$

where N is the principal quantum number, Σ stands for the spin projection on the symmetry axis and the $a_{l\Lambda}$'s are constant coefficients characteristic of the deformation of a given nucleus. S. G. Nilsson [26]) introduced a spin-orbit coupling $C\,\mathbf{L}\cdot\mathbf{S}$ into the single particle hamiltonian. As a result the $\Lambda\Sigma$-states go over into Ω-states with $\Omega = \Lambda+\Sigma = \Lambda\pm\frac{1}{2}$. It is interesting to attempt a derivation of such an effective spin-orbit potential using K_{LS} and Nilsson intrinsic wave functions for the core particles. In view of the deformed non-spherical shape of the core density we cannot expect to obtain the simple form $V_{LS}(R)\mathbf{L}\cdot\mathbf{S}$ anyway. Let us use Nilsson wave functions for the intrinsic wave functions and let us describe the state of the whole nucleus by the usual

$$\psi_{IMK} = \sqrt{\frac{2I+1}{16\pi^2}}\,[D^{I}_{MK=\Omega}(\theta^i)\psi_{N\Omega}(1')\phi(2',\ldots A') + \text{the symmetrizing part}]. \tag{26}$$

The primed coordinates refer to the body frame of reference, ϕ is the spin-saturated core wave function built of Nilsson wave functions or, approximately, of asymptotic Nilsson wave functions.

It is easy to show that the expressions for the energy shifts $(\Delta E)_{\mathrm{d}}$ and $(\Delta E)_{\mathrm{ex}}$, where $(\Delta E)_{LS} = \langle N\Omega|(\Delta E)_{LS}|N\Omega\rangle$, are of the form of eqs. (8) and (14), respectively, with $\psi_0(\mathbf{R})$ replaced by $|N\Omega; \mathbf{R}'\rangle$ and $(1/R)\mathrm{d}\rho(R/\mathrm{d}R)$ $\mathbf{L}$ replaced by $\nabla_{\mathbf{R}'}\rho(\mathbf{R}')\times(-i\hbar\nabla_{\mathbf{R}'})$, where $\mathbf{R}'$ is the radius vector in the body frame. When realistic and self-consistent densities $\rho(\mathbf{R}')$ of spheroidal nuclei become available, it will be interesting to calculate the form of the operator $(\Delta E)_{LS}$ and test the appropriate approximate Nilsson type model.

The author feels greatly indebted to Professor K. A. Brueckner for his private communication on the K-matrix and to him and to Drs. Gammel and Rotenberg for some further correspondence on this subject. Several stimulating and helpful discussions with Drs. C. Levinson, R. Folk, B. Nigam, T. Skyrme, J. Blair, B. French and H. Mitler are gratefully acknowledged. Thanks are due to Drs. J. Clark and C. Class for providing the author with preprints of their papers.

References

1) J. Sawicki and R. Folk, Nuclear Physics **11** (1959) 368, referred to as I
2) K. A. Brueckner, J. L. Gammel and H. Weitzner, Phys. Rev. **110** (1958) 443
3) J. Dąbrowski, Proc. Phys. Soc. A **71** (1958) 658
4) K. A. Brueckner, Proceedings of the International Conference on the Nuclear Optical Model (Tallahassee 1959) p. 145–160
5) A. M. Lockett III, M. Rotenberg and K. A. Brueckner, Bull. Am. Phys. Soc. **4** (1959) 156
6) K. A. Brueckner, private communication
7) J. L. Gammel and R. M. Thaler, Phys. Rev. **107** (1957) 1337
8) S. A. Moszkowski, Bull. Am. Phys. Soc. **4** (1959) 256; Technical Report No. 2, UCLA (April 1959)
9) C. M. Class, R. H. Davis and J. H. Johnson, Phys. Rev. Letters **3** (1959) 41
10) C. K. Bockelman and W. W. Brueckner, Phys. Rev. **107** (1957) 1366
11) R. D. Bent and T. H. Kruse, Phys. Rev. **109** (1958) 1240
12) T. H. R. Skyrme, Nuclear Physics **9** (1958) 635
13) J. W. Clark, preprint
14) B. P. Nigam and M. K. Sundaresan, Phys. Rev. **111** (1958) 284
15) L. S. Kisslinger, Phys. Rev. **104** (1956) 1077
16) R. Hofstaedter, Revs. Mod. Phys. **28** (1956) 214
17) D. Kurath, Phys. Rev. **91** (1953) 1430
18) C. A. Levinson and K. W. Ford, Phys. Rev. **99** (1955) 792
19) R. H. Nussbaum, Revs. Mod. Phys. **28** (1956) 423
20) W. Heisenberg, Theorie des Atomkerns (Goettingen 1951)
21) R. J. Blin-Stoyle, Phil. Mag. **46** (1955) 973
22) W. W. True, K. W. Ford, Phys. Rev. **109** (1958) 1675
23) A. M. Feingold, Phys. Rev. **101** (1956) 258
24) J. Hughes and K. J. Le Couteur, Proc. Phys. Soc. A **63** (1950) 1219
25) S. A. Moszkowski, Phys. Rev. **99** (1955) 803; Handbuch d. Physik **39** (1957) 411–548
26) S. G. Nilsson, Mat. Fys. Medd. Dan. Vid. Selsk. **29**, No. 16 (1955)

1.D.4 *Nuclear Physics* **13** (1959) 360—381; © *North-Holland Publishing Co., Amsterdam*
Not to be reproduced by photoprint or microfilm without written permission from the publisher

COLLECTIVE VIBRATIONS OF CLOSED-SHELL NUCLEI

J. M. ARAÚJO
Universidade do Porto, Portugal †

Received 2 July 1959

Abstract: Collective vibrations in atomic nuclei are studied, assuming a time-dependent nuclear well potential. The collective frequencies (and the collective parameters B_λ and C_λ) are obtained by imposing the condition of time-independence on the expectation value of the energy. The calculations are carried through without the use of the adiabatic approximation. For some closed-shell nuclei it is found that the lowest vibrational state should not be of the quadrupole type. The life-times of vibrational states are also calculated. The related problem of static deformations of a finite well potential is discussed. Some numerical results for the quadrupole and octupole vibrations in O^{16} and the quadrupole vibration in Si^{28} are given.

1. Introduction

The present knowledge about collective vibrations in atomic nuclei is, both from the theoretical and experimental points of view, still very incomplete ††. Collective rotations have been studied much more extensively and are far better understood. Still, one expects collective vibrations to be a more general type of collective motion, inasmuch as they may occur for both spherical and deformed nuclei. However, the excitation energies for the vibrational modes are, in general, much higher than for the rotational states, and this fact alone implies a less clear separation between the intrinsic and vibrational excitations.

Already a few years ago, it became clear that the hydrodynamical description of the collective motions was perhaps even more inadequate for vibrations than for rotations. The experimental data could, however, be qualitatively understood as exhibiting the effects of the nuclear shell structure and residual interactions [1]). One may hope to be able to make quantitative estimates by examining the model recently studied by Belyaev [5]), who analysed some effects of the pairing correlations on the nuclear collective excitations.

In this paper, we set ourselves the much less far reaching task of trying to explore, somewhat more fully than has hitherto been done [6, 7, 8]), the results

† Now at the Institute for Theoretical Physics, University of Copenhagen.

†† Several reviews of the present situation have recently been published by Alder, Bohr, Huus, Mottelson and Winther [1]) (especially section V); Villars [2]); Moszkowski [3]) (section III F); Tamura [4]).

of a semi-classical model in which the nuclear well potential is allowed to oscillate. We have used a finite square well potential plus spin-orbit coupling and a $\mathbf{l}^2$ term, which plays the role of an interpolation between the square well and the harmonic oscillator potential. It is assumed that, when a deformation (static or dynamical) takes place, only the well boundary changes, the well depth remaining unaffected; this is a much smaller change than the one usually assumed for the harmonic oscillator potential. The nucleon wave functions for such a time-dependent potential are calculated in section 2 and used in section 3 to obtain the expectation value of the energy. Since the deformation parameters are treated as classical observables, the eigenfrequency equation is obtained by requiring that the expectation value of the energy (calculated to second order in the deformation parameters) should be time-independent. The additional energy brought in by the time dependence of the well potential then assumes the same form as in the hydrodynamical picture, and one gets expressions for the collective parameters B_λ and C_λ. No use is made of the adiabatic approximation which one tends to regard with some suspicion when dealing with collective vibrations. But we also give, for the purpose of comparison, the equations corresponding to the adiabatic approximation.

The model bears to the collective vibrations the same relation as the cranking model to collective rotations. One may perhaps say that, after all, treating the collective variables as classical observables should not make such a difference, since the resulting expression for the additional energy is of the usual harmonic oscillator type. Also the potential, seen by one particle, calculated from the wave functions obtained in section 2, turns out to have the same dependence on time as assumed to start with; this may be regarded as a somewhat trivial consistency condition.

In section 4, we calculate the lifetimes of states of collective vibration and, in section 5, we briefly discuss the related problem of small static deformations (of any multipolarity) of a finite square well. Finally, in section 6, some numerical results are presented and discussed.

Collective vibrations of closed-shell nuclei have also been recently studied by Griffin [9]) and by Ferrell and Visscher [10]). The rigidities of closed-shell nuclei against small static quadrupole and octupole deformations have been treated by Marumori, Suekane and Yamamoto [11]), Suekane [12]), and Lane and Pendlebury [13]). The present paper is partly based on previous work by Taylor [14]) and the author [15]).

2. Nucleon Wave Functions

We shall look for solutions of the time-dependent Schrödinger equation

$$H\psi = i\hbar \frac{\partial \psi}{\partial t}, \tag{1}$$

for a Hamiltonian

$$H = \mathbf{p}^2/2M - 2\hbar^{-2}V\gamma\,\mathbf{l}\cdot\mathbf{s} + \hbar^{-2}\sigma\mathbf{l}^2 + V(t), \tag{2}$$

where the time-dependent potential $V(t)$ is defined as

$$V(t) = 0 \quad \text{for} \quad r < R(\theta, \varphi, t); \qquad V(t) = V \quad \text{for} \quad r > R(\theta, \varphi, t). \tag{3}$$

The surface of discontinuity of the potential is given, in the usual way, by

$$R(\theta, \varphi, t) = R_0[1 + \sum_{\lambda\mu} \alpha_{\lambda\mu}(t) Y_{\lambda\mu}(\theta, \varphi)]; \tag{4}$$

the deformation parameters $\alpha_{\lambda\mu}(t)$, assumed to be small ($|\alpha_{\lambda\mu}(t)| \ll 1$), may be written as

$$\alpha_{\lambda\mu}(t) = \sum_n \alpha_{\lambda\mu n} \exp(i\omega_{\lambda\mu n} t). \tag{5}$$

The Hamiltonian (2) contains, besides the kinetic and potential energy terms, a spin-orbit coupling term as well as the term $\hbar^{-2}\sigma\mathbf{l}^2$ which allows a better reproduction of the experimental level spacings.

We shall write our wave functions as

$$\psi^{(i)} = \sum_{jlm} \int d\omega \exp(-i\omega t) g(j, l, m, \omega) j_l(K_{jl\omega} r) \Phi_{jlm}, \tag{6}$$

$$\psi^{(e)} = \sum_{jlm} \int d\omega \exp(-i\omega t) f(j, l, m, \omega) h_l(i\kappa_{jl\omega} r) \Phi_{jlm}, \tag{6'}$$

for $r < R(\theta, \varphi, t)$ and $r > R(\theta, \varphi, t)$ respectively. In eqs. (6) and (6'), Φ_{jlm} denote the usual angular momentum eigenfunctions, j_l and h_l the spherical Bessel and Hankel functions. The coefficients $K_{jl\omega}$ and $\kappa_{jl\omega}$ are given in terms of j, l and ω by the equations

$$\hbar\omega = (\hbar K_{jl\omega})^2/(2M) - \gamma V \alpha(j, l) + \sigma l(l+1) \tag{7}$$

and

$$K_{jl\omega}^2 + \kappa_{jl\omega}^2 = 2MV\hbar^{-2}, \tag{8}$$

where

$$\alpha(j, l) = \begin{cases} +l \\ -(l+1) \end{cases} \quad \text{for} \quad j = \begin{cases} l+\frac{1}{2} \\ l-\frac{1}{2} \end{cases}. \tag{9}$$

We shall take for the coefficients $g(j, l, m, \omega)$ and $f(j, l, m, \omega)$ series expansions in powers of the $\alpha_{\lambda\mu n}$

$$g(j, l, m, \omega) = g\delta_{jlm, j_0 l_0 m_0}\delta(\omega - \omega_0) + g^{(1)}(j, l, m, \omega) + g^{(2)}(j, l, m, \omega) + \ldots, \tag{10}$$

$$f(j, l, m, \omega) = f\delta_{jlm, j_0 l_0 m_0}\delta(\omega - \omega_0) + f^{(1)}(j, l, m, \omega) + f^{(2)}(j, l, m, \omega) + \ldots; \tag{10'}$$

the choice made for the zero order terms corresponds to solutions which go over to an eigenfunction of the energy when the deformation parameters tend to zero †.

† For the sake of simplicity, we shall usually drop indices j_0, l_0, m_0, ω_0 (or n_0), corresponding to the predominant state, in symbols like $\psi^{(i)}$, $g(j, l, m, \omega)$, etc.

The conditions of continuity of the wave function and its gradient on the surface of discontinuity of the potential (eq. (4)) now give in zeroth order (with respect to the $\alpha_{\lambda\mu n}$)

$$g j_{l_0}(x) = f h_{l_0}(y), \tag{11}$$

$$g x j'_{l_0}(x) = f y h'_{l_0}(y), \tag{11'}$$

where we have put

$$x = x_{j_0 l_0 \omega_0}, \qquad x_{jl\omega} = K_{jl\omega} R_0; \qquad y = y_{j_0 l_0 \omega_0}, \qquad y_{jl\omega} = i\kappa_{jl\omega} R_0. \tag{12}$$

The elimination of g and f between (11) and (11') leads to the usual equation

$$x j'_{l_0}(x)/j_{l_0}(x) = y h'_{l_0}(y)/h_{l_0}(y) \tag{13}$$

which, together with

$$x^2 - y^2 = x_{jl\omega}^2 - y_{jl\omega}^2 = 2MVR_0^2\hbar^{-2} = \beta^2, \tag{14}$$

determines the energy levels of a particle in a static, spherical well potential.

The continuity conditions give, in first order,

$$g^{(1)}(j, l, m, \omega) j_l(x_{jl\omega}) = f^{(1)}(j, l, m, \omega) h_l(y_{jl\omega}), \tag{15}$$

$$g^{(1)}(j, l, m, \omega) x_{jl\omega} j'_l(x_{jl\omega}) - f^{(1)}(j, l, m, \omega) y_{jl\omega} h'_l(y_{jl\omega}) = g j_{l_0}(x) \beta^2 \sum_{\lambda\mu n} \alpha_{\lambda\mu n} (j_0 l_0 m_0 | \lambda\mu | jlm) \delta(\omega - \omega_0 + \omega_{\lambda\mu n}). \tag{15'}$$

In the last equation, $(j_0 l_0 m_0 | \lambda\mu | jlm)$ denotes the result of an integration over angular variables and summation over the spin coordinate

$$(j_0 l_0 m_0 | \lambda\mu | jlm) = \int \Phi^*_{jlm} Y_{\lambda\mu}(\theta, \varphi) \Phi_{j_0 l_0 m_0} \mathrm{d}\Omega, \tag{16}$$

and the remaining symbols are explained by eqs. (12) and (14).

From (15) and (15') one gets

$$g^{(1)}(j, l, m, \omega) j_l(x_{jl\omega}) [j, l, \omega]^{-1} = g j_{l_0}(x) \beta^2 \sum_{\lambda\mu n} \alpha_{\lambda\mu n} (j_0 l_0 m_0 | \lambda\mu | jlm) \delta(\omega - \omega_0 + \omega_{\lambda\mu n}), \tag{17}$$

if one puts

$$[j, l, \omega] = (\alpha_{jl\omega} - \beta_{jl\omega})^{-1}. \tag{18}$$

with

$$\alpha_{jl\omega} = x_{jl\omega} j'_l(x_{jl\omega})/j_l(x_{jl\omega}), \qquad \beta_{jl\omega} = y_{jl\omega} h'_l(y_{jl\omega})/h_l(y_{jl\omega}). \tag{19}$$

For $f^{(1)}$ (j, l, m, ω) one gets a similar equation which can be obtained from (17) by changing g into f and interchanging j_l with h_l, $x_{jl\omega}$ with $y_{jl\omega}$ (therefore β^2 is changed into $-\beta^2$).

Finally, the continuity conditions give, in second order,

$$g^{(2)}(j, l, m, \omega) j_l(x_{jl\omega}) - f^{(2)}(j, l, m, \omega) h_l(y_{jl\omega}) = -\tfrac{1}{2} g j_{l_0}(x) \beta^2 \times \sum_{\lambda\mu n \lambda'\mu' n' j' l' m'} \alpha_{\lambda\mu n} \alpha_{\lambda'\mu' n'} (j_0 l_0 m_0 | \lambda\mu | j' l' m') (j' l' m' | \lambda' \mu' | jlm) \delta(\omega - \omega_0 + \omega_{\lambda\mu n} + \omega_{\lambda'\mu' n'}), \tag{20}$$

$$g^{(2)}(j,l,m,\omega)x_{jl\omega}j'_l(x_{jl\omega})-f^{(2)}(j,l,m,\omega)y_{jl\omega}h'_l(y_{jl\omega}) = gj_{l_0}(x)\beta^2$$
$$\times\sum_{\lambda\mu n\lambda'\mu'n'j'l'm'}\alpha_{\lambda\mu n}\alpha_{\lambda'\mu'n'}(j_0l_0m_0|\lambda\mu|j'l'm')(j'l'm'|\lambda'\mu'|jlm)\delta(\omega-\omega_0+\omega_{\lambda\mu n}+\omega_{\lambda'\mu'n'}) \quad (20')$$
$$\times\{1+\tfrac{1}{2}\alpha+\beta^2[j',l',\omega_0-\omega_{\lambda\mu n}]\},$$

where we have put $\alpha = \alpha_{j_0l_0\omega_0} = \beta_{j_0l_0\omega_0}$ (see eqs. (19) and (13)). From (20) and (20′) one gets

$$g^{(2)}(j,l,m,\omega)j_l(x_{jl\omega})[j,l,\omega]^{-1} = gj_{l_0}(x)\beta^2\sum_{\lambda\mu n\lambda'\mu'n'j'l'm'}\alpha_{\lambda\mu n}\alpha_{\lambda'\mu'n'}(j_0l_0m_0|\lambda\mu|j'l'm')$$
$$(j'l'm'|\lambda'\mu'|jlm)\delta(\omega-\omega_0+\omega_{\lambda\mu n}+\omega_{\lambda'\mu'n'})\{1+\tfrac{1}{2}(\alpha+\beta_{jl\omega})+\beta^2[j',l',\omega_0-\omega_{\lambda\mu n}]\}, \quad (21)$$

and a similar result for $f^{(2)}(j,l,m,\omega)$.

The process may be carried as far as one wishes without difficulty. However, we are interested only in the second order approximation and therefore the wave function will be given by equations (6), (6′), (10), (10)′, (17) and (21); the quantities x, y, $x_{jl\omega}$, $y_{jl\omega}$ are given by (7), (12), (13) and (14).

It is sometimes convenient to have $g^{(1)}(j,l,m,\omega)$, $f^{(1)}(j,l,m,\omega)$, etc. expressed in terms of the complex conjugates of the $\alpha_{\lambda\mu n}$. That can be easily done, since $R(\theta,\varphi,t)$ (given by eq. (4)) is real and

$$\int\Phi^*_{jlm}Y^*_{\lambda\mu}(\theta,\varphi)\Phi_{j_0l_0m_0}\mathrm{d}\Omega = (jlm|\lambda\mu|j_0l_0m_0),$$

because the integrals defined in (16) are also real. Instead of (17) one may also write

$$g^{(1)}(j,l,m,\omega)j_l(x_{jl\omega})[j,l,\omega]^{-1}$$
$$= gj_{l_0}(x)\beta^2\sum_{\lambda\mu n}\alpha^*_{\lambda\mu n}(jlm|\lambda\mu|j_0l_0m_0)\delta(\omega-\omega_0-\omega_{\lambda\mu n}); \quad (17')$$

for $g^{(2)}(j,l,m,\omega)$ one has also a similar alternative equation.

The orthogonality of wave functions $\psi_{j_0l_0m_0\omega_0}$, $\psi_{j'_0l'_0m'_0\omega'_0}$ having different predominant states can easily be checked in the used second order approximation.

3. Energy and Collective Parameters B_λ and C_λ

The expectation value of the Hamiltonian (2) corresponding to the wave functions obtained in the previous section may be easily calculated. In order to have the wave functions normalized one must choose g such that

$$-gg^*R_0^3j_{l_0}(x)^2\beta^2(2x^2y^2)^{-1}[\alpha^2+\alpha-l_0(l_0+1)] = 1;$$

f is then determined by (11).

One has then

$$
\begin{aligned}
E_{j_0 l_0 m_0 \omega_0} &= \langle \psi_{j_0 l_0 m_0 \omega_0} | H | \psi_{j_0 l_0 m_0 \omega_0} \rangle \\
&= \hbar\omega_0 + \hbar^2 (2MR_0^2)^{-1} 2x^2 y^2 [\alpha^2 + \alpha - l_0(l_0+1)]^{-1} \\
&\times \{ \sum_{\lambda\mu} \alpha_{\lambda\mu}(t) (j_0 l_0 m_0 | \lambda\mu | j_0 l_0 m_0) + \sum_{\lambda\mu n \lambda'\mu' n' j l m} \alpha_{\lambda\mu n} \alpha_{\lambda'\mu' n'} \exp i(\omega_{\lambda\mu n} + \omega_{\lambda'\mu' n'}) t \\
&\times (j_0 l_0 m_0 | \lambda\mu | j l m)(j l m | \lambda'\mu' | j_0 l_0 m_0) [1 + \alpha + \beta^2 \omega_{\lambda'\mu' n'} (\omega_{\lambda\mu n} + \omega_{\lambda'\mu' n})^{-1} \qquad (22) \\
&\times [j, l, \omega_0 - \omega_{\lambda\mu n}] + \beta^2 \omega_{\lambda\mu n} (\omega_{\lambda\mu n} + \omega_{\lambda'\mu' n'})^{-1} [j, l, \omega_0 + \omega_{\lambda'\mu' n'}]] \},
\end{aligned}
$$

in the used approximation.

If we were to assume self-consistency for the spherical and deformed potential (dynamical or static) and that only two-body forces are important, the expectation value of the nuclear Hamiltonian

$$\mathscr{H} = \sum_i T_i + \sum_{i<j} \sum v_{ij}$$

would simply be

$$\langle \mathscr{H} \rangle = \sum_i \langle H_i \rangle - \tfrac{1}{2} \sum_i \langle V_i \rangle,$$

where $H_i = T_i + V_i$ denotes the single-particle Hamiltonian. The second term of the last equation should therefore be taken into account when calculating the change in the expectation value of the energy resulting from a deformation of the self-consistent field. Still, that term is very often disregarded, even when one knows that the assumption of self-consistency implies that it is rather large; e.g., in the case of the harmonic oscillator potential the term $\frac{1}{2}\langle V_i \rangle$ amounts to one fourth of $\langle H_i \rangle$, the same relation holding also for the changes in those terms †. In our case the subtractive term is not so important, since the main contribution to $\delta\langle H_i \rangle$ comes from $\delta\langle T_i \rangle$; the $\delta\langle V_i \rangle$ corresponds simply to the change with deformation in the probability for the particle to be inside the well whose volume is kept constant. This depends on the well depth (it is obviously zero for an infinitely deep well); for the depths we shall use in our numerical calculations $\delta\langle V_i \rangle$ is of the order of 20 to 30 % of $\delta\langle H_i \rangle$. Therefore, one would have a correction to the results of 10 to 15 % ††. On the other hand, the subtractive term would complicate appreciably all the equations; since its effect is not very big and, in any case, the model is rather schematic, we prefer not to take it into account.

If one is interested in the collective vibrations of closed-shell nuclei, the summation over m_0 greatly simplifies the results; in fact, one has (e.g., Racah [16]))

† However, a detailed calculation of Inglis [6]), assuming two-body forces giving saturation, gave for $\delta\langle \mathscr{H} \rangle$ a result closer to $\Sigma_i \delta\langle H_i \rangle$ than to $\frac{1}{4}\Sigma_i \delta\langle H_i \rangle$; this may be regarded as an indication of the deviation of the model potential from a self-consistent field.

†† These figures correspond to static deformations of O^{16} considered in table 3 of section 6.

$$\sum_{m_0} (j_0 l_0 m_0|\lambda\mu|j_0 l_0 m_0) = \delta_{\lambda 0}\delta_{\mu 0}(2j_0+1)(4\pi)^{-\frac{1}{2}}, \tag{23}$$

$$\sum_{mm_0} (j_0 l_0 m_0|\lambda\mu|jlm)(jlm|\lambda'\mu'|j_0 l_0 m_0)$$
$$= (-1)^{\mu}\delta_{\lambda\lambda'}\delta_{\mu(-\mu')}(4\pi)^{-1}(-1)^{j+j_0+1}(j_0 l_0||c^{\lambda}||jl)(jl||c^{\lambda}||j_0 l_0), \tag{24}$$

where

$$(l\pm\tfrac{1}{2}, l||c^{\lambda}||l'\pm\tfrac{1}{2}, l') = (-1)^{\frac{1}{2}(j'+\lambda-j)}\left[\frac{(j+j'-\lambda)!(j'+\lambda-j)!(j+\lambda-j')!}{(j+j'+\lambda+1)!}\right]^{\frac{1}{2}}$$
$$\times \frac{(j+j'+\lambda+1)!!}{(j+j'-\lambda-1)!!(j'+\lambda-j)!!(j+\lambda-j')!!}, \tag{25}$$

$$(l\pm\tfrac{1}{2}, l||c^{\lambda}||l'\mp\tfrac{1}{2}, l') = (-1)^{\frac{1}{2}(j'+\lambda-j-1)}\left[\frac{(j+j'-\lambda)!(j'+\lambda-j)!(j+\lambda-j')!}{(j+j'+\lambda+1)!}\right]^{\frac{1}{2}}$$
$$\times \frac{(j+j'+\lambda)!!}{(j+j'-\lambda)!!(j'+\lambda-j-1)!!(j+\lambda-j'-1)!!}.$$

We shall consider only deformations without change of volume (of the well potential) and therefore, in the second order approximation, one must have

$$\alpha_{00}(t) = -(4\pi)^{-\frac{1}{2}}\sum_{\lambda\mu}|\alpha_{\lambda\mu}(t)|^2.$$

Putting

$$A(j_0, l_0; \lambda; j, l) = (-1)^{j+j_0+1}(j_0 l_0||c^{\lambda}||jl)(jl||c^{\lambda}||j_0 l_0), \tag{26}$$

one gets, for a closed-shell nucleus,

$$\sum_{j_0 l_0 m_0 \omega_0} E_{j_0 l_0 m_0 \omega_0} = \sum_{j_0 l_0 \omega_0}(2j_0+1)\hbar\omega_0 + \hbar^2(4\pi M R_0^2)^{-1}\sum_{j_0 l_0 \omega_0} x^2_{j_0 l_0 \omega_0} y^2_{j_0 l_0 \omega_0}$$
$$[\alpha^2_{j_0 l_0 \omega_0} + \alpha_{j_0 l_0 \omega_0} - l_0(l_0+1)]^{-1}\sum_{\lambda\mu nn'}\alpha_{\lambda\mu n}\alpha^{*}_{\lambda\mu n'}\exp i(\omega_{\lambda\mu n}-\omega_{\lambda\mu n'})t$$
$$\times\{(2j_0+1)\alpha_{j_0 l_0 \omega_0} + \beta^2\sum_{jl} A(j_0, l_0; \lambda; j, l)(\omega_{\lambda\mu n}-\omega_{\lambda\mu n'})^{-1}$$
$$\times(\omega_{\lambda\mu n}[j, l, \omega_0-\omega_{\lambda\mu n'}] - \omega_{\lambda\mu n'}[j, l, \omega_0-\omega_{\lambda\mu n}])\}, \tag{27}$$

since

$$\sum_{jl} A(j_0, l_0; \lambda; j, l) = 2j_0+1.$$

In general, our result for the energy (eq. (27)) will be a function of time; but it can be time-independent if the frequencies $\omega_{\lambda\mu n}$ are such as to satisfy the condition

$$F_{\lambda}(\omega) = \hbar^2(4\pi M R_0^2)^{-1}\sum_{j_0 l_0 \omega_0} x^2_{j_0 l_0 \omega_0} y^2_{j_0 l_0 \omega_0}[\alpha^2_{j_0 l_0 \omega_0} + \alpha_{j_0 l_0 \omega_0} - l_0(l_0+1)]^{-1}$$
$$\times\{2(2j_0+1)\alpha_{j_0 l_0 \omega_0} + \beta^2\sum_{jl} A(j_0, l_0; \lambda; j, l)([j, l, \omega_0+\omega]+[j, l, \omega_0-\omega])\} = 0, \tag{28}$$

where the symbols are explained by eqs. (12), (14), (18), (19), (25) and (26).

Putting

$$\delta E = \sum_{j_0 l_0 m_0 \omega_0} (E_{j_0 l_0 m_0 \omega_0} - \hbar\omega_0),$$

one can then rewrite eq. (27) as

$$\delta E = \tfrac{1}{2} \sum_{\lambda\mu n} \{C_\lambda(\omega_{\lambda n}) |\alpha_{\lambda\mu n}(t)|^2 + B_\lambda(\omega_{\lambda n}) |\dot{\alpha}_{\lambda\mu n}(t)|^2\}, \tag{29}$$

where $\alpha_{\lambda\mu n}(t)$ denotes the sum of the terms in eq. (5) containing $\exp(i\omega_{\lambda n} t)$ or $\exp(-i\omega_{\lambda n} t)$, $\omega_{\lambda n}$ the roots of the eigenfrequency equation (28), and

$$C_\lambda(\omega) = F_\lambda(\omega) - \tfrac{1}{2}\omega F'_\lambda(\omega), \tag{30}$$

$$B_\lambda(\omega) = -\tfrac{1}{2}\omega^{-1} F'_\lambda(\omega). \tag{31}$$

Of course, the condition $C_\lambda(\omega) = B_\lambda(\omega)\omega^2$ leads again to $F_\lambda(\omega) = 0$ (eq. (28)).

Eqs. (28), (30), (31) determine the energies corresponding to collective vibrations of any multipolarity, as well as the collective parameters C_λ and B_λ. We have not used the adiabatic approximation in deriving our equations; nevertheless we shall compare, in a later section, the results with those corresponding to the adiabatic approximation. Therefore we shall also give the equations for that case.

Since $F_\lambda(\omega)$ is an even function of ω, its series expansion in powers of ω may be written

$$F_\lambda(\omega) = F_\lambda(0) + \frac{\omega^2}{2!} F''_\lambda(0) + \frac{\omega^4}{4!} F^{\mathrm{IV}}_\lambda(0) + \ldots.$$

The adiabatic approximation replaces $F_\lambda(\omega)$ by the first two terms of the series, with the result that one has

$$(C_\lambda)_{\text{adiab.}} = F_\lambda(0) = C_\lambda(0), \tag{30'}$$

$$(B_\lambda)_{\text{adiab.}} = -\tfrac{1}{2} F''_\lambda(0). \tag{31'}$$

In eq. (30'), the quantity $C_\lambda(0)$ denotes the "rigidity" of a closed-shell nucleus against small static deformations of multipolarity 2^λ; its value can be obtained from (28) by making ω go to zero. One gets

$$\begin{aligned} C_\lambda(0) = {} & \hbar^2 (4\pi M R_0^2)^{-1} \sum_{j_0 l_0 \omega_0} x^2_{j_0 l_0 \omega_0} y^2_{j_0 l_0 \omega_0} [\alpha^2_{j_0 l_0 \omega_0} + \alpha_{j_0 l_0 \omega_0} - l_0(l_0+1)]^{-1} \\ & \{2(2j_0+1)\alpha_{j_0 l_0 \omega_0} + \sum_{jl} A(j_0, l_0; \lambda; j, l) \{2\beta^2[j, l, \omega_0] \varepsilon_{jl, j_0 l_0} \\ & + [(2\alpha_{j_0 l_0 \omega_0} + 3)(x^2_{j_0 l_0 \omega_0} + y^2_{j_0 l_0 \omega_0})(\alpha^2_{j_0 l_0 \omega_0} + \alpha_{j_0 l_0 \omega_0} - l_0(l_0+1))^{-1} \\ & + (2\alpha_{j_0 l_0 \omega_0} + 1) x^2_{j_0 l_0 \omega_0} y^2_{j_0 l_0 \omega_0} (\alpha^2_{j_0 l_0 \omega_0} + \alpha_{j_0 l_0 \omega_0} - l_0(l_0+1))^{-2}] \delta_{jl, j_0 l_0}\}\}, \end{aligned} \tag{32}$$

with $\varepsilon_{jl, j_0 l_0} = 1 - \delta_{jl, j_0 l_0}$.

It is possible to set an upper limit for the smallest solution of eq. (28) without any calculations. In fact, $F_\lambda(0) > 0$ and $F_\lambda(\omega) \to -\infty$ when ω

tends to $\hbar^{-1}(E_{jl}-E_{j_0l_0})$, the quantity within brackets being the smallest energy difference between one unoccupied and one occupied level such that the quantity $A(j_0, l_0; \lambda; j, l)$ is different from zero †. The smallest solution of (28) is therefore necessarily smaller than the value of ω quoted above (fig. 1). This upper limit is not always a monotonic function of λ. For instance,

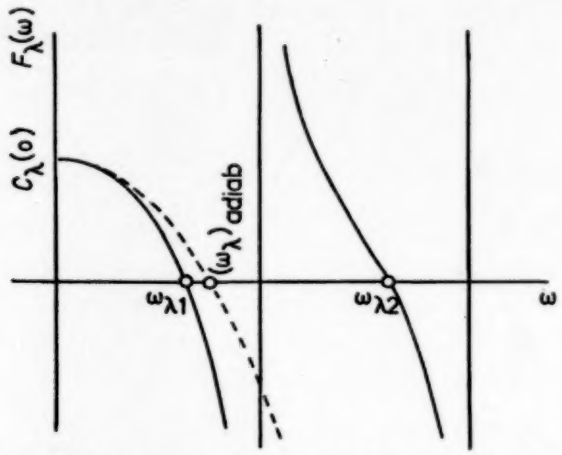

Fig. 1. The figure shows two branches of a function $F_\lambda(\omega)$; $\omega_{\lambda 1}$ and $\omega_{\lambda 2}$ are eigenfrequencies for deformations of order λ. The dashed curve is a parabola corresponding to the adiabatic approximation. Probably only the first eigenfrequency ($\omega_{\lambda 1}$) may have some physical meaning; we only discuss this smallest zero of the functions $F_\lambda(\omega)$.

whenever the last occupied level and the first unoccupied level have opposite parities they may not be connected by a quadrupole deformation. If they are connected, e.g., by an octupole deformation, the upper limit set for the smallest ω_2 is greater than that of ω_3; and one may expect that the same inequality holds for the actual values of ω_2 and ω_3. As we shall see in a later section, this situation does occur for some closed-shell nuclei. However, one has to bear in mind that the above conclusion was reached by considering only terms up to second order in a series expansion. If such a series converges slowly, the approach is inadequate and the conclusion does not hold any longer. That will happen, for instance, if there is a low-lying unoccupied level 'connected', by the deformation considered, to the occupied level immediately below. In such a case it would obviously be wrong to conclude that there would be a very low-lying state of collective vibration.

On the other hand, the fact that the functions $F_\lambda(\omega)$ become infinite when ω takes a value corresponding to an energy difference between two levels (one occupied and the other unoccupied) connected by the deformation of order λ, is clearly associated with the resonance that would then

† We shall say of two such levels that they are 'connected' by the deformation of order λ.

occur. In such cases, some of the quantities $g^{(1)}(j, l, m, \omega)$ (and $f^{(1)}(j, l, m, \omega)$) would become infinite and cause $F_\lambda(\omega)$ to go to infinity. However, the zeros of the functions $F_\lambda(\omega)$ seem to occur (at least for the cases considered in section 6) for values of ω sufficiently far from the conditions of resonance. Then none of the quantities $g^{(1)}(j, l, m, \omega)$ (and $f^{(1)}(j, l, m, \omega)$) becomes unduly large (as compared with g or f), when one takes for the amplitudes $\alpha_{\lambda\mu n}$ the values derived from the collective parameters B_λ and C_λ. In such cases, the present approach seems to remain adequate.

We have just seen that, in spite of the formal analogy between (29) and the liquid drop Hamiltonian, some characteristic differences do remain. Still, the analogy can be carried further; e.g., the expectation value of the angular momentum comes out to be

$$\langle \mathbf{M} \rangle = i \sum_{\lambda n} B_\lambda(\omega_{\lambda n}) \sum_{\mu\mu'} \alpha^*_{\lambda\mu n}(t) \dot{\alpha}_{\lambda\mu' n}(t) [\mathbf{m}_\lambda]_{\mu'\mu},$$

where $B_\lambda(\omega_{\lambda n})$ is given by (31) and $\mathbf{m}_\lambda$ denotes the matrices associated with the representation of an angular momentum $\hbar\lambda$.

It may be interesting to know what becomes of the eigenfrequency eq. (28) when the well depth goes to infinity. Then, $\beta \to \infty$, $y \to i\infty$ and x becomes one zero of a spherical Bessel function. From

$$i^{l+1} y h_l(y) = \exp(iy) \sum_{K=0}^{l} \frac{(l+K)!\, i^K}{(l-K)!\, 2^K K!\, y^K}$$

one gets

$$\alpha = iy - 1 - \frac{i}{2y} l_0(l_0+1) - \frac{1}{2y^2} l_0(l_0+1) + \ldots,$$

$$\beta_{jl\omega} = iy - 1 - \frac{i}{2y} l(l+1) + \frac{i}{2y} (x^2_{jl\omega} - x^2) - \frac{1}{2y^2} l(l+1) + \ldots.$$

It is then easy to see that, when $V \to \infty$, the eigenfrequency equation becomes

$$F_\lambda(\omega) = \hbar^2 (4\pi M R_0^2)^{-1} \sum_{j_0 l_0 \omega_0} x^2_{j_0 l_0 \omega_0} \{4(2j_0+1) + \sum_{jl} A(j_0, l_0; \lambda; j, l) \times [\alpha_{jl\omega_0+\omega} + \alpha_{jl\omega_0-\omega}]\} = 0. \quad (28')$$

In a similar way, the quantity $C_\lambda(0)$ given in eq. (32) now becomes

$$C_\lambda(0) = \hbar^2 (4\pi M R_0^2)^{-1} \sum_{j_0 l_0 \omega_0} x^2_{j_0 l_0 \omega_0} \{4(2j_0+1) + \sum_{jl} A(j_0, l_0; \lambda; j, l) \times [\delta_{jl, j_0 l_0} + 2\alpha_{jl\omega_0} \varepsilon_{jl, j_0 l_0}]\}. \quad (32')$$

If we further make γ and σ go to zero, we get eqs. (39) and (44) of ref. [7]).

4. Lifetimes

Since we have been treating the deformation parameters as classical observables, the charge density for a state of collective vibration appears as a sum of a time-independent term and time-dependent terms of orders one, two, etc, with respect to the deformation parameter

$$\rho(\mathbf{r}, t) = \rho^{(0)}(r)+\rho^{(1)}(\mathbf{r}, t)+\rho^{(2)}(\mathbf{r}, t)+ \ldots .$$

The first-order term is simply

$$\rho^{(1)}(\mathbf{r}, t) = \rho_1{}^{(1)}(\mathbf{r}, t)H(R_0-r)+\rho_e{}^{(1)}(\mathbf{r}, t)H(r-R_0),$$

where $H(x)$ is Heaviside's function and $\rho_1{}^{(1)}$, $\rho_e{}^{(1)}$ denote the first-order terms of the charge density corresponding to the wave functions (6) and (6′). From this, one can get the reduced transition probability for an electric multipole transition from a state of collective vibration to the ground state. It comes out as

$$B(\mathrm{E}\lambda) = \{(2\pi)^{-1}eR_0{}^{\lambda}\sum_{j_0 l_0 \omega_0} x^2y^2[\alpha^2+\alpha-l_0(l_0+1)]^{-1}\sum_{jl} A(j_0, l_0; \lambda; j, l) \tag{33}$$
$$\times [C(j_0, l_0, \omega_0; \lambda; j, l, \omega_0+\omega_\lambda)+C(j_0, l_0, \omega_0; \lambda; j, l, \omega_0-\omega_\lambda)]\}^2 \cdot \tfrac{1}{2}\hbar/(B_\lambda C_\lambda)^{\frac{1}{2}},$$

where the A's are given by eqs. (26) and (25) and the C's are connected with integrals of the type

$$J_n(l, a; m, b) = \int_0^{R_0} z^n j_l(az) j_m(bz)\mathrm{d}z,$$

and similar integrals involving spherical Hankel functions

$$H_n(l, a; m, b) = \int_{R_0}^{\infty} z^n h_l(az) h_m(bz)\mathrm{d}z,$$

in the following way

$$R_0{}^{\lambda+3}C(j_0, l_0, \omega_0; \lambda; j, l, \omega) = J_{\lambda+2}(l_0, K_{j_0 l_0 \omega_0}; l, K_{jl\omega})[j_{l_0}(x)j_l(x_{jl\omega})(\alpha_{jl\omega}-\beta_{jl\omega})]^{-1}$$
$$+H_{\lambda+2}(l_0, i\kappa_{j_0 l_0 \omega_0}; l, i\kappa_{jl\omega})[h_{l_0}(y)h_l(y_{jl\omega})(\alpha_{jl\omega}-\beta_{jl\omega})]^{-1}.$$

We are mainly interested in the lifetimes of excited states corresponding to quadrupole or octupole vibrations. One needs then to calculate the above integrals for $n = 4$ and $m = l+2$, l, $l-2$ and for $n = 5$ and $m = l+3$, $l+1$, $l-1$, $l-3$. It can be shown that all such integrals may be reduced to $J_4(l, a; l, b)$; and this may be calculated by a method due to Sonine [17]). One gets

$$J_4(l, a; l, b) = 2z(a^2-b^2)^{-2}[(a^2+b^2)z^2-2l(l+1)]j_l(az)j_l(bz)$$
$$+az^2(a^2-b^2)^{-3}[-(a^2-b^2)^2z^2+2(3a^2+b^2)]j'_l(az)j_l(bz)$$
$$+bz^2(a^2-b^2)^{-3}[(a^2-b^2)^2z^2-2(3b^2+a^2)]j_l(az)j'_l(bz)$$
$$+4abz^3(a^2-b^2)^{-2}j'_l(az)j'_l(bz).$$

The expressions of the C's are rather long; they are given in the appendix for $\lambda = 2$ and $\lambda = 3$.

5. Static Deformations

The determination of the energy levels and wave functions of a particle in a slightly distorted square well potential may be easily carried out. The method we shall outline is again based on a series expansion and therefore applicable only to small deformations; but otherwise the deformation is arbitrary i.e., it may be of any multipolarity. However, we shall consider only deformations preserving axial symmetry, that is, we shall put

$$R(\theta) = R_0 + R_0 \sum_{\lambda} \alpha_\lambda Y_{\lambda 0}(\theta).$$

The single-particle Hamiltonian will be again the one given in (2), but the potential will now be a function $V(r, \theta)$ of two spatial coordinates alone. For the wave functions we shall have now

$$\psi^{(1)} = \sum_{jlm} g(j, l, m) j_l(K_{jl} r) \Phi_{jlm}, \tag{34}$$

$$\psi^{(e)} = \sum_{jlm} f(j, l, m) h_l(i\kappa_{jl} r) \Phi_{jlm}, \tag{34'}$$

with

$$K_{jl}^2 + \kappa_{jl}^2 = 2MV\hbar^{-2}, \tag{35}$$

for any j and l.

For $g(j, l, m)$ and $f(j, l, m)$ we shall have expansions similar to (10) and (10'). But the wave function (34), (34') will be an energy eigenfunction only if the quantities K_{jl} are such that the expression

$$E = (\hbar K_{jl})^2/(2M) - \gamma V \alpha(j, l) + \sigma l(l+1), \tag{36}$$

where $\alpha(j, l)$ is given by (9), is independent of j and l. If so, eq. (36) gives the corresponding energy eigenvalue.

Now, if we expand K_{jl} and κ_{jl} in series of powers of the α_λ's,

$$K_{jl} = K_{jl}^{(0)} + K_{jl}^{(1)} + K_{jl}^{(2)} + \ldots,$$
$$\kappa_{jl} = \kappa_{jl}^{(0)} + \kappa_{jl}^{(1)} + \kappa_{jl}^{(2)} + \ldots,$$

the condition (35) leads to

$$K_{jl}^{(0)2} + \kappa_{jl}^{(0)2} = 2MV\hbar^{-2},$$
$$K_{jl}^{(0)} K_{jl}^{(1)} + \kappa_{jl}^{(0)} \kappa_{jl}^{(1)} = 0,$$
$$2(K_{jl}^{(0)} K_{jl}^{(2)} + \kappa_{jl}^{(0)} \kappa_{jl}^{(2)}) + (K_{jl}^{(1)2} + \kappa_{jl}^{(1)2}) = 0,$$

etc., which must be satisfied for any j and l.

On the other hand, the energy eigenvalue also takes the form of a series

$$E = (\hbar K_{jl}^{(0)})^2/(2M) - \gamma V \alpha(j, l) + \sigma l(l+1) + \hbar^2/2M \cdot 2K_{jl}^{(0)} K_{jl}^{(1)} + \hbar^2/(2M) \cdot (2K_{jl}^{(0)} K_{jl}^{(2)} + K_{jl}^{(1)2}) + \ldots, \tag{36'}$$

where again the terms of orders zero, one, two, etc. must have the same values whatever the values of j and l.

The conditions of continuity of the wave function and its gradient on the boundary of the well potential now lead to equations which determine $g^{(1)}(j, l, m), f^{(1)}(j, l, m), g^{(2)}(j, l, m), f^{(2)}(j, l, m)$, etc., for $(j, l, m) \neq (j_0, l_0, m_0)$, that is, for angular momentum quantum numbers different from those of the predominant state. One gets

$$g^{(1)}(j, l, m) j_l(x_{jl})[\alpha_{jl}-\beta_{jl}] = g j_{l_0}(x)\beta^2 \sum_{\lambda} \alpha_\lambda (j_0 l_0 m_0|\lambda|jlm), \tag{37}$$

$$\begin{aligned} g^{(2)}(j, l, m) j_l(x_{jl})[\alpha_{jl}-\beta_{jl}] &= g j_{l_0}(x)\beta^2 \sum_{\lambda\lambda' j' l' m'} \alpha_\lambda \alpha_{\lambda'} (j_0 l_0 m_0|\lambda|j' l' m') \\ &\times (j' l' m'|\lambda'|jlm)\{\tfrac{1}{2}(\alpha+\beta_{jl}+2)+\beta^2[\alpha_{j'l'}-\beta_{j'l'}]^{-1}\varepsilon_{j'l'm', j_0 l_0 m_0} \\ &+x^2y^2[\alpha^2+\alpha-l_0(l_0+1)]^{-1}\{\tfrac{1}{2}(2\alpha+3)x^{-2}y^{-2}(x^2+y^2)+\tfrac{1}{2}(2\alpha+1) \\ &\times[\alpha^2+\alpha-l_0(l_0+1)]^{-1}+[\alpha_{jl}-\beta_{jl}]^{-1}[l(l+1)\beta^2 x_{jl}^{-2}y_{jl}^{-2}+(1+\beta_{jl}) \\ &\times(x_{jl}^{-2}\alpha_{jl}-y_{jl}^{-2}\beta_{jl})]\}\delta_{j'l'm', j_0 l_0 m_0}\}, \end{aligned} \tag{38}$$

and similar equations for $f^{(1)}(j, l, m)$ and $f^{(2)}(j, l, m)$.

In eqs. (37) and (38) we have put, similarly to what had been done in section 2,

$$x_{jl} = K_{jl}^{(0)} R_0, \qquad y_{jl} = i\kappa_{jl}^{(0)} R_0, \qquad x = x_{j_0 l_0}, \qquad y = y_{j_0 l_0}, \qquad \beta^2 = x_{jl}^2 - y_{jl}^2,$$
$$\alpha_{jl} = x_{jl} j'_l(x_{jl})/j_l(x_{jl}), \qquad \beta_{jl} = y_{jl} h'_l(y_{jl})/h_l(y_{jl}),$$

while $\varepsilon_{jlm, j_0 l_0 m_0} = 1-\delta_{jlm, j_0 l_0 m_0}$ and $(jlm|\lambda|j' l' m') = (jlm|\lambda 0|j' l' m')$ (compare with eq. (16)).

But, for $j = j_0$, $l = l_0$, $m = m_0$, the continuity conditions, both in first and second order, lead to two equations which are not independent. One cannot then determine $g^{(1)}(j_0, l_0, m_0), f^{(1)}(j_0, l_0, m_0)$, etc.; but the compatibility of the pairs of equations fixes the first and second order terms of the energy eigenvalue. One gets

$$2K_{jl}^{(0)} K_{jl}^{(1)} = 2R_0^{-2}x^2y^2[\alpha^2+\alpha-l_0(l_0+1)]^{-1} \sum_{\lambda} \alpha_\lambda (j_0 l_0 m_0|\lambda|j_0 l_0 m_0), \tag{39}$$

$$\begin{aligned} 2K_{jl}^{(0)} K_{jl}^{(2)} + K_{jl}^{(1)2} &= R_0^{-2}x^2y^2[\alpha^2+\alpha-l_0(l_0+1)]^{-1} \sum_{\lambda\lambda' jlm} \alpha_\lambda \alpha_{\lambda'} (j_0 l_0 m_0|\lambda|jlm) \\ &(jlm|\lambda'|j_0 l_0 m_0)\{2(\alpha+1)+[(2\alpha+3)(x^2+y^2)(\alpha^2+\alpha-l_0(l_0+1))^{-1} \\ &+(2\alpha+1)x^2y^2(\alpha^2+\alpha-l_0(l_0+1))^{-2}]\delta_{jlm, j_0 l_0 m_0}+2\beta^2[\alpha_{jl}-\beta_{jl}]^{-1}\varepsilon_{jlm, j_0 l_0 m_0}\}. \end{aligned} \tag{40}$$

The determination of $g^{(1)}(j_0, l_0, m_0), f^{(1)}(j_0, l_0, m_0)$, etc. can be achieved by means of the normalization condition; besides giving g (and f), it leads to

$$\begin{aligned} g^{(1)}(j_0, l_0, m_0) &= \tfrac{1}{2}g[\alpha^2+\alpha-l_0(l_0+1)]^{-1}\{2\alpha x^2+3(x^2+y^2) \\ &+(2\alpha+1)x^2y^2[\alpha^2+\alpha-l_0(l_0+1)]^{-1}\} \sum_{\lambda} \alpha_\lambda (j_0 l_0 m_0|\lambda|j_0 l_0 m_0), \end{aligned}$$

as well as to equations for $f^{(1)}(j_0, l_0, m_0)$, $g^{(2)}(j_0, l_0, m_0)$, $f^{(2)}(j_0, l_0, m_0)$.

From (36'), (39), and (40) one can obtain the 'rigidity' against deformations of any order λ. The value thus obtained for $C_\lambda(0)$ coincides, as it should, with eq. (32), obtained as a limiting case of the dynamical problem. From the value of $C_\lambda(0)$ one may obtain a corresponding 'surface tension' $S_\lambda(0)$. Of course there is, in the adopted model, no sharp nuclear boundary. Still, if we consider as 'nuclear surface' in the undeformed state a spherical surface of some radius R (e.g., the root-mean-square radius), the change in area for a volume preserving deformation of order λ will be, to second order,

$$\delta_\lambda S = \tfrac{1}{2} R^2(\lambda-1)(\lambda+2)\alpha_\lambda{}^2$$

if the deformation of the "nuclear surface" is defined by the same parameters as the deformation of the well potential boundary. Putting $R = rA^{\frac{1}{3}}$, one has

$$4\pi r^2 S_\lambda(0) = 4\pi[(\lambda-1)(\lambda+2)A^{\frac{2}{3}}]^{-1} C_\lambda(0), \tag{41}$$

to be compared with the value 15.4 MeV accepted in the hydro-dynamical model for any nucleus and any type of deformation.

The wave functions obtained in this section may be used to calculate the intrinsic quadrupole moment associated with a small deformation of a closed-shell structure. For a wave function having a given predominant state (j_0, l_0, m_0, n_0), one gets

$$Q_{j_0 l_0 m_0 n_0} = Q^{(0)} + Q^{(1)} + \ldots,$$

with

$$Q^{(0)} = 4(\pi/5)^{\frac{1}{2}}(j_0 l_0 m_0 | 2 | j_0 l_0 m_0)\langle r^2\rangle,$$

$$Q^{(1)} = -4(\pi/5)^{\frac{1}{2}} \cdot 4R_0{}^2 x^2 y^2[\alpha^2+\alpha-l_0(l_0+1)]^{-1} \sum_{\lambda j l} \alpha_\lambda (j_0 l_0 m_0 | 2 | j l m_0)$$

$$(j l m_0 | \lambda | j_0 l_0 m_0) C(j_0, l_0; 2; j, l),$$

where the coefficients $C(j_0, l_0; 2; j, l)$ are substantially the same as those of the previous section †.

For a closed-shell structure, one gets simply

$$Q = -(5\pi)^{-\frac{1}{2}} \alpha_2 \sum_{j_0 l_0 n_0} 4R_0{}^2 x^2 y^2[\alpha^2+\alpha-l_0(l_0+1)]^{-1} \times \sum_{j l} A(j_0, l_0; 2; j, l) C(j_0, l_0; 2; j, l), \tag{42}$$

to first order in the α_λ's. This result will have to be compared with

$$Q = 3(5\pi)^{-\frac{1}{2}} Z R^2 \alpha_2,$$

corresponding to the usually assumed uniform charge distribution inside a sphere of radius R.

† The only significant difference occurs for $l = l_0$ and $j = j_0$ (see appendix).

6. Some Numerical Results. Discussion

We have made numerical calculations for only two light closed-shell nuclei, O^{16} and Si^{28}. The latter is a 'normal' nucleus in the sense that we expect its lowest collective vibration to be of the quadrupole type. But for O^{16} we expect, on the contrary, the lowest vibrational state to be of the octupole type, since the last occupied and first unoccupied levels are 'connected' by an octupole deformation, but not by a quadrupole deformation.

6.1. O^{16}

The parameters of the model are the well depth V and radius R_0, the spin-orbit coupling constant γ and the constant σ (eq. (2)). For O^{16} we took $\sigma = 0$ and $\gamma V = 1$ MeV; this value of γ corresponds to a $d_{\frac{3}{2}}-d_{\frac{5}{2}}$ splitting of 5 MeV. For the well depth and radius ($R_0 = r_0 A^{\frac{1}{3}}$) we used different sets of values given in the first two columns of table 1. In the third column of the table are the radius parameters $r = R_{eq.} A^{-\frac{1}{3}}$ corresponding to the equivalent uniform distribution †, in column four the energy differences between the first unoccupied and last occupied levels and in the last column the energy of the last occupied level counted from the top of the well potential.

TABLE 1

Different sets of values of parameters used for O^{16}

	V (MeV)	r_0 (10^{-13} cm)	r (10^{-13} cm)	$1d_{\frac{5}{2}}-1p_{\frac{1}{2}}$ (MeV)	$V-1p_{\frac{1}{2}}$ (MeV)
I	45	1.44	1.38	9.1	21.1
II	35	1.44	1.45	8.2	12.3
III	41	1.32	1.33	10.4	14.4

We have not tried to choose the best possible values of V and r_0, taking as a criterion the corresponding values for r and $V-1p_{\frac{1}{2}}$. Still, one may remark that the values of r for cases I and III are reasonable, while that of II is much too large. In fact, the electron scattering experiments [18]) gave for O^{16} a root mean square radius of 2.64×10^{-13} cm, corresponding to $r = 1.35\times10^{-13}$ cm. Also, the charge distribution for cases I and III, given in fig. 2, is quite similar to the distribution which was used to fit the electron scattering results [18]).

In table 2 we give the energy $\hbar\omega_3$ of the octupole vibration and the collective parameters C_3 and B_3 and compare them with the hydrodynamical values for the same root-mean-square radius. In both cases the effect of the Coulomb forces has been neglected.

† The root-mean-square radius can be easily calculated by means of a formula due to Schafheitlin [17]).

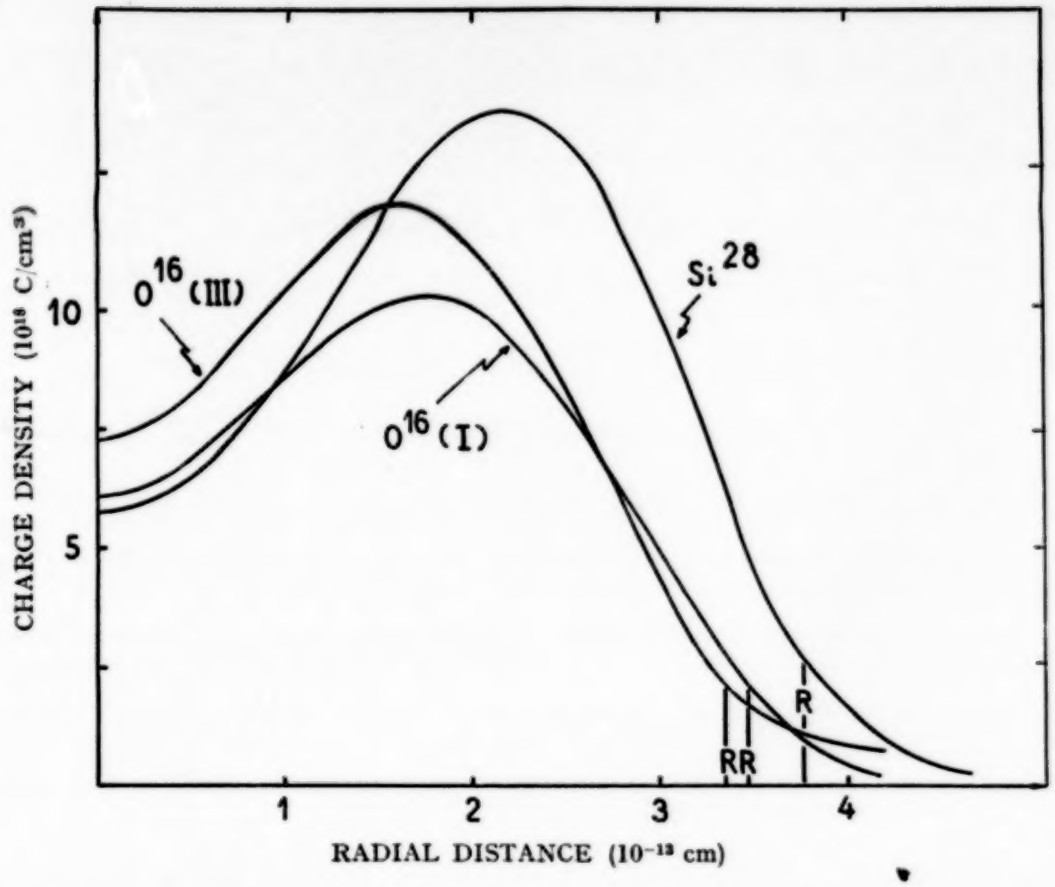

Fig. 2. The charge distributions in O^{16} (cases I and III of table 1) and Si^{28} corresponding to the used wave functions. The symbol R denotes radius of the equivalent uniform distribution.

TABLE 2

The octupole vibration of O^{16}

	$\hbar\omega_3$ (MeV)	C_3 (MeV)	B_3 (10^{-44} MeV · sec^2)	$(\hbar\omega_3)_{\text{hydr.}}$ (MeV)	$C_3/C_{3\text{hydr.}}$	$B_3/B_{3\text{hydr.}}$
I	6.29	105.4	115.3	14.5	1.35	7.17
II	5.34	77.4	117.8	13.8	0.99	6.66
III	6.88	96.8	88.6	15.0	1.24	5.91

We have also studied the quadrupole vibration for case I. We got $\hbar\omega_2 = 17.6$ MeV, $C_2 = 220.5$ MeV, $B_2 = 30.9 \times 10^{-44}$ MeV · sec^2; comparing with the hydrodynamical estimates, one has $C_2 = 7.09\ (C_2)_{\text{hydr.}}$, $B_2 = 1.28\ (B_2)_{\text{hydr.}}$. The value of ω_2 is of the same order of magnitude as the frequencies of nucleon radial motion: $\omega_2 = 0.74\omega_{1s} = 0.48\ \omega_{1p}$. But the frequency of the octupole vibration is already several times smaller; e.g., for case I one has $\omega_3 = 0.27\ \omega_{1s} = 0.17\ \omega_{1p}$.

In table 3, we give the rigidities $C_2(0)$ and $C_3(0)$ against small static deformations of the quadrupole and octupole types and compare the corre-

sponding 'surface tensions' with the value $4\pi r^2 S = 15.4$ MeV, assumed in the hydrodynamical model for any type of deformation.

TABLE 3

Quadrupole and octupole static deformations of O^{16}

	$C_2(0)$ (MeV)	$4\pi r^2 S_2(0)/15.4$	$C_3(0)$ (MeV)	$4\pi r^2 S_3(0)/15.4$
I	115.9	3.72	64.1	0.82
III	114.4	3.67	59.8	0.77

As expected, we found that O^{16} is a very rigid nucleus against quadrupole deformations, but not so against octupole deformations. We also found $\omega_3 < \omega_2$. The energy $\hbar\omega_3$ is less than half the hydrodynamical value, C_3 of the same order of magnitude as $(C_3)_{\text{hydr.}}$, while B_3 is 6 to 7 times larger than $(B_3)_{\text{hydr.}}$. Since, according to the considerations of section 3, the energy difference $1d_{\frac{5}{2}} - 1p_{\frac{1}{2}}$ sets an upper limit for ω_3, it is reasonable that ω_3 should be an increasing function of $1d_{\frac{5}{2}} - 1p_{\frac{1}{2}}$. One can also understand the variation of B_3 with that energy difference: if $1d_{\frac{5}{2}} - 1p_{\frac{1}{2}}$ increases, ω_3 also increases, while $F'_3(\omega_3)$ decreases (see fig. 1); with the result that B_3 will decrease (eq. (31)) †. On the other hand the energy $\hbar\omega_2$ which we obtained is more than twice the hydrodynamical value, owing not to a decrease in the value of B_2, but to a considerable increase in the value of C_2.

Griffin [9]) has recently studied the monopole and quadrupole vibrations of O^{16} using the 'generating coordinate method'. In both cases he got an energy of about 15 MeV (see however tables 2 and 3 of ref.[9])). For the 2+ state, Griffin obtained $B_2 \approx (B_2)_{\text{hydr.}}$, but a value for C_2 much larger than $(C_2)_{\text{hydr.}}$. Our results for the quadrupole vibration agree fairly well with those of Griffin. However, as Griffin remarked, since ω_0 and ω_2 are of the same order of magnitude as the frequencies of nucleon motion, such collective monopole or quadrupole excitations should not occur in O^{16}, at least in a pure form. But, for the octupole vibration, ω_3 is only about one sixth of the characteristic frequency for the 1p nucleons (whose probability of presence near the 'nuclear surface' is much larger than for the s nucleons). Therefore, it is perhaps not certain that such a state of octupole vibration should not exist. Still, one may remark that even for the 3− state the adiabatic approximation would be inadequate; eqs. (30′) and (31′) give, for the set of parameters denoted by I,

$$(\hbar\omega_3)_{\text{adiab.}} = 7.95 \text{ MeV}; \qquad (C_3)_{\text{adiab.}} = 64.1 \text{ MeV};$$
$$(B_3)_{\text{adiab.}} = 43.8 \times 10^{-44} \text{ MeV} \cdot \text{sec}^2.$$

† The same effect occurs if, using the adiabatic approximation, one calculates B by means of a cranking formula.

Comparing with the results of the first line of table 2 one has

$$\omega_3 = 0.79(\omega_3)_{\text{adiab.}}; \qquad C_3 = 1.65(C_3)_{\text{adiab.}}; \qquad B_3 = 2.63(B_3)_{\text{adiab.}}.$$

The adiabatic approximation thus leads to a higher value for ω_3 and smaller values for C_3 and B_3. The most seriously affected quantity is the mass parameter B_3: the value obtained in the adiabatic approximation is only about 40 % of the value calculated without that approximation.

The second excited state of O^{16} is a 3− state, at 6.14 MeV, with a mean life of $(1.2\pm 0.6)\times 10^{-11}$ sec (Kohler and Hilton[19]). The shell-model lifetime is some 10 times larger and, in order to get a value of the right order of magnitude, Elliott and Flowers [20]) had to introduce a semi-empirical nucleon effective charge. The α-particle model, after adjustment of the parameters to give the right excitation energy, leads to a lifetime of 3.2×10^{-11} sec (Kameny [21])). Since we got, for the energy of the octupole vibration of O^{16}, a value of the same order of magnitude as the experimental excitation energy of the 3− state, we also calculated the lifetime. For the set of parameters denoted by III we got a reduced transition probability (eq. (33)) $B(E3) = 27.6\times 10^{-90}$ MeV · cm^7 and, using the experimental energy of 6.14 MeV, a lifetime of 2.8×10^{-11} sec. Apparently, the experimental lifetime cannot be explained without introducing correlations in the ground-state wave function [19]). Still, one might perhaps say that, even without playing around with the values of the parameters, the energy and lifetime of the octupole vibration of O^{16} correspond reasonably well with the properties of the 3− state.

The possibility of such an identification was contemplated before by Wilkinson [22]), but discarded, because it was believed, at the time, that the energy of the quadrupole vibration in O^{16} was 14.7 MeV and that the energy of collective vibrations was always an increasing function of the spin. But, as we saw, O^{16} is just an exception to such a rule, if this nucleus has states of collective vibration at all.

We have also calculated the intrinsic quadrupole moment associated with a small quadrupole deformation of the O^{16} shells; for the well depth and radius denoted by I we got

$$Q = 0.596\times 3(5\pi)^{-\frac{1}{2}} \cdot 8R^2\alpha_2,$$

that is only about 60 % of the value corresponding to a uniform charge distribution with the same root-mean-square radius. The experimental quadrupole moment of O^{17}(−0.026b), although much larger than the single-particle value (−0.0013b), is a good deal smaller than the value obtained in the hydrodynamical version of the unified model (−0.16b). Horie and Arima[23]) and Amado [24]) have obtained values of the right order of magnitude by taking into account configuration mixing. Marumori, Suekane and Yamamoto [11]) have also studied the problem of static deformations of a

square well potential which we considered in section 5. They used the values of $C_2(0)$ obtained to calculate quadrupole moments of nuclei with closed shells plus a nucleon or hole; for O^{17} they got -0.031b, a value very close to the new experimental value. However, their calculations would have to be revised, since the hydrodynamical estimate of the mass parameters, which they have used, is known to be, in general, inadequate. Besides, the assumption of uniform charged distribution may, in some cases, be a poor approximation. Still, apart from those points, we believe that their approximation of replacing the finite well of depth V and radius R_0 by an infinite well of radius $R'_0 = R_0+\lambda_0$, with $\lambda_0 = (\hbar^2/2MV)^{\frac{1}{2}}$ is not legitimate. In fact, we have solved, in section 5, the problem of small deformations of a finite square well. The rigidity $C_2(0)$ is given by eq. (32) for the case of a finite well and by eq. (32′) for an infinitely deep well. Eq. (32′) is actually equivalent to the equations given in the paper of Marumori *et al.*[11]); and for case I it leads, after replacing R_0 by R'_0, to a value (222.2 MeV) which is about twice the value calculated for the finite well (115.9 MeV). Of course, this remark does not invalidate qualitatively the fluctuations of $C_2(0)$ obtained by Marumori *et al.* (see also ref. [7])); it only shows that their numerical values are not very reliable.

Recently Suekane [12]) and Lane and Pendlebury [13]) calculated the rigidities against octupole deformations of closed-shell nuclei. They also got, for O^{16}, $C_3(0) < C_2(0)$. Still, their work appears open to the same criticism as that of Marumori, Suekane and Yamamoto.

6.2. Si^{28}

For Si^{28} we took

$$V = 48\ \text{MeV}; \quad r_0 = 1.23\times 10^{-13}\ \text{cm}; \quad \gamma V = 1.7\ \text{MeV}; \quad \sigma = 0.69\ \text{MeV}.$$

These values of the parameters give †

$$r = 1.24\times 10^{-13}\ \text{cm}; \quad 1d_{\frac{3}{2}}-2s_{\frac{1}{2}} = 4.1\ \text{MeV}; \quad 2s_{\frac{1}{2}}-1d_{\frac{5}{2}} = 4.4\ \text{MeV};$$
$$V-1d_{\frac{5}{2}} = 13.0\ \text{MeV}.$$

According to the experimental results of Helm [25]), which gave, for Si^{28}, $r = 1.29\times 10^{-13}$ cm, our value of r is somewhat small. Besides, the results on electron scattering by Si^{28} have been interpreted with a charge distribution (called by Helm a gauss-uniform distribution) considerably different from that of fig. 2. However, the results are not very sensitive, for the electron energy used by Helm (187 MeV), to the details of the charge distribution in the central region; the central dip of fig. 2 may be too pronounced, but some dip might well exist.

For the quadrupole vibration of Si^{28} we got

† The values of $1d_{\frac{3}{2}}-2s_{\frac{1}{2}}$ and $2s_{\frac{1}{2}}-1d_{\frac{5}{2}}$ are approximately the same as those used by Marumori *et al.*[11]).

$\hbar\omega_2 = 1.31$ MeV; $C_2 = 29.5$ MeV; $B_2 = 743.6\times 10^{-44}$ MeV · sec^2,

The adiabatic approximation leads to

$$(\hbar\omega_2)_{\text{adiab.}} = 1.38\ \text{MeV}; \qquad (C_2)_{\text{adiab.}} = 26.7\ \text{MeV};$$
$$(B_2)_{\text{adiab.}} = 613.3\times 10^{-44}\ \text{MeV}\cdot\text{sec}^2,$$

while the hydrodynamical model gives

$$(\hbar\omega_2)_{\text{hydr.}} = 6.29\ \text{MeV}; \qquad (C_2)_{\text{hydr.}} = 45.2\ \text{MeV};$$
$$(B_2)_{\text{hydr.}} = 49.4\times 10^{-44}\ \text{MeV}\cdot\text{sec}^2.$$

Therefore we get, in this case, an energy much smaller than the hydrodynamical energy, due partly to a decrease in C_2 but mainly to a much bigger mass parameter ($B_2 \approx 15\ (B_2)_{\text{hydr.}}$). The collective frequency ω_2 is now considerably smaller than the characteristic nucleon frequencies: $\omega_2 = 0.06$ $\omega_{1s} = 0.04$ $\omega_{1p} = 0.03$ ω_{1d}. Still, $B_2 = 1.21\ (B_2)_{\text{adiab.}}$. This seems to indicate that the adiabatic approximation will, in many cases, be inadequate for the study of collective vibrations in nuclei. Si^{28} appears to be much less rigid than O^{16} for quadrupole deformations; in fact, $4\pi r^2 S_2(0) = 0.59\times 15.4$ MeV (compare with table 3). On the other hand, Si^{28} is rather rigid against octupole deformations; for the values of the parameters quoted above, we found $C_3(0) = 276.1$ MeV, which corresponds to a 'surface tension' for octupole deformations $4\pi r^2 S_3(0) = 2.44\times 15.4$ MeV. Suekane [12]) and Lane and Pendlebury [13]) have also found, for Si^{28}, $C_2(0) < C_3(0)$.

One may contemplate the possibility of identifying the rather low-lying quadrupole vibration of Si^{28} with the first excited state of this nucleus. That state lies at 1.78 MeV, an energy somewhat higher than our estimate, but both its lifetime [26]) and the cross-section for its excitation by inelastic electron scattering [25]) seem to indicate the presence of some collective effect. It has been suggested [27]) that Si^{28} may be a deformed nucleus; however, we have treated it as spherical.

If we consider the next few closed-shell nuclei, Si^{30}, S^{32}, S^{36}, Ca^{40}, we see that for all but Ca^{40} we expect the lowest vibrational state to be of the quadrupole type. For Ca^{40} one should have again a 3− state, as for O^{16}. But we have no results for those nuclei; the calculations even for such relatively light nuclei would imply a very considerable amount of numerical work.

It is a pleasure to thank Professor Rosenfeld for his criticism and advice. Thanks are due also to the Instituto de Alta Cultura for financial support.

Appendix

We give here the expressions of the quantities $C(j_0, l_0, \omega_0; \lambda; j, l, \omega)$ referred to in section 4:

$\lambda = 2, l = l_0+2$

$$C = (x^2-x_{jl\omega}^2)^{-1}\{1+4(x^2-x_{jl\omega}^2)^{-1}[-(l_0+1)+\alpha+\beta^2(\alpha_{jl\omega}-\beta_{jl\omega})^{-1}]+4(x^2-x_{jl\omega}^2)^{-2}$$
$$[-(y^2+y_{jl\omega}^2)+2(2l_0+3)(l_0-\alpha)-2\beta^2(\alpha_{jl\omega}-\beta_{jl\omega})^{-1}(2l_0+3+\alpha_{jl\omega}-\alpha)]\};$$

$\lambda = 2, \quad l = l_0$

$$C = (x^2-x_{jl\omega}^2)^{-1}\{1+(x^2-x_{jl\omega}^2)^{-1}[2+4\alpha+4\beta^2(\alpha_{jl\omega}-\beta_{jl\omega})^{-1}]+4(x^2-x_{jl\omega}^2)^{-2}$$
$$[-(y^2+y_{jl\omega}^2)+2\beta^2(\alpha_{jl\omega}-\beta_{jl\omega})^{-1}(\alpha-\alpha_{jl\omega})]\};$$

$\lambda = 3, l = l_0+3$

$$C = (x^2-x_{jl\omega}^2)^{-1}\{1+6(x^2-x_{jl\omega}^2)^{-1}[-(l_0+2)+\alpha+\beta^2(\alpha_{jl\omega}-\beta_{jl\omega})^{-1}]+12(x^2-x_{jl\omega}^2)^{-2}[4(l_0+2)$$
$$\times(l_0+1-\alpha)+2-(y^2+y_{jl\omega}^2)+2\beta^2(\alpha_{jl\omega}-\beta_{jl\omega})^{-1}(\alpha-\alpha_{jl\omega}-2(l_0+2))]+24(x^2-x_{jl\omega}^2)^{-3}$$
$$\times[(3l_0+5-\alpha)(y^2+y_{jl\omega}^2)+2(2l_0+3)(2l_0+5)(\alpha-l_0)+2\beta^2(\alpha_{jl\omega}-\beta_{jl\omega})^{-1}(-\beta^2$$
$$-(y^2+y_{jl\omega}^2)-(2l_0+3)(2l_0+5)+(3l_0+5-\alpha)(3l_0+7+\alpha_{jl\omega}))]\};$$

$\lambda = 3, l = l_0+1$

$$C = (x^2-x_{jl\omega}^2)^{-1}\{1+2(x^2-x_{jl\omega}^2)^{-1}[-(l_0+1)+3\alpha+3\beta^2(\alpha_{jl\omega}-\beta_{jl\omega})^{-1}]+4(x^2-x_{jl\omega}^2)^{-2}$$
$$[4(l_0+1)(l_0-\alpha)-3(y^2+y_{jl\omega}^2)+2\beta^2(\alpha_{jl\omega}-\beta_{jl\omega})^{-1}(3(\alpha-\alpha_{jl\omega})-2(l_0+1))]$$
$$+24(x^2-x_{jl\omega}^2)^{-3}[(l_0-\alpha)(y^2+y_{jl\omega}^2)+2\beta^2(\alpha_{jl\omega}-\beta_{jl\omega})^{-1}(-\beta^2-(y^2+y_{jl\omega}^2)$$
$$+(l_0-\alpha)(l_0+2+\alpha_{jl\omega}))]\}.$$

The expression for $\lambda = 2$, $l = l_0-2$ may be obtained from that for $\lambda = 2$, $l = l_0+2$ by changing l_0 into $-(l_0+1)$; and similarly for $\lambda = 3$, $l = l_0-3$ and $l = l_0+3$ and for $\lambda = 3$, $l = l_0-1$ and $l = l_0+1$.

Essentially the same quantities appear also when one calculates the quadrupole moment associated with a small static deformation of a closed-shell structure (eq. (42), where the ω's have now been dropped). As we have mentioned, the only significant difference occurs for $l = l_0$ and $j = j_0$, because then $x^2-x_{jl}^2$ becomes zero. One has then (for $\lambda = 2$)

$$6C(j_0, l_0; 2; j_0, l_0) = 2\alpha[\alpha^2+\alpha-l_0(l_0+1)]^{-1}-\tfrac{1}{4}(2\alpha-1)(2\alpha+1)^2[\alpha^2+\alpha-l_0(l_0+1)]^{-2}$$
$$-x^{-2}y^{-2}(2\alpha+5)[l_0(l_0+1)-\tfrac{3}{4}]+x^{-2}y^{-2}(x^2+y^2)\{-1+(2\alpha+1)[\alpha^2+\alpha-l_0(l_0+1)]^{-1}$$
$$\times[\tfrac{1}{2}(2\alpha-1)-(l_0(l_0+1)-\tfrac{3}{4})]\}+2x^{-4}y^{-4}(x^2+y^2)^2[l_0(l_0+1)-\tfrac{3}{4}].$$

References

1) K. Alder, A. Bohr, T. Huus, B. Mottelson and A. Winther, Revs. Mod. Phys. **28** (1956) 432
2) F. Villars, Ann. Rev. Nucl. Sci. **7** (1957) 185
3) S. A. Moszkowski, Models of Nuclear Structure, in Vol. **39** of Handbuch der Physik (Springer Verlag, 1957)

4) T. Tamura, Fortschr. der Phys. **6** (1958) 109
5) S. T. Belyaev, Mat. Fys. Medd. Dan. Vid. Selsk. **31**, No. 11 (1959)
6) D. R. Inglis, Phys. Rev. **97** (1955) 701
7) J. M. Araújo, Nuclear Physics **1** (1956) 259
8) A. Mouhasseb, Compt. Rend. **242** (1956) 2111; **243** (1956) 1289
9) J. J. Griffin, Phys. Rev. **108** (1957) 328
10) R. A. Ferrell and W. M. Visscher, Phys. Rev. **102** (1956) 450; **104** (1956) 475; R. A. Ferrell, Phys. Rev. **107** (1957) 1631
11) T. Marumori, S. Suekane and A. Yamamoto, Progr. Theor. Phys. **16** (1956) 320
12) S. Suekane, Progr. Theor. Phys. **21** (1959) 74
13) A. M. Lane, Comptes Rendus du Congrès International de Physique Nucléaire (Paris, juillet 1958)
14) D. F. Taylor, Ph. D. Thesis, Manchester (October 1955) (unpublished).
15) J. M. Araújo, Aspectos colectivos da estrutura nuclear (Porto 1957)
16) G. Racah, Phys. Rev. **62** (1942) 438
17) G. N. Watson, Theory of Bessel Functions (New York, 1945)
18) R. Hofstadter, Ann. Rev. Nucl. Sci. **7** (1957) 231
19) D. Kohler and H. H. Hilton, Phys. Rev. **110** (1958) 1094
20) J. P. Elliott and B. H. Flowers, Proc. Roy. Soc. A **242** (1957) 57
21) S. L. Kameny, Phys. Rev. **103** (1956) 358
22) D. H. Wilkinson, Phil. Mag. **1** (1956) 127
23) H. Horie and A. Arima, Phys. Rev. **99** (1955) 778
24) R. D. Amado, Phys. Rev. **108** (1957) 1462
25) R. H. Helm, Phys. Rev. **104** (1956) 1466
26) S. Devons, G. Manning and J. H. Towle, Proc. Phys. Soc. A **69** (1956) 173
27) A. G. Rubin, Phys. Rev. **108** (1957) 62

2.D *Nuclear Physics* **13** (1959) 382—396; © *North-Holland Publishing Co., Amsterdam*
Not to be reproduced by photoprint or microfilm without written permission from the publisher

COMPOUND NUCLEUS PROCESSES IN MEDIUM MASS NUCLEI

A. C. DOUGLAS and N. MACDONALD

Atomic Weapons Research Establishment, Aldermaston

Received 29 June 1959

Abstract: In applying compound nucleus theory to a reaction involving many states of the compound and final nucleus, one usually assumes that the level density of the final nucleus depends on the spin I as $\rho_I \propto (2I+1)$. This leads to the predictions that the angular distribution is isotropic and that the cross-section has the product form

$$\sigma(\mathrm{A}+\mathrm{a} \to \mathrm{B}+\mathrm{b}) = cF_{\mathrm{aA}}F_{\mathrm{bB}}.$$

Recent experiments on (n, p) and (n, α) reactions in nuclei of mass $A \leqq 65$ show quite strong angular anisotropies, with symmetry about 90°. We have examined the consequences of using the more correct form

$$\rho_I \propto (2I+1)\exp\left\{\frac{-(I+\frac{1}{2})^2}{2\sigma^2}\right\}.$$

Anisotropies in the direction found experimentally are predicted. The degree of anisotropy depends sensitively on σ, and the measurement of angular distributions therefore gives a means of determining this important parameter. The deviation of $\sigma(\mathrm{A}+\mathrm{a} \to \mathrm{B}+\mathrm{b})$ from the product form is quite small.

1. Introduction

At sufficiently high bombarding energies individual resonances are not resolved and many states of the compound nucleus are excited simultaneously. It is customary to assume that the signs of the matrix elements for the formation and decay of the various intermediate states are uncorrelated. It has sometimes been stated that this random sign approximation implies that the angular distribution in a compound nucleus process A(a, b)B is isotropic, and that the cross-section has the form

$$\sigma(\mathrm{A}+\mathrm{a} \to \mathrm{B}+\mathrm{b}) = cF_{\mathrm{aA}}F_{\mathrm{bB}} \tag{1.1}$$

implying independence of formation and decay of the compound nucleus. Various authors [1]) have pointed out that to obtain isotropy it is necessary to assume that the level density $\rho(\varepsilon_{\mathrm{B}}, I_{\mathrm{B}})$ of B has the form

$$\rho(\varepsilon_{\mathrm{B}}, I_{\mathrm{B}}) = \rho(\varepsilon_{\mathrm{B}})(2I_{\mathrm{B}}+1). \tag{1.2}$$

Here ε_{B} is the excitation energy and I_{B} the spin of a level in B. The random sign approximation only implies symmetry about 90°. Lane and Thomas [1]) have pointed out that the result (1.1) also depends on the use of (1.2). These results are also discussed by Satchler [2]).

We have examined these aspects of compound nucleus theory using the more correct form

$$\rho(\varepsilon_B, I_B) = \frac{\rho_0(\varepsilon_B)(2I_B+1)}{2\sigma^2(\varepsilon_B)} \exp\left\{\frac{-(I_B+\frac{1}{2})^2}{2\sigma^2(\varepsilon_B)}\right\} \tag{1.3}$$

as given by Bethe and by Bloch [3]). This is itself an approximation, good to within 5 % in the range of values of σ which we use, to the form

$$\rho(\varepsilon_B, I_B) = \rho_0(\varepsilon_B)\left\{\exp\left[\frac{-I_B{}^2}{2\sigma^2}\right] - \exp\left[\frac{-(I_B+1)^2}{2\sigma^2}\right]\right\}.$$

Wolfenstein [1]) discussed the angular distribution using the forms

$$\rho(\varepsilon, I) = \rho(\varepsilon)$$

and

$$\begin{aligned} \rho(\varepsilon, I) &= \rho(\varepsilon)(2I+1), \quad I \leqq I_{\max} \\ &= 0, \qquad\qquad\quad I > I_{\max}. \end{aligned}$$

Ericson and Strutinski [4]) have examined, using a form similar to (1.3) for ρ, the angular distribution of alpha particles inelastically scattered at Ni^{58}. In this process the target nucleus and the incoming and outgoing particle have zero spin, and they deal with 18 MeV alpha particles so that the average value of the total angular momentum is large. These facts enable them to work in the classical limit. We discuss the case of reactions induced by 14 MeV neutrons, for which this is not a good approximation. No theoretical work has appeared on the question of how much the cross-section differs from the product form (1.1).

A further assumption which is involved in obtaining the two results of the simplified theory is that the collision matrix $U^J_{al_1s_1, bl_2s_2}$ is independent of the initial and final channel spins s_1 and s_2. To obtain (1.1) it must also be assumed that when U is expressed in terms of transmission factors, as in equation (3.5) below, these depend on the orbital angular momenta l_1, l_2 and not on the total angular momentum J. We retain these assumptions.

We examine the angular distribution of the processes

$$\begin{aligned} &Cu^{63}(n, p)Ni^{63}, \\ &Fe^{54}(n, p)Mn^{54}, \\ &Fe^{54}(n, \alpha)Cr^{51}, \end{aligned}$$

and the formation and decay of the compound nucleus Cu^{64} by neutron and proton channels. Our main reason for selecting these processes is that there are experimental data available on these (n, p) angular distributions [5]) and also on the (n, α) angular distributions for one or two nuclei in this mass region [6]). The experiments of Allan [5]) and Kumabe [6]) give evidence of anisotropy with approximate symmetry about 90°. Ghoshal [7]) has used induced activity measurements to compare the cross sections of the reactions

$Ni^{60}(\alpha, n)Zn^{63}$	$Cu^{63}(p, n)Zn^{63}$
$Ni^{60}(\alpha, 2n)Zn^{62}$	$Cu^{63}(p, 2n)Zn^{62}$
$Ni^{60}(\alpha, pn)Cu^{62}$	$Cu^{63}(p, pn)Cu^{62}$.

He regarded his results as consistent with (1.1). John [8]) has examined similar processes involving the compound nucleus Po^{210}. He states that his results and Ghoshal's are inconsistent with (1.1), the proton induced reactions giving larger yields than expected, but the small deviation from the simple theory could be the result of a contribution from direct processes. Cohen [9]) compared the cross sections for (n, p), (n, n'), (p, p') and (p, n) processes in this mass region, without however examining any case in which the same compound nucleus is formed. (Of any pair of nuclei X_Z^A and Y_{Z-1}^A one is in general unstable.) His results indicate that the ratio of protons to neutrons formed in a proton induced reaction is of the order of four times the value predicted by the simple form of the compound nucleus theory, although this theory gives quite well the same ratio in neutron induced processes, and although he can assign a nuclear temperature to his energy spectra indicating that the statistical compound nucleus theory is appropriate.

2. The Parameter σ

In the form (1.3) of $\rho(\varepsilon, I)$, $\sigma^2 = \tau\mathscr{I}/\hbar^2$ where τ is the nuclear temperature and $\mathscr{I}$ has the form of a moment of inertia. Using an independent particle model with a square potential well of radius R, Bloch [3]) derived the value

$$\mathscr{I}_R = \tfrac{2}{5}MAR^2 \tag{2.1}$$

where A is the mass number and M the mass of a nucleon. This corresponds to the moment of inertia of a rigid sphere. With a harmonic oscillator well Bloch derived the value $\mathscr{I} = \frac{1}{4}MAR^2$.

The most direct method of obtaining σ is by counting the number of levels with various spins. This has been done by Hibdon [10]) for neutron resonances in Al^{28}. He obtains $\mathscr{I}/\mathscr{I}_R \approx \frac{1}{3}$. It would be useful to have the spin assignments, from (d, p) or (p, p') processes, for as many states as possible in one nucleus. Ericson [11]) has estimated σ for several nuclei in the following manner. Using data from (pp') and (dp) reactions he plots against excitation energy ε the logarithm of $N(\varepsilon)$, the number of states of energy $\leqq \varepsilon$. This can be fitted by a straight line, corresponding to a constant temperature. He extrapolates this line to the energy of the states obtained by low energy neutron scattering. From the known density of these states (which have low spin values) and (1.3) he can find $\log N(\varepsilon)$ for a particular σ, and so obtains the value of σ which makes $\log N(\varepsilon)$ fall on the extrapolated line. The values obtained correspond to

$$\mathscr{I}/\mathscr{I}_R \approx 1.6 \quad \text{for} \quad S^{33},$$
$$\mathscr{I}/\mathscr{I}_R \approx 1.5 \quad \text{for} \quad Mn^{56},$$
$$\mathscr{I}/\mathscr{I}_R \approx 0.9 \quad \text{for} \quad Fe^{57}.$$

Theoretical level densities have been compared [12]) with experimental data on low energy neutron scattering. In general the approximate form

$$\rho(\varepsilon, I) = \rho_0(\varepsilon)\,\frac{(2I+1)}{2\sigma^2(\varepsilon)} \tag{2.2}$$

has been used, ρ_0 having the form

$$\rho_0(\varepsilon) = f(\varepsilon)\exp{(a\varepsilon)^{\frac{1}{2}}} \tag{2.3}$$

where f is a slowly varying function of ε, the main energy dependence coming from the exponential. The results in each case imply a value of $\mathscr{I}/\mathscr{I}_R$ because of the presence of the factor $1/\sigma^2(\varepsilon)$ in (2.2). Near mass $A = 60$ and for $R = r_0 A^{\frac{1}{3}}$ with $r_0 = 1.2\times 10^{-13}$ cm, $\mathscr{I}_R \approx 15$ MeV^{-1}. The values of $\mathscr{I}/\mathscr{I}_R$ are [12])

Ross	0.84
Lang and Le Couteur	0.30
Newton	0.13
Cameron	0.03

Clearly, with the smaller values of σ implied by these results, eq. (2.2) is a poor approximation to (1.3) even for small values of I. However, Cameron [12]) presents evidence that (2.2) is a reasonable form for ρ. This consists of a graph of the ratio of the observed level spacing to the calculated spacing, plotted against the spin I of the target nucleus. The compound nucleus spin is $I+\frac{1}{2}$ because only s wave neutrons are involved in most of the experiments. The fit is about equally good for all values of I considered.

The present situation with regard to the determination of the important parameter σ is unsatisfactory, since the valus of σ obtained from the results of Newton and Cameron [12]) differ greatly from those found by Ericson, and since the work discussed above gives information for a fairly limited range of excitation energies. It is apparent that any evidence on the value of σ from angular distributions will be useful.

3. Theory

Our account of the theory of the process A(ab)B follows that of Lane and Thomas [1]). We use the channel spin representation: $\mathbf{I}_1$, $\mathbf{i}_1$ denote the spins of the target nucleus A and the projectile a respectively, and $\mathbf{s}_1$ is the channel spin in the incident channel:

$$\mathbf{s}_1 = \mathbf{I}_1 + \mathbf{i}_1.$$

The total spin is

$$\mathbf{J} = \mathbf{s}_1 + \mathbf{l}_1$$

where $\mathbf{l}_1$ is the angular momentum in the incident channel. Similar quantities in the outgoing (bB) channel are denoted by $\mathbf{I}_2$, $\mathbf{i}_2$, $\mathbf{s}_2$, $\mathbf{l}_2$ where

$$\mathbf{J} = \mathbf{s}_2 + \mathbf{l}_2.$$

The differential cross-section per unit solid angle and unit interval of energy of the emitted particle is

$$\langle \mathrm{d}^2\sigma_{\mathrm{ab}} \rangle = [k_{\mathrm{a}} \hat{I}_1 \hat{i}_1]^{-2} \sum_{L, s_1, s_2, I_2} B_L(\mathrm{b}E_{\mathrm{b}} s_2, \mathrm{a}s_1) P_L(\cos\theta) \rho_{\mathrm{B}}(\varepsilon_{\mathrm{B}} I_2) \mathrm{d}E_{\mathrm{b}} \mathrm{d}\Omega_{\mathrm{b}}. \quad (3.1)$$

In this expression k_{a} is the wave number of the incident particle, E_{b} the kinetic energy of b and θ the angle between the direction of b and the incident beam. $\hat{\chi}$ stands for $(2\chi+1)^{\frac{1}{2}}$. The function B_L is [13])

$$B_L = \sum_{JJ'} \sum_{l_1 l'_1} \sum_{l_2 l'_2} \tfrac{1}{4} (-1)^{s_2 - s_1} \{U^J_{\mathrm{b}l_2 s_2, \mathrm{a}l_1 s_1}\}^* U^{J'}_{\mathrm{b}l'_2 s_2, \mathrm{a}l'_1 s_1} \times Z'(l_1 J l'_1 J'; s_1 L) Z'(l_2 J l'_2 J'; s_2 L); \quad (3.2)$$

Z' is defined in terms of the Racah coefficient W and the Clebsch-Gordan coefficient $(a0c0|f0)$ by

$$Z'(abcd; ef) = \hat{a}\hat{b}\hat{c}\hat{d}(a0c0|f0) W(abcd; ef); \quad (3.3)$$

U is the collision matrix. We assume that $U^J_{\mathrm{b}l_2 s_2, \mathrm{a}l_1 s_1} = U^J_{\mathrm{b}l_2, \mathrm{a}l_1}$. In the following we make the random sign assumption, implying that only $l_1 = l'_1$, $l_2 = l'_2$, $J = J'$ need be considered. From (3.3) this implies that L is even, that is that the angular distribution is symmetric about 90°. This gives us

$$\begin{aligned} \langle \mathrm{d}^2\sigma_{\mathrm{ab}} \rangle = {} & [k_{\mathrm{a}} \hat{I}_1 \hat{i}_1]^{-2} \sum_{L s_1 s_2 I_2} P_L(\cos\theta) \tfrac{1}{4} (-1)^{s_2 - s_1} \\ & \times \sum_{l_1 l_2 J} |U^J_{\mathrm{b}l_2, \mathrm{a}l_1}|^2 Z'(l_1 J l_1 J; s_1 L) \\ & \times Z'(l_2 J l_2 J; s_2 L) \rho_{\mathrm{B}}(\varepsilon_{\mathrm{B}} I_2) \mathrm{d}E_{\mathrm{b}} \mathrm{d}\Omega_{\mathrm{b}}. \end{aligned} \quad (3.4)$$

We take $|U^J_{\mathrm{b}l_2, \mathrm{a}l_1}|^2$ of the form

$$|U^J_{\mathrm{b}l_2, \mathrm{a}l_1}|^2 = \frac{T^J_{\mathrm{a}l_1}(E_{\mathrm{a}}) T^J_{\mathrm{b}l_2}(E_{\mathrm{b}})}{\sum_{\mathrm{b}'l'_2 s'_2 I'_2} \int_0^{\varepsilon_{\mathrm{B}'\max}} \mathrm{d}\varepsilon_{\mathrm{B}'} T^J_{\mathrm{b}'l'_2}(E_{\mathrm{b}'}) \rho_{\mathrm{B}'}(\varepsilon_{\mathrm{B}'} I'_2)} \quad (3.5)$$

where the sum over b′ is over all competing channels and we make use of the transmission factors $T^J_{\mathrm{a}l_1}$, $T^J_{\mathrm{b}l_2}$.

Writing the denominator in (3.5) as $g(J)$ we have

$$\begin{aligned} \langle \mathrm{d}^2\sigma_{\mathrm{ab}} \rangle = {} & [k_{\mathrm{a}} \hat{I}_1 \hat{i}_1]^{-2} \sum_{l_1 l_2 J} \sum_{L s_1 s_2 I_2} P_L(\cos\theta) \frac{(-1)^{s_2 - s_1}}{4g(J)} \\ & \times T^J_{\mathrm{a}l_1} T^J_{\mathrm{b}l_2} Z'(l_1 J l_1 J; s_1 L) Z'(l_2 J l_2 J; s_2 L) \rho_{\mathrm{B}}(\varepsilon_{\mathrm{B}} I_2) \mathrm{d}E_{\mathrm{b}} \mathrm{d}\Omega_{\mathrm{b}}. \end{aligned} \quad (3.6)$$

If we assume the form (1.2) for ρ_B we can perform the sum over I_2:

$$\sum_{I_2} (2I_2+1) = (2s_2+1)(2i_2+1). \tag{3.7}$$

This can be shown to lead to an isotropic distribution as follows. We sum over s_2 first: s_2 occurs only in the factors

$$W(l_1 J l_1 J; s_1 L) W(l_2 J l_2 J; s_2 L)(-1)^{s_2-s_1}(2s_2+1)$$
$$= (2s_2+1)\sum_{\lambda}(2\lambda+1)(-1)^{2s_1-\lambda-L} W^2(l_2 J \lambda s_1; s_2 l_1) W(l_1 l_2 l_1 l_2; \lambda L).$$

We use the relation

$$\sum_{s_2} (2s_2+1) W^2(l_2 J \lambda s_1; s_2 l_1) = 1$$

so that sum over s_2 becomes

$$(-1)^{2s_1-L}\sum_{\lambda}(2\lambda+1)(-1)^{\lambda} W(l_1 l_2 l_1 l_2; \lambda L)$$
$$= (-1)^{2s_1-L+l_1+l_2}\frac{1}{\hat{l}_1\hat{l}_2}\sum_{\lambda}(2\lambda+1) W(l_1 l_2 l_1 l_2; \lambda L) W(l_1 l_2 l_1 l_2; \lambda 0)$$
$$= \frac{(-1)^{2s_1-L+l_1+l_2}}{\hat{l}_1\hat{l}_2}\delta_{L0}.$$

Hence the distribution is isotropic. By the same method we have shown that the angular distribution of particle c in the reaction A(a, bc)C, b not being observed, is isotropic if the random sign assumption is made and if ρ_c is given the form (1.2) (see appendix). Using the form (1.3) for ρ in the A(a, b)B case we evaluate the angular distributions using the published tables of Z and W functions [14]).

Assuming now that T_{al_1} and T_{bl_2} are independent of J we have for the averaged total cross-section

$$\langle\sigma_{ab}\rangle dE_b = \pi[k_a\hat{I}_1\hat{i}_1]^{-2}\sum_{l_1 l_2} T_{al_1} T_{bl_2}\sum_{J s_1 s_2 I_2}\frac{(2J+1)\rho_B(\varepsilon_B I_B)dE_b}{g(J)}. \tag{3.8}$$

Using (1.2) for ρ_B and summing over I_2 as in (3.7) we have

$$\langle\sigma_{ab}\rangle dE_b = \pi[k_a\hat{I}_1\hat{i}_1]^{-2}\sum_{l_1 l_2} T_{al_1} T_{bl_2}$$
$$\times\sum_{J s_1 s_2}\frac{(2i_2+1)(2s_2+1)\rho_B(\varepsilon_B)(2J+1)dE_b}{\sum_{b' s'_2 l'_2}(2s'_2+1)(2i'_2+1)\int_0^{\varepsilon_{B'\max}} d\varepsilon_{B'} T_{b' l'_2}(E_{b'})\rho_{B'}(\varepsilon_{B'})}$$
$$= \pi(2i_2+1)[k_a\hat{I}_1\hat{i}_1]^{-2}\sum_{J s_1 l_1 l_2}\frac{(2J+1)\{(2l_2+1)T_{bl_2}\}T_{al_1}\rho_B(\varepsilon_B)dE_b}{\sum_{b' l'_2}(2i'_2+1)\int_0^{\varepsilon_{B'\max}} d\varepsilon_{B'}\{(2l'_2+1)T_{b' l'_2}\}\rho_{B'}(\varepsilon_{B'})}.$$

The sum over J and s_1 then leads to

$$\langle\sigma_{ab}\rangle dE_b = \frac{(2i_2+1)\sigma_a(\text{c.n.})\sigma_b(\text{c.n.})k_b^2\rho_B(\varepsilon_B)dE_b}{\sum_{b'}(2i'_2+1)\int_0^{\varepsilon_{B'max}} d\varepsilon_{B'}\sigma_{b'}(\text{c.n.})k_{b'}^2\rho_{B'}(\varepsilon_{B'})} \tag{3.9}$$

where we define the cross-section for formation of the compound nucleus by

$$\sigma_a(\text{c.n.}) = \frac{\Pi}{k_a^2}\sum_{l_1}(2l_1+1)T_{al_1}(E_a). \tag{3.10}$$

The result (3.9) has the form of (1.1). If we consider incident neutrons n_1 and protons p_1 which give the same excitation energy of the compound nucleus, and final neutrons of energy E_{n_2} and protons of energy E_{p_2} then (3.9) implies that the quantity

$$R = \frac{\langle\sigma_{n_1n_2}\rangle\langle\sigma_{p_1p_2}\rangle}{\langle\sigma_{n_1p_2}\rangle\langle\sigma_{p_1n_2}\rangle} = 1. \tag{3.11}$$

We have calculated R using the more general form (1.3) for ρ for the case of the compound nucleus Cu^{64}. The result (3.9) can be generalized to the process A(a, bc)C using (1.2) for the level densities of the final and intermediate nuclei (see appendix).

4. The Angular Distributions of Cu^{63}(n, p)Ni^{63} and Fe^{54}(n, p)Mn^{54} for 14 MeV Neutrons

We simplify (3.8) by ignoring the energy dependence of σ. We consider only (n, n′) and (np) processes in the denominator of (3.8), and take the same value of σ for the final nuclei N and P in the two cases, so that $g(J)$ has the form

$$g(J) = \sum_{I'_2 s'_2 I'_2}\frac{(2I'_2+1)}{2\sigma^2(\bar{\varepsilon}_N)}\exp\left\{\frac{-(I'_2+\frac{1}{2})^2}{2\sigma^2(\bar{\varepsilon}_N)}\right\} \times\left[\int_0^{\varepsilon_{Nmax}} d\varepsilon_N T_{I'_2 n}(E_n)\rho_{N0}(\varepsilon_N) + \int_0^{\varepsilon_{Pmax}} d\varepsilon_P T_{I'_2 p}(E_p)\rho_{P0}(\varepsilon_P)\right],$$

in which we have assumed the transmission factors independent of J. $\bar{\varepsilon}_N$ is the most probable value of ε_N. Taking $\sigma(\bar{\varepsilon}_N)$ for both the contributions to $g(J)$ is a reasonable approximation because the proton integrals are relatively small. Taking the same value of σ for $\rho(\varepsilon_B I_B)$ as for $g(J)$ in (3.8) is a good approximation when we consider final nucleus excitation energies not far from $\bar{\varepsilon}_N$, since one expects $2\sigma^2$ to be proportional to $\varepsilon^{\frac{1}{2}}$.

We have used $\rho_0(\varepsilon)$ in the form given by Newton [12]) the exponential part of (2.3) having $\sqrt{a} = 4.92\ \text{MeV}^{-\frac{1}{2}}$. We use the nuclear radius $R = r_0 A^{\frac{1}{3}}$ with $r_0 = 1.45\times10^{-13}$ cm, in calculating the transmission factors. For neutrons these were calculated using the simple square well theory [13]) and the tables

of Monahan *et al.* [16]). The proton transmission factors were calculated from the graphs of Sharp *et al.* [17]).

TABLE 1

The ratio $\sigma(0°)/\sigma(90°)$ for the process $Cu^{63}(n,p)Ni^{63}$ for various values of $2\sigma^2$ and of proton energy, and $r_0 = 1.45 \times 10^{-13}$ cm

$2\sigma^2$ \ E_p	5.2 MeV	3.3 MeV	2.1 MeV
25	1.05	1.03	1.02
10	1.22	1.14	1.12
5	1.47	1.32	1.27
2.5	1.70	1.48	1.40

Table 1 presents results for four values of $2\sigma^2$ and three proton energies, in the case of Cu^{63}. In fig. 1 the angular distribution for 5 MeV proton energy is compared with the latest (1959) data of Allan [5]). There is a slight forward peak. (At energies $>$ 5 MeV the direct process, with a strong forward peak, is important.) We therefore look at the angular distribution for backward angles in the energy range 4—5 MeV and see that it is consistent with $2\sigma^2 \geqq 10$. Taking $2\sigma^2(\bar{\varepsilon}_N) = 10$ and the appropriate value of $2\sigma^2$ for the excitation energy corresponding to 5 MeV protons we have verified that for this order of magnitude of σ, ignoring the energy dependence of σ is a good approximation.

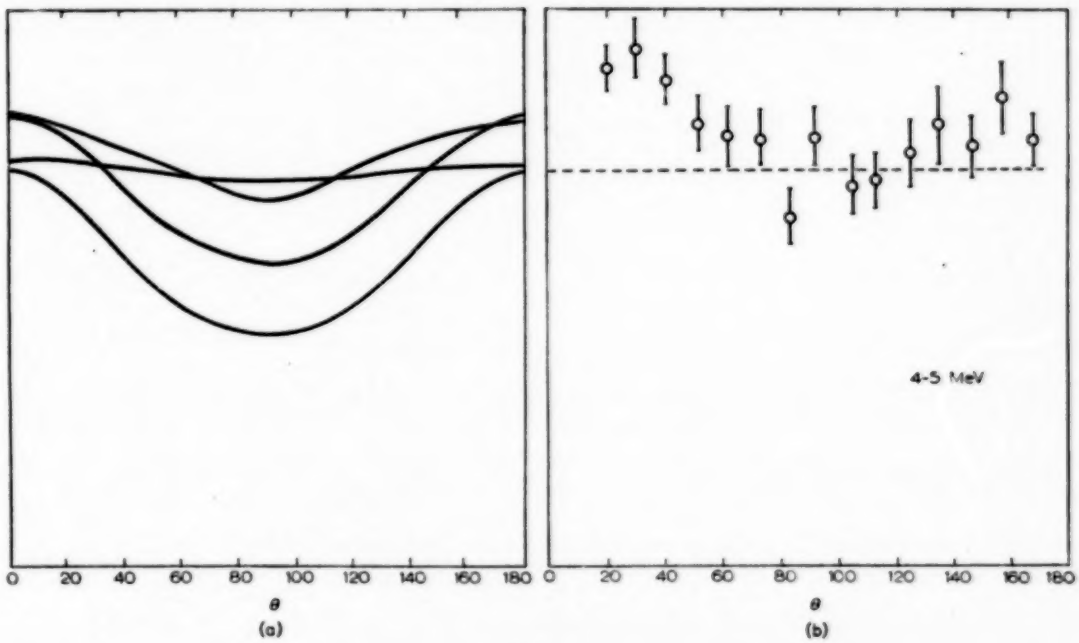

Fig. 1

(a) Angular distributions calculated for the process $Cu^{63}(n, p)Ni^{63}$ with $r_0 = 1.45 \times 10^{-13}$ cm, $\sqrt{a} = 4.92$ MeV$^{-\frac{1}{2}}$, proton energy 5 MeV. In increasing order of anisotropy, curves are for $2\sigma^2 = 25$, 10, 5 and 2.5.

(b) Results of Allan [5]) for energy range 4.5 MeV.

Our results are not sensitive to the value of a. We calculated the case of $2\sigma^2 = 5$ with $\sqrt{a} = 5.9$ MeV$^{-\frac{1}{2}}$, thus covering the range of values of a given in ref.[10]) and found a 1 % increase in $\sigma(0°)/\sigma(90°)$. The anisotropy increases appreciably as r_0 increases but not so as to qualitatively alter our results (see table 2).

TABLE 2

The ratio $\sigma(0°)/\sigma(90°)$ for the process $Cu^{63}(n,p)Ni^{63}$ for various values of $2\sigma^2$ and of proton energy, and $r_0 = 1.45 \times 10^{-13}$ cm

$2\sigma^2$ \ E_p	5.2 MeV	3.3 MeV
25	1.03	1.02
10	1.14	1.10
2.5	1.67	1.42

Cu^{63} has spin $\frac{3}{2}$. To examine the effect of changing I_1 and i_1, we evaluated the case of $2\sigma^2 = 5$ for $I_1 = 0$, with $i_1 = \frac{1}{2}$ and 0. The results are shown in table 3. As expected, the introduction of randomly oriented spins in the

TABLE 3

Values of $\sigma(0°)/\sigma(90°)$ with $2\sigma^2 = 5$, $r_0 = 1.25 \times 10^{-13}$ cm, 5.2 MeV proton energy and various initial state spins

$i_1 = \frac{1}{2}$	$I_1 = \frac{3}{2}$	1.47
$i_1 = \frac{1}{2}$	$I_1 = 0$	1.59
$i_1 = 0$	$I_1 = 0$	1.87

initial state smooths out the angular distribution. We have not used our $I_1 = 0$ results for comparison with the experimental data on $Fe^{54}(n,p)Mn^{54}$. It is apparent from figs. 2 a, b that the difference between the results below and above 5 MeV makes it impossible to estimate σ.

Our results for low proton energy in table 1 illustrate the energy dependence of the anisotropy in the (n ,p) process, but cannot be compared with experiment because below about 4 MeV the dominant processes [5]) are $Cu^{63}(n, np)Ni^{62}$ and $Fe^{54}(n, np)Mn^{53}$. This is unfortunate since it is in one of the low energy cases that the most striking example of anisotropy with symmetry about 90° is found (fig. 2c). Although it is straightforward to derive a formula for the angular distribution of an (n, np) reaction (see appendix) we have not calculated this angular distribution because of the great labour involved and because the low excitation energies in the final state may well make our form (1.3) of the spin dependence of levels incorrect. This is indicated by the fact that the results for Cu and Fe differ greatly

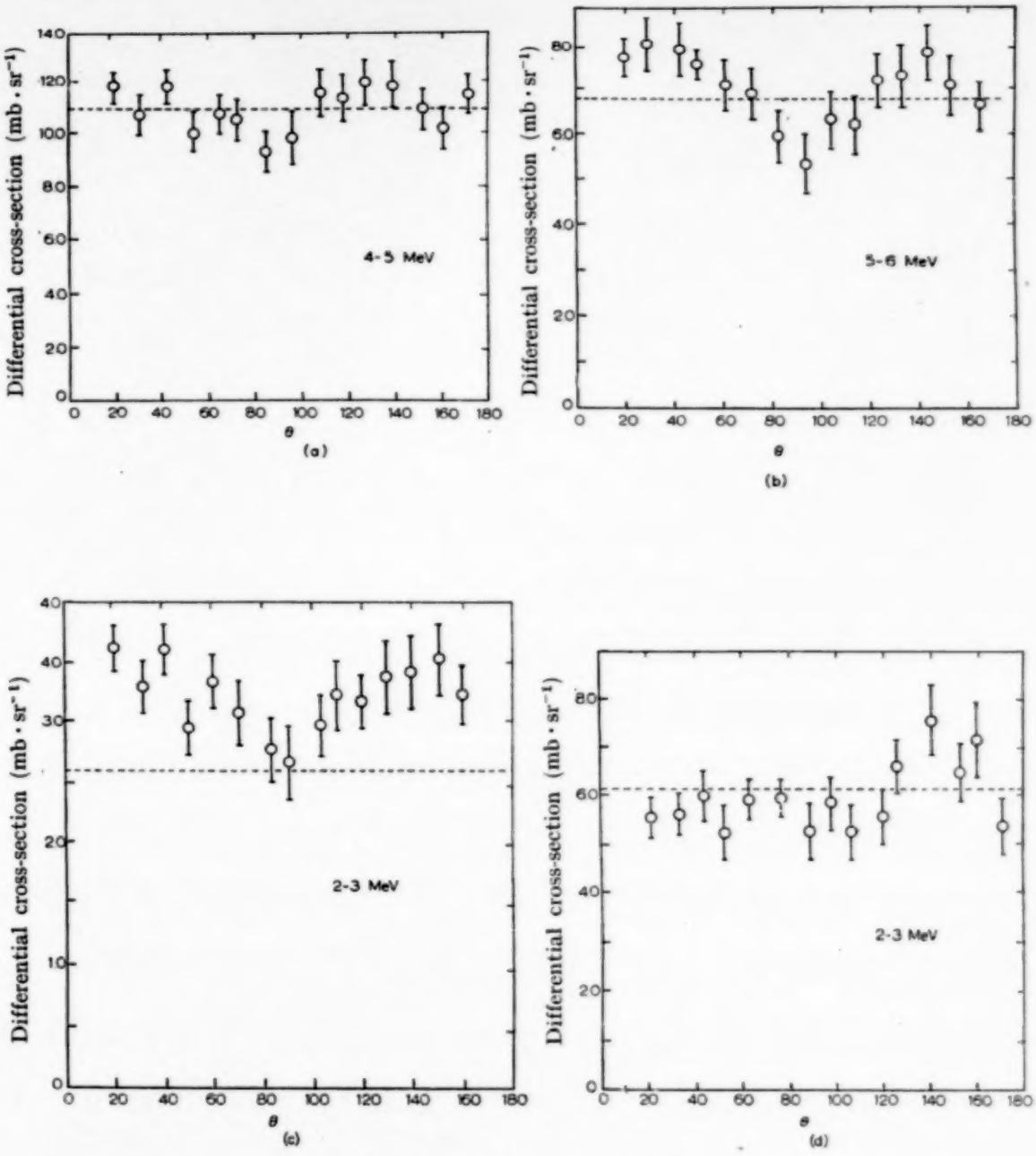

Fig. 2. Experimental results of D. L. Allan [5])

(a) 4—5 MeV protons from neutron bombardment of Fe^{54}.

(b) 5—6 MeV protons from neutron bombardment of Fe^{54}.

(c) 2—3 MeV protons from neutron bombardment of Cu^{63}.

(d) 2—3 protons from neutron bombardment of Fe^{54}.

(figs. 2, c, d). The energy dependence of the anisotropy in the (n, p) process could be studied in Fe^{56} where even at low energies the (n, np) process is unimportant. The results of March and Morton [5]) in this case show no departure from isotropy for protons with energy $\leqq 4$ MeV. Further work on this nucleus would be of interest, especially since Mn^{56} is one of the nuclei for which Ericson [11]) has estimated σ.

5. The Angular Distribution in the (n, α) Process

For (n, α) processes Kumabe [6]) presents results which exhibit a very marked anisotropy with symmetry about 90°. His results, summarized in table 4, are for all alpha energies, with 14.8 MeV neutrons. The peak of

TABLE 4

Approximate values of $\sigma(0°)/\sigma(90°$ from results of Kumabe, for (n, α) process in various elements

Target nucleus	Spin	$\sigma(0°)/\sigma(90°)$
Al^{27}	$\frac{5}{2}$	2.4
S^{32}	0	2.7
V^{51}	$\frac{7}{2}$	2.75
Mn^{55}	$\frac{5}{2}$	3.2
Co^{59}	$\frac{7}{2}$	3.2

the alpha energy spectrum is at about 5 MeV. We have calculated the case of $2\sigma^2 = 5$, $I_1 = 0$ with 14 MeV neutrons and alpha energies 4.55 MeV and 5.95 MeV. The radius of the compound nucleus is taken as $r_0(A^{\frac{1}{3}}+4^{\frac{1}{3}})$ with r_0 again 1.45×10^{-13} cm. The results are $\sigma(0°)/\sigma(90°) = 2.1$ and 2.3 at the lower and higher energy respectively. These results show that Kumabe's data require $2\sigma^2 < 5$, which is not consistent with the value indicated by the (n, p) data. (Kumabe's results in our mass region are for $I_1 = \frac{5}{2}$ and $\frac{7}{2}$, but they do not depend strongly on spin.)

6. Independence of Formation and Decay of the Compound Nucleus Cu^{64}

Table 5 shows the value of $R(3.11)$ for a number of values of E_{n_2}, E_{p_2} and σ. E_{n_1} is 14 MeV again and E_{p_1} 14.72 MeV, giving the same excitation energy of the compound nucleus, so that for $\sigma = \infty$, we have $R = 1$. We assume that Ni^{63} and Cu^{63} have the same spin. Recalling that the angular distribution results indicate that $2\sigma^2 \geqq 10$ we can see that departures from $R = 1$ are small. Even for smaller σ, if $E_{n_2} = 1$—2 MeV, $E_{p_2} \approx 5$ MeV, that is for the maxima of the (nn') and (np) energy spectra we have $R \approx 1$, and an experiment like those of [7, 8]), is therefore not likely to detect this effect.

TABLE 5

Values of $R = \dfrac{\langle\sigma_{n_1n_2}\rangle\langle\sigma_{p_1p_2}\rangle}{\langle\sigma_{n_1p_2}\rangle\langle\sigma_{p_1n_2}\rangle}$ for three values of $2\sigma^2$, and various values of E_{n_2}, E_{p_2}.

$2\sigma^2$	E_{p_2} (MeV) / E_{n_2} (MeV)	5.2	3.3	2.1
2.5	4.5	1.23	1.34	1.37
	2.6	1.06	1.15	1.18
	1.4	0.95	1.03	1.06
5	4.5	1.15	1.19	1.24
	2.6	1.04	1.08	1.12
	1.4	0.97	1.01	1.05
10	4.5	1.07	1.08	1.10
	2.6	0.99	1.00	1.02
	1.4	0.97	0.98	1.00

Our values of R are much smaller than would correspond to Cohen's result [9]) mentioned in section 1. Also our largest values are a consequence of an increase in $R_n = \langle\sigma_{n_1n_2}\rangle/\langle\sigma_{n_1p_2}\rangle$ over its value for $\sigma = \infty$, partially cancelled

TABLE 6

Proton energy $E_{p_2} = 3.3$ MeV and neutron energy $E_{n_2} = 2.6$ MeV. Ratio R_n of $\langle\sigma_{n_1n_2}\rangle/\langle\sigma_{n_1p_2}\rangle$ to its value with $\sigma = \infty$, and ratio R_p of $\langle\sigma_{p_1n_2}\rangle\langle\sigma_{p_1p_2}\rangle$ to its value with $\sigma = \infty$.

$2\sigma^2$	$\dfrac{R_n(\sigma)}{R_n(\infty)}$	$\dfrac{R_p(\sigma)}{R_p(\infty)}$
10	0.99	0.99
5	1.20	1.11
2.5	1.42	1.23

by a smaller increase in $R_p = \langle\sigma_{p_1n_1}\rangle/\langle\sigma_{p_1p_2}\rangle$ as we show in table 6. Cohen's result on the other hand is that $\sigma(pp')/\sigma(pn)$ greatly exceeds the value given by the simple compound nucleus theory.

7. Conclusions

The angular distributions in the compound nucleus processes considered depend mainly on the parameter σ, and so provide a means of estimating σ. The value we obtain from comparison with (n, p) experimental data is consistent with the values obtained by Ericson [11]). (nα) is a more favourable case than (n, p) for detecting the effect, and experiments to confirm Kumabe's results would be useful.

In the case of a projectile such as an alpha particle or heavy ion, if the incident energy is sufficient, the average value of the square of the total

spin $\overline{J^2}$ is much greater than $\overline{l_2^2}$ for an outgoing nucleon. Under these circumstances, and if the classical limit is appropriate, one can use the approximation (eq. (16) of ref. [4])),

$$\frac{\sigma(0°)}{\sigma(90°)} = 1 + \frac{\overline{J^2}\,\overline{l_2^2}}{8\sigma^4}.$$

While this overestimates the effect in the case of neutron induced processes, and gives too rapid an increase with decreasing σ, it does illustrate the significance of the increase in the anisotropy when we increase the proton energy (table 1), increase r_0 (table 2), or change from (np) to (nα). All these changes increase $\overline{l_2^2}$ while increasing r_0 also increases $\overline{J^2}$.

Our results show that the detection of departures from (1.1) is not very useful as a means of determining σ. Also, the results we obtain do not help to explain Cohen's [9]) results on (pp') cross-sections.

Our attention was drawn to this problem by Dr. A. M. Lane. It is a pleasure to thank Dr. Lane for many helpful discussions. We also wish to thank Dr. D. L. Allan for providing information about the (n, p) experiments, and Dr. T. Ericson for a most interesting conversation.

Appendix

The angular distribution of the particle c when the first emitted particle b is not observed is readily obtained using the formalism [17]) of statistical and efficiency tensors. Making the random sign approximation it has the form

$$W(\theta) = \frac{1}{8\pi}(-1)^{i_2} \sum_{Jl_1l_2l_3s_1s_2s_3L} P_L(\cos\theta)(2J+1)(2s_2+1)(-1)^{s_1+s_3+l_2}|U|^2$$
$$\times Z'(l_1Jl_1J; s_1L)Z'(l_3I_2l_3I_2; s_3L)W(I_2s_2I_2s_2; i_2L)W(Js_2Js_2; l_2L); \quad \text{(A.1)}$$

$|U|^2$ is taken to have the form

$$|\langle s_3l_3s_2l_2J|U|s_1l_1J\rangle|^2$$
$$= \int dE_b \frac{\sum_{I_2I_3} T_{l_1}(a)T_{l_2}(b)T_{l_3}(c)\rho_B(\varepsilon_B I_2)\rho_C(\varepsilon_C I_3)}{\sum_{b'l'_2s'_2I'_2} \int_0^{\varepsilon_{B'\max}} d\varepsilon_{B'} T_{l'_2}(b')\rho_{B'}(\varepsilon_{B'}I'_2) \sum_{c'l'_3s'_3I'_3} \int_0^{\varepsilon_{C'\max}} d\varepsilon_{C'} T_{l'_3}(c')\rho_{C'}(\varepsilon_{C'}I'_3)}. \quad \text{(A.2)}$$

Here, of course, ε_B and $\varepsilon_{C'_{max}}$ are functions of E_b, while ε_C is a function of E_b and E_c; $\mathbf{i}_2$ is the spin of b and $\mathbf{I}_2$ the spin of the intermediate nucleus B; $\mathbf{s}_2 = \mathbf{i}_2+\mathbf{I}_2$ and $\mathbf{J} = \mathbf{s}_2+\mathbf{l}_2$, $\mathbf{l}_2$ being the orbital angular momentum in channel (bB); $\mathbf{i}_3$, $\mathbf{I}_3$, $\mathbf{s}_3$, $\mathbf{l}_3$ are corresponding quantities in the channel (cC); $\mathbf{I}_3 = \mathbf{s}_3+\mathbf{l}_3$.

The factor $Z'(l_3I_2l_3I_2; s_3L)$ implies that L is even. When we assume $\rho_C(\varepsilon_C I_3) \propto (2I_3+1)$ we can perform the sum over s_3 by the introduction of a

summation over λ in the product $Z'(l_3 I_2 l_3 I_2; s_3 L) W(I_2 s_2 I_2 s_2; i_2 L)$ as in section 3. This summation again gives a factor δ_{L0}. Setting $L = 0$ in (A.1) and using the form (1.2) for each of the level densities in (A.2) we obtain for the cross-section the form

$$\langle \mathrm{d}\sigma_{\mathrm{ac}} \rangle \mathrm{d}E_{\mathrm{c}} = \frac{(2i_2+1)(2i_3+1)\sigma_{\mathrm{a}}(\mathrm{c.n.})\, k_{\mathrm{c}}^2 \sigma_{\mathrm{c}}(\mathrm{c.n.})\, \mathrm{d}E_{\mathrm{c}}}{\sum_{\mathrm{b}'} \int_0^{\varepsilon_{\mathrm{B}'\max}} \mathrm{d}\varepsilon_{\mathrm{B}'} \sigma_{\mathrm{b}'}(\mathrm{c.n.}) k_{\mathrm{b}'}^2 \rho_{\mathrm{B}'}(\varepsilon_{\mathrm{B}'}) (2i'_2+1)} \times \int \mathrm{d}E_{\mathrm{b}} \left\{ \frac{\sigma_{\mathrm{b}}(\mathrm{c.n.}) k_{\mathrm{b}}^2 \rho_{\mathrm{B}}(\varepsilon_{\mathrm{B}}) \rho_{\mathrm{C}}(\varepsilon_{\mathrm{C}})}{\sum_{\mathrm{c}'} \int_0^{\varepsilon_{\mathrm{C}'\max}} \mathrm{d}\varepsilon_{\mathrm{C}'} \sigma_{\mathrm{c}'}(\mathrm{c.n.}) k_{\mathrm{c}'}^2 \rho_{\mathrm{C}'}(\varepsilon_{\mathrm{C}'}) (2i'_3+1} \right\}. \tag{A.3}$$

Note added in proof: Since obtaining the results given above we have, thanks to the courtesy of Dr. J. Howlett, A.E.R.E. Harwell, had computing facilities made available for a calculation of the (n, np) anisotropy. In this calculation the spins of all particles have been neglected, and the comparison with the (n, p) results is indirect, making use of a calculation of the anisotropy in the (n, p) process when the spins are ignored. We find that in this case it is important to take account of the dependence of σ on energy since the average excitation energy available is much less in the second stage of the process than in the first. The three values of $2\sigma^2$ given in the (n, np) column are used in ρ_{B} and $\rho_{\mathrm{B}'}$, ρ_{C}, $\rho_{\mathrm{C}'}$ respectively (see eq. (A.2)). The sets 5.3.2. and 10.6.4. correspond to $2\sigma^2(\bar{\varepsilon}) \propto \bar{\varepsilon}^{\frac{1}{2}}$. In all the results in the table we have 14 MeV incoming neutron, 1.35 MeV outgoing neutron, and 2.1 MeV proton.

It is clear that the effect of the extra stage in the process, if σ is kept constant, is to reduce the anisotropy, but that this can be more than compensated by reducing σ in the second stage. The observed anisotropies suggest that σ does in fact increase with ε.

n, np		np (no spins)		np (with spins)	
$2\sigma^2$	$\sigma(0°)/\sigma(90°)$	$2\sigma^2$	$\sigma(0°)/\sigma(90°)$	$2\sigma^2$	$\sigma(0°)/\sigma(90°)$
5, 3, 2	1.47	5	1.40	5	1.27
5, 3, 3	1.36				
5, 5, 5	1.18				
10, 6, 4	1.30	10	1.14	10	1.12
10, 6, 6	1.21				
10, 10, 10	1.09				

References

1) L. Wolfenstein, Phys. Rev. **82** (1951) 690;
W. Hauser and H. Feshbach, Phys. Rev. **87** (1952) 366;
A. M. Lane and R. G. Thomas, Revs. Mod. Phys. **30** (1958) 257

2) G. R. Satchler, Proceedings of the Conference on Reactions between Complex Nuclei (Gatlinburg) ORNL 2606 (1958) p. 79
3) H. A. Bethe, Revs. Mod. Phys. **9** (1937) 69;
C. Bloch, Phys. Rev. **93** (1954) 1094
4) T. Ericson and V. Strutinski, Nuclear Physics **8** (1958) 284; **9** (1959) 689
5) D. L. Allan, Proc. Phys. Soc. A **70** (1957) 195;
Columbia Conference on Neutron Interactions with the Nucleus TID 7547 (1958) 207;
Nuclear Physics **6** (1958) 464;
Nuclear Physics **10** (1959) 348;
P. V. March and W. T. Morton, Phil. Mag. **3** (1958) 143
6) I. Kumabe, E. Takekoshi, H. Ogata, Y. Tsuneka and S. Oki, Phys. Rev. **106** (1957) 155;
Journal Phys. Soc. Japan **13** (1958) 129
I. Kumabe, Journal Phys. Soc. Japan **13** (1958) 325
7) S. N. Ghoshal, Phys. Rev. **80** (1950) 939
8) W. John, Phys. Rev. **103** (1956) 704
9) B. L. Cohen and A. G. Rubin, Phys. Rev. **113** (1959) 579
10) C. T. Hibdon, Bull. Am. Phys. Soc. **3** (1958) 48;
Proceedings of 2nd Geneva Conference on the Peaceful Uses of Atomic Energy (1958)
11) T. Ericson, Nuclear Physics **11** (1959) 481
12) J. M. B. Lang and K. J. LeCouteur, Proc. Phys. Soc. A **67** (1954) 586;
T. D. Newton, Can. Journ. Phys. **34** (1956) 804;
A. A. Ross, Phys. Rev. **108** (1957) 720;
A. G. W. Cameron, Can. Journ. Phys. **36** (1958) 1040
13) J. M. Blatt and L. C. Biedenharn, Revs. Mod. Phys. **24** (1952) 258
14) L. C. Biedenharn, ORNL 1501 (1953);
L. C. Biedenharn and A. Simon, ORNL 1501 Supplement (1954);
S. Obi, T. Ishidzu, H. Horie, S. Yanagawa, Y. Tanabe and M. Sato, Annals of the Tokyo Astronomical Observatory, Series 2. **3** (1957) 89; **4** (1954) 1; **4** (1955) 77;
W. T. Sharp, J. M. Kennedy, B. J. Sears and M. G. Hoyle, Chalk River Report, C.R.T. 556 (1954)
15) J. M. Blatt and V. F. Weisskopf, Theoretical Nuclear Physics (Wiley, 1952)
16) J. E. Monahan, L. C. Biedenharn and J. P. Schiffer, A.N.L. 5846 (1958)
17) W. T. Sharp, H. E. Gove and E. B. Paul, Chalk River Report, T.P.I. 70 (1955)
18) S. Devons and L. J. B. Goldfarb, Handbuch der Physik, Vol. **42** (Springer, 1957) p. 362

2.L *Nuclear Physics* **13** (1959) 397—406; © *North-Holland Publishing Co., Amsterdam*
Not to be reproduced by photoprint or microfilm without written permission from the publisher

DIFFUSIONS ÉLASTIQUES ET INÉLASTIQUES DE PROTONS DE 11 MeV SUR LES ISOTOPES ^{64}Zn, ^{66}Zn, ^{68}Zn

R. BEURTEY, P. CATILLON, R. CHAMINADE, H. FARAGGI, A. PAPINEAU et J. THIRION

Section des Réactions Nucléaires à Moyenne Energie,
C.E.N. *Saclay, Gif sur Yvette* (*S. & O*), *France*

Reçu le 22 juin 1959

Abstract: The elastic and inelastic scattering of 11 MeV protons on separated isotopes of zinc (64, 66, 68) is presented. The curves of elastic scattering exhibit differences which will be compared with theoretical curves in a later article. Inelastic spectra with good resolution are studied and the curves corresponding to the first excited state obtained. Theoretical computations are in progress.

1. Introduction

L'étude de la diffusion élastique des protons sur des isotopes séparés [1]) semble indiquer, dans plusieurs cas, des différences de distributions angulaires difficiles à attribuer à une variation monotone du rayon des noyaux. Les données expérimentales étant encore fragmentaires, l'interprétation reste à faire. Nous avons étudié les diffusions élastiques sur les trois isotopes pairs du zinc (64, 66, 68).

La diffusion inélastique sur ces trois isotopes a été également étudiée. En particulier, il a été possible d'obtenir des distributions angulaires précises concernant le premier niveau excité dans chacun des cas. Si la comparaison avec la théorie des sections efficaces absolues est difficile, du moins devrait-il être possible de rendre compte des variations de sections efficaces entre les divers isotopes, les niveaux ayant les mêmes caractéristiques et pratiquement les mêmes énergies d'excitation. Les expériences déjà faites concernent ^{54}Fe, ^{56}Fe, ^{65}Cu, ^{58}Ni, ^{66}Zn [2]); en outre, de nombreuses expériences [3]) ont porté sur le niveau excité du carbone-12. Dans ce dernier cas, une interprétation complète a été donnée par Levinson et Banerjee [4]) et les mesures de diffusion élastique montrent que la contribution de niveaux particuliers du noyau composé ne peut être négligée. Dans les autres cas mentionnés, les calculs de Hayakawa et Yoshida [5]) montrent bien qu'il s'agit d'interaction directe, mais il n'existe pas d'interprétation aussi complète que celle de Levinson et Banerjee. La présomption que les niveaux particuliers du noyau composé sont sans influence est ici grandement justifiée a priori; elle est

d'ailleurs contrôlable en étudiant des diffusions élastiques à des énergies voisines et en constatant que les distributions angulaires sont effectivement très semblables; c'est ce que nous avons constaté dans le cas des trois isotopes du zinc.

2. Ensemble Expérimental

2.1. FAISCEAU

Le faisceau de protons du cyclotron de Saclay [6]) est focalisé sur des fentes objet, puis analysé par un aimant à gradient $n = \frac{1}{2}$ [7]). Celui-ci donne une définition en énergie de 2×10^{-3} pour une largeur des fentes objet et image de 2 mm. Dans une première série de mesures, l'énergie était 11.10 ± 0.05 MeV. Cette énergie a été abaissée à 10.45 ± 0.02 MeV en plaçant un absorbant de béryllium près des fentes objet.

2.2. CHAMBRE À CIBLES

Elle est cylindrique ($\phi = 170$ mm), de hauteur 115 mm; elle contient un collimateur limitant la hauteur du faisceau à 6 mm et un porte-cibles manœuvrable sous vide, susceptible de contenir 4 cibles. Deux fenêtres de Mylar de 10 mm de hauteur, d'épaisseur 2.5/100 mm permettent l'étude des particules diffusées de 15° à 165°. La chambre est supportée par une colonne centrale de même axe vertical, autour duquel un bras supportant l'ensemble de détection peut pivoter. Ce bras supporte des diaphragmes de définition angulaire de détection, de largeur 6 mm, le premier à 90 mm de l'axe, le second à 120 mm.

A l'opposé du collimateur, est située une cage de Faraday doublée intérieurement de graphite, comportant un anneau porté à -500 V pour éliminer l'influence de l'émission secondaire d'électrons qui ne serait d'ailleurs que de 2 % sans cette précaution.

Un orifice de monitorage se trouve à 20° dans la direction perpendiculaire au plan d'observation. Un scintillateur NaI(Tl) et un photomultiplicateur EMI 6097 F suivis d'un amplificateur 2 Mc/s et d'une échelle permettent le monitorage par isolement du pic élastique.

2.3. ENSEMBLE DE DÉTECTION [8])

A partir de la fenêtre de Mylar, on trouve successivement (fig. 1):

(a) un dispositif de mesure de perte d'énergie de la particule. Nous avons utilisé la scintillation dans CsI(Tl) qui est proportionnelle à dE/dx pour de grandes variations de cette quantité. Le scintillateur est obtenu par évaporation sous vide qui permet de fabriquer une lame de 2/100 mm d'épaisseur; il est placé au centre d'un réflecteur en aluminium et suivi d'un photomultiplicateur 6292 DuMont. La largeur à mi-hauteur des impulsions est de 20 % pour une perte d'énergie de 300 keV.

(b) un dispositif de mesure de l'énergie. Cette mesure se fait à l'aide d'un deuxième scintillateur clivé carré de NaI(Tl), d'épaisseur 2 mm, de 10 mm de côté, scellé hermétiquement dans un boîtier comportant une fenêtre d'entrée en mica aluminé de 2 mg/cm². Ce scintillateur n'a subi aucune évolution mesurable depuis un an.

Un photomultiplicateur EMI 6097 F, sélectionné en uniformité et en sensibilité de photocathode, est suivi, comme pour le premier détecteur, d'un amplificateur à double mise en forme par ligne à retard, permettant un taux de comptage élevé sans dérive. La largeur à mi-hauteur obtenue est comprise entre 1.5 et 2 % suivant le straggling introduit par l'absorption due à l'air et aux fenêtres.

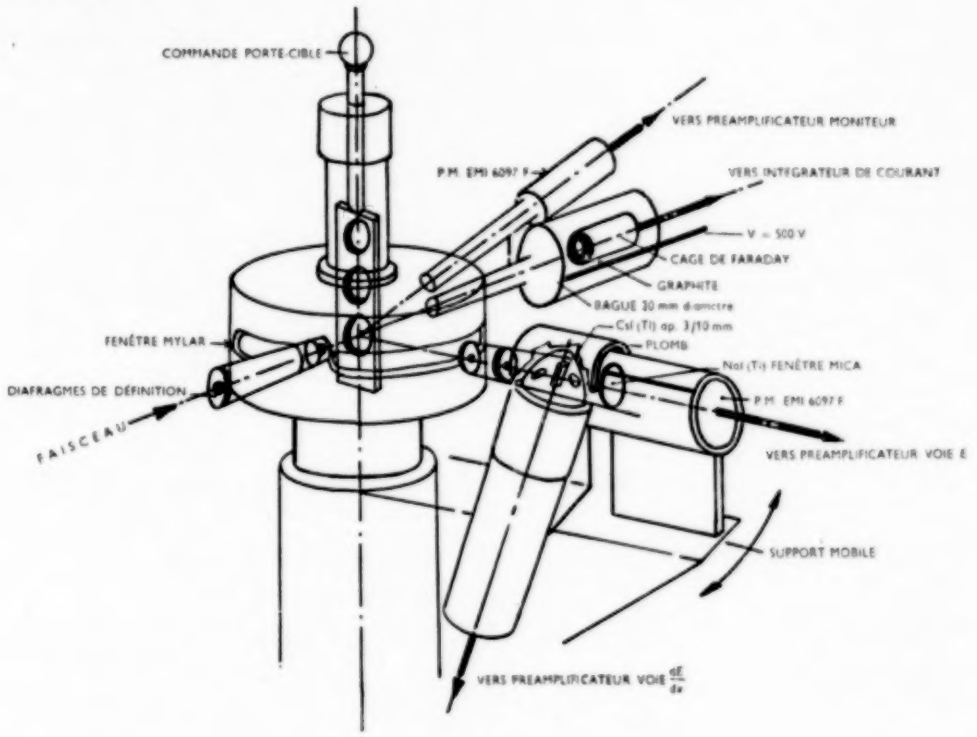

Fig. 1.

2.4. SÉLECTION DES PARTICULES ÉMISES

La sélection des particules se fait en fonction du produit $E\mathrm{d}E/\mathrm{d}x$ en utilisant un dispositif électronique dérivé de celui utilisé par Aschenbrenner [9]).

Un tube à rayons cathodiques, alimenté par une haute tension stabilisée, est attaqué symétriquement sur les plaques de déviation horizontale par les impulsions rectangulaires symétriques issues de l'amplificateur couplé au scintillateur mince. La paire de plaques de déflexion verticale est excitée symétriquement par les impulsions rectangulaires symétriques sortant de l'amplificateur mesurant l'énergie de la particule diffusée. Le wehnelt de ce tube est excité après retard convenable par les impulsions d'un circuit à coïncidences relié aux deux amplificateurs précités. Un même type de

particules se présente sur l'écran dans une zone hyperbolique correspondant à un produit $E\mathrm{d}E/\mathrm{d}x$ approximativement proportionnel à MZ^2, c'est-à-dire sensiblement constant pour un type donné de particules.

Un guide de lumière associé à des caches convenablement placés collecte les impulsions lumineuses obtenues sur la zone présélectionnée pendant la commande du wehnelt et les dirige vers un photomultiplicateur. Les impulsions de celui-ci commandent, après mise en forme, l'ouverture de l'analyseur à 256 canaux dont l'entrée est reliée à l'amplificateur mesurant l'énergie des particules étudiées.

2.5. MATIÈRE DES CIBLES

La matière des cibles a été fournie par le groupe de séparation isotopique de Harwell. Les cibles sans support ont été préparées à Saclay par évaporation sous vide, selon la méthode employée par Prugne [10]).

3. Résultats

3.1. SPECTRE DES PROTONS DIFFUSÉS

Les figures 2 (a, b, c) montrent trois exemples de spectres obtenus. Le premier pic inélastique est parfaitement séparé, sauf dans la zone d'angles de

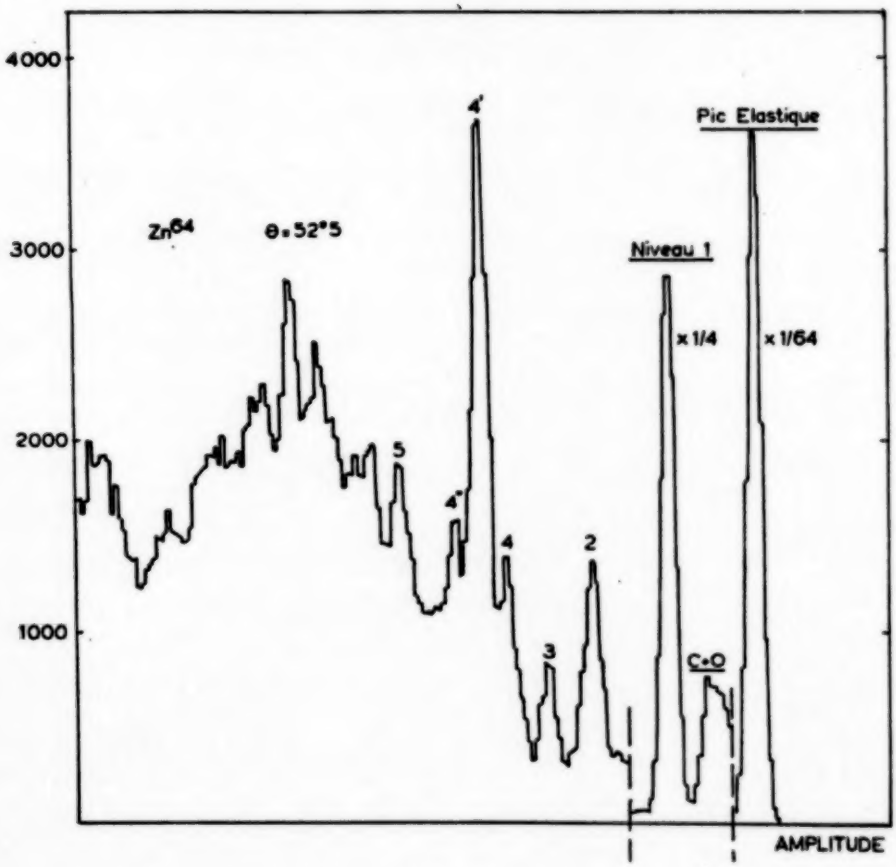

Fig. 2a.

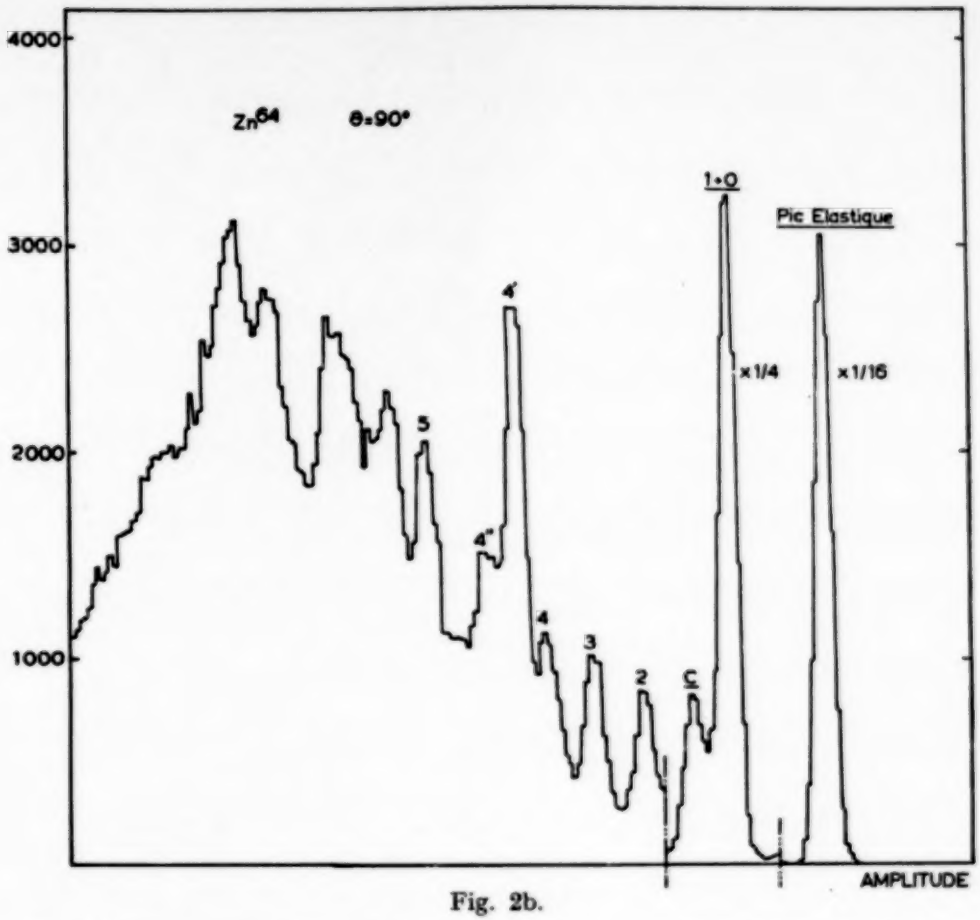
4000
3000
2000
1000
Zn^{64} θ=90°
1+0
Pic Elastique
×1/4
×1/16
5
4'
4''
4
3
2
C
AMPLITUDE

Fig. 2b.

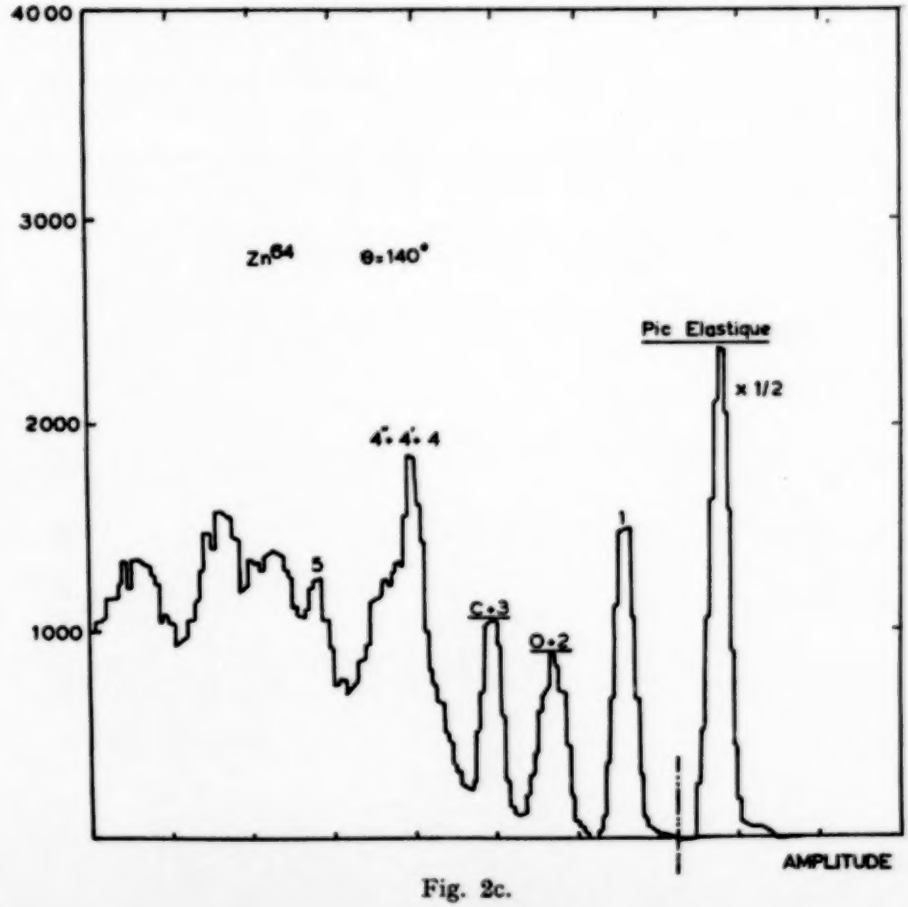
4000
3000
2000
1000
Zn^{64} θ=140°
Pic Elastique
x 1/2
4''+4'+4
5
C+3
O+2
1
AMPLITUDE

Fig. 2c.

75 à 115° où les pics parasites dus à la diffusion élastique sur l'oxygène et le carbone viennent graduellement se superposer. La diffusion élastique sur le carbone et l'oxygène a été mesurée dans une expérience séparée; les résultats

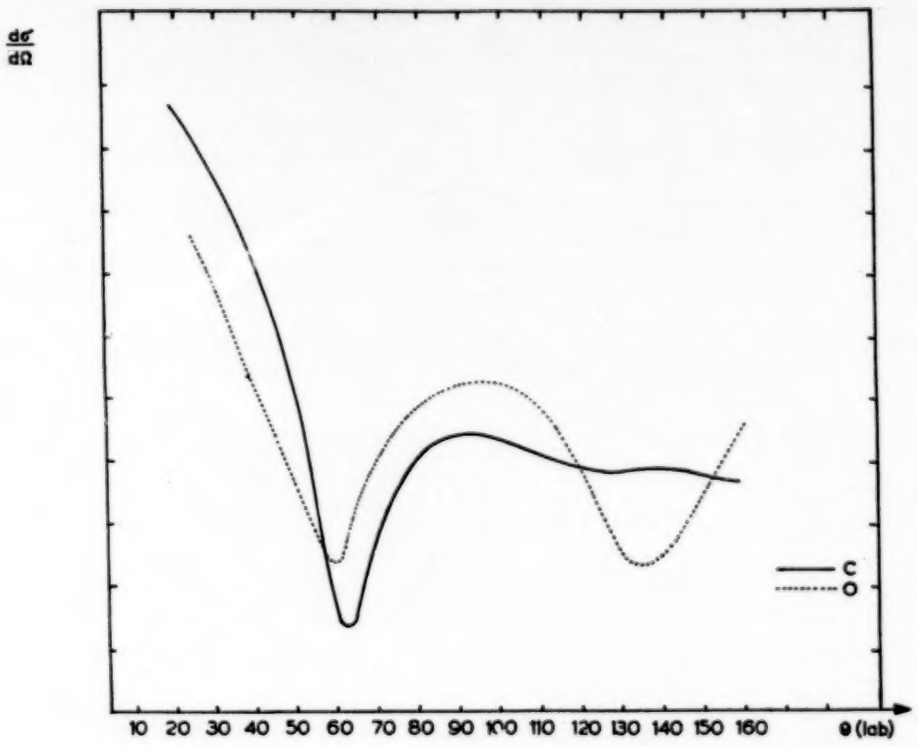

Fig. 3.

sont présentés sur la figure 3. Les proportions d'oxygène et de carbone des cibles sont obtenues sur les spectres aux angles supérieurs à 115°, les pics correspondants étant alors entièrement séparés. Il est alors facile de sous-

TABLEAU 1

Énergies des premiers niveaux excités

	No	1	2	3	4'
^{64}Zn	Nos mesures	0.995±0.03	(1.79±0.04)	(2.29±0.05)	2.93±0.05
	Van Patter *et al.*[11])	0.991			
	Sinclair *et al.*[12])	1.000	1.77		
	Temmer et Heydenburg[13])	1.00			
^{66}Zn	Nos mesures	1.055±0.03	(1.89±0.04)	(2.41±0.05)	2.87±0.05
	Van Patter *et al.*[11])	1.038			
	Sinclair *et al.*[12])	1.051	1.89		
	Temmer et Heydenburg[13])	1.04			
^{68}Zn	Nos mesures	1.075±0.03	(1.60±0.04)	(2.40±0.05)	2.76±0.05
	Van Patter *et al.*[11])	1.078			

Énergies en MeV.

traire les contributions dues à C et O dans la zone angulaire où les pics sont confondus.

Il faut remarquer, pour les trois isotopes, outre ce premier pic simple, la présence d'un certain nombre de groupes de protons diffusés inélastiquement correspondant à des énergies *moyennes* d'excitation, indiquées sur le tableau 1. On voit, en particulier, que le pic n° 4' est fortement excité.

En plus des références indiquées sur le tableau, signalons la concordance de nos résultats avec les valeurs obtenues par $^{63}Cu(p, \gamma)$ et $^{65}Cu(p, \gamma)$ par Weller et Grosskreutz [14]).

La distribution angulaire du pic n° 1, seule précise, sera seule présentée.

3.2. DIFFUSION ÉLASTIQUE

Les résultats sont présentés sur les figures 4, 5. L'étalonnage absolu a été réalisé en mesurant l'épaisseur des cibles par ralentissement des alpha du

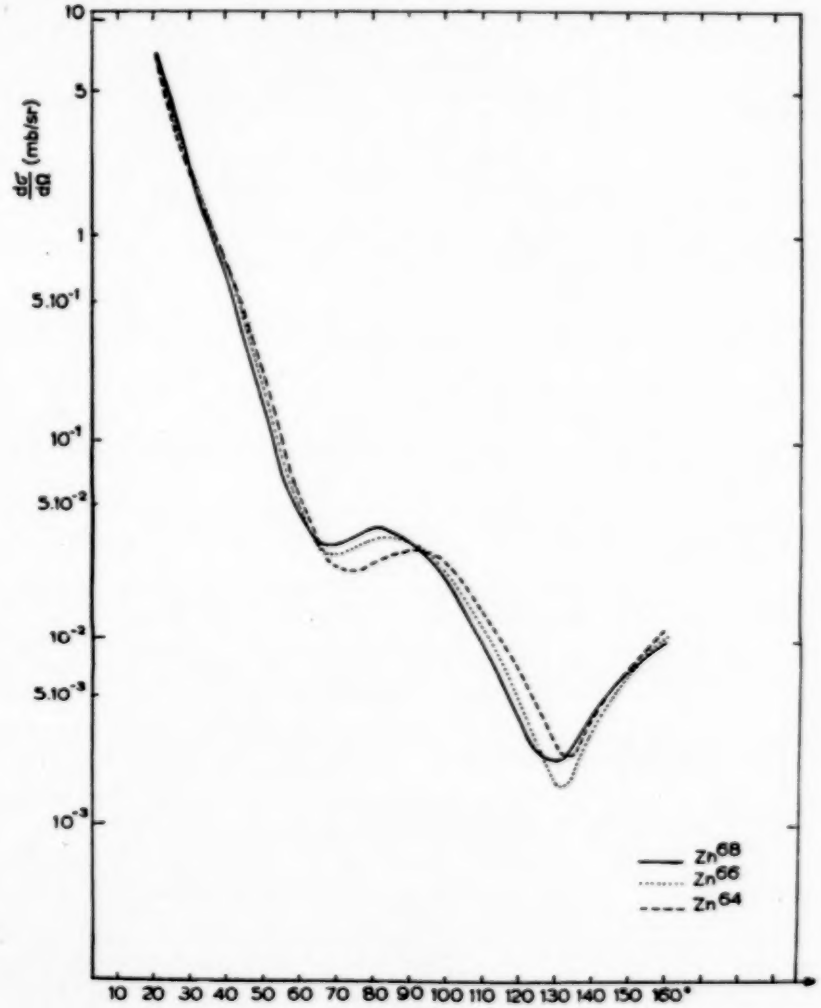

Fig. 4.

thorium; ce ralentissement a été préalablement calibré par des cibles de zinc naturel d'épaisseurs connues par pesée. Nous avons trouvé pour $(\sigma/\sigma_{\text{Ruth}})_{20°}$ la valeur 0.72, la même pour les trois zincs aux erreurs de mesure près ($\pm$ 6 %).

On constate que les déplacements des minima d'un isotope à l'autre sont trois fois supérieurs à ceux prédits par la théorie simpliste de la diffraction par

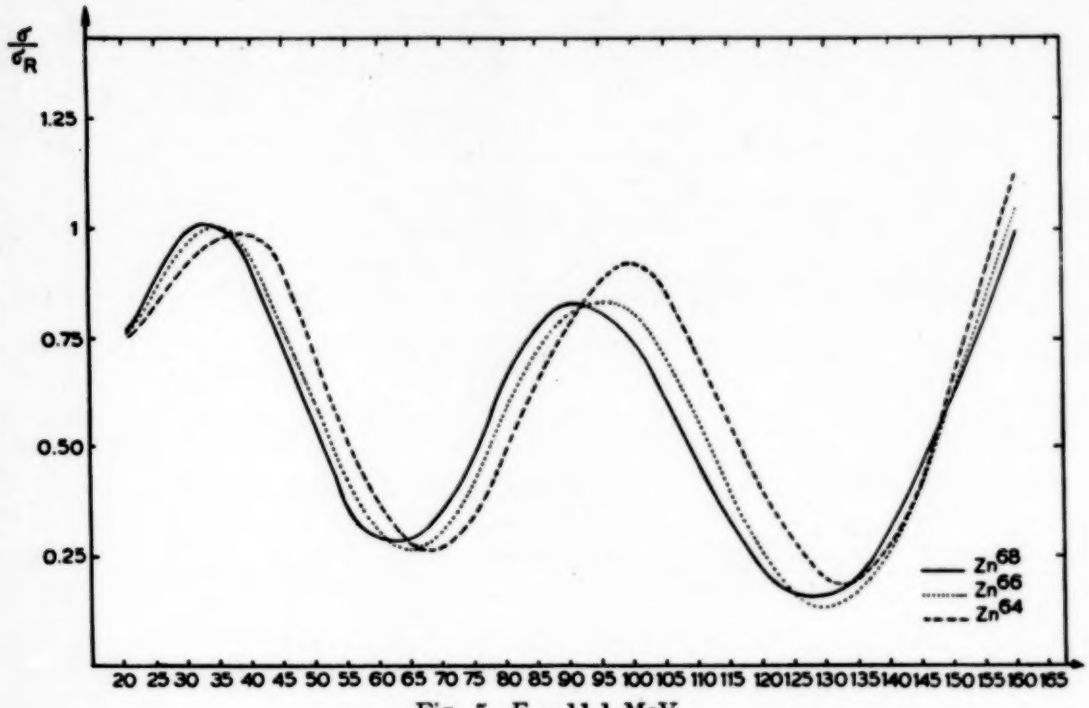

Fig. 5. E_p=11.1 MeV.

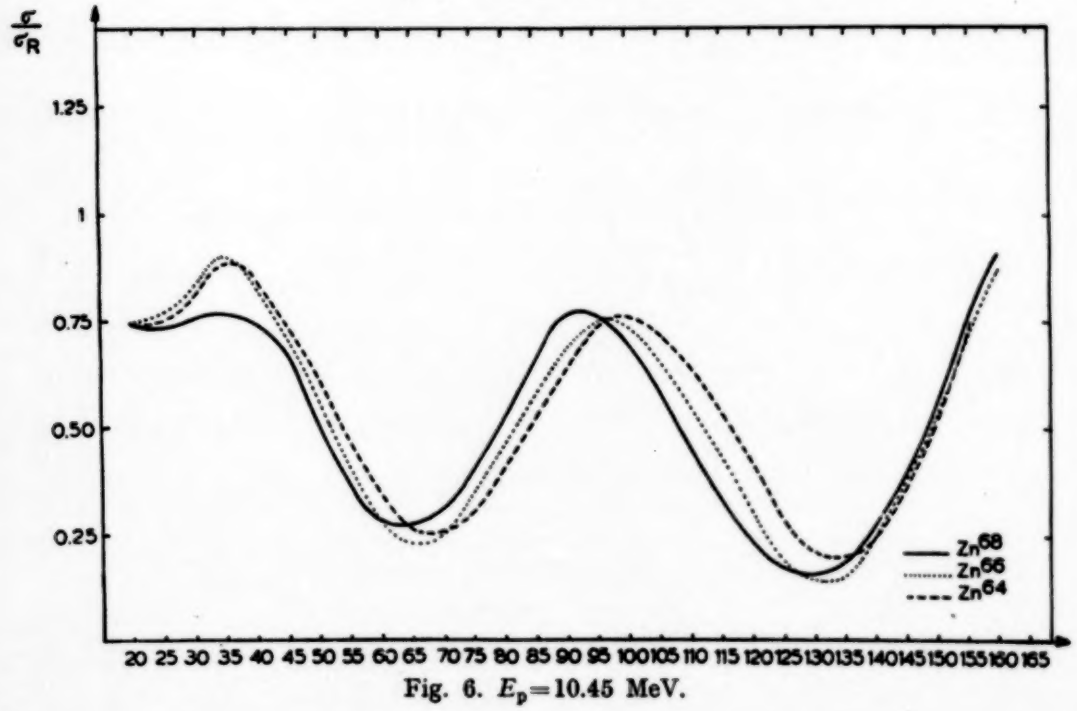

Fig. 6. E_p=10.45 MeV.

un noyau totalement absorbant en supposant une loi en $A^{\frac{1}{3}}$ pour la variation du rayon. Les résultats des calculs entrepris à Saclay (utilisant un potentiel complexe et une surface diffuse) seront prochainement publiés et permettront de tirer des conclusions sûres. Les premiers résultats semblent donner un déplacement théorique des minima légèrement inférieur à celui constaté expérimentalement toujours en supposant une loi en $A^{\frac{1}{3}}$ pour la variation du rayon. La valeur expérimentale de $\sigma/\sigma_{\text{Ruth}}$ à 20° est en bon accord avec les résultats théoriques de Glassgold [16]).

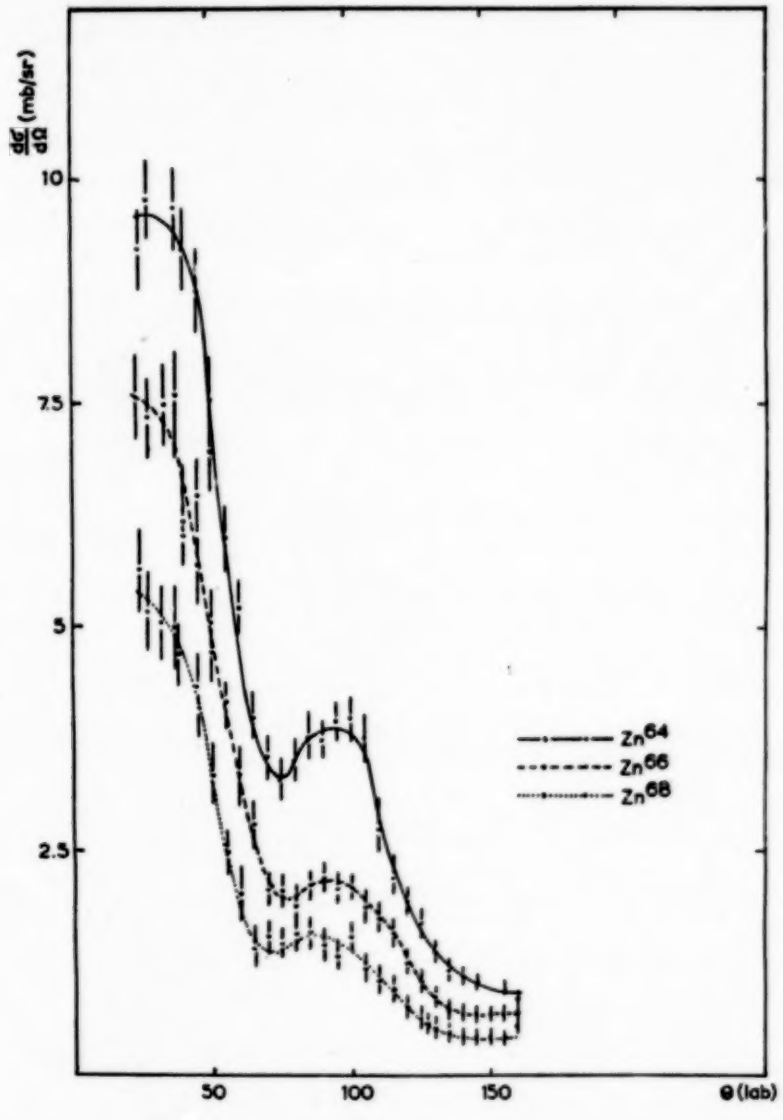

Fig. 7.

Des mesures semblables effectuées à une énergie $E_p = 10.45$ MeV sont présentées sur la figure 6. On constate que l'allure des courbes est la même que celle obtenue à 11.1 MeV. Il ne semble donc pas y avoir de contribution appréciable due à une éventuelle résonance étroite.

3.3. DIFFUSION INÉLASTIQUE

La figure 7 présente les courbes de distributions angulaires relatives au premier niveau. Les courbes présentent une distribution préférentielle vers l'avant du type interaction directe. Les ondulations semblent indiquer le rôle d'une surface diffuse du noyau.

Les trois transitions sont du type $0+ \rightarrow 2+$. Les niveaux $2+$ ont un aspect collectif, les transitions E2 mesurées par excitation coulombienne étant notablement plus rapides que les transitions à une particule. Les valeurs de $B(\mathrm{E2})/B(\mathrm{E2})_{\mathrm{sp}}$ sont, d'après Alder *et al.*[16]), pour ^{64}Zn: 15, pour ^{66}Zn : 11. Comme dans les théories simplifiées (approximation de Born) d'interaction directe du type surface, les transitions sont proportionnelles au carré de la déformabilité du noyau, un rapport peut exister entre les sections efficaces de diffusion inélastique et les valeurs de $B(\mathrm{E2})$. Les courbes présentées supportent cet argument qualitatif. Malheureusement la valeur de $B(\mathrm{E2})$ de ^{68}Zn n'est pas connue.

Nous tenons à remercier vivement l'équipe du Cyclotron pour son impeccable fonctionnement, ainsi que Mlle M. Marçay qui a assuré la fabrication des cibles et Mme M. Cros qui contribua à la mise au point de l'ensemble de détection.

Bibliographie

1) R. A. Vanetsian *et al.*, Comptes rendus Congrès Int. Phys. Nucl., Paris 1958, p. 607 (éditions Dunod, Paris, 1959)
2) Univ. Minnesota, Ann. Progr. Rep. mars 1958, p. 39;
T. Tamura et D. C. Choudhury, Phys. Rev. **113** (1959) 552
3) W. E. Burcham *et al.*, Phys. Rev. **92** (1953) 1266
4) C. A. Levinson et M. K. Banerjee, Ann. Physics **2** (1957) 471
5) Hayakawa et Yoshida, Proc. phys. Soc. **68** (1955) 656
6) Bariaud et Roche (á paraître)
7) Thirion et Saudinos (à paraître)
8) Chaminade (à paraître)
9) F. Aschenbrenner, Phys. Rev. **98** (1955) 657
10) P. Prugne *et al.*, J. Phys. Radium **16** (1955) 730
11) D. M. van Patter *et al.*, Phys. Rev. **107** (1957) 171
12) Sinclair *et al.*, Research Report 60 (1956) 945
13) G. M. Temmer et N. P. Heydenburg, Phys. Rev. **104** (1956) 967
14) C. E. Weller et J. C. Grosskreutz, Phys. Rev. **102** (1956) 1149
15) A. E. Glassgold *et al.*, Phys. Rev. **106** (1957) 1207
16) Alder *et al.*, Revs. Mod. Phys. **28** (1956) 536

2.F *Nuclear Physics* **13** (1959) 407—419; © *North-Holland Publishing Co., Amsterdam*
Not to be reproduced by photoprint or microfilm without written permission from the publisher

$C^{12}(p, 2p)B^{11}$ IN THE IMPULSE APPROXIMATION

K. F. RILEY
Cavendish Laboratory, Cambridge University

Received 29 June 1959

Abstract: The cross-section for $C^{12}(p, 2p)B^{11}$ is calculated on the basis of the impulse approximation using a W.K.B. method, in which absorption is taken into account. The effects of reflection and refraction are discussed, and the former is treated approximately. The effect of finite energy resolution on the observed angular distribution of the two protons is found.

1. Introduction

Recently, experiments have been carried out to investigate reactions of the type

$$\text{Nucleus}_A^Z + \text{p} \rightarrow \text{Nucleus}_{A-1}^{Z-1} + 2\text{p}.$$

In this paper we calculate the differential cross-sections for this process on the assumption that it is a direct reaction and that the impulse approximation applies.

Experiments at Uppsala [1]) at 185 MeV have been carried out for small values of A, in the range 7—16, whilst for medium sized nuclei, e.g. Ni, measurements have been made at Minnesota at 40 MeV [2]). Further experiments at 80 MeV and 140 MeV at A.E.R.E., Harwell, and at 380 MeV at Liverpool, are either under way or being planned. The results at 185 MeV and 40 MeV differ considerably, but perhaps not unexpectedly, in view of the differences in energy and in target nuclei. Whilst at the higher energy, it was found that a shell model could reasonably explain the results, the measurements at 40 MeV could only be fitted by ascribing to the struck proton a momentum much less than it would have if the shell model were applicable. It was suggested [2]) that the differences between the two sets of results could be mainly ascribed to absorption restricting the interaction to take place on the nuclear edge.

Other authors [3]) have considered the reaction from the viewpoint that the interaction takes place in the 'rim' of the nucleus and assume that, because of absorption, no interaction which would require any one of the protons to pass through the central part of the nucleus can make any contribution to the cross-section. This approach, however, is only correct in the extreme limit of total absorption, which is not in practice the case.

We assume that the incident proton and the outgoing protons move in a complex potential and that the internucleon collision takes place throughout the nuclear volume. We calculate the cross-section for the reaction in a first order W.K.B. approximation and use a square well for the complex potential. This choice of well shape is discussed later. The t-matrix elements for the nucleon-nucleon interactions are obtained by suitably transforming matrix elements derived from free p—p scattering data. The influences of refraction and reflection are discussed and the effect of the latter is treated approximately. Finally the effect of conservation of isobaric spin is considered.

2. Physical Assumptions

We consider clean knock-out processes, which leave the remainder of the nucleus unaffected. On the basis of the shell model, when the knocked-out proton comes from the outermost shell of the target nucleus, this will be the case, and the final state of the nucleus will be its ground state. This assumes that the residual nucleons in the outer shell are left in a state of coupled angular momenta which is the ground state of the final nucleus. Such an assumption implies that the fractional parentage coefficient to this state is dominant. This is likely to be a good approximation if the nearest excited state is several MeV away. If an inner shell nucleon is ejected the residual nucleus will be left in an excited state and rearrangement will take place. For sufficiently energetic nucleons, the decay time of this excited state will be long compared with the time taken for the nucleons to leave the nucleus, and for the purposes of calculating the matrix element for the reaction, the excited state of the nucleus can be taken as the final state. Our calculations are for a reaction proceeding directly to the ground state of the final nucleus, and accordingly, the only rearrangement to be considered is that due to the nucleus contracting to its new size; the effect of this, however, will be small and has been disregarded.

In order to make specific calculations, we have replaced the nuclear potential by an equivalent spin independent square well, in so far as strength and size are concerned. We have neglected refraction of the nucleons caused by the changing nuclear potential, an assumption that will be more justified, the higher the energy of the nucleon considered. The effects of refraction are considered further in the discussion of the results.

Coulomb effects are neglected, but at the energies considered, the error due to this should not be serious. The calculation as it stands applies, apart from minor changes, equally well to (n, 2n) reactions, for which no approximations are required for Coulomb effects; practically, however, such experiments are much more difficult to perform than (p, 2p).

3. The Cross Section

In the following work, we use the subscripts 0 and 3 to indicate the incident and struck nucleon respectively, before the collision; 1 and 2 will refer to the two final nucleons and n will denote the recoiling nucleus. In the W.K.B. approximation the cross-section for a system consisting initially of an unpolarized proton of momentum $\hbar\mathbf{k}_0$ and a nucleus of A nucleons initially at rest, going into a state consisting of 2 protons with momenta between $\hbar\mathbf{k}_j$ and $\hbar\mathbf{k}_j+\hbar\mathrm{d}\mathbf{k}_j (j = 1, 2)$ and a recoil nucleus of $A-1$ nucleons is

$$\frac{\mathrm{d}^2\sigma_{12,0}}{\mathrm{d}\mathbf{k}_1\mathrm{d}\mathbf{k}_2} = \frac{2\pi}{\hbar}\frac{1}{v_0}\delta(E_0-E_1-E_2-E_n-E_b)|t_{03,21}|^2\sum_{fm}|g'(\mathbf{k}_0, \mathbf{k}_1, \mathbf{k}_2)|^2, \quad (3.1)$$

where E_b is the binding energy of the struck nucleon and $\sum_{fm}$ indicates summation over spins and final states; $t_{03,21}$ is the t-matrix element for the internucleon collision, and

$$g'(\mathbf{k}_0, \mathbf{k}_1, \mathbf{k}_2) = (2\pi)^{-\frac{3}{2}}\int \mathrm{e}^{i(\mathbf{k}_0-\mathbf{k}_1-\mathbf{k}_2)\cdot\mathbf{r}_1}\psi_f^*(2, \ldots, A)\psi_1(1, \ldots, A)$$

$$\times \exp\left[\sum_{j=0}^{2}\tfrac{1}{2}d_j(\mathbf{r}_1)\left(i\frac{V_jk_j}{E_j}-W_j\left(\frac{2m}{\hbar^2(E_j+V_j)}\right)^{\frac{1}{2}}\right)\right]\mathrm{d}1\ldots\mathrm{d}A, \quad (3.2)$$

where $V_j(k_j)+iW(k_j)$ is the potential depth for a nucleon of energy $E_j = \hbar^2k_j^2/2m$, and $d_j(\mathbf{r}_1)$ is the distance travelled in the potential by the j-th proton to or from the collision point.

The factor

$$\phi(1) = \int\psi_f^*(2, \ldots, A)\psi_1(1, \ldots, A)\mathrm{d}2\ldots\mathrm{d}A \quad (3.3)$$

is the overlap function between the antisymmetrized initial and final wave functions of the nucleus. If an independent particle model is assumed for these two states, the factor $\phi(1)$ reduces to a single particle wave function. However, in the more general case, $\phi(1)$ is essentially a fractional parentage coefficient, and not a single particle wave function. By varying the form of $\phi(1)$ to reach agreement with experiment, we should be able to gain information as to the form of the nuclear wave function.

Since we have assumed that the incident proton is unpolarized and in practice the initial and final orientations of the nucleus are not observed, we average over initial spins and sum over all final states consistent with the struck proton having been initially in the outermost shell of the nucleus.

4. Momentum and Energy Considerations

From conservation of momentum in the laboratory system we have

$$\mathbf{k}_0 = \mathbf{k}_1+\mathbf{k}_2+\mathbf{k}_n. \quad (4.1)$$

A nucleon, upon entering or leaving a potential well, suffers a change in wave number. If we denote the momentum of a nucleon inside the potential by $\hbar\mathbf{k}'$, where for a square well potential $\mathbf{k}'$ is independent of the nucleon's spatial coordinates, then by momentum conservation in the internucleon collision we have

$$\mathbf{k}'_0+\mathbf{k}'_3 = \mathbf{k}'_1+\mathbf{k}'_2. \tag{4.2}$$

However, (4.1) and (4.2) are not independent, since the residual nucleus receives, in addition to momentum $-\mathbf{k}'_3$, a momentum

$$\sum_{j=0}^{2} \pm(\mathbf{k}'_j-\mathbf{k}_j),$$

the + or − sign depending upon whether the j^{th} proton leaves or enters the nucleus, and hence we also have the relationship

$$\mathbf{k}_n = -\mathbf{k}'_3-(\mathbf{k}'_0-\mathbf{k}_0)+(\mathbf{k}'_1-\mathbf{k}_1)+(\mathbf{k}'_2-\mathbf{k}_2) \tag{4.3}$$

which, when substituted in (4.1), yields (4.2).

Further, we have from energy conservation

$$E_0 = E_1+E_2+E_n+E_b. \tag{4.4}$$

It should be noted that, as a result of our assumption that the residual nucleus is left in its ground state, no excitation energy appears in our energy conservation equation.

To simplify the calculation we now further restrict ourselves to events that are coplanar. In view of our neglect of refraction, this simplification means that our results will apply to experiments in which the two counters are in the same plane as the incident proton beam and the target.

With this restriction to coplanarity we can describe the two emergent protons by four quantities k_1, k_2, θ_1 and θ_2, where $\theta_j (j = 1, 2)$ are the angles defined by $\mathbf{k}_j \cdot \mathbf{k}_0 = k_j k_0 \cos\theta_j$, and are such that θ_1 and θ_2 are measured in opposite senses from the axis of the experiment. From (4.1) $\mathbf{k}_n$ is determined in terms of $\mathbf{k}_0$, $\mathbf{k}_1$ and $\mathbf{k}_2$, and hence from (4.4) we see that, if a definite binding energy for the struck nucleon is assumed, only three of the four quantities are independent.

5. Reflection at the Nuclear Surface

When a particle passes from a medium in which its wave number is k into one in which it has wave number k', the transmission coefficient at the boundary is given by

$$T = \frac{4k\cos\phi k'\cos\phi'}{(k\cos\phi+k'\cos\phi')^2},$$

where ϕ is the angle between the direction of motion and the normal at the

boundary. Now, if the angle of refraction is small, $\phi' \approx \phi$ and T becomes

$$T = \frac{4kk'}{(k+k')^2}.$$

This is the form we shall use for T at each crossing of the nuclear boundary by a proton.

6. The t-Matrix Element

We now return to the t-matrix element for the internucleon collision $t_{03,21}$. We have shown the equivalence of the two statements of conservation of momentum, and now use, from (4.3),

$$\mathbf{k}'_0+\mathbf{k}'_3 = \mathbf{k}'_1+\mathbf{k}'_2.$$

We reduce the interaction to the centre of mass system by applying $-\frac{1}{2}(\mathbf{k}'_0+\mathbf{k}'_3)$ to the whole system, and it is then easily shown that the centre of mass scattering angle $\bar{\theta}$ is given by

$$\cos\bar{\theta} = \frac{(\mathbf{k}'_1-\mathbf{k}'_2)\cdot(2\mathbf{k}'_0-(\mathbf{k}'_1+\mathbf{k}'_2))}{|\mathbf{k}'_1-\mathbf{k}'_2||2\mathbf{k}'_0-(\mathbf{k}'_1+\mathbf{k}'_2)|}. \tag{6.1}$$

We now use a non-relativistic expansion of the relativistic transformation of t-matrix elements developed by Møller [4]). If $E_\alpha{}^0$ and $E_\beta{}^0$ are the energies of 2 particles involved in a mutual scattering, before the scattering takes place, in a system of reference s, and $E_\alpha{}^1$, $E_\beta{}^1$ are the corresponding energies after the scattering, and if further a bar $(-)$ indicates the same quantities measured in a different frame of reference $\bar{\mathrm{s}}$, then

$$(\bar{E}_\alpha{}^1\bar{E}_\beta{}^1\bar{E}_\alpha{}^0\bar{E}_\beta{}^0)^{\frac{1}{2}}\langle\bar{k}_\beta{}^1\bar{k}_\alpha{}^1|\bar{t}|\bar{k}_\beta{}^0\bar{k}_\alpha{}^0\rangle = (E_\alpha{}^1E_\beta{}^1E_\alpha{}^0E_\beta{}^0)^{\frac{1}{2}}\langle k_\beta{}^1k_\alpha{}^1|t|k_\beta{}^0k_\alpha{}^0\rangle. \tag{6.2}$$

Now let us take s to be the laboratory system of coordinates and $\bar{\mathrm{s}}$ the centre of mass system of the incident and struck protons. Then we have

$$\bar{E}_\alpha{}^0 = \bar{E}_\beta{}^0 = mc^2+\frac{\hbar^2}{2m}\cdot\tfrac{1}{4}|\mathbf{k}'_0-\mathbf{k}'_3|^2$$

and

$$\bar{E}_\alpha{}^1 = \bar{E}_\beta{}^1 = mc^2+\frac{\hbar^2}{2m}\cdot\tfrac{1}{4}|\mathbf{k}'_1-\mathbf{k}'_2|^2,$$

whilst

$$E_\alpha{}^0, E_\beta{}^0, E_\alpha{}^1, E_\beta{}^1 = mc^2+(\hbar^2k_j'^2)/(2m) \quad \text{for} \quad j = 0, 3, 1, 2,$$

respectively. The indistinguishability of protons 1 and 2 is taken into account by the symmetry between α and β, and the fact that experimentally measured (p, p) cross-sections include the effects due to the necessary anti-symmetry. Hence,

$$(1+\tfrac{1}{4}\gamma|\mathbf{k}'_0-\mathbf{k}'_3|^2)^2(1+\tfrac{1}{4}\gamma|\mathbf{k}'_1-\mathbf{k}'_2|^2)^2|\bar{t}|^2 = \prod_{j=0}^{3}(1+\gamma k_j'^2)|t|^2 \tag{6.3}$$

where $\gamma = \hbar^2/2m^2c^2$.

Now, measurements of free p—p scattering determine the cross-section for a process in which a proton of laboratory momentum $\mathbf{K}_0$ is scattered through a laboratory angle $\frac{1}{2}\theta_{\rm cm}$ into a state of laboratory momentum $\mathbf{K}_1$, with $|\bar{\mathbf{K}}_1| = |\bar{\mathbf{K}}_0| = \frac{1}{2}|\mathbf{K}_0|$. If we denote the t-matrix element for this process by T_{01},

$$\frac{\mathrm{d}\bar{\sigma}_{01}}{\mathrm{d}\bar{\mathbf{K}}_1} = \frac{4\pi}{\hbar}\frac{m}{|\mathbf{K}_0|}\frac{1}{\hbar}|\bar{T}_{01}|^2\,\Delta(\text{Energy}). \tag{6.4}$$

Thus, if we write

$$\mathbf{K}_0 = 2\mathbf{k}'_0 - (\mathbf{k}'_1 + \mathbf{k}'_2), \quad \bar{\mathbf{K}}_1 = \tfrac{1}{2}(\mathbf{k}'_1 - \mathbf{k}'_2), \tag{6.5}$$

we have the required transition in terms of variables for which we know the corresponding cross-section involving the same t-matrix element. Further, after summing over spins and final states, we have

$$\frac{\mathrm{d}\sigma_{21,0}}{\mathrm{d}\mathbf{k}_1\mathrm{d}\mathbf{k}_2} = \sum_{\rm mf}|g'(\mathbf{k}_0, \mathbf{k}_1, \mathbf{k}_2)|^2\frac{\mathrm{d}\sigma_{21,03}}{\mathrm{d}\mathbf{k}_1},$$

where

$$\frac{\mathrm{d}\sigma_{21,03}}{\mathrm{d}\mathbf{k}_1} = \frac{2\pi}{\hbar^2}\frac{m}{k_0}|t_{21,03}|^2$$

and (6.4) can be rewritten as

$$\frac{\mathrm{d}\bar{\sigma}_{01}}{\mathrm{d}\bar{E}_1\mathrm{d}\bar{\Omega}_1} = 4\pi\left(\frac{m}{\hbar^2}\right)^2\frac{|\bar{\mathbf{K}}_1|}{|\mathbf{K}_0|}|\bar{T}_{01}|^2\,\Delta(\text{Energy}). \tag{6.6}$$

Thus, since $|\bar{T}_{01}|^2 = |\bar{t}_{21,03}|^2$, and writing (6.3) as $|t_{21,03}|^2 = F|\bar{t}_{21,03}|^2$ we have, using (6.5) and (6.6)

$$\frac{\mathrm{d}\sigma_{21,0}}{\mathrm{d}E_1\mathrm{d}E_2\mathrm{d}\Omega_1\mathrm{d}\Omega_2} = \frac{mk_1k_2}{\hbar^2|\mathbf{k}'_1 - \mathbf{k}'_2|}\frac{|\mathbf{k}'_0 - \mathbf{k}'_3|}{k_0}\mathrm{F}\frac{\mathrm{d}\bar{\sigma}_{01}}{\mathrm{d}\bar{E}_1\mathrm{d}\bar{\Omega}_1}\sum_{\rm mf}|g'(\mathbf{k}_0, \mathbf{k}_1, \mathbf{k}_2)|^2.$$

It should be noted that although we have written two differentials with respect to energy on the left hand side, there is, because of the necessary energy conservation, only one degree of freedom in the energy, if we take Ω_1 and Ω_2 as independent variables.

We now use the relationship

$$\bar{E}_1 = \bar{E}_0 = \frac{\hbar^2}{2m}\frac{|\mathbf{k}'_0 - \mathbf{k}'_3|}{4} = \tfrac{1}{4}E_{\rm inc}$$

where $E_{\rm inc}$ is the effective incident energy of the bombarding proton to give finally,

$$\frac{d\sigma_{21,0}}{dE_1 dE_2 d\Omega_1 d\Omega_2}$$

$$= \frac{4m}{\hbar^2} \frac{k_1 k_2}{|\mathbf{k}'_1 - \mathbf{k}'_2|} \frac{|\mathbf{k}'_0 - \mathbf{k}'_3|}{k_0} \frac{(1+\frac{1}{4}\gamma|2\mathbf{k}'_0 - (\mathbf{k}'_1+\mathbf{k}'_2)|^2)^2 (1+\frac{1}{4}\gamma|\mathbf{k}'_1 - \mathbf{k}'_2|^2)^2}{\prod_{j=0}^{3}(1+\gamma k_j'^2)}$$

$$\times \frac{d\bar{\sigma}_{01}}{dE_{\text{inc}} d\bar{\Omega}_1}(E_{\text{inc}}, \theta_{\text{cm}}) \sum_{\text{mf}} |g'(\mathbf{k}_0, \mathbf{k}_1, \mathbf{k}_2)|^2. \tag{6.8}$$

In deriving this expression for the cross-section, we have used a t-matrix element for which energy is conserved between the momentum components, whereas in actual fact, energy is not conserved between $\mathbf{k}'_0$, $\mathbf{k}'_3$, $\mathbf{k}'_1$, $\mathbf{k}'_2$. However, since the t-matrix for p—p scattering is fairly constant with regards to both energy and angle, except at low incident energies, this off-energy shell effect should not be serious. Since we are averaging over spins, we may use the free p—p cross-section for unpolarized protons.

7. $C^{12}(p, 2p)B^{11}$

We now consider a specific example, that of the ground state of C^{12} proceeding via a (p, 2p) reaction to the ground state of B^{11}. Carbon has a ground state 0^+, whilst the ground state of B^{11} is $\frac{3}{2}^-$; hence the angular momentum change is $\frac{3}{2}$ and from considerations of parity we have $\Delta l = 1$. Thus, if we take C^{12} to be jj-coupled, this transition is brought about by the ejection of a $p_{\frac{3}{2}}$ proton from the carbon nucleus. We use jj-coupling and take as the ground state wave function for C^{12} an antisymmetrized product of spherical harmonic oscillator wave functions, with parameters chosen to fit electron scattering data [5]). Summation over spins and final states consistent with the ejection of a p-shell proton leads directly to the result

$$\sum_{\text{fm}} |g'(\mathbf{k}_0, \mathbf{k}_1, \mathbf{k}_2)|^2 = \tfrac{4}{3}\{\sum_{\mu=-1}^{1} |g'_{1\mu}(\mathbf{k}_0, \mathbf{k}_1, \mathbf{k}_2)|^2\},$$

where $g'_{1\mu}(\mathbf{k}_0, \mathbf{k}_1, \mathbf{k}_2)$ is (3.2) evaluated with $\phi(1)$, defined by (3.3), put equal to

$$\left(\frac{8\nu^{\frac{5}{2}}}{3\pi^{\frac{1}{2}}}\right)^{\frac{1}{2}} r e^{-\frac{1}{2}\nu r^2} Y_1{}^{\mu}.$$

Consideration of isobaric spin, which, for reactions involving low lying states of light nuclei, is a good quantum number, leads to a further factor in the calculated cross-section. The initial state is a $T = \frac{1}{2}$, $T_3 = \frac{1}{2}$ state. The final state is obtained by coupling the $T = \frac{1}{2}$, $T_3 = -\frac{1}{2}$ state of B^{11} to the $T = 1$, $T_3 = 1$ state of the two protons, to obtain $T = \frac{1}{2}$, $T_3 = \frac{1}{2}$. This gives as our reduction factor

$$(1, 1, \tfrac{1}{2}, -\tfrac{1}{2}|1\ \tfrac{1}{2}\ \tfrac{1}{2}\ \tfrac{1}{2})^2 = \tfrac{2}{3},$$

and the required t-matrix element that for a $T = 1$ state. However, since in the free scattering process, the interaction proceeds wholly through a $T = 1$ state, the required t-matrix element is simply the one given by the free p—p scattering cross-section.

The value of ν used in calculation was 0.3741, and the radius of the potential well 2.4×10^{-13} cm. The dependence of the complex potential depth upon nucleon energy was taken from UCRL 5028, whilst the free p—p scattering cross-section in the centre of mass system, was taken as

$$\frac{\mathrm{d}^2\sigma}{\mathrm{d}\Omega \mathrm{d}E} = \left(1.9 + \frac{230}{E} + \frac{4850}{E^2}\right)(1 + 0.1 \cos^2 \theta).$$

This analytic form is in good agreement with the energy dependence of the cross-section given by Hess [6]), for the range $20 \leqq E \leqq 200$ MeV. A binding energy of 16 MeV for a p-shell proton was assumed.

8. Results and Discussion

Calculations were carried through for an incident proton energy of 80 MeV

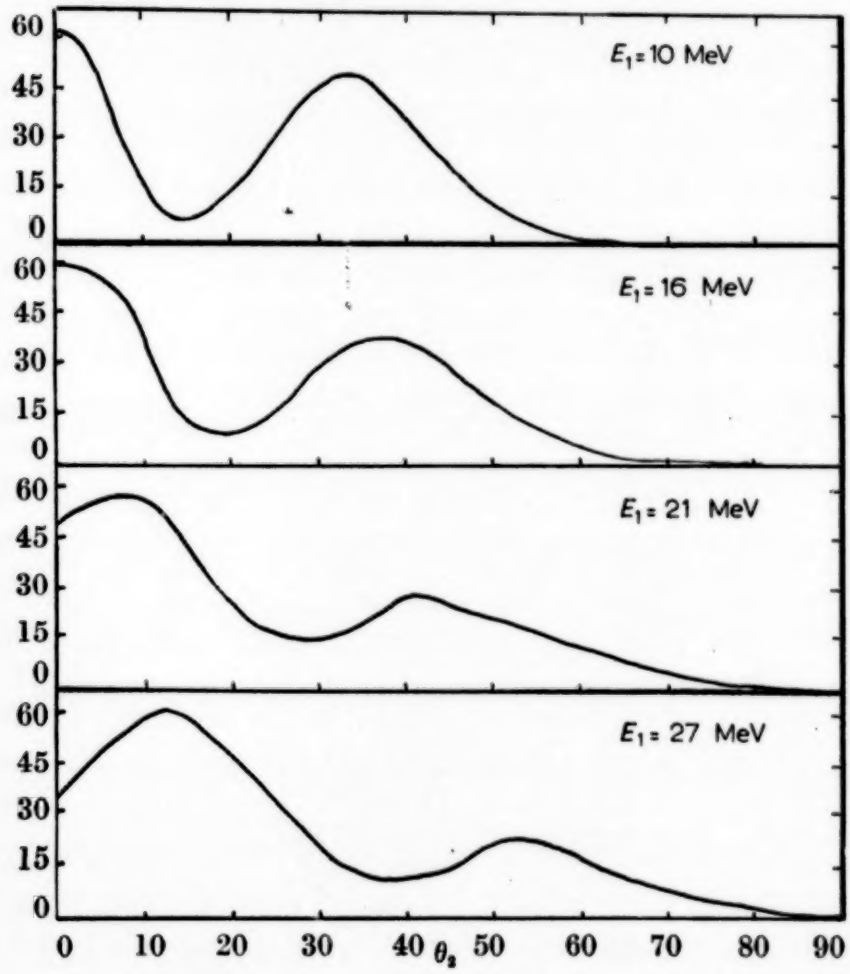

Fig. 1. The cross-section as a function of θ_2 for different values of E_1 with $\theta_1 = 45°$, in units of $\mu\mathrm{b} \cdot \mathrm{sr}^{-2} \cdot \mathrm{MeV}^{-1}$.

and with θ_1 fixed at 45°. The angular variation of the cross-section with θ_2, for various values of the energy E_1, in the range 10—50 MeV, was determined. For each pair of values θ_2 and E_1, E_2, and hece k_2, were found from (4.1) and (4.4). These angular distributions are plotted in figs. 1 and 2.

Bearing in mind that for a p-state spherical harmonic oscillator wave function, the density distribution in **k**-space is zero at the origin, it is easy to

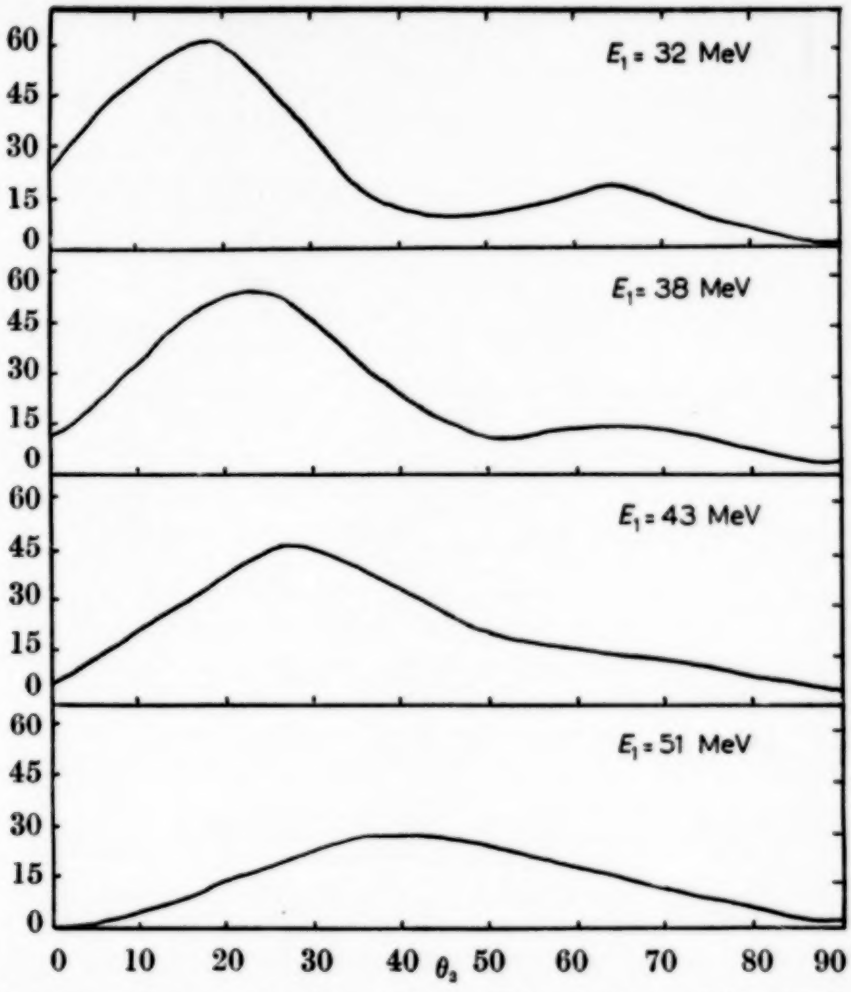

Fig. 2. The cross-section as a function of θ_2 for different values of E_1 with $\theta_1 = 45°$, in units of $\mu b \cdot sr^{-2} \cdot MeV^{-1}$.

understand the general form of the curves. Varying θ_2 and E_1 corresponds to varying the part of the absorption-modified momentum distribution of the struck nucleon which we are examining, and, in particular, the minima in the plotted curves correspond to struck nucleons of almost zero momenta.

The influence of the larger value of the free p—p scattering cross-section at lower relative energies can be seen in fig. 3, which shows the forms of the differential cross section for the actual t-matrix elements (full line) and for a constant t-matrix (broken line), for the case $E_1 \approx E_2$. Smaller values of θ_2 correspond, classically speaking, to the struck nucleon moving in the same

direction as the incident nucleon; hence a smaller relative momentum and larger t-matrix element.

The cross-section for coplanor coincident emission with $\theta_1 = 45°$, integrated over all energies and over θ_2 between 0° and 90° is $1.4\,\mathrm{mb \cdot sr^{-1} \cdot rad^{-1}}$. This is not the total cross-section for $\theta_1 = 45°$ since no account has been taken of cases where both protons leave the nucleus on the same side of the

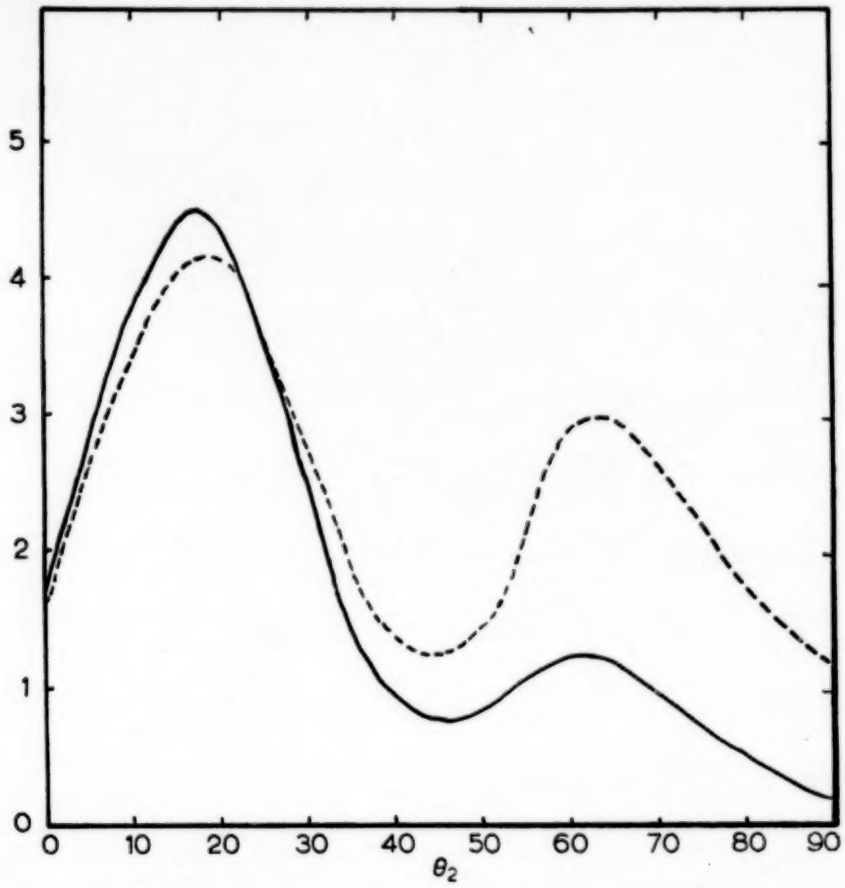

Fig. 3. Variation of the calculated cross-section with the form of the free p—p cross-section, (the experimental p—p cross-section falls with increasing energy). The cross-section is shown for the actual t-matrix (full line) and for a constant t-matrix (broken line). The vertical scales are in arbitrary units.

axis. This contribution will not be negligible since the maximum value of the differential cross-section occurs at $\theta_2 \approx 10°$, i.e. $\theta_1+\theta_2 \approx 55°$, and by not including contributions for $\theta_2 < 0$ we are cutting off the distribution at $\theta_1+\theta_2 = 45°$. However, the value given will apply to any experiment which does not measure events in which $\theta_1+\theta_2 < 45°$ for $\theta_1 = 45°$.

We would expect that for a struck nucleon of 16 MeV binding energy, initially at rest, and equal final energies, the peak in the cross-section would occur at $\theta_1+\theta_2$ given by

$$\cos(\theta_1+\theta_2) = \frac{E_b}{2E_1}.$$

This gives $\theta_1+\theta_2 = 75°$. However, as has been noted above, the most probable value of the momentum of the struck nucleon in a p-shell is not zero and, in general, this causes two peaks in the cross-section, one on either side of $\theta_1+\theta_2 = 75°$. This, together with the larger t-matrix element for smaller relative nucleon-nucleon energies, causes the maximum in the cross-section to move to smaller values of $\theta_1+\theta_2$.

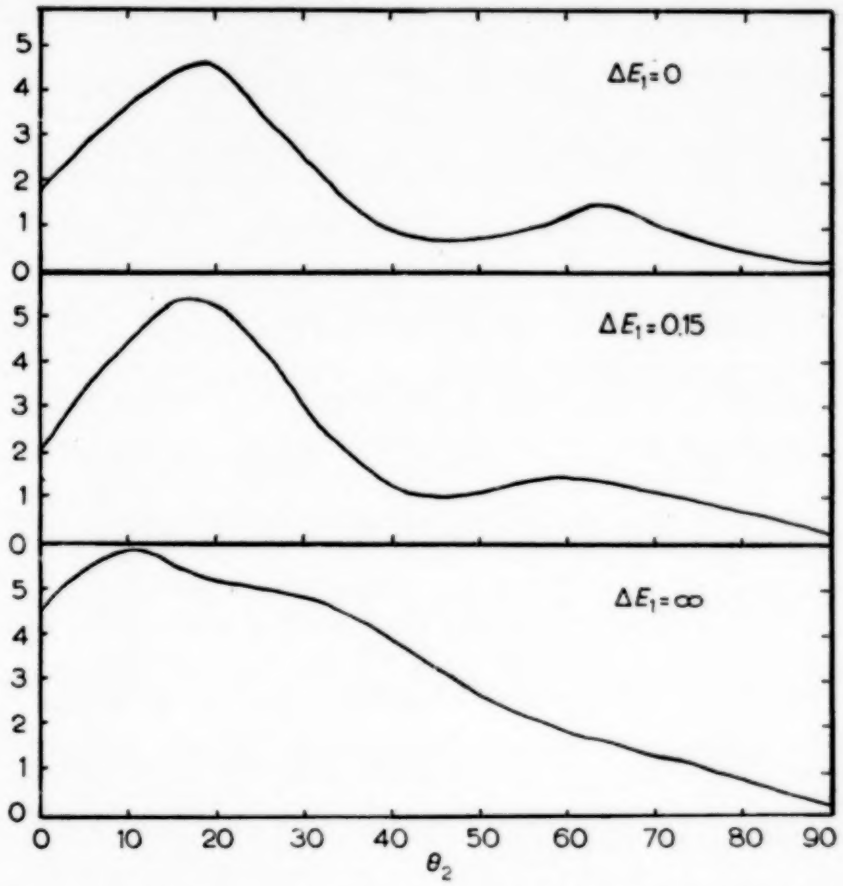

Fig. 4. The cross-section as a function of θ_2 for different values of ΔE_1, with a mean energy for $E_1 = 32$ MeV. The vertical scales are expressed in arbitrary units and are not equal in the three cases.

The choice of spherical harmonic oscillator wave functions will have shortened the tail of the spatial distribution of protons in the target nucleus and this may be important if most of the interactions occur in the outer part of the nucleus. More serious errors may have been introduced by the neglect of refraction, which would have two possible effects. Refraction at the nuclear surface would cause a general smearing out of the angular distribution and might, in extreme cases, cause a shift of the peaks and troughs in the angular distributions. Also, large refraction effects would mean that our treatment of reflection at the nuclear boundary is not sufficiently accurate. The effects due to refraction could be estimated by treating the problem by the method of partial waves.

9. Effects of Energy Resolution

The cross-sections plotted in figs. 1 and 2 are those calculated for perfect energy resolution. This position is not, of course, obtainable in practice and a general smearing out of the observed angular distribution occurs. Fig. 4 shows the effect of different energy resolutions on the cross-section as a function of θ_2, for mean energies $E_1 = E_2 = 32$ MeV. If we define ΔE_1 as the ratio of the full width at half height of the energy resolution curve to the mean energy E_1, then $\Delta E_1 = 0$ represents perfect energy resolution, and $\Delta E_1 = \infty$ gives the case of no energy resolution, or alternatively the angular distribution integrated over energies. The case of $\Delta E_1 = 0.15$ is also shown. As would be expected, as the energy resolution decreases the structure of the cross-section disappears. However, even with $\Delta E_1 = 0.15$, a value that should not be too difficult to attain, and good statistics, some structure should still be observed.

10. Conclusion

An order of magnitude calculation has been carried out for the cross-section in the absence of any effects due to absorption or changes in wave number. It was found that, at 80 MeV, the main effect of absorption was to reduce the cross-section by a factor of the order of 0.03. Absorption also smears out the angular distribution, but, as we have seen, does not eliminate the structure of the cross-section completely. With sufficiently good resolution, both in angle and energy, it should be possible to observe this structure and hence obtain information about the parameters of the nuclear wave function.

Qualitatively, our results agree with those of Maris [7]) for Li^7, although detailed comparison is not possible as he considers only symmetric scattering. Thus, we conclude that the approximation to the exponential factor in (3.2), made by Maris to obtain a closed form expression for the cross-section, is justified.

As has been mentioned previously, probably the least justified physical assumption that has been made is the neglect of refraction, which may, if strong enough, cause displacements of the peaks in the cross-section. A calculation by the method of partial waves, which will take these effects into account is being undertaken by the author and J. Nuttall.

The author wishes to acknowledge the help of the University Mathematical Laboratory in making time available on EDSAC II and to thank Dr. R. J. Eden for much helpful encouragement and for suggesting the problem. This work was carried out whilst the author was a holder of a D.S.I.R. research studentship.

References

1) Th. A. J. Maris, P. Hillman and H. Tyrén, Nuclear Physics **7** (1958) 1
2) R. J. Griffiths and R. N. Eisberg, (to be published)
3) I. E. McCarthy, University of Minnesota Linear Accelerator Progress Report (Nov. 1958)
4) C. Møller, Mat, Fys. Medd. Dan. Vid. Selsk, Nos. 22—23 (1945)
5) R. Hofstadter, Rev. Mod. Phys. **28** (1956) 3
6) W. N. Hess, Revs. Mod. Phys. **30** (1958) 368
7) Th. A. J. Maris, Nuclear Physics **9** (1959) 4

2.L *Nuclear Physics* **13** (1959) 420—434; © *North-Holland Publishing Co., Amsterdam*
Not to be reproduced by photoprint or microfilm without written permission from the publisher

ON DIFFRACTIONAL DISINTEGRATION OF DEUTERONS

A. G. SITENKO and V. K. TARTAKOVSKY
Physico-Technical Institute, Ukranian SSR Academy of Sciences,
Kharkov University, Kharkov

Received 30 March 1959

Abstract: Diffraction disintegration of deuterons on nuclei is considered under the assumption that the radius of the deuteron is appreciably less than that of the nucleus. A differential cross section of the process is determined, giving the energy distribution of the disintegration products in the deuteron's centre-of-mass system and in the laboratory system, their angular distribution, the momentum distribution of the recoil nuclei, and the angular correlation between the disintegration products. The polarization of these particles is likewise considered.

1. Introduction

The interaction of deuterons with nuclei at high energies, when the wave length of the incident deuteron is small compared to the nucleus size, is of diffractional character. Treating the nucleus as a black body and using the analogy with optical phenomena one may evolve a theory of diffractional phenomena arising in deuteron-nucleus interactions. In addition to pure elastic scattering similar to the diffractional scattering of elementary particles, in the case of deuterons there also occurs an inelastic scattering leading to a disintegration of the deuteron into a neutron and a proton. This diffractional disintegration takes place far from the nucleus and is due to the small binding energy of the deuteron [1–4]).

The diffractional disintegration of deuterons can be detected experimentally through energy spectra and angular correlation between neutrons and protons produced in deuteron nucleus interaction. Energy and angular distribution of neutrons and protons liberated in diffractional disintegration of deuterons can be calculated by assuming that the nucleus is absolutely black and that the deuteron radius R_d is considerably smaller than the nucleus radius R. Taking into account the spin-orbit interaction with the nucleus of the neutron and the proton that constitute the deuteron one may find the polarization of the particles released in diffractional disintegration of deuterons.

The present work reports the results obtained on diffractional energy and angular distributions, angular correlation, and polarization of neutrons and protons liberated in diffractional disintegration of deuterons.

2. Differential Cross-Section of Diffractional Disintegration

The cross-section of the deuteron diffractional disintegration, according to ref. [4]), is determined by the following formula:

$$d\sigma = |a_{\varkappa \mathbf{f}}|^2 \frac{d\varkappa}{(2\pi)^2} \frac{d\mathbf{f}}{(2\pi)^3}, \tag{1}$$

where $\varkappa$ and $\mathbf{f}$ are the wave vectors of the centre-of-mass motion and of the relative motion of the neutron-proton system in the final state, while $a_{\varkappa \mathbf{f}}$ is the amplitude in the expansion of the diffracted wave function of a deuteron into a series of functions $\varphi_{\mathbf{f}}\psi_{\varkappa}$:

$$a_{\varkappa \mathbf{f}} = -\int e^{-i\varkappa \cdot \varrho_d} I_{\mathbf{f}}(\varrho_d) d\varrho_d, \tag{2}$$

$$I_{\mathbf{f}}(\varrho_d) = \int \varphi_{\mathbf{f}}^*(\mathbf{r})\{\omega_n + \omega_p - \omega_n\omega_p\}\varphi_0(r)d\mathbf{r}. \tag{3}$$

(The notations are the same as in ref. [4]).)

Assuming that the nuclear radius R is considerably larger than the deuteron radius R_d, the curvature of the nucleus boundary can be neglected in (3), i.e., in calculating $I_{\mathbf{f}}(\varrho_d)$ the boundary of the nucleus can be considered plane. In this case, if $\rho_d < R$, the term in brackets in (3) may be taken to be equal to unity, and the integral (3) vanishes owing to the orthogonality of the functions $\varphi_{\mathbf{f}}$ and φ_0. If $\rho_d > R$, the integration in (3) should be performed over the area outside a plane layer of thickness $2(\rho_d - R)$, perpendicular to the normal $\mathbf{n}$ to the boundary of the nucleus:

$$I_{\mathbf{f}}(b) = \int_{|\mathbf{r}\cdot\mathbf{n}|>2b} \varphi_{\mathbf{f}}^*(\mathbf{r})\varphi_0(r)d\mathbf{r}, \quad b = \mathbf{r}\cdot\mathbf{n} - R > 0. \tag{4}$$

Let us take the x-axis along the normal, and the y-axis along the tangent to the boundary of the nucleus shadow. Carrying out the integration in (4) we obtain

$$I_{\mathbf{f}}(b) = \frac{2\sqrt{2\pi\alpha}}{\alpha^2+f^2}\left\{\frac{1}{2P'}\left[(P'-if_x)e^{-2b(P'+if_x)} + (P'+if_x)e^{-2b(P'-if_x)}\right] - \int_1^\infty \frac{e^{-2(\alpha-if)b\xi}}{\xi^2}d\xi\right\}, \tag{5}$$

$$P' = \sqrt{\alpha^2+f^2-f_x^2}.$$

Since in the chosen system of coordinates $I_{\mathbf{f}}(b)$ does not depend on y_d, the integration in (2) over y_d yields a delta-function, and

$$a_{\varkappa \mathbf{f}} = -2\pi\delta(\kappa_y)e^{-i\kappa_x R}\int_0^\infty e^{-i\kappa_x b} I_{\mathbf{f}}(b)db. \tag{6}$$

Substituting this expression into (1) and noticing that $\delta^2(\kappa_y) \to R\delta(\kappa_y)$ (the circumference of the nucleus $2\pi R$ should be taken for the interval of variation of the variable y_d), we find

$$d\sigma = R\left|\int_0^\infty e^{-i\kappa_x b} I_f(b)db\right|^2 \delta(\kappa_y)\,d\varkappa\,\frac{df}{(2\pi)^3}. \tag{7}$$

Introducing cylindrical coordinates $d\varkappa = \kappa d\kappa d\psi$ (the angle ψ is counted from the direction of $\mathbf{n}$) and integrating in (7) over the angle ψ, we obtain, owing to the delta-function,

$$d\sigma = R\left\{\left|\int_0^\infty e^{-i\kappa b} I_f(b)\,db\right|^2 + \left|\int_0^\infty e^{i\kappa b} I_f(b)db\right|^2\right\}\frac{df}{(2\pi)^3}\,d\kappa. \tag{8}$$

The first term in (8) corresponds to parallel orientations of vectors $\varkappa$ and $\mathbf{n}$, the second term to antiparallel orientations of these vectors. Evidently, if we introduce the angle φ between the vector $\varkappa$ and the projection of vector $\mathbf{f}$ on a plane perpendicular to the wave vector of the incident deuteron, then after substituting $f_\perp \cos\varphi$ for f_x in the first term and $-f_\perp \cos\varphi$ for f_x in the second term, we obtain a differential cross-section which does not depend on the choice of the frame of reference. Performing the integration in (8) and introducing dimensionless quantities $\mathbf{u} = \mathbf{f}/\alpha$ and $z = \kappa/2\alpha$, we finally obtain the differential cross-section of the deuteron diffractional disintegration in the form

$$d\sigma = \frac{1}{\pi^2} R R_d \left\{\left|\frac{1}{2P}\left(\frac{P - iu_\perp\cos\varphi}{P + iu_\perp\cos\varphi + iz} + \frac{P + iu_\perp\cos\varphi}{P - iu_\perp\cos\varphi + iz}\right)\right.\right.$$
$$\left. + \frac{i}{z} + \frac{1-iu}{z^2}\ln\frac{1-iu}{1-iu+iz}\right|^2 + \left|\frac{1}{2P}\left(\frac{P + iu_\perp\cos\varphi}{P - iu_\perp\cos\varphi - iz} + \frac{P - iu_\perp\cos\varphi}{P + iu_\perp\cos\varphi - iz}\right)\right.$$
$$\left.\left. - \frac{i}{z} + \frac{1-iu}{z^2}\ln\frac{1-iu}{1-iu+iz}\right|^2\right\}\frac{du}{(1+u^2)^2}\,dz, \tag{9}$$

$$P = \sqrt{1 + u^2 - u_\perp^2\cos^2\varphi}.$$

The wave vectors of the neutron and the proton released in the diffractional disintegration of the deuteron are related to the wave vector $\mathbf{k}$ of the centre of mass and the wave vector $\mathbf{f}$ of the relative motion by means of

$$\mathbf{k}_n + \mathbf{k}_p = \mathbf{k}, \quad \mathbf{k}_n - \mathbf{k}_p = 2\mathbf{f}. \tag{10}$$

Employing these relations we can easily obtain from (9) the differential wave vector distribution of the released particles.

3. Relative Energy Distribution of Disintegration Products

To determine the relative energy distribution in the centre-of-mass system we shall use expression (7). Integration of this expression over $\varkappa$ gives the relative momentum distribution of the deuteron disintegration products:

$$d\sigma = \frac{R}{(2\pi)^2}\int_0^\infty db|I_f(b)|^2 df. \tag{11}$$

Integrating over b and going over to the dimensionless vector $\mathbf{u} = \mathbf{f}/\alpha$, we obtain

$$d\sigma = RR_d\phi(\mathbf{u})d\mathbf{u}, \tag{12}$$

$$\phi(\mathbf{u}) = \frac{2}{\pi}\frac{1}{(1+u^2)^2}\left\{\frac{2P^4-P^2u_x^2+u_x^4}{4P^3(1+u^2)} - \mathrm{Re}\,\frac{1}{P}\int_1^\infty \frac{d\xi}{\xi^2}\left[\frac{P-iu_x}{(1-iu)\xi+P+iu_x}\right.\right.$$
$$\left.\left. + \frac{P+iu_x}{(1-iu)\xi+P-iu_x}\right] + \int_1^\infty \frac{d\xi}{\xi^2}\int_0^\infty \frac{d\eta}{\eta^2}\frac{1}{(1-iu)\xi+(1+iu)\eta}\right\}. \tag{13}$$

Integration of (12) over the angles of vector $\mathbf{u}$ yields the relative energy distribution. (In calculating the second term in (13) it is convenient to start directly from the expression

$$-\frac{2\alpha^3}{\pi^2}\frac{1}{1+u^2}\mathrm{Re}\int_0^\infty db\int_1^\infty \frac{d\xi}{\xi^2}e^{-2(1+iu)\alpha b\xi}\int_{|x|>2b} d\mathbf{r}\,\frac{e^{-\alpha r}}{r}e^{-i\alpha\mathbf{u}\cdot\mathbf{r}},$$

which should be first integrated over the angles of vector $\mathbf{u}$, after which the remaining integration can be performed.) The resulting formula for the relative energy distribution of the disintegration products has the form

$$d\sigma = RR_d I(u)u\,du,$$

$$I(u) = \frac{2}{(1+u^2)^2}\left(u - \mathrm{arctg}\,u + \frac{2u}{1+u^2}\right) - \frac{32}{3}(1-\ln 2)\frac{u}{(1+u^2)^3}.$$

Fig. 1 shows the dependence of the cross-section on $u = f/\alpha$. The peak in distribution corresponds to $u \approx 0.6$, consequently the average energy of the relative motion of neutron and proton in the diffractional disintegration of a deuteron will, in order of magnitude, be equal to the binding energy of the deuteron.

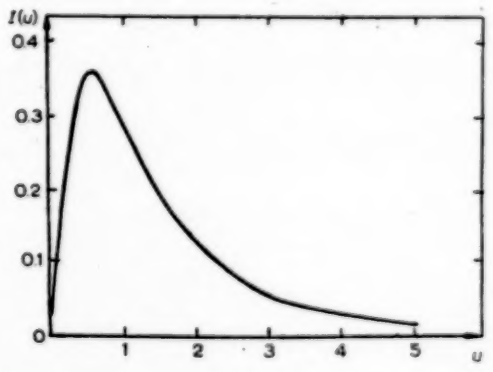

Fig. 1. Relative energy distribution of the deuteron diffractional disintegration products.

4. Energy Distribution of Neutrons and Protons in the Laboratory System

At high energies of incident deuterons the energy distribution of the disintegration products in the laboratory system of coordinates will be

determined by the distribution along the projection of the relative wave vector **u** on the direction of deuteron motion. The neutron energy E_n is related to this projection by

$$u_z = \frac{E_n - \frac{1}{2}E_d}{\sqrt{\varepsilon E_d}}, \tag{15}$$

where E_d is the energy of the incident deuteron. The u_z distribution can be obtained by integrating (12) over the perpendicular components of the vector **u**:

$$d\sigma = RR_d F(u_z)du_z,$$

$$F(u_z) = \int_{-\infty}^{\infty}\int_{-\infty}^{\infty} du_x du_y \frac{2}{\pi(1+u^2)^2}\left\{\frac{2P^4 - P^2u_x^2 + u_x^4}{4P^3(1+u^2)}\right. \tag{16}$$

$$\left. -2\,\frac{P-iu_x}{P}\int_1^{\infty}\frac{d\xi}{\xi^2}\,\frac{\xi+P+iu_x}{(\xi+P+iu_x)^2+u^2\xi^2} + \int_1^{\infty}\frac{d\xi}{\xi^2}\int_1^{\infty}\frac{d\eta}{\eta^2}\,\frac{1}{(1-iu)\xi+(1+iu)\eta}\right\}.$$

If the interaction between neutron and proton in the final state is neglected (i.e. if $\varphi_f(\mathbf{r})$ is replaced by the plane wave $e^{i\mathbf{q}\cdot\mathbf{r}}$), only the first term will remain in the expression between brackets in (16). Integrating over u_x and u_y we obtain in this case the following expression for the distribution function:

$$F^0(u_z) = \tfrac{1}{4}\pi(1+u_z^2)^{-\frac{3}{2}}. \tag{17}$$

It is to be noted that this formula coincides with the formula for the distribution of neutrons stripped from deuterons by non-transparent nuclei [5]).

In calculating the second term in (16) it is convenient to integrate first over u_z by the method of residues; the resulting rational function of ξ can then easily be integrated. In calculating the third term in (16) integration is easier to perform first over ξ and η, and then over $u_\perp$.

We finally obtain the following expression for the energy distribution function of neutrons and protons:

$$F(u_z) = \frac{\pi}{6}\frac{1}{\sqrt{1+u_z^2}} + \frac{11+3u_z^2}{18(1+u_z^2)^2} + \frac{1+9u_z^2}{9(1+u_z^2)^3}\ln\frac{4}{1+u_z^2} \tag{18}$$

$$-\frac{3-16u_z^2-3u_z^4}{9(1+u_z^2)^3}u_z\,\mathrm{arctg}\,u_z + \tfrac{1}{6}(1-3u_z^2)\left[(\mathrm{arctg}\,u_z)^2 - \tfrac{1}{4}\pi^2\right] - u_z\,\mathrm{arctg}\,u_z - \tfrac{1}{2}.$$

Note that the term (17) is cancelled by a part of the second term.

Substituting (18) into (16) and integrating over u_z we obtain the total cross-section of the deuteron diffractional disintegration [3, 4])

$$\sigma_d = \tfrac{1}{3}\pi(2\ln 2 - \tfrac{1}{2})RR_d. \tag{19}$$

The energy distribution of particles in the diffractional disintegration of a deuteron is plotted in fig. 2. The distribution is characterized by a sharp peak at an energy of released particles equal to half the energy of the incident deuteron.

The maximum of distribution (17) is approximately twice higher than the maximum of (18). If, however, the maximum of the distribution, obtained in neglecting neutron-proton interaction in the final state, is normalized with respect to the maximum of the real distribution (18), the resultant distribution will be close to (18). For comparison, a dotted line for such distribution has also been plotted in fig. 2.

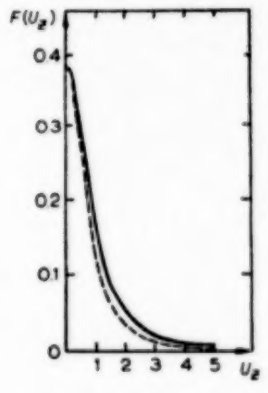

Fig. 2. Energy distribution of the deuteron diffractional disintegration products in the laboratory system.

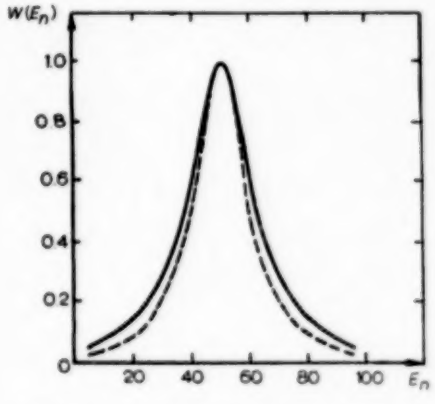

Fig. 3. Energy distribution of neutrons produced in the deuteron diffractional disintegration at 100 MeV.

Fig. 3 shows the energy distribution of neutrons for incident deuterons of 100 MeV. For comparison, the dotted line represents the energy distribution of neutrons produced in stripping reaction for deuterons of the same energy. The width of the energy distribution of neutrons produced in diffractional disintegration is somewhat greater than that of neutrons produced in stripping reaction.

5. Angular Correlation between Neutrons and Protons in Diffractional Disintegration of Deuterons

Angular correlation between neutrons and protons released in diffractional disintegration of deuterons is determined by the distribution along the component of the relative vector **u** perpendicular to the incident deuteron momentum. The modulus of the perpendicular component of vector **u** is connected with the angle between neutron and proton by the relation

$$u_\perp = u \sin \theta.$$

Integrating (12) over different directions of the vector $\mathbf{u}_\perp$ we obtain the u_z and $u_\perp$ distributions

$$\begin{aligned} d\sigma &= RR_0 G(u_\perp, u_z) u_\perp du_\perp du_z, \\ G(u_\perp, u_z) &= \int_0^{2\pi} d\varphi \phi(\mathbf{u}). \end{aligned} \tag{20}$$

First of all let us determine the angular correlation for particles released with energies equal to half the energy of the incident deuteron. For such energies $u_z = 0$ and therefore the correlation will be determined by the $G(u_\perp, 0)$ distribution. Since the u_z-distribution is characterized by a sharp peak at $u_z = 0$, these particles constitute the main contribution to the diffractional disintegration.)

Using expression (13), with the previously performed integration over ξ and η, we obtain the following expression for $G(u_\perp, 0)$:

$$\begin{aligned} G(u_\perp, 0) = \frac{2}{\pi} \Bigg\{ & \frac{(u_\perp^2 - 11) E\left(\frac{u_\perp}{\sqrt{1+u_\perp^2}}\right) + 5K\left(\frac{u_\perp}{\sqrt{1+u_\perp^2}}\right)}{(1+u_\perp^2)^{\frac{5}{2}}} - \frac{4N(u_\perp)}{(1+u_\perp^2)^4} \Bigg\} \\ & + \frac{8}{3} \left\{ \frac{1}{(1+u_\perp^2)^3} + \frac{3u_\perp^2 - 1}{2(1+u_\perp^2)^4} \ln \frac{4}{1+u_\perp^2} + \frac{u_\perp^2 - 3}{(1+u_\perp^2)^4} u_\perp \operatorname{arctg} u_\perp \right\}, \end{aligned} \tag{21}$$

where E and K are complete elliptical integrals while $N(u_\perp)$ is representable as a single integral which cannot be expressed in terms of elementary functions:

$$\begin{aligned} N(u_\perp) = \int_0^\pi \frac{d\varphi}{P} \Bigg\{ & \frac{P(P^2 - 3u_x^2) + u_\perp u_x (u_x^2 - 3P^2)}{2} \ln \frac{1+u_\perp^2}{(P+1)^2 + (u_\perp - u_x)^2} \\ & + [u_x(u_x^2 - 3P^2) - u_\perp P(P^2 - 3u_x^2)] \operatorname{arctg} \frac{u_\perp P + u_x}{P + 1 + u_\perp(u_\perp - u_x)} \Bigg\}, \\ P = \sqrt{1+u_y^2}. \end{aligned}$$

At small angles ($u_\perp \ll 1$) the correlation function $G(u_\perp, 0)$ is approximately expressed by

$$G(u_\perp, 0) = \tfrac{16}{3} \ln 2 - \tfrac{10}{3} - (\tfrac{64}{3} \ln 2 - \tfrac{83}{6}) u_\perp^2 + \ldots, \quad u_\perp \ll 1.$$

If we neglect the neutron-proton interaction in the final state, i.e. drop the second and the third terms between brackets in (13), the $u_\perp$ distribution at $u_z = 0$ will have the form

$$G^0(u_\perp, 0) = \frac{2}{\pi} \frac{(5+u_\perp^2) E\left(\frac{u_\perp}{\sqrt{1+u_\perp^2}}\right) - 3K\left(\frac{u_\perp}{\sqrt{1+u_\perp^2}}\right)}{(1+u_\perp^2)^{\frac{5}{2}}}. \tag{22}$$

The functions $G(u_\perp, 0)$ and $G^0(u_\perp, 0)$ have sharp maxima at $u_\perp = 0$. The ratio of their maxima is

$$G^0(0, 0)/G(0, 0) \approx 5.5.$$

Fig. 4 shows the graphs of the correlation functions $G(u_\perp, 0)$ and $G^0(u_\perp, 0)$. The dotted line refers to $G^0(u_\perp, 0)$ with maximum normalized onto the maximum of $G(u_\perp, 0)$. It is seen that both curves are close to each other.

The total $u_\perp$ distribution can be obtained by integrating (20) over u_z:

$$\mathrm{d}\sigma = RR_\mathrm{d} L(u_\perp) u_\perp \mathrm{d}u_\perp, \quad L(u_\perp) = \int_{-\infty}^{\infty} \mathrm{d}u_z \int_0^{2\pi} \mathrm{d}\varphi \phi(\mathbf{u}). \tag{23}$$

The distribution $L(u_\perp)$ is not obtainable in explicit form. However, one may find an expression for $L^0(u_\perp)$, i.e. for the distribution when only a plane wave

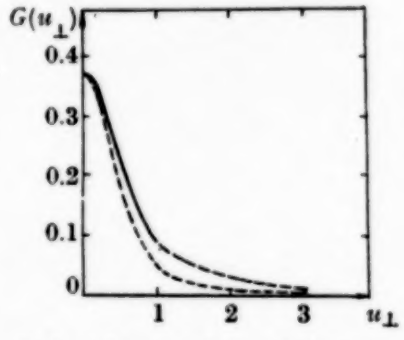

Fig. 4. Angular correlation between neutrons and protons produced in diffractional disintegration of deuterons ($u_z = 0$).

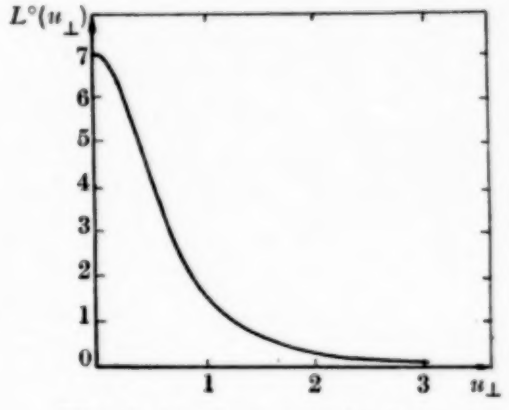

Fig. 5. Angular correlation between neutrons and protons produced in diffractional disintegration of deuterons.

is left in the wave function $\varphi_t(\mathbf{r})$ which describes the relative motion of neutron and proton:

$$L^0(u_\perp) = \frac{2u_\perp^4 + 7u_\perp^2 + 2}{u_\perp^2 (1+u_\perp^2)^{\frac{5}{2}}} - \frac{3u_\perp^2 + 2}{u_\perp^3 (1+u_\perp^2)^{\frac{3}{2}}} \operatorname{arctg} u_\perp. \tag{24}$$

The maximum of the function $L(u_\perp)$ can also be calculated:

$$L(0) = 6G - \tfrac{13}{36}\pi - \tfrac{11}{3}, \tag{25}$$

where G is the Catalan constant equal to 0.915.... The ratio of the distribution maxima $L^0(u_\perp)$ and $L(u_\perp)$ thus equals

$$L^0(u_\perp)/L(0) \approx 3.84.$$

If the maximum $L^0(u_\perp)$ is normalized onto the maximum of $L(u_\perp)$, one may expect that the resulting distribution will be close to the real one. The

corresponding curve is plotted in fig. 5. Apparently, the distribution $L(u_\perp)$ decreases somewhat more slowly with increasing $u_\perp$ than is represented by this curve.

6. Centre-of-Mass Momentum Distribution

The centre-of-mass momentum distribution of the neutron-proton system after the diffractional disintegration of a deuteron can be found by integrating (8) over the vector $\mathbf{u}$ of the relative motion:

$$d\sigma = RR_d H(z)dz,$$

$$H(z) = \frac{1}{\pi^3}\int d\mathbf{u}\left\{\frac{1}{2\pi}\left|\int_0^\infty d\beta e^{2i\beta z}\int d\mathbf{x}\,\frac{e^{-x}}{x}e^{-i\mathbf{u}\cdot\mathbf{x}}\right|^2\right.$$

$$-\frac{4}{1+u^2}\mathrm{Re}\left(\int_0^\infty d\beta e^{2i\beta z}\int_{|\mathbf{n}\cdot\mathbf{x}|>2\beta} d\mathbf{x}\,\frac{e^{-x}}{x}e^{-i\mathbf{u}\cdot\mathbf{x}}\right)\left(\int_0^\infty d\beta e^{2i\beta z}\int_1^\infty d\xi\,\frac{e^{-2(1-iu)\beta\xi}}{\xi^2}\right)^*$$

$$\left.+\frac{8\pi}{(1+u^2)^2}\left|\int_0^\infty d\beta e^{2i\beta z}\int_1^\infty d\xi\,\frac{e^{-2(1-iu)\beta\xi}}{\xi^2}\right|^2\right\}. \tag{26}$$

In calculating (26) one should first perform integration over the directions of the vector $\mathbf{u}$. (This integration may be carried out in the same way as when finding the relative energy distribution of the deuteron disintegration products. In this case the third term in (26) is cancelled by part of the second term.) As a result we obtain the following expression for the distribution:

$$H(z) = H^0(z)$$

$$+\frac{8}{\pi}\int_0^\infty du\int_1^\infty\int_1^\infty\frac{d\xi}{\xi^2}\,\frac{d\eta}{\eta^2}\,\mathrm{Re}\,\frac{u}{(u+i)(u-i)^3(\xi u-z-i\xi)(\eta u+z-i\eta)}, \tag{27}$$

where $H^0(z)$ is the distribution obtained without taking account of the neutron-proton interaction in the final state:

$$H^0(z) = \frac{4}{z^2} - \frac{8}{z^3}\mathrm{arctg}\,\frac{z}{2}. \tag{28}$$

The function under the integral in (27) is even in u, therefore, integration over u can be extended from $-\infty$ to $+\infty$, the integral being simultaneously multiplied by $\frac{1}{2}$. After that, the integration over u is easily performed with the help of the method of residues by choosing the contour in a lower semiplane which contains only one simple pole in the point $u = -i$. Integrating then over ξ and η, we finally obtain the following formula for the centre-of-

mass momentum distribution of the neutron-proton system after the deuteron disintegration:

$$H(z) = \frac{2}{z^2} - \frac{2}{z^4} \ln^2 \left(\frac{z^2}{4} + 1 \right) - \frac{8}{z^4} \left(\operatorname{arctg} \frac{z}{2} \right)^2 . \tag{29}$$

The distribution $H(z)$ is plotted in fig. 6. It should be noted that this curve will also be valid for the momentum distribution of recoil nuclei.

If the distribution maximum (28) is normalized onto the maximum of (29) the resultant distribution will almost coincide with (29). Deviations will be noticeable only at large values of z for which the curve corresponding to the

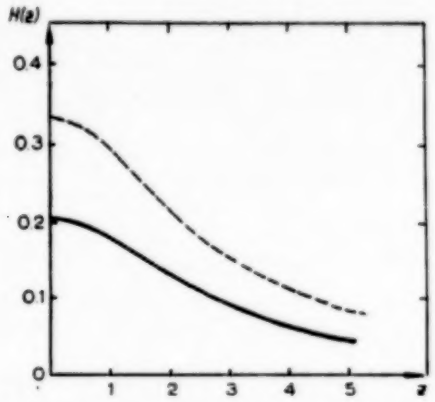

Fig. 6. Centre-of-mass momentum distribution of the neutron proton system after the diffractional disintegration of the deuteron.

normalized $H^0(z)$ will be somewhat higher than the curve of the real distribution (29).

7. Angular Distribution of Neutrons and Protons in Diffractional Disintegration of Deuterons

The emission angle of a neutron or a proton in diffractional disintegration of the deuteron is determined by the wave vector component perpendicular to the incident deuteron, $\zeta_n = \varkappa_n/\alpha$ and $\zeta_p = \varkappa_p/\alpha$. Using equation (9) and relation (10) we obtain the following general formula for the angular distribution of neutrons:

$$\begin{aligned} d\sigma &= RR_d W(\zeta_n) \zeta_n d\zeta_n , \\ W(\zeta_n) &= \int_{-\infty}^{\infty} du_x \int_{-\infty}^{\infty} du_z \int_0^{2\pi} d\varphi_n C(u_x, u_z, \zeta_n, \varphi_n), \end{aligned} \tag{30}$$

$$\begin{aligned} C(u_x, u_z, \zeta_n, \varphi_n) = \frac{1}{\pi^2} \frac{1}{(1+u^2)^2} \Bigg| \frac{1}{2P} \left[\frac{P - iu_x}{P + i\zeta_{nx}} + \frac{P + iu_x}{P + i\zeta_{nx} - 2iu_x} \right] \\ - \int_1^{\infty} \frac{d\xi}{\xi^2} \frac{1}{(1 - iu)\xi + i\zeta_{nx} - iu_x} \Bigg|^2 , \end{aligned} \tag{31}$$

where

$$P = \sqrt{1+u_z^2+\zeta_{ny}^2}, \quad \zeta_{nx} = \zeta_n \cos\varphi_n \quad \text{and} \quad \zeta_{ny} = \zeta_n \sin\varphi_n.$$

Expression (30) cannot be integrated analytically. However, since the u_x and u_z distributions are characterized by a sharp peak at $u_x = 0$ and $u_z = 0$, the nature of the angular distribution can be found through the expression

$$W'(\zeta_n) = \int_0^{2\pi} d\varphi_n C(0, 0, \zeta_n, \varphi_n),$$

$$C(0, 0, \zeta_n, \varphi_n) = \frac{1}{\pi^2} \frac{1}{(1+\zeta_n^2 \sin^2\varphi_n)^2} \left| \frac{1}{\sqrt{1+\zeta_n^2 \sin^2\varphi_n}+i\zeta_n \cos\varphi_n} \right. \tag{32}$$

$$\left. -\int_1^\infty \frac{d\xi}{\xi^2} \frac{1}{(1-i\zeta_n|\sin\varphi_n|)\xi+i\zeta_n \cos\varphi_n} \right|^2.$$

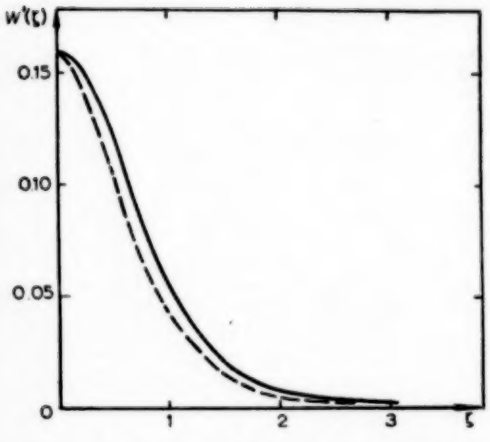

Fig. 7. Angular distribution of neutrons produced in diffractional disintegration of deuterons ($u_x = 0$, $u_z = 0$).

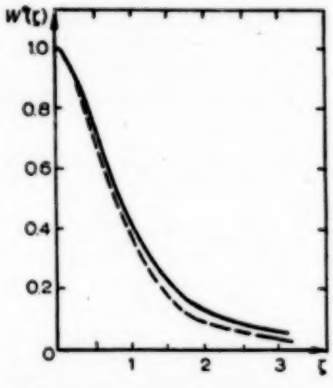

Fig. 8. Angular distribution of neutrons produced in diffractional disintegration of deuterons.

The distribution $W'(\zeta_n)$ obtained by numerical integration of (32) is shown in fig. 7. In the region of small emission angles of neutrons the following approximate formula is valid:

$$W'(\zeta_n) = \frac{1}{2\pi} - \frac{5}{9\pi}\zeta_n^2 + \ldots, \quad \zeta_n \ll 1.$$

If the neutron-proton interaction in the final state is neglected, the distribution can be represented by the expression

$$W'^0(\zeta_n) = \frac{1}{\pi} \frac{2+\zeta_n^2}{(1+\zeta_n^2)^{\frac{3}{2}}}. \tag{33}$$

The ratio of maxima (33) and (32) equals 4. The dotted line in fig. 7 is for distribution (33) normalized onto the maximum $W'(\zeta_n)$. As is seen, the obtained distributions do not reveal any considerable difference.

Neglecting the neutron-proton interaction in the final state one can find the total angular distribution of the released particles

$$W^0(\zeta_n) = \int_{-\infty}^{\infty} du_x \int_{-\infty}^{\infty} du_z \int_0^{2\pi} d\varphi_n \frac{1}{\pi^2} \frac{1}{(1+u^2)^2} \frac{1}{4P^2} \left| \frac{P-iu_x}{P+i\zeta_{xn}} + \frac{P+iu_x}{P+i\zeta_{nx}-2iu_x} \right|^2. \quad (34)$$

Integrating over u_x, u_z, and the angle φ_n we obtain the following formula for the angular distribution of neutrons (or protons) in diffractional disintegration of deuterons:

$$W^0(\zeta_n) = \frac{2(1+2\zeta_n^2)}{\zeta_n^2(1+\zeta_n^2)^{\frac{1}{2}}} - \frac{1}{2\zeta_n^3\sqrt{1+\zeta_n^2}} \operatorname{arctg} \zeta_n - \frac{9+17\zeta_n^2}{2\zeta_n^3(1+\zeta_n^2)^{\frac{1}{2}}} \operatorname{arctg} \frac{\zeta_n}{3}. \quad (35)$$

At small and large emission angles the following approximate formulas are valid:

$$W^0(\zeta_n) = \tfrac{8}{9} - (1+\tfrac{67}{405})\zeta_n^2 + \ldots, \quad \zeta_n \ll 1,$$

$$W^0(\zeta_n) = \frac{4}{\zeta_n^3} + \ldots, \quad \zeta_n \gg 1.$$

The angular distribution of particles liberated in diffractional disintegration of deuterons, with maximum normalized to unity, is plotted in fig. 8. For comparison, the dotted line represents the angular distribution of particles stripped from a deuteron by a black nucleus. The width of the latter distribution is somewhat smaller than that of the distribution (35).

8. Polarization of Deuteron Disintegration Products

The spin-orbit interaction of the neutron and the proton constituting the deuteron with a nucleus leads to the possibility of polarization of the particles produced in diffractional disintegration. Account of spin-orbit interaction of neutron and proton with the nucleus reduces to the substitution of the operator factors

$$\hat{\omega}_n = \left\{1 - \gamma_n e^{i\delta_n} \boldsymbol{\sigma}_n \left(\tfrac{1}{2}\mathbf{k}_d \times \frac{\partial}{\partial \boldsymbol{\varrho}_n}\right)\right\} \omega_n,$$

$$\hat{\omega}_p = \left\{1 - \gamma_p e^{i\delta_p} \boldsymbol{\sigma}_p \left(\tfrac{1}{2}\mathbf{k}_d \times \frac{\partial}{\partial \boldsymbol{\varrho}_p}\right)\right\} \omega_p$$

for the factors ω_n and ω_p in expression (3) [7]). Then the probability amplitude of the deuteron diffractional disintegration takes the form

$$\begin{aligned} \hat{a} = a &+ \gamma_n e^{i\delta_n} \int d\boldsymbol{\varrho}_n \int d\boldsymbol{\varrho}_p \int dz e^{-i\boldsymbol{\varkappa}\cdot\boldsymbol{\varrho}_d} \varphi_f^*(\mathbf{r}) \boldsymbol{\sigma}_n \left(\tfrac{1}{2}\mathbf{k}_d \times \frac{\partial}{\partial \boldsymbol{\varrho}_n}\right) \omega_n \Omega_p \varphi_0(r) \\ &+ \gamma_p e^{i\delta_p} \int d\boldsymbol{\varrho}_n \int d\boldsymbol{\varrho}_p \int dz e^{-i\boldsymbol{\varkappa}\cdot\boldsymbol{\varrho}_d} \varphi_f^*(\mathbf{r}) \boldsymbol{\sigma}_p \left(\tfrac{1}{2}\mathbf{k}_d \times \frac{\partial}{\partial \boldsymbol{\varrho}_p}\right) \omega_p \Omega_n \varphi_0(r), \end{aligned} \quad (37)$$

where a is the probability amplitude (2). (It is to be noted that the operator factors $\hat{\omega}_n$ and $\hat{\omega}_p$ commute only when we choose ϱ_n and ϱ_p as independent variables.) We have neglected the quadratic terms in the constants γ_n and γ_p of the spin-orbit interaction.

Integrating (37) by parts and introducing the unit vectors

$$\mathbf{n}_n = \frac{\mathbf{k}_d \times \boldsymbol{\varkappa}_n}{k_d \kappa_n}, \quad \mathbf{n}_p = \frac{\mathbf{k}_d \times \boldsymbol{\varkappa}_p}{k_d \kappa_p}, \quad (\boldsymbol{\varkappa}_n, \boldsymbol{\varkappa}_p \perp \mathbf{k}_d),$$

we can represent the matrix of diffractional disintegration in the form

$$\hat{a} = a + b_n(\boldsymbol{\sigma}_n \cdot \mathbf{n}_n) + b_p(\boldsymbol{\sigma}_p \cdot \mathbf{n}_p), \tag{38}$$

where

$$b_n = \tfrac{1}{2} i \gamma_n e^{i\delta_n} k_d \kappa_n \int d\boldsymbol{\varrho}_d \int d\mathbf{r} e^{-i\boldsymbol{\varkappa}\cdot\boldsymbol{\varrho}_d} \varphi_f^*(\mathbf{r}) \omega_n \Omega_p \varphi_0(r),$$

$$b_p = \tfrac{1}{2} i \gamma_p e^{i\delta_p} k_d \kappa_p \int d\boldsymbol{\varrho}_d \int d\mathbf{r} e^{-i\boldsymbol{\varkappa}\cdot\boldsymbol{\varrho}_d} \varphi_f^*(\mathbf{r}) \omega_p \Omega_n \varphi_0(r).$$

To simplify the calculations we shall neglect interaction between neutrons and protons after the disintegration. In this case a equals

$$a = -\frac{\pi\sqrt{2\pi\alpha}}{P'[P'^2 + \frac{1}{4}(\kappa_{nx} - \kappa_{px})^2]} \left\{ \frac{P' - \frac{1}{2}i(\kappa_{nx} - \kappa_{px})}{P' + i\kappa_{nx}} + \frac{P' + \frac{1}{2}i(\kappa_{nx} - \kappa_{px})}{P' + i\kappa_{px}} \right\} \delta(\kappa_{ny} + \kappa_{py}). \tag{39}$$

In calculating the integrals in b_n and b_p it is convenient to integrate first over $\boldsymbol{\varrho}_d$ with the fixed $\mathbf{r}$. In the limiting case of $R \gg R_d$ this integration, owing to the presence of factors $\omega_n \Omega_p$ and $\omega_p \Omega_n$, reduces to integrating over an infinite band of width x (integration in b_n over x_d being from $\frac{1}{2}x$ to $-\frac{1}{2}x$, in b_p from $-\frac{1}{2}x$ to $\frac{1}{2}x$, while integration over y_d is from $-\infty$ to ∞).
As a result we obtain

$$b_n = 2\pi\sqrt{2\pi\alpha}\gamma_n e^{i\delta_n} k_d \kappa_n \frac{\kappa_{px} - \kappa_{nx}}{(P'^2 + \kappa_{px}^2)(P'^2 + \kappa_{nx}^2)} \delta(\kappa_{ny} + \kappa_{py}),$$

$$b_p = 2\pi\sqrt{2\pi\alpha}\gamma_p e^{i\delta_p} k_d \kappa_p \frac{\kappa_{nx} - \kappa_{px}}{(P'^2 + \kappa_{px}^2)(P'^2 + \kappa_{nx}^2)} \delta(\kappa_{ny} + \kappa_{py}). \tag{40}$$

Choosing the initial density matrix ρ_0 in the form

$$\rho_0 = \tfrac{1}{12}(3 + \boldsymbol{\sigma}_n \cdot \boldsymbol{\sigma}_p),$$

we arrive at the following expression for the density matrix of the neutron-proton system after the deuteron disintegration:

$$\rho = \tfrac{1}{12}\{|a|^2(3+\boldsymbol{\sigma}_n\cdot\boldsymbol{\sigma}_p)+a^*b_n(\boldsymbol{\sigma}_n\cdot\mathbf{n}_n)(3+\boldsymbol{\sigma}_n\cdot\boldsymbol{\sigma}_p)+a^*b_p(\boldsymbol{\sigma}_p\cdot\mathbf{n}_p)(3+\boldsymbol{\sigma}_n\cdot\boldsymbol{\sigma}_p)$$
$$+ab_n^*(3+\boldsymbol{\sigma}_n\cdot\boldsymbol{\sigma}_p)(\boldsymbol{\sigma}_n\cdot\mathbf{n}_n)+|b_n|^2(\boldsymbol{\sigma}_n\cdot\mathbf{n}_n)(3+\boldsymbol{\sigma}_n\cdot\boldsymbol{\sigma}_p)(\boldsymbol{\sigma}_n\cdot\mathbf{n}_n)$$
$$+b_pb_n^*(\boldsymbol{\sigma}_p\cdot\mathbf{n}_p)(3+\boldsymbol{\sigma}_n\cdot\boldsymbol{\sigma}_p)(\boldsymbol{\sigma}_n\cdot\mathbf{n}_n) \qquad (41)$$
$$+ab_p^*(3+\boldsymbol{\sigma}_n\cdot\boldsymbol{\sigma}_p)(\boldsymbol{\sigma}_p\cdot\mathbf{n}_p)+b_nb_p^*(\boldsymbol{\sigma}_n\cdot\mathbf{n}_n)(3+\boldsymbol{\sigma}_n\cdot\boldsymbol{\sigma}_p)(\boldsymbol{\sigma}_p\cdot\mathbf{n}_p)$$
$$+|b_p|^2(\boldsymbol{\sigma}_p\cdot\mathbf{n}_p)(3+\boldsymbol{\sigma}_n\cdot\boldsymbol{\sigma}_p)(\boldsymbol{\sigma}_p\cdot\mathbf{n}_p)\}.$$

The polarization of neutrons released in diffractional disintegration of deuterons is determined by the formula

$$P_n = \frac{\mathrm{tr}\{(\boldsymbol{\sigma}_n\cdot\mathbf{n}_n)\rho\}}{\mathrm{tr}\,\rho} = \frac{2\,\mathrm{Re}\,a\{b_n+\frac{1}{3}b_p(\mathbf{n}_n\cdot\mathbf{n}_p)\}^*}{|a|^2+|b_n|^2+|b_p|^2+\frac{2}{3}\,\mathrm{Re}\,b_nb_p^*(\mathbf{n}_n\cdot\mathbf{n}_p)}. \qquad (42)$$

It should be noted that the polarization of particles released in the deuteron diffractional disintegration vanishes if $f_\perp = 0$ or $\kappa = 0$.

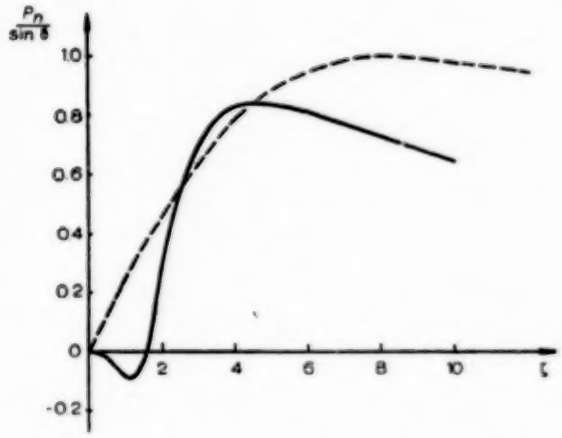

Fig. 9. Polarization of neutrons produced in diffractional disintegration of deuterons at 100 MeV ($\zeta_p = 0$).

Let us consider the polarization of neutrons in the case $\kappa_p = 0$, i.e. when the momentum of the proton does not change its direction in the deuteron disintegration. In this case $b_p = 0$ and the formula for the polarization of the neutron is simplified:

$$P_n = \frac{2\,\mathrm{Re}\,ab_n^*}{|a|^2+|b_n|^2}. \qquad (43)$$

Integrating the numerator and denominator in (43) over the direction of the two-dimensional vector $\varkappa_n$ as well as over f_z, we shall find the polarization as a function of the emission angle of the neutron:

$$
\begin{aligned}
P_n(\zeta) &= \frac{\sin \delta\gamma\alpha k_d \varphi_1(\zeta)}{\varphi_2(\zeta)+(\gamma\alpha k_d)^2\varphi_3(\zeta)}, \quad \zeta = \frac{\kappa_n}{\alpha}, \\
\varphi_1(\zeta) &= 2\zeta - \frac{32}{\zeta} + \frac{128}{3\zeta}\frac{1}{\sqrt{1+\frac{1}{4}\zeta^2}} - \frac{32}{3\zeta}\frac{1}{\sqrt{1+\zeta^2}} - \frac{2\zeta}{(1+\zeta^2)^{\frac{3}{2}}}, \\
\varphi_2(\zeta) &= 1 - \frac{26}{\zeta^2} + \frac{64}{3\zeta^2}\frac{1}{\sqrt{1+\frac{1}{4}\zeta^2}} + \frac{4}{(1+\frac{1}{4}\zeta^2)^{\frac{3}{2}}} + \frac{14}{3\zeta^2}\frac{1}{\sqrt{1+\zeta^2}}, \\
\varphi_3(\zeta) &= \zeta^2 - 4 + \frac{4}{\sqrt{1+\zeta^2}} + \frac{\zeta^2}{(1+\zeta^2)^{\frac{3}{2}}}.
\end{aligned}
\tag{44}
$$

The polarization $P_n(\zeta)$ vanishes at $\zeta = 0$ and $\zeta = 1.57$, having negative values between these points. At the point $\zeta = 1.57$ the polarization changes sign and at large values of ζ it becomes positive.

The fig. 9 shows the dependence of the polarization on the neutron emission angle ζ for 100 MeV incident deuterons. For comparison the dotted line represents the polarization due to the scattering of free neutrons by nuclei at an energy equal to half the energy of the deuteron.

The authors are sincerely thankful to A. I. Akhiezer for discussion of the results of this work.

References

1) A. I. Akhiezer and A. G. Sitenko, Uchyonie Zapiski of the Kharkov Univ. **64** (1955) 9
2) E. L. Feinberg, JETP **29** (1955) 115
3) R. Glauber, Phys. Rev. **99** (1955) 1515
4) A. Akhiezer and A. Sitenko, Phys. Rev. **106** (1957) 1236
5) R. Serber, Phys. Rev. **72** (1947) 1008
6) I. I. Ivanchik and V. S. Popov, JETP **36** (1959) 499
7) A. Sitenko, Nuclear Physics **9** (1959) 412

8.B *Nuclear Physics* **13** (1959) 435—446; © *North-Holland Publishing Co., Amsterdam*

Not to be reproduced by photoprint or microfilm without written permission from the publisher

LOW-TYPE INTEGRAL EQUATIONS FOR THE ABSORPTION AND PRODUCTION OF K MESONS

SAUL BARSHAY †

Institute for Theoretical Physics, University of Copenhagen

Received 25 June 1959

Abstract: A discussion is given of Low-type integral equations for approximate transition amplitudes which describe the processes $\overline{\mathrm{K}}+\mathrm{N}\to\pi+\mathrm{Y}$ and $\pi+\mathrm{N}\to\mathrm{K}+\mathrm{Y}$. Isobaric spin and angular momentum decompositions of the equations are performed, and the resulting sets of integral equations for the various amplitudes are discussed with non-relativistic approximations for the interaction current operators. Certain assumptions are made with regard to the as yet unknown relative parities, coupling strengths, and scattering properties of the strange particles, in a preliminary effort to utilize the field equations as a model for correlating certain features of the present experimental data on the absorption of low-energy K^- mesons by protons.

1. Introduction

In this paper an attempt is made to derive and to investigate Low-type [1]) equations for the scattering amplitudes which describe two of the simpler processes involving pions, nucleons, K mesons, and hyperons. These processes, which are related by the crossing symmetry, are

$$\begin{aligned} &\text{a)}\ \overline{\mathrm{K}}+\mathrm{N}\to\pi+\mathrm{Y}, \\ &\text{b)}\ \pi+\mathrm{N}\to\mathrm{K}+\mathrm{Y}. \end{aligned} \tag{1}$$

The particle symbols are used to denote the mesons and the symbol Y stands for either a Λ or a Σ hyperon and N for a nucleon. The approximate equations to be considered are linear integral equations for the desired amplitudes, the inhomogeneous terms being "renormalized" Born approximations, and the kernels of the integral terms being related to pion-nucleon and pion-hyperon scattering amplitudes. The equations may be useful in going somewhat beyond the Born approximation calculations of the amplitudes, and in this respect they are somewhat similar to the Chew-Low [2]) development of photopion production. For simplicity, the equations are derived within the static approximation for the baryon fields (that is, the bilinear combinations of baryon field operators in the Hamiltonian are considered as replaced by source functions and virtual antibaryons are removed from consideration). However, the final equations may be generalized to their relativistic analo-

† National Science Foundation Postdoctoral Fellow.

gues in the same manner as the Chew-Low equation for photopion production [2]) derived within the static model may be generalized to the corresponding Low equation [1]).

In a preliminary discussion of the equations, we shall examine the scattering amplitudes for the processes (1a) for $\overline{\mathrm{K}}$ kinetic energies of zero to $\approx$ 100 MeV, utilizing static model approximations for the current operators under several assumptions about the unknown relative parities, coupling strengths, and scattering properties of the strange particles. This discussion is meant to see whether a semi-phenomenological analysis of the equations may provide any correlation of the accumulating experimental data on K^--proton interactions leading to pion-hyperon final states. The discussion is, at present, rather limited by a crude treatment of the strong K-meson interaction current.

2. Derivation

We consider the total Hamiltonian to be $H = H_0+H_1+H_2$, where H_0 is the free-field Hamiltonian (with the observed masses), H_1 describes the pion-baryon interactions, and H_2 describes the K meson-baryon interactions. Suppressing the mass counter-terms which must be subtracted from the interaction Hamiltonians, we may define the pion and K-meson current operators, j_1 and j_2, by

$$\begin{aligned} H_1 &= \sum_p \{c_p j_1(p)+c_p^\dagger j_1^\dagger(p)\}, \\ H_2 &= \sum_p \{C_p j_2(p)+C_p^\dagger j_2^\dagger(p)\}, \end{aligned} \tag{2}$$

where the c_p (C_p) and $c_p^\dagger$ ($C_p^\dagger$) are annihilation and creation operators, respectively, for pions (K mesons) of momentum $\mathbf{p}$ and energy $\omega = \{\mathbf{p}^2+\mu^2(m^2)\}^{\frac{1}{2}}$. Here the symbol † denotes the hermitian adjoint, μ is the pion mass, m is the K-meson mass; the isobaric spin indices may be considered to be included in the symbol p. We denote by χ_a and χ_b the initial and final free particle states for the reaction (1a); these are eigenstates of H_0 corresponding to a total energy $E = \omega_\mathrm{a}+E_\mathrm{N} = \omega_\mathrm{b}+E_\mathrm{Y}$, where ω_a, ω_b, E_N and E_Y are, respectively, the total energies of K meson, pion, nucleon and hyperon. We denote by $\psi_\mathrm{a}^{(+)}$ the exact state vector (with outgoing waves) for the initial state; it satisfies

$$\begin{aligned} H\psi_\mathrm{a}^{(+)} &= E\psi_\mathrm{a}^{(+)}, \\ \psi_\mathrm{a}^{(+)} &= \Omega^{(+)}\chi_\mathrm{a}, \end{aligned} \tag{3}$$

where

$$\Omega^{(+)} = 1+(E-H+i\eta)^{-1}(H_1+H_2).$$

Finally, we denote by $\varphi_\mathrm{b}^{(-)}$ a state vector for the final state, corresponding

to the situation with $H_2 = 0$. It satisfies

$$\begin{aligned}(H_0+H_1)\varphi_b^{(-)} &= E\varphi_b^{(-)},\\ \varphi_b^{(-)} &= \overline{\Omega}^{(-)}\chi_b,\end{aligned} \tag{4}$$

where

$$\overline{\Omega}^{(-)} = 1+(E-H_0-H_1-i\eta)^{-1}H_1.$$

The exact matrix element is given by

$$T_{ab} = \langle\chi_b|T|\chi_a\rangle, \tag{5}$$

where

$$T = (H_1+H_2)\Omega^{(+)}.$$

This may be transformed into

$$T_{ab} = \langle\varphi_b^{(-)}|H_2|\psi_a^{(+)}\rangle = \langle\chi_b|\overline{\Omega}^{(-)\dagger}H_2\Omega^{(+)}|\chi_a\rangle. \tag{6}$$

The equivalence of the two forms is established simply by noting that the difference,

$$T-\overline{\Omega}^{(-)\dagger}H_2\Omega^{(+)} = D \propto E-H_0,$$

gives a zero contribution to the matrix element, i.e., $\langle\chi_b|D|\chi_a\rangle = 0$. We now perform a straightforward reduction of the last form of the matrix element in eq. (6). We write the initial free-particle state containing a K meson of momentum and isobaric spin denoted by a, and a nucleon of specified momentum, spin, and isobaric spin, $|\chi_a\rangle = C_a^\dagger|\chi_N\rangle$. For the final free-particle state containing a pion of momentum and isobaric spin denoted by b, and a hyperon of specified momentum, spin, and isobaric spin, we write, $|\chi_b\rangle = c_b^\dagger|\chi_Y\rangle$. Then, the matrix element is given by

$$T_{ab} = \langle\chi_Y|[c_b, [\overline{\Omega}^{(-)\dagger}H_2\Omega^{(+)}, C_a^\dagger]]|\chi_N\rangle = \langle\chi_Y|[c_b, Z]|\chi_N\rangle. \tag{7}$$

The square brackets denote the commutator. By calculation of the commutator we obtain

$$\begin{aligned}Z = [\overline{\Omega}^{(-)\dagger}H_2\Omega^{(+)}, C_a^\dagger] &= \overline{\Omega}^{(-)\dagger}j_2(a)\Omega^{(+)}\\ &-\overline{\Omega}^{(-)\dagger}j_2(a)\{(E-H+i\eta)^{-1}-(E-H-\omega_a+i\eta)^{-1}\}(H_1+H_2)\\ &+\overline{\Omega}^{(-)\dagger}H_2(E-H+i\eta)^{-1}j_2(a)+\overline{\Omega}^{(-)\dagger}H_2(E-H+i\eta)^{-1}j_2(a)\\ &\times(E-H-\omega_a+i\eta)^{-1}(H_1+H_2).\end{aligned} \tag{8}$$

The first and second terms of eq. (8) combine to give the following contribution to the matrix element (7):

$$\langle\chi_Y|c_b\overline{\Omega}^{(-)\dagger}j_2(a)\{1+(E_N-H+i\eta)^{-1}(H_1+H_2)\}|\chi_N\rangle = \langle\varphi_b^{(-)}|j_2|N\rangle, \tag{9}$$

where $|N\rangle$ denotes an eigenstate of H corresponding to the physical nucleon. The last two terms of eq. (8) combine to give the following contribution to the matrix element (7):

$$\langle\chi_Y|c_b\overline{\Omega}^{(-)\dagger}H_2(E-H+i\eta)^{-1}j_2(a)\{1+(E_N-H+i\eta)^{-1}(H_1+H_2)\}|\chi_N\rangle = \langle\varphi_b^{(-)}|H_2(E-H+i\eta)^{-1}j_2|N\rangle. \quad (10)$$

The complete matrix element is then

$$T_{ab} = \langle\varphi_b^{(-)}|j_2|N\rangle+\langle\varphi_b^{(-)}|H_2(E-H+i\eta)^{-1}j_2|N\rangle. \quad (11)$$

This form of the matrix element is particularly convenient if we wish to begin an examination of the problem by treating the K-meson current, j_2, as acting only once. If we neglect the K-meson self-field effects in the state vector $|N\rangle$, we have the first term in eq. (11) written in terms of eigenstates of $H' = H_0+H_1$. A perturbation expansion of the second term allows identification of all effects of higher order in j_2 (including K-meson contributions to vertex renormalizations). We will turn our attention in the next section to an expansion of the first term in eq. (11) in intermediate eigenstates of H', that is, we start by considering the K-meson current j_2, to act once (note, however, the phenomenological modification discussed at the end of this section). We may state this in another way. The exact matrix element is given by $\langle\varphi_b^{(-)}|J|N\rangle$, where J is a new current operator defined by $J = j_2 + H_2(E-H+i\eta)^{-1}j_2$. We approximate J by j_2 (as we have, at present, no better representation). The coupling constants that will appear will then be renormalized in the pionic sense, that is, pionic corrections to the vertex function are taken into account by embedding the Heisenberg operators between eigenstates of H'. The term we shall analyze contains many of the effects of the one coupling which we know experimentally to be very strong (as measured by $g^2/4\pi \approx 15$), the pion-nucleon coupling.

We note, however, that an important contribution from higher order effects in the K-meson interaction could be included phenomenologically in the following manner. Expand the first term of eq. (11) in intermediate eigenstates of the total Hamiltonian and retain the physical baryon and the "one-pion" states, as we shall do explicitly in the next section. Then, approximate all the matrix elements, except those relating to pion-hyperon scattering, by "turning off" the K-meson interactions in the state vectors. This will express all the matrix elements except the above-mentioned ones in terms of the eigenstates of H'. However, matrix elements for pion-hyperon scattering, exact within an approximation which involves incorporating the K-meson self-field effects back into the hyperon eigenstates of H', will appear in the "one-pion" terms of the integral equation. Since we will resort to a purely phenomenological description of these matrix elements, we can include in the latter description the possible important effects [3]) of the K-meson interaction on pion-hyperon scattering in the vicinity of the K^-—p threshold. In section 4, in which we deal in a preliminary manner with the phenomenology of the equations, we shall consider that this approx-

imation procedure has been carried out and that the pion-hyperon scattering amplitudes that appear in the integral equation can be correlated with the physical pion-hyperon scattering properties †.

By standard techniques, we may write

$$\begin{aligned}\langle \varphi_b^{(-)}|j_2|\mathrm{N}\rangle = {} & \langle \mathrm{Y}|U_1^\dagger(E-H'+i\eta)^{-1}j_2|\mathrm{N}\rangle \\ & +\langle \mathrm{Y}|j_2(E_\mathrm{N}-\omega_b-H')^{-1}V_1^\dagger|\mathrm{N}\rangle.\end{aligned} \tag{12}$$

In this equation, U_1 and V_1 refer to the parts of j_1 corresponding to the interaction of pions with hyperons and nucleons, respectively, $|\mathrm{Y}\rangle$ denotes a hyperon eigenstate of H', and we may substitute $E = E_\mathrm{Y}+\omega_b$. Eq. (12) satisfies a simple "crossing" symmetry which may be summarized by the following equations:

$$\begin{aligned} & U_1^\dagger \rightleftarrows j_2 \quad \text{(in the first term)}, \\ & V_1^\dagger \rightleftarrows j_2 \quad \text{(in the second term)}, \\ & U_1 \rightleftarrows V_1, \\ & \omega_b \rightarrow -\omega_b, \\ & E_\mathrm{N} \rightleftarrows E_\mathrm{Y}. \end{aligned} \tag{13}$$

The first three equations are, of course, simply more explicit writing of the operation $j_1^\dagger \rightleftarrows j_2$. If we denote the operator between the baryon states in eq. (12) by $T_\mathrm{K}(\pi)$ and further, define $T_\pi(\mathrm{K})$ by

$$T_\pi(\mathrm{K}) = j_2^\dagger(E-H'+i\eta)^{-1}U_1+V_1(E_\mathrm{N}-\omega_b-H')^{-1}j_2^\dagger, \tag{14}$$

then we have the following unitarity condition:

$$T_\pi^\dagger(\mathrm{K})-T_\mathrm{K}(\pi) = 2\pi i \sum_n \delta(E-E_n)T_\pi^\dagger(n)T_\mathrm{K}(n). \tag{15}$$

3. Analysis of the "One-Pion" Approximation

We consider now the approximation of retaining only the baryon and the baryon plus-one-pion states in an expansion of eq. (12) obtained by introducing a complete set of eigenstates of H' (with incoming waves) between the energy denominator and the current operators. We do this because we would like to make a crude investigation of the effect upon the $\overline{\mathrm{K}}$ absorption

† A standard Low equation [1]), with the exact matrix element written in terms of the operators j_1 and j_2 embedded between eigenstates of H, may of course, be written down quite analogously to eq. (12) below. The "renormalized" Born approximations would then contain the completely renormalized couplings. We have explicitly separated off the effects of pion-hyperon couplings induced by the K-meson and pion-nucleon couplings. (However, we have not attempted to calculate such effects in this paper.) The pion-renormalized Born approximations represent the effects of primary pion-baryon couplings. A separation of these effects is possible in a simple, non-relativistic (i.e., cut-off and finite) model. Aside from the model, it is an interesting question to what extent pion-hyperon couplings are induced by the strong pion-nucleon and K-meson interactions. (However, we have not attempted to calculate such effects in this paper; since we make no explicit use of the separation, the concluding remarks with regard to the pion-renormalized couplings are also applicable if the couplings are considered to have been completely renormalized.)

processes of certain assumptions concerning the interaction properties of the pion-baryon system whose scattering amplitudes enter linearly in the "one-pion" terms. The equation for the truncated transition amplitude now reads

$$\begin{aligned}\langle\varphi_{\mathrm{b}}^{(-)}|j_2|\mathrm{N}\rangle \approx{}& \langle\mathrm{Y}|U_1^{\dagger}|\mathrm{Y}'\rangle\langle\mathrm{Y}'|j_2|\mathrm{N}\rangle(E-E_{\mathrm{Y}'}+i\eta)^{-1}\\ &+\langle\mathrm{Y}|j_2|\mathrm{N}'\rangle\langle\mathrm{N}'|V_1^{\dagger}|\mathrm{N}\rangle(E_{\mathrm{N}}-\omega_{\mathrm{b}}-E_{\mathrm{N}'})^{-1}\\ &+\langle\mathrm{Y}|U_1^{\dagger}|\mathrm{Y}',\pi^{(-)}\rangle\langle^{(-)}\pi,\mathrm{Y}'|j_2|\mathrm{N}\rangle(E-E_{\mathrm{Y}'}-\omega+i\eta)^{-1}\\ &+\langle\mathrm{Y}|j_2|\mathrm{N}',\pi^{(-)}\rangle\langle^{(-)}\pi,\mathrm{N}'|V_1^{\dagger}|\mathrm{N}\rangle(E_{\mathrm{N}}-\omega_{\mathrm{b}}-\omega-E_{\mathrm{N}'})^{-1}.\end{aligned}\tag{16}$$

In this equation, hyperon intermediate states (with energy $E_{\mathrm{Y}'}$) and nucleon intermediate states (with energy $E_{\mathrm{N}'}$) are denoted by $|\mathrm{Y}'\rangle$ and $|\mathrm{N}'\rangle$, respectively; the pion-hyperon and pion-nucleon intermediate states (with energies $E_{\mathrm{Y}'}+\omega$ and $E_{\mathrm{N}'}+\omega$) are denoted by $|\mathrm{Y}',\pi^{(-)}\rangle$ and $|\mathrm{N}',\pi^{(-)}\rangle$, respectively; sums over the various charge combinations, as well as an integration over the intermediate momentum, are to be understood.

We perform a decomposition of eq. (16) in isobaric spin space. First consider reaction (1a) in which a pion and a Σ hyperon are produced; we want the equations for the production amplitudes in the states of isobaric spin zero and one. It is convenient to introduce two auxiliary amplitudes, A and B such that the isobaric dependence of the matrix element we are considering is given by

$$\langle\varphi_{\mathrm{b}}^{(-)}|j_2|\mathrm{N}\rangle=\tfrac{1}{3}\{A(3\delta_{\pi\mathrm{Y}}-\tau_{\mathrm{Y}}^{\dagger}\tau_{\pi})+B\tau_{\mathrm{Y}}^{\dagger}\tau_{\pi}\},\tag{17}$$

where τ_{π} and τ_{Y} refer to the components of the Pauli isobaric spin operator along the pion and hyperon states appropriate to the reaction (1b) obtained from (1a) by "crossing" the pion and K-meson fields. The isobaric spin zero and one amplitudes are then given by

$$A_1=\tfrac{2}{3}(A-B),\qquad A_0=\tfrac{1}{3}\sqrt{6}(2A-B).\tag{18}$$

We now write the integral equations satisfied by the amplitudes A and B:

$$\begin{aligned}\text{(a)}\quad A(\omega_{\mathrm{b}},\mathbf{b},\mathbf{a})={}&(\text{b.a.})_A+(1/2\pi^2)\int d^3\mathbf{p}[(\Delta+\omega_{\mathrm{b}}-\omega+i\eta)^{-1}\\ &\times z_1^{\dagger}(\omega,\mathbf{p},\mathbf{b})D(\omega,\mathbf{p},\mathbf{a})+(\omega_{\mathrm{b}}-\omega+i\eta)^{-1}\{(\tfrac{2}{3}\alpha_0^{\dagger}(\omega,\mathbf{p},\mathbf{b})+\tfrac{1}{3}\alpha_1^{\dagger}(\omega,\mathbf{p},\mathbf{b}))\\ &\times A(\omega,\mathbf{p},\mathbf{a})+(\tfrac{1}{3}\alpha_0^{\dagger}(\omega,\mathbf{p},\mathbf{b})-\tfrac{1}{3}\alpha_1^{\dagger}(\omega,\mathbf{p},\mathbf{b}))B(\omega,\mathbf{p},\mathbf{a})\}\\ &+(\omega_{\mathrm{b}}+\omega)^{-1}A(-\omega^*,-\mathbf{p},\mathbf{a})\beta_3(\omega,\mathbf{p},\mathbf{b})],\end{aligned}\tag{19}$$

$$\begin{aligned}\text{(b)}\quad B(\omega_{\mathrm{b}},\mathrm{b},\mathrm{a})={}&(\text{b.a.})_B+(1/2\pi^2)\int d^3\mathbf{p}[(\Delta+\omega_{\mathrm{b}}-\omega+i\eta)^{-1}\\ &\times(-\sqrt{\tfrac{2}{3}})z_1^{\dagger}(\omega,\mathbf{p},\mathbf{b})D(\omega,\mathbf{p},\mathbf{a})+(\omega_{\mathrm{b}}-\omega+i\eta)^{-1}\{(\tfrac{1}{3}\alpha_0^{\dagger}(\omega,\mathbf{p},\mathbf{b})\\ &+\tfrac{2}{3}\alpha_1^{\dagger}(\omega,\mathbf{p},\mathbf{b}))B(\omega,\mathbf{p},\mathbf{a})+(\tfrac{2}{3}\alpha_0^{\dagger}(\omega,\mathbf{p},\mathbf{b})-\tfrac{2}{3}\alpha_1^{\dagger}(\omega,\mathbf{p},\mathbf{b}))\\ &\times A(\omega,\mathbf{p},\mathbf{a})\}+(\omega_{\mathrm{b}}+\omega)^{-1}B(-\omega^*,-\mathbf{p},\mathbf{a})\beta_1(\omega,\mathbf{p},\mathbf{b})].\end{aligned}$$

In these equations, $D(\omega,\mathbf{p},\mathbf{a})$ is an amplitude for the process $\overline{\mathrm{K}}+\mathrm{N}\to\pi+\Lambda$

(this matrix element is written $\langle q_{\mathbf{b}}{}^{(-)}|j_2|\mathrm{N}\rangle = -D(\omega, \mathbf{b}, \mathbf{a})\tau_\pi/\sqrt{3}$); z_1 is an amplitude for the scattering of the isobaric spin one part of a $\pi-\Sigma$ state into a $\pi-\Lambda$ state; α_0 and α_1 are amplitudes for $\pi-\Sigma$ scattering in the isobaric spin zero and one states, respectively; β_3 and β_1 are the P-wave amplitudes for pion-nucleon scattering in the states of isobaric spin $\frac{3}{2}$ and $\frac{1}{2}$, respectively; Δ is the difference in mass between the Σ and Λ; (b.a.) denotes the respective pion-renormalized Born approximations.

For the amplitude describing the production of Λ hyperons we have the following equation:

$$\begin{aligned} D(\omega_{\mathbf{b}}, \mathbf{b}, \mathbf{a}) = (\text{b.a.})_D + (1/2\pi^2)\int \mathrm{d}^3\mathbf{p}[&(-\Delta+\omega_{\mathbf{b}}-\omega+i\eta)^{-1} \\ &\times\sqrt{\tfrac{2}{3}}\,\tilde{z}_1{}^{\dagger}(\omega, \mathbf{p}, \mathbf{b})\{B(\omega, \mathbf{p}, \mathbf{a})-A(\omega, \mathbf{p}, \mathbf{a})\}+(\omega_{\mathbf{b}}-\omega+i\eta)^{-1} \\ &\times\tilde{\alpha}_1{}^{\dagger}(\omega, \mathbf{p}, \mathbf{b})D(\omega, \mathbf{p}, \mathbf{a})+(\omega_{\mathbf{b}}+\omega)^{-1}D(-\omega^*, -\mathbf{p}, \mathbf{a}) \\ &\times\beta_1(\omega, \mathbf{p}, \mathbf{b})]. \end{aligned} \tag{20}$$

Here, $\tilde{z}_1$ is an amplitude for the scattering of a $\pi-\Lambda$ state into the isobaric spin one part of a $\pi-\Sigma$ state, and $\tilde{\alpha}_1$ is an amplitude for $\pi-\Lambda$ scattering.

We now perform an angular momentum decomposition of eqs. (19) and (20) for two possible situations with regard to the relative parities of the strange particles.

Case A) The relative $\Sigma-\Lambda$ parity is even and the K *meson is pseudoscalar.*

We then obtain the following set of integral equations for the production amplitudes ${}^{\nu}A$, ${}^{\nu}B$, ${}^{\nu}D$, from an initial P-state $\overline{\mathrm{K}}$-nucleon system to a final P-state $\pi-$ hyperon system (the superscript $\nu = 2j+1$ (on all of the amplitudes entering into the equations) refers to the state of total angular momentum j):

$$\begin{aligned} \text{(a)}\quad {}^1A(\omega_{\mathbf{b}}) &= 3(\mathrm{ab}/\mu m)\{-(\omega_{\mathbf{b}})^{-1}f_{\Sigma\pi}f_{\Sigma\mathrm{K}}+(\Delta+\omega_{\mathbf{b}})^{-1}f_{\Lambda\pi}f_{\Lambda\mathrm{K}}\} \\ &+(1/\pi)\int_{\mu}^{\infty}-p\mathrm{d}\omega[(\Delta+\omega_{\mathbf{b}}-\omega+i\eta)^{-1}(-1/3\sqrt{6})^1z_1{}^*(\omega)\,{}^1D(\omega) \\ &+(\omega_{\mathbf{b}}-\omega+i\eta)^{-1}\tfrac{1}{9}\{(2\,{}^1\alpha_0{}^*(\omega)+{}^1\alpha_1{}^*(\omega))\,{}^1A(\omega)+({}^1\alpha_0{}^*(\omega)-{}^1\alpha_1{}^*(\omega))\,{}^1B(\omega)\} \\ &-(\omega_{\mathbf{b}}+\omega)^{-1}\tfrac{1}{27}\{(-4\,{}^1\beta_3(\omega)+4\,{}^3\beta_3(\omega))\,{}^3A(-\omega^*)+({}^1\beta_3(\omega)+\gamma\,{}^3\beta_3(\omega)) \\ &\times{}^1A(-\omega^*)\}], \end{aligned} \tag{21}$$

$$\begin{aligned} \text{(b)}\quad {}^3A(\omega_{\mathbf{b}}) &= (1/\pi)\int_{\mu}^{\infty}p\mathrm{d}\omega[(\Delta+\omega_{\mathbf{b}}-\omega+i\eta)^{-1}(-1/3\sqrt{6})^3z_1{}^*(\omega)\,{}^3D(\omega) \\ &+(\omega_{\mathbf{b}}-\omega+i\eta)^{-1}\tfrac{1}{9}\{(2\,{}^3\alpha_0{}^*(\omega)+{}^3\alpha_1{}^*(\omega))\,{}^3A(\omega)+({}^3\alpha_0{}^*(\omega)-{}^3\alpha_1{}^*(\omega)) \\ &\times{}^3B(\omega)\}-(\omega_{\mathbf{b}}+\omega)^{-1}\tfrac{1}{27}\{(8\,{}^1\beta_3(\omega)+{}^3\beta_3(\omega))\,{}^3A(-\omega^*) \\ &+(-2\,{}^1\beta_3(\omega)+2\,{}^3\beta_3(\omega))\,{}^1A(-\omega^*)\}], \end{aligned}$$

$$(c)\quad {}^1D(\omega_b) = -\sqrt{3}(ab/\mu m)\{3(\omega_b-\Delta)^{-1}f_{A\pi}f_{\Sigma K}-(\omega_b)^{-1}ff_{AK}\}$$
$$+(1/\pi)\int_\mu^\infty p\,d\omega[(-\Delta+\omega_b-\omega+i\eta)^{-1}(\sqrt{2}/3\sqrt{3})\,{}^1\bar{z}_1{}^*(\omega)\{{}^1B(\omega)-{}^1A(\omega)\}$$
$$+(\omega_b-\omega+i\eta)^{-1}\tfrac{1}{3}\,{}^1\bar{\alpha}_1{}^*(\omega)\,{}^1D(\omega)-(\omega_b+\omega)^{-1}\tfrac{1}{27}\{(-4\,{}^1\beta_1(\omega)+4\,{}^3\beta_1(\omega))$$
$$\times{}^3D(-\omega^*)+({}^1\beta_1(\omega)+8\,{}^3\beta_1(\omega))\,{}^1D(-\omega^*)\}],\qquad(21)$$

$$(d)\quad {}^3D(\omega_b) = 2\sqrt{3}(ab/\mu m)(\omega_b)^{-1}ff_{AK}$$
$$+(1/\pi)\int_\mu^\infty p\,d\omega[(-\Delta+\omega_b-\omega+i\eta)^{-1}(\sqrt{2}/3\sqrt{3})\,{}^3\bar{z}_1{}^*(\omega)$$
$$\times\{{}^3B(\omega)-{}^3A(\omega)\}+(\omega_b-\omega+i\eta)^{-1}\tfrac{1}{3}\,{}^1\bar{\alpha}_1{}^*(\omega)\,{}^3D(\omega)$$
$$-(\omega_b+\omega)^{-1}\tfrac{1}{27}\{(8\,{}^1\beta_1(\omega)+{}^3\beta_1(\omega))\,{}^3D(-\omega^*)$$
$$+(-2\,{}^1\beta_1(\omega)+2\,{}^3\beta_1(\omega))\,{}^1D(-\omega^*)\}].$$

The equation for ${}^1B(\omega_b)$ is obtained from (22a) by replacing the Born approximation by

$$3(ab/\mu m)\{2(\omega_b)^{-1}f_{\Sigma\pi}f_{\Sigma K}+(\omega_b)^{-1}ff_{\Sigma K}+(\Delta+\omega_b)^{-1}f_{A\pi}f_{AK}\}$$

and by the substitutions

$$D\to -2D;\quad \beta_3\to\beta_1;\quad (2\,{}^1\alpha_0{}^*+{}^1\alpha_1{}^*)\,{}^1A\to({}^1\alpha_0{}^*+2\,{}^1\alpha_1{}^*)\,{}^1B;$$
$$({}^1\alpha_0{}^*-{}^1\alpha_1{}^*)\,{}^1B\to(2\,{}^1\alpha_0{}^*-2\,{}^1\alpha_1{}^*)\,{}^1A.$$

Similarly, the equation for ${}^3B(\omega_b)$ is obtained from (22b) by replacing the Born apprximation by $-6(ab/\mu m)(\omega_b)^{-1}ff_{\Sigma K}$ and by the same substitutions as enumerated above, with the superscripts on the amplitudes α, A and B changed from 1 to 3. In these equations, f is the pion-renormalized, unrationalized, pseudovector, pion-nucleon coupling constant, and the other quantities f are similar coupling constants for the interactions indicated by the subscripts. The symbol * denotes complex conjugation.

The transition operators are constructed from the amplitudes and standard projection operators appropriate to the transition. For example, for the process $K^-+p\to\pi^-+\Sigma^+$, we have, in this case,

$$A(\omega_b, \mathbf{b}, \mathbf{a}) = (4\omega_a\omega_b)^{-\frac{1}{2}}\{{}^1A(\omega_b)\tfrac{1}{3}\boldsymbol{\sigma}\cdot\mathbf{b}\,\boldsymbol{\sigma}\cdot\mathbf{a}$$
$$+{}^3A(\omega_b)\tfrac{1}{3}(3\mathbf{b}\cdot\mathbf{a}-\boldsymbol{\sigma}\cdot\mathbf{b}\,\boldsymbol{\sigma}\cdot\mathbf{a})\}\{\delta_{\pi Y}-\tfrac{1}{3}\tau_Y{}^\dagger\tau_\pi\}.\qquad(22)$$

By the "crossing" symmetry, we may construct from the scalar amplitudes taken at negative values of the energy argument (however, very different in magnitude from those appropriate to $\overline{K}$ absorption) the transition operators for the associated production processes (1b)†.

† An earlier consideration [11]) of the equations for these high-energy processes came to naught because of the probable necessity of, and the difficulty in, estimating the effects of intermediate states with pairs.

Case B) The relative $\Sigma-\Lambda$ parity is odd and the relative $K-\Sigma$ parity is even.

This model has some nice features when applied to K^+-nucleon scattering [4]), allowing for both S and P-wave scattering in the non-relativistic limit of the interaction, in a manner that is in qualitative agreement with recent experimental data [5]). The set of integral equations for the production amplitudes now reads

$$
\begin{aligned}
\text{(a)}\quad {}^1A(\omega_b) &= -(b/\mu)(\omega_b)^{-1} f_{\Sigma\pi} g_{\Sigma K} \\
&+ 1/\pi \int_\mu^\infty p\,d\omega \big[(\Delta+\omega_b-\omega+i\eta)^{-1}(-1/\sqrt{6})\,{}^0z_1^*(\omega)\,{}^0D(\omega) \\
&+ (\omega_b-\omega+i\eta)^{-1}\tfrac{1}{9}\{(2\,{}^1\alpha_0^*(\omega)+{}^1\alpha_1^*(\omega))\,{}^1A(\omega) \\
&+ ({}^1\alpha_0^*(\omega)-{}^1\alpha_1^*(\omega))\,{}^1B(\omega)\}-(\omega_b+\omega)^{-1}\tfrac{1}{3}\,{}^1\beta_3(\omega)\,{}^1A(-\omega^*)\big],
\end{aligned}
$$

$$
\begin{aligned}
\text{(b)}\quad {}^0A(\omega_b) &= (1/\pi)\int_\mu^\infty p\,d\omega\big[(\Delta+\omega_b-\omega+i\eta)^{-1}(-1/3\sqrt{6})\,{}^1z_1^*(\omega)\,{}^1D(\omega) \\
&+ (\omega_b-\omega+i\eta)^{-1}\tfrac{1}{3}\{(2\,{}^0\alpha_0^*(\omega)+{}^0\alpha_1^*(\omega))\,{}^0A(\omega) \\
&+ ({}^0\alpha_0^*(\omega)-{}^0\alpha_1^*(\omega))\,{}^0B(\omega)\}\big],
\end{aligned}
$$

$$
\begin{aligned}
\text{(c)}\quad {}^0D(\omega_b) &= -\sqrt{3}(\omega_b-\Delta)^{-1} g_{\Lambda\pi} g_{\Sigma K}+(1/\pi)\int_\mu^\infty p\,d\omega \\
&\times\big[(-\Delta+\omega_b-\omega+i\eta)^{-1}\sqrt{\tfrac{2}{3}}\,{}^1\tilde{z}_1^*(\omega)\{{}^1B(\omega)-{}^1A(\omega)\} \\
&+ (\omega_b-\omega+i\eta)^{-1}\,{}^0\tilde{\alpha}_1^*(\omega)\,{}^0D(\omega)\big],
\end{aligned}
\qquad (23)
$$

$$
\begin{aligned}
\text{(d)}\quad {}^1D(\omega_b) &= -\sqrt{3}(ab/\mu m)(\omega_b)^{-1} f f_{\Lambda K}+(1/\pi)\int_\mu^\infty p\,d\omega\big[(-\Delta+\omega_b-\omega+i\eta)^{-1} \\
&\times\sqrt{6}\,{}^0\tilde{z}_1^*(\omega)\{{}^0B(\omega)-{}^0A(\omega)\}+(\omega_b-\omega+i\eta)^{-1}\tfrac{1}{3}\,{}^1\tilde{\alpha}_1^*(\omega)\,{}^1D(\omega) \\
&-(\omega_b+\omega)^{-1}\tfrac{1}{27}\{(-4\,{}^1\beta_1(\omega)+4\,{}^3\beta_1(\omega))\,{}^3D(-\omega^*) \\
&+({}^1\beta_1(\omega)+8\,{}^3\beta_1(\omega))\,{}^1D(-\omega^*)\}\big],
\end{aligned}
$$

$$
\begin{aligned}
\text{(e)}\quad {}^3D(\omega_b) &= 2\sqrt{3}(ab/\mu m)(\omega_b)^{-1} f f_{\Lambda K}+(1/\pi)\int_\mu^\infty p\,d\omega \\
&\times\big[(\omega_b-\omega+i\eta)^{-1}\tfrac{1}{3}\,{}^3\tilde{\alpha}_1^*(\omega)\,{}^3D(\omega)-(\omega_b+\omega)^{-1}\tfrac{1}{27}\{(8\,{}^1\beta_1(\omega) \\
&+{}^3\beta_1(\omega))\,{}^3D(-\omega^*)+(-2\,{}^1\beta_1(\omega)+2\,{}^3\beta_1(\omega))\,{}^1D(-\omega^*)\}\big].
\end{aligned}
$$

The equation for ${}^1B(\omega_b)$ is obtained from (23a) by replacing the Born approximation by

$$2(b/\mu)(\omega_b)^{-1} g_{\Sigma K}\{f_{\Sigma\pi}-\tfrac{3}{2}f\}$$

and by the substitutions

$$
\begin{gathered}
D \to -2D;\quad \beta_3 \to \beta_1;\quad (2\,{}^1\alpha_0^*+{}^1\alpha_1^*)\,{}^1A \to ({}^1\alpha_0^*+2\,{}^1\alpha_1^*)\,{}^1B; \\
({}^1\alpha_0^*-{}^1\alpha_1^*)\,{}^1B \to 2({}^1\alpha_0^*-{}^1\alpha_1^*)\,{}^1A.
\end{gathered}
$$

Finally, the equation for ${}^0B(\omega_b)$ is obtained from (23b) by replacing the Born approximation by $(a/m)(\Delta+\omega_b)^{-1}g_{\Lambda\pi}f_{\Lambda K}$, and by the above substitutions with the superscripts on the amplitudes α, A and B changed from 1 to 0. The pion-renormalized, unrationalized, scalar couplings are denoted by g with appropriate subscripts. In eqs. (23), the superscripts on the amplitudes A, B and α, only, refer to the orbital angular momentum of the pion-hyperon state (in the case of a P state, $j = \frac{1}{2}$). In eq. (23c), the superscripts on the amplitudes D and $\tilde{\alpha}_1$ also refer to the pion-hyperon orbital angular momentum. The superscripts on the amplitudes z_1 and $\tilde{z}_1$ refer to the orbital angular momentum of the pion-hyperon state produced by the amplitude multiplying z_1 and $\tilde{z}_1$, respectively.

4. Discussion

We limit ourselves to a few, perhaps somewhat academic, remarks, in the light of the present crude approximation $J \approx j_2$, and also in the light of the somewhat unclear experimental situation with regard to the production processes in low-energy K^-—p interactions. Let us first outline our picture of the latter situation. We assume that the original data [6]) on K^-—p captures represents predominantly interactions from initial S Bohr orbits, and therefore that the observed branching ratios [6]), $\Sigma^- : \Sigma^+ : \Sigma^0 : \Lambda \approx 4 : 2 : 2 : \frac{1}{2}$, will be continuous with those to be observed in K^-—p interactions at the bottom of the continuum (perhaps with a suitable allowance made for some at-rest captures from P Bohr orbits). We then consider two interesting variations as the K^- energy is raised. Perhaps the most striking is that inferred from a number of emulsion studies [7,8]), namely that the "direct" Λ production, so infrequent in captures at rest (contrary to simple phase space considerations), appears to rise sharply with energy, becoming comparable with the total charged Σ production at K^- kinetic energies of the order of 100 MeV. Secondly, there appears to be a variation over the first 100 MeV energy interval in the Σ^-/Σ^+ ratio [7,9]), from a value of ≈ 2 in captures at rest to a value of ≈ 1.

Consider now the situation A). The non-relativistic reduction of the pseudoscalar interactions of pions and K mesons leaves us only with equations for the transition amplitudes from initial $\overline{K}$-nucleon P states to final pion-hyperon P states. We may, under the assumption stated above, take the S-state to S-state branching ratios from experiment (as we have no theoretical feeling for the S-wave effects induced by the operator γ_5) and attempt to understand the increasing Λ production as a feature of an increasingly significant P-wave interaction. The variation in the Σ^-/Σ^+ ratio may be partially due to a suitable energy dependence [10]) in the S-state transition amplitudes, but one would also expect the P-state transition amplitudes (if

these are also of increasing importance in Σ production) to confirm the tendency of this ratio to be ≈ 1. In perhaps the simplest situation (since there is no "a priori" reason why similar renormalized pseudovector coupling strengths should differ markedly), in which we take $|f_{\Sigma\pi}| \approx |f_{\Lambda\pi}| \approx |f|$ and $|f_{\Sigma K}| \approx |f_{\Lambda K}|$, one finds that a crude examination of eq. (22) (under, for example, the "global" symmetry hypothesis that the important pion-baryon scattering amplitudes, other than ${}^3\beta_3$, are likely to be the pion-hyperon amplitudes in the states of isotopic spin one and angular momentum $\frac{3}{2}$) suggests that, *if* the P-wave interaction is indeed responsible for an increasing Λ production, then a non-negligible P-wave Σ production is also likely; and that this production strongly favours Σ^- over Σ^+, except in the case $f_{\Lambda\pi} f_{\Sigma K} \approx f f_{\Lambda K}$, $f_{\Sigma\pi} \approx -f$.

In case B), we have found a slightly better reconciliation of the two variations with energy which we are considering. In this case, the very low energy continuum transitions are from an initial $\overline{K}$-nucleon S state to a final $\pi-\Sigma$ P state or a final $\pi-\Lambda$ S state. A crude examination of the eqs. (23), under the assumption that the important integral term involves the mixing amplitude z_1, suggests that, if $f_{\Sigma\pi} \approx f$, and if the pion-renormalized scalar coupling, $g_{\Lambda\pi}$, is about an order of magnitude smaller than the pion-renormalized pseudoscalar coupling g, corresponding to f, then the at-rest branching ratios $\Sigma^- : \Sigma^+ : \Sigma^0 \approx 2 : 1 : 1$ are roughly obtained (from the Born approximation), with strong suppression of Λ production. Further, if we choose the pion-renormalized scalar K-meson coupling, $g_{\Sigma K}$, to be about an order of magnitude smaller than the pion-renormalized pseudoscalar coupling, $g_{\Lambda K}$, corresponding to $f_{\Lambda K}$, then, at about 60 MeV K^- laboratory kinetic energy, the P-state Λ production can become comparable with the total charged Σ production. At this energy, there is sufficient absorption of P-wave $\overline{K}$ leading to S-wave $\pi-\Sigma$ systems (with these transitions characterized by a Σ^-/Σ^+ ratio < 1) to reduce the overall Σ^-/Σ^+ ratio by perhaps about 35 %, in the crude approximation in which we neglect any energy variation in the ratio characteristic of the S-state to P-state transitions.

A further remark may be made in case B) with regard to the hyperon angular distributions and polarizations. The above crude estimates of the amplitudes suggest that, either the and Σ^+ and Σ^- angular distributions in the centre-of-mass system are of the form $|A| \pm |B| \cos\theta$, respectively, at those energies where Λ production has become significant, or, if these angular distributions are largely isotropic, then the charged hyperons must have a significant polarization induced by the production process. Absence of both angular anisotropy *and* evidence for polarization in charged Σ production at energies where Λ production has increased would weaken an attempt to understand the latter effect as due to significant P wave $\overline{K}$-nucleon interactions.

In conclusion, we remark that a better representation of the operator J, embodying higher order effects in the strong K-meson interaction current, might make the Low-type field equations discussed in this paper useful models for correlating the accumulating experimental data and the purely phenomenological considerations concerning the absorption of $\overline{K}$ mesons by nucleons. From the experimental side, it would be useful to know whether the energy variations we have discussed here in a preliminary way are indeed significant, i.e., whether the Λ production increases markedly over the first 100 MeV in K^-—p interactions, and whether the Σ^-/Σ^+ ratio tends to unity in the same energy interval, and further, whether the branching ratios at the bottom of the continuum are continuous with those at rest.

I would like to thank Professor Niels Bohr, Professor Aage Bohr and Professor C. Møller, as well as the other members and guests of the institute for Theoretical Physics for their kind hospitality and stimulating interest during my stay in Copenhagen. I would like to acknowledge my debt to the National Science Foundation for fellowship support.

References

1) F. Low, Phys. Rev. **97** (1955) 1392
2) G. F. Chew and F. Low, Phys. Rev. **101** (1956) 1579
3) R. H. Dalitz and S. F. Tuan, Annals of Physics (to be published)
4) S. Barshay, Phys. Rev. Letters **1** (1958) 97
5) Keefe, Kernan, Montwill, Grilli, Guerriero and Salandin, Nuovo Cimento **3** (1959) 241
6) Alvarez, Bradner, Falk-Variant, Gow, Rosenfeld, Solmitz and Tripp. U.C.R.L. **3775** (unpublished)
7) Eisenberg, Koch, Lohrmann, Mikolić, Schneeberger and Winzeler, Nuovo Cimento **9** (1958) 745
8) Eisenberg, Koch, Mikolić, Schneeberger and Winzeler, Nuovo Cimento (to be published)
9) Preliminary data kindly supplied to the author by Professor A. Rosenfeld of Berkeley
10) R. H. Dalitz, Report to the 1958 Conference on High-Energy Physics at C.E.R.N.
11) S. Barshay, Phys. Rev. **107** (1957) 1454; **108** (1957) 1648

8.B *Nuclear Physics* **13** (1959) 447—450; © *North-Holland Publishing Co., Amsterdam*
Not to be reproduced by photoprint or microfilm without written permission from the publisher

ON A POSSIBLE CONNECTION BETWEEN ISOBARIC SPIN AND STRANGENESS AND INVERSION PROPERTIES OF SPINORS

A. M. BRODSKY and D. D. IVANENKO
Physical Department, State University, Moscow

Received 5 July 1959

Habitually isobaric and strangeness properties of particles are treated by the introduction of an iso-space of 2, 3 or 4 dimensions (and possibly allowing transitions to ordinary space). On the other side, one can try to describe these properties by remaining in ordinary pseudo-euclidean space, but by using new possibilities exhibited by the behaviour of spinors for spatial and temporal inversions, which up to now have not yet been fully exploited, and by taking account of parity non-conservation.

As was occasionally remarked previously, it is possible to introduce in the formulae describing transformations of spinors in space or time inversions extra factors other than those, -1; $\pm i$, considered by Yang and Tiomno [1]), viz. [8, 9]) $\pm\gamma_5$, $\pm i\gamma_5$. For instance, for the space inversion $x_{1,2,3} \to -x_{1,2,3}$ not only the ordinary Racah formula $\psi' \to \gamma_4\psi$, but e.g. also $\psi' \to \gamma_5\gamma_4\psi$ as well as $\psi \to i\gamma_4\psi$, are possible; in covariant form, one may have not only $\psi' = a_\mu\gamma_5\gamma_\mu\psi$, but also $ia_\mu\gamma_5\gamma_\mu\psi$ or $a_\mu\gamma_\mu\psi$ etc. for reflexion at a hypersurface with normal a_μ. In such manner there arise different spinor representations of the total Lorentz group, some of which are equivalent for unitary transformations, but differ from one another on charge conjugation. A more essential difference between spinors arises if the above-mentioned extra factors -1, i, γ_5 or their products are introduced only for space or only for time inversions.

Let us characterize each spinor by two pairs of indices: a, b and α, β. Index a takes the value 1 (or 2) if for space reflexion an extra factor γ_5 is (or is not) added. Analogously, index b characterizes the geometrical time reflexion T^0, which is connected with the Schwinger-inversion by $T^S = T^0 \times (\tilde{\ }) = TC$, where $(\tilde{\ })$ means transposition in Hilbert space and, T Wigner time inversion. Indices α, β take the 4 values $-1, 0, 1, 2$, corresponding to occurrence of extra-factors i^α for space and i^β for time inversions. We emphasize that from the proposed point of view the most essential difference between spinors is characterized by the values of the differences a—b and α—β or by the moduli of such differences.

"Mixed" spinors with $a-b \neq 0$, introduced previously by us, realize without any doubling of the number of components, a spinor representation, which may be called "anomalous", leading to $T^0 P = +PT^0$, in contradistinction from the "normal" case, when $T^0 P = -TP^0$. It is convenient to denote "normal" spinors by ψ^{11}, relating the first index to spatial inversions. Yang-Tiomno classes $(\pm 1, \pm i)$ may be indicated as ψ^{1A1A}, ψ^{1A1B} etc. The presence of the extra factor γ_5 may be indicated by an index 2, as ψ^{2A2A}, ψ^{2B2A} etc. Then, for mixed spinors one must use the symbols ψ^{12}, ψ^{21}, with various subscripts A, B, C, D if desired. For "mixed" spinors the construction of a Dirac equation with non-vanishing mass is possible only at the expense of violating P-invariance, but conserving strong (combined) invariance $P^S = PC$.

If one has only invariance under strong inversions, P^S and T^S, one must ask first of all about characterizing different spinors in these cases. The most straightforward solution of this problem can be achieved by introducing alongside with any ordinary ("small") spinor ψ a pair of self-conjugate ("large") spinors $\Psi(\gamma_5^2 = -1)$

$$\Psi(1) = \tfrac{1}{2}[(1+i\gamma_5)\psi + (1-i\gamma_5)\psi^c], \qquad \Psi(2) = \tfrac{1}{2}[(1-i\gamma_5)\psi + (1+i\gamma_5)\psi^c];$$

$$\Psi^c(1, 2) = c\Psi^*(1, 2) = \Psi(1,2),$$

where Ψ^c denote the charge conjugate spinor. Under combined inversions (P^S and T^S) each large spinor $\Psi(1)$ or $\Psi(2)$ is transformed independently and linearly, in a way analogous to the transformation of ordinary ψ under "geometrical" inversions. Let us point that for phase transformations of ordinary spinors $\psi \to e^{i\alpha}\psi$, the large spinors $\Psi(1, 2)$ transform like $\Psi(1, 2) = e^{\pm i\alpha\gamma_5}\Psi(1, 2)$. For self-conjugated small spinors ψ (neutrino), the large spinor $\Psi(1)$ coincides with $\Psi(2)$. A supplementary difference in the $\Psi(1, 2)$ is connected with the presence of identical or different signs for inversions. Self-conjugate spinors ψ are possible only for such $\Psi(1)$, $\Psi(2)$ which have the same signs. For the description of combined space and time inversions of large spinors $\Psi(1, 2)$it is sufficient to introduce only one pair of indices I, K, and correspondingly only one difference

$$N = I-K = a-b+(\alpha-\beta) \pmod 2.$$

Here a, b, α, β belong to the initial "small" ψ. The large spinors $\Psi(1)$, $\Psi(2)$ build up a doublet, whose components transform among themselves for geometrical inversions or charge conjugation of the initial "small" ψ. One can essentially put such transformations, together with Salam-Toushek transformations, in correspondence with 3-dimensional isobaric rotations.

This behaviour of spinors for inversions makes it tempting to connect the difference N with, say, baryonic number, further $(\alpha—\beta)$ with strangeness $(-S)$ and $(a—b)$ with hypercharge $(+Y)$. Then, these quantities will obey the required relation

$$N = Y - S.$$

One can also assign corresponding numbers to bosons constructed as bilinear forms of spinors.

The construction of bilinear combinations (bosons), possessing habitual covariant properties for strong inversions (scalar, vector, pseudoscalar, etc.), from a pair of spinors, one of which has $N = 1$ ("mixed" spinor) and the other $N = 0$ ("normal" spinor) proves to be impossible. In the same way, it is impossible to build up habitual bilinear combinations from spinors which differ in $(a-b)$ or $(\alpha-\beta)$ (mod 2) values, i.e. possess in inversions extra factors i or γ_5 [2,5]). Moreover, bosons constructed from spinors with different N, S, Y will always build up doublets, whose components transform among themselves for inversions, i.e. one has bosons of the type of K-mesons.

Thus, one gets new conservation laws, when only N is conserved strictly, but S and Y are conserved only if invariance for geometrical inversions holds. In such manner the empirical fact of simultaneous break of conservation of S, Y, P, which appeared previously as somewhat accidental, can also find a plausible explanation from the present point of view. If one takes as an universal conservation law the conservation of strong inversion $P^S = PC$, ordinary space parity P would not be conserved if there is no iso-spin invariance, in agreement with suggestion of Soloviev [11]). Keeping in mind the above considerations, one is led to a most natural characterization of leptons by large spinors $\Psi(1, 2)$ normal"'" for combined inversions. This would correspond to their description, for geometrical ("weak") inversions, by ordinary small spinors, either also of "normal" type, or of "mixed" type, the latter with respect to a supplementary factor $i\gamma_5$, and not only γ_5. Then one can describe the various leptons e, ν, μ by spinors which differ in inversions by factors ± 1, $\pm i$ (following Yang-Tiomno) and also by factors $\pm\gamma_5$ (i.e. in the above mentioned form, by $\psi^{1A1A} \ldots \psi^{1D2D}$ etc.).

It is proposed to characterize baryons by large spinors $\Psi(1, 2)$ "mixed" (i.e. anomalous) for combined inversions, which induces for ordinary small ψ the presence of a factor γ_5; this leads either to anomalous commutation rules for the small ψ, or only to the presence of a weaker relative difference in the form of a factor i for space and time inversions. Such a description of the baryons proves to be closely related to an investigation of Salam [3]) and Taylor [4]), who used, however, anomalous rules $PT = +TP$ for geometrical, but not for combined inversions, as proposed here, and introduced a doubling of components. The doubling can be used also in our treatment, but we can also without doubling of components apply the new possibilities of representation of space and time inversions. In the notation of the present note one can say that Taylor uses for strangeness the difference $(\alpha-\beta)$ and takes account of $(a-b)$ via the iso-spin matrix τ_2 (and not via the γ_5-matrix).

Our point of view, as well as that of Taylor, does not coincide with the

proposition of Gürsey [10]) to characterize baryons by ordinary ("normal") spinors, using Yang-Tiomno A, B, C, $D(\pm 1, \pm i)$ classes for different strangeness values. On the other side, we agree with ideas of M. Mirianashvili [2]) and Gürsey [5]), who proposed to describe some bosons not only by bilinear combinations of spinors of the same kind, but also by fusion of different spinors. It is tempting, in generalizing their hypothesis, to allow even the fusion of, say, normal with mixed (anomalous) spinors etc. Then we can arrive at strange bosons of the type of K-mesons.

The development of these ideas will show whether one has here only one of the phenomenological schemes of particles, or the difference in behaviour for space and time inversions really represents one of the chief properties of particles. If the latter case would prove to be reasonable, then also in constructing a unitary non-linear spinor theory of matter one would be led to the necessity of using many kinds of fundamental spinors.

Note added in proof: Owing to the lack of absolute conservation of baryonic number in the proposed hypothetical formalism there exists in principle a possibility of transmutation of baryons into mesons and leptons; this has, however, a very small probability, owing to other conservation laws and the necessity of realizing a contact interaction for many particles. We acknowledge valuable remarks on the last point by Professor A. Salam and Professor L. Rosenfeld during the Kiev conference.

References

1) C. N. Yang and J. Tiomno, Phys. Rev. **79** (1950) 495
2) M. Mirianashvili, Proc. Inst. Phys. Georgian SSR **4** (1958)
3) A. Salam, Proc. 7-th Rochester Conference (1957)
4) J. C. Taylor, Nuclear Physics **3** (1957) 606;
McLennan, Phys. Rev.
5) F. Gürsey, Phys. Rev. Lett. **1** (1958) 98
6) Ogievetsky, Chow Kuang-Chao, Journ. Exp. Theor. Phys. **36** (1959) 264;
Nuclear Physics **10** (1959) 235
7) H. Sokolik, Journ. Exp. Theor. Phys. **36** (1959) 1098
8) A. Brodsky and D. Ivanenko, Journ. Exp. Theor. Phys. **36** (1959) 1279;
C.R. (Dokl. Acad. Sci.) **120** (1958) 995
9) I. Shapiro, Journ. Exp. Theor. Phys. **23** (1952) 4
10) F. Gürsey, Nuovo Cimento **7** (1958) 411
11) V. Soloviev, Journ. Theor. Exp. Phys. **33** (1957) 537

1.D.2:
2.G

Nuclear Physics **13** (1959) 451—455; © *North-Holland Publishing Co., Amsterdam*
Not to be reproduced by photoprint or microfilm without written permission from the publisher

$Cl^{35}(d, p)Cl^{36}$ IN THE UNIFIED MODEL

M. L. MEHTA and C. S. WARKE

Tata Institute of Fundamental Research, Bombay

Received 27 April 1959

Abstract: The general expression for the angular distribution of protons derived from Sawicki's transition matrix elements is given. The angular distribution of protons in the reaction $Cl^{35}(d, p)Cl^{36}$ is calculated assuming the strong coupling unified model. Calculation of the integral in the stripping formula takes into account the effect of the deformed surface of the nucleus. The value of the deformation obtained from fitting the observed angular distribution is found to agree roughly with those derived from the quadrupole and magnetic moments.

1. Introduction

For some nuclei the angular distribution of protons in the (d, p) reaction does not agree with the Butler theory and the single particle shell model, as for example in $F^{19}(d, p)F^{20}$, $Cl^{35}(d, p)Cl^{36}$, $Mg^{25}(d, p)Mg^{26}$ etc. The fitting of the experimental angular distribution in these cases requires two l values. One may then consider configuration mixing and this has been done for Cl^{35} by Sueji Okai and Mitsuo Sano [1]). Alternatively, one may use the unified model, in which, for strong coupling, this mixing of angular momenta is an immediate consequence of the deformation of the nucleus; this has been shown by Sawicki [2, 3]). The magnetic moment and quadrupole moment are calculated using Nilsson's [4]) wave functions and formulae.

2. The General Expression for Angular Distribution

The transition matrix element for stripping is [2, 3])

$$\begin{aligned} I^{K}_{\Omega_n}(M_1\mu_d, M_f\mu_p) \propto\ & (\tfrac{1}{2}\tfrac{1}{2}1;\ \mu_p,\ \mu_d-\mu_p,\ \mu_d) \\ & \times \sum_{ll'jZM} [\sqrt{2l'+1}(i)^{l'}(l'\tfrac{1}{2}j;\ 0,\ \mu_d-\mu_p,\ \mu_d-\mu_p) \\ & \times (l'\tfrac{1}{2}j;\ M-\Sigma,\ \Sigma,\ M)(I_1jI_f;\ M_1,\ \mu_d-\mu_p,\ M_f) \\ & \times (I_1I_f;\ K_1,\ M,\ K_f)a_{l,\Omega_n-\Sigma}S_{ll',\Omega_n-\Sigma,M-\Sigma}G(K)]. \end{aligned} \tag{1}$$

where the a's are the coefficients used by Nilsson to express the normalised wave function in the cylindrically symmetric oscillator potential in terms of spherically symmetric wave functions, and $G(K)$ is the deuteron term

$$G(K) = 1 - \frac{K^2+\alpha_d^2}{K^2+\beta_d^2} \tag{2}$$

where

$$\mathbf{K} = \tfrac{1}{2}\mathbf{k}_d - \mathbf{k}_p,$$

and β_d and α_d are the parameters in the Hulthén wave function. In eq. (1) the last term is given by

$$S_{ll'mm'} = \int_{r_n \geq r_0(1+\beta Y_2^0)} R_{Nl}\, j_{l'}(kr_n) Y_{lm}^* Y_{l'm'}\, d\mathbf{r}_n, \tag{3}$$

where R_{Nl} is the radial part of the spherically symmetric wave function and β is the deformation parameter as defined by Bohr [5]). The nuclear surface is not sharply defined but we assume that it is $r_n = r_0(1+\beta Y_2^0)$; the arguments of Y_2^0 in this expression being measured with respect to the nuclear symmetry axis. With this boundary, and up to first order in β, eq. (3) becomes

$$\begin{aligned} S_{ll'mm'} &= \mathscr{R}_{Nl}\delta_{ll'}\delta_{mm'} \\ &\quad - r_0^3 R_{Nl}(r_0) j_{l'}(kr_0)\beta \sqrt{\frac{5(2l'+1)}{4\pi(2l+1)}}\, (l'\,2l;\,0,\,0,\,0)\,(l'\,2l;\,m',\,0,\,m), \\ \mathscr{R}_{Nl} &= \int_{r_0}^{\infty} R_{Nl}(x) j_l(kx) x^2\, dx, \\ \mathbf{k} &= \mathbf{k}_d - \mathbf{k}_p. \end{aligned} \tag{4}$$

This expression is $\neq 0$ only for $m = m'$. We shall write

$$\varphi_{ll'm} \equiv r_0^3 R_{Nl}(r_0) j_{l'}(kr_0)\beta \sqrt{\frac{5(2l'+1)}{4\pi(2l+1)}}\, (l'\,2l;\,000)\,(l'\,2l;\,m,\,0,\,m). \tag{5}$$

Since we do not want the absolute value of the cross section we shall neglect the common factors. We have

$$\sigma(\theta) \propto \sum_{\mu_p \mu_d M_1 M_f} |I^{K_1}_{\Omega_n}(M_1\mu_d;\, M_f\mu_p)|^2. \tag{6}$$

From eqs. (1) and (4), using the symmetry properties of the Clebsch-Gordan coefficients (ref. [7]), chapter 3), and the orthogonality relations between them, the sum over μ_p, μ_d, M_1 and M_f in eq. (6) can easily be performed. The result is

$$\begin{aligned} \frac{\sigma(\theta)}{|G(K)|^2} \propto \sum_j\, & (I_1 j I_f;\, K_1,\, \Omega_n,\, K_f)^2 \Big[c_j \mathscr{R}_{Nl'} \\ & - \sum_{l\Sigma} a_{l,\,\Omega_n-\Sigma}(l'\tfrac{1}{2}j;\, \Omega_n-\Sigma,\, \Sigma,\, \Omega_n)\varphi_{l,\,l',\,\Omega_n-\Sigma}\Big]^2 \end{aligned} \tag{7}$$

where

$$c_j = \sum_{\Sigma} a_{l',\,\Omega_n-\Sigma}(l'\,\tfrac{1}{2}j;\, \Omega_n-\Sigma,\, \Sigma,\, \Omega_n)$$

as defined by Nilsson (ref.[4]), p. 26) and $l' = \frac{1}{2}[2j+(-1)^{P+j+\frac{1}{2}}]$; $(-1)^P$ is the parity of the state in which neutron is captured.

If one takes the integration outside the sphere, $\beta = 0$, eq. (7) reduces to

$$\frac{\sigma(\theta)}{|G(K)|^2} \propto \sum_j (I_1 j I_f; K_1, \Omega_n, K_f)^2 c_j^2 \mathscr{R}^2_{Nl'}. \tag{8}$$

In both eqs. (7) and (8) the angular distribution of protons in the (d, p) reaction is a sum of squares over j.

3. The Angular Distribution of Protons in Cl^{35}(d, p)Cl^{36}

The ground state of Cl^{35} is $\frac{3}{2}^+$. The quadrupole moment shows that the deformation is negative. According to Nilsson's [4]) diagram of energy levels, the odd proton of Cl^{35} has $\Omega_p = \frac{3}{2}$; this is consistent with $I_1 = K_1 = \frac{3}{2}$ for the ground state of Cl^{35}, since the rotational energy is smallest in this case (ref. [5]), p. 22). The configuration of Cl^{36} contains one odd proton in the $\Omega_p = \frac{3}{2}$ state and one odd neutron in the $\Omega_n = \frac{1}{2}$ state. This means that the neutron from the deuteron is absorbed in the state $\Omega_n = \frac{1}{2}$. The selection rule for the stripping reaction [2]) which follows from eq. (1) is $K_1 = K_f + \Omega_n$; therefore, $K_f = 2$. Also, $I_f = 2$, since the ground state of Cl^{36} is known to be 2^+. With these quantum numbers the differential cross section $\sigma(\theta)$ derived from eq. (8) is given by

$$\begin{aligned}\frac{\sigma(\theta)}{|G(K)|^2} \propto\ & a_{00}^2 \mathscr{R}^2_{20} + 0.1(\sqrt{2}a_{2,0} - \sqrt{3}a_{2,1})^2 \mathscr{R}^2_{22} \\ & + 0.004(\sqrt{2}a_{2,1} + \sqrt{3}a_{2,0})^2 \mathscr{R}^2_{22}.\end{aligned} \tag{9}$$

Here, the first term gives the contribution from $l = 0$; the last two correspond to $l = 2$. The first, second and the third terms correspond respectively to $j = \frac{1}{2}, \frac{3}{2}$ and $\frac{5}{2}$, which are the allowed values of j in eq. (1). Note that the $j = \frac{5}{2}$ term is small compared to the other terms. As usual, we shall take the factor $G(K)$ to be nearly constant for variations of θ; in fact, $|G(K)|^2$ varies from 0.8 to 0.65 in the range $0 \leqq \theta \leqq 80°$. In eq. (9), the $a_{l,m}$ are calculated for any value of the deformation by interpolation in the tabulated values (see ref. [4]), p. 49). A close fit with the experimental angular distribution is obtained with $\beta = -0.1$ and $r_0 = 6.36 \times 10^{-13}$ cm.

We shall now consider the effect of integrating outside the deformed boundary and obtain the deformation parameter by fitting the angular distribution. Using the above quantum numbers and eq. (7), the differential cross section is given by

$$\begin{aligned}\frac{\sigma(\theta)}{|G(K)|^2} \propto\ & \left[-a_{00}\mathscr{R}_{20} + \frac{2}{3\sqrt{5}}\, a_{20}\beta k_1^3 r_0^3 R_{22}(k_1 r_0) j_0(k r_0)\right]^2 \\ & + \left[-\tfrac{2}{5} a_{00}\beta k_1^3 r_0^3 R_{20}(k_1 r_0) j_2(k r_0) + \frac{1}{\sqrt{10}}(\sqrt{2}a_{20} - \sqrt{3}a_{21})\right. \\ & \left. \times (\mathscr{R}_{22} - \tfrac{4}{21}\beta k_1^3 r_0^3 R_{22}(k_1 r_0) j_2(k r_0))\right]^2.\end{aligned} \tag{10}$$

Since in eq. (9) the $j = \frac{5}{2}$ term is already small compared to other terms we have neglected it in (10). A good fit with the experimental angular distribution is obtained with $\beta = -0.15$ and $r_0 = 6.36 \times 10^{-13}$ cm (see fig. 1). We

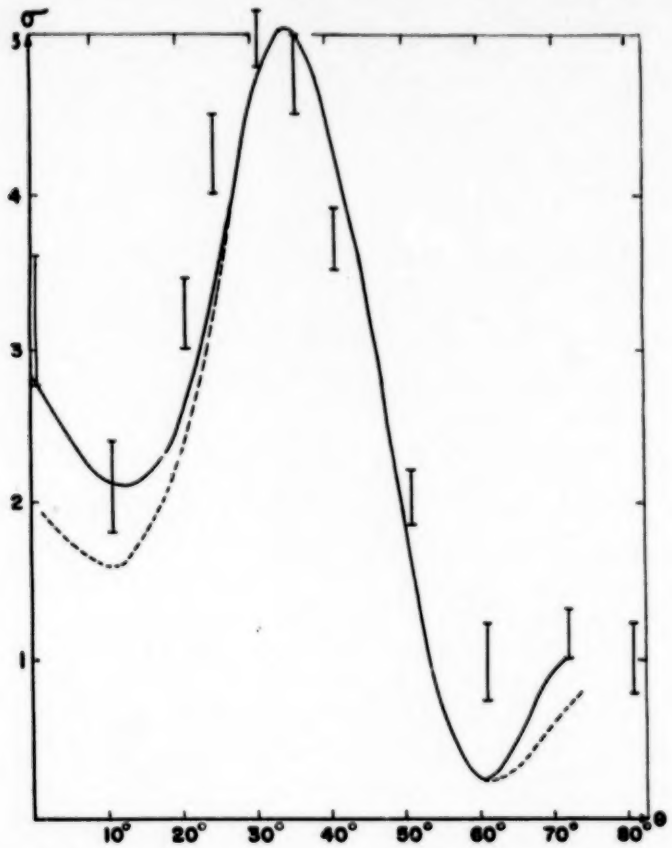

Fig. 1. The angular distribution of protons (in arbitrary units) associated with the ground state for the reaction Cl^{35}(d, p)Cl^{36}.

Incident deuteron energy $E = 6.9$ MeV; gain in kinetic energy $Q = 6.3$ MeV; radius parameter $r_0 = 6.36 \times 10^{-13}$ cm.

The solid line corresponds to $\beta = -0.15$ and the dotted line to $\beta = -0.1$.

see that the required value of the deformation is affected considerably when one takes into account the deformed boundary of the nucleus in evaluating the overlap integral of the stripping amplitude. In both cases it is found that, for a fixed r_0, as β takes larger negative values, the cross section, in the range $0 \leqq \theta \leqq 20°$, increases relatively to the peak as is shown in fig. 1. This being the range where there is effective contribution from $l = 0$ only, we conclude that larger negative values of β increase the contribution from $l = 0$. For fixed β, as we increase r_0, the peak occurs at larger angles and the height of the peak also increases.

4. Discussion

Let us now consider the magnetic and quadrupole moments of the nucleus. The values of the magnetic moment and quadrupole moment of Cl^{35} are given

in table 1 for $\beta = -0.1, -0.15, -0.2$, using the formulae given by Nilsson [4]). For the quadrupole moment, the single particle contribution is comparable to the surface contribution and hence has not been neglected. The single particle quadrupole moment calculated from Nilsson's [4]) wave function is -0.015, and is included in the values shown in table 1. As seen from table 1,

TABLE 1

	Experimental	Single particle shell model	Unified Model		
			-0.1	-0.15	-0.20
Q.M.	-0.079	-0.055	-0.053	-0.070	-0.089
M.M.	0.82	0.12	0.86	1.15	1.53

the experimental values of the quadrupole and magnetic moments can only be fitted by rather different values of the deformation parameter: whereas $\beta = -0.1$ gives the correct magnetic moment, β has to be -0.18 for the quadrupole moment. However, for β -0.15, which, according to section 3, is the best value to fit the stripping experiments, the overall agreement is not bad.

In making this conclusion it must be remembered that the expressions for the magnetic moment and the stripping amplitude are only approximate, due to the neglect of corrections such as the exchange magnetic moment in the former and the interaction of the proton and nucleus in the latter.

We found that the situation is only worsened by the inclusion of rotational mixing in the strong coupling model.

The authors wish to express their thanks to Dr. G. Abraham for suggesting the calculations and for discussions and to Drs. A. Rahman and K. Kumar for helpful criticisms.

References

1) Sueji Okai and Mitsuo Sano, Prog. Theor. Phys. **14** (1955) 399
2) J. Sawicki, Nuclear Physics **6** (1958) 575
3) J. Sawicki, Nuclear Physics **7** (1958) 289
4) S. G. Nilsson, Mat. Fys. Medd. Dan. Vid. Selsk. **29**, No 16 (1955)
5) A. Bohr and B. R. Mottelson, Mat. Fys. Medd. Dan. Vid. Selsk. **27**, No. 16 (1953)
6) G. R. Satchler, Annals of Physics **3** (1958) 275
7) M. E. Rose, Elementary Theory of Angular Momentum (1957)

8.B *Nuclear Physics* **13** (1959) 456—460; © *North-Holland Publishing Co., Amsterdam*
Not to be reproduced by photoprint or microfilm without written permission from the publisher

PARITY NON-CONSERVATION IN HYPERON DECAYS

FERNANDO E. PRIETO †

Institute for Theoretical Physics, University of Copenhagen, Denmark

Received 6 July 1959

Abstract: The suggestion made by Tati, relating parity conservation or non-conservation to the type of particles involved in the weak interaction vertex responsible for the decay, is examined in the framework of d'Espagnat and Prentki's formalism for strong and weak interactions. It is found that, as long as one considers only second-order effects, the results are in reasonable agreement with the available experimental data, but that, if higher order corrections are considered, serious discrepancies are found with the experimental data on parity non-conservation for the Λ and Σ^- decays into a charged pion and a nucleon.

1. Introduction

It has been suggested by Tati [1]) that the non-conservation of parity in weak interactions might be related to the type of ingoing or outgoing particles in a weak interaction vertex involving four fermions in such a way that, in general, parity is not conserved in this interaction, but is conserved if the vertex involves two identical particles. Tati obtains results that seem to be in agreement with the available experimental data on parity non-conservation in hyperon decay. From this point of view, however, parity conservation or non-conservation depends strongly on the possible decay mechanisms for a given particle, and one may wonder whether the mechanisms assumed by Tati are the only possible mechanisms by which each particle may decay. With this in mind, it seems to be of some interest to find out whether Tati's suggestion works well within the framework of a consistent model for strong and weak interactions, such as that proposed by d'Espagnat and Prentki [2]), in which it is possible to account at least in a qualitative way for most of the available experimental data on the decay of elementary particles. Another important question is that of the effect of higher order corrections due to pion exchange. It seems that it is necessary to consider at least fourth order terms, because then higher order corrections could be possibly taken into account by some cut-off technique.

2. Classification of Decays

The experimental data on parity non-conservation in weak decays have been summarized by Tati as follows:

† On leave of absence from the University of Mexico and the National Institute for Scientific Research, Mexico.

a) The asymmetry parameter α is large in β, μ, π, and $\Lambda \to p+\pi^-$ decays.

b) There is some degree of parity non-conservation in Σ^+ decay.

c) This asymmetry is very small in Σ^- decay.

In order to obtain qualitative agreement with these experimental results, Tati makes the following assumptions:

T1. The interaction between four fermions is the only primary weak interaction.

T2. In general, parity is not conserved in this interaction, but is conserved in the exceptional case in which there are two indistinguishable particles among the particles created or annihilated in the weak interaction vertex.

T3. The process nucleon + antinucleon → pion is considerably stronger than the process hyperon + antihyperon → pion.

With these assumptions, any decay process may belong to one of the following three classes:

I) *Parity non-conserving decays.* For these decays, there are only distinguishable particles present in every state connected by the weak interaction; in this case, parity is not conserved and the asymmetry parameter is large. Tati includes in this class the following decays: $n \to p+e^-+\bar{\nu}$, $\mu \to e+\nu+\bar{\nu}$, $\pi^+ \to p+\bar{n} \to \mu^++\nu$, $\pi^- \to \bar{p}+n \to \mu^-+\bar{\nu}$, $\Lambda \to p+n+\bar{p} \to p+\pi^-$, and $\Sigma^+ \to n+p+\bar{n} \to n+\pi^+$.

II) *Mixed decays.* These decays may occur either through parity conserving or parity non-conserving vertex, and the asymmetry parameter is expected to be relatively small compared with those of class I. According to Tati, to this class belong the decays $\Lambda \to n+\pi^0$ and $\Sigma^+ \to p+\pi^0$. The Λ decay may go via the parity conserving vertex $\Lambda \to n+n+\bar{n}$ or via the parity non-conserving vertex $\Lambda \to n+p+\bar{p}$. The parity conserving vertex in the Σ^+ decay is $\Sigma^+ \to p+p+\bar{p}$, and the parity non-conserving vertex is $\Sigma^+ \to p+n+\bar{n}$.

III) *Parity conserving decays.* The decays may go only through parity conserving vertices, and the asymmetry parameter is expected to be very small. Tati includes in this class the decay $\Sigma^- \to n+n+\bar{p} \to n+\pi^-$.

Before going into the details of the decay interactions, we should like to remark that it seems that there is not yet enough experimental evidence to support the classification of decays in the three cited groups. It is true that the degree of parity non-conservation has been found to be large for the $\Lambda \to p+\pi^-$ decay [3,4]) and very small for the $\Sigma^- \to n+\pi^-$ decay [3,4,5]); however, the experimental evidence is not so conclusive for the Σ^+ decays, for which rather dissimilar data are cited by Crawford *et al.* [3]) and by Cool *et al.* [5]); and for the $\Lambda \to n+\pi^0$ decay there are no data at all. Therefore, it is perhaps better to be cautious, and take the theoretical results as an estimation of the relative value of the asymmetry parameter, avoiding any statement about agreement or disagreement with the experimental data on

Σ^+ decays; only for the Λ and Σ^- decays into a charged pion can such statements be made.

3. Second Order Effects

In d'Espagnat-Prentki formalism [2]) (hereafter referred to as E.P.), hyperon decay may occur to the second order either through the annihilation of a nucleon or a cascade particle pair.

For the Λ decay into a charged pion, for which the possible decay modes are

$$\Lambda \to \mathrm{p}+\mathrm{n}+\bar{\mathrm{p}} \to \mathrm{p}+\pi^-, \tag{1}$$

$$\Lambda \to \mathrm{p}+\Xi^-+\bar{\Xi}^0 \to \mathrm{p}+\pi^-, \tag{2}$$

it is obvious that even without T3, which would eliminate reaction (2), there are only distinguishable particles involved in the weak interaction vertex responsible for the decay; consequently, it belongs to class I, in agreement with Tati's results, and also in agreement with the experimental data. This is also the case for the Σ^+ decay into a charged pion,

$$\Sigma^+ \to \mathrm{n}+\mathrm{p}+\bar{\mathrm{n}} \to \mathrm{n}+\pi^+, \tag{3}$$

$$\Sigma^+ \to \mathrm{n}+\Xi^0+\bar{\Xi}^- \to \mathrm{n}+\pi^+, \tag{4}$$

but as we have previously said, it is difficult to make any statement about agreement with the experimental data.

In the Σ^- decay, for which the possible reactions are

$$\Sigma^- \to \mathrm{n}+\mathrm{n}+\bar{\mathrm{p}} \to \mathrm{n}+\pi^-, \tag{5}$$

$$\Sigma^- \to \mathrm{n}+\Xi^-+\bar{\Xi}^0 \to \mathrm{n}+\pi^-, \tag{6}$$

process (5) involves a parity conserving vertex, and reaction (6) involves a parity non-conserving vertex. Without T3, which eliminates reaction (6), this decay should belong to class II, in disagreement with the experimental data; it is only the assumption that nucleon pair annihilation into a pion is stronger than hyperon pair annihilation that improves the situation and permits the inclusion of this decay in class II, in agreement with Tati and with the experimental data.

Now, we are left with the Λ and Σ^+ decays into a neutral pion, shown in eqs. (7) to (11):

$$\Lambda \to \mathrm{n}+\mathrm{p}+\bar{\mathrm{p}} \to \mathrm{n}+\pi^0, \tag{7}$$

$$\Lambda \to \mathrm{n}+\Xi^-+\bar{\Xi}^- \to \mathrm{n}+\pi^0, \tag{8}$$

$$\Lambda \to \mathrm{n}+\Xi^0+\bar{\Xi}^0 \to \mathrm{n}+\pi^0, \tag{9}$$

$$\Sigma^+ \to \mathrm{p}+\mathrm{n}+\bar{\mathrm{n}} \to \mathrm{p}+\pi^0, \tag{10}$$

$$\Sigma^+ \to \mathrm{p}+\Xi^0+\bar{\Xi}^0 \to \mathrm{p}+\pi^0. \tag{11}$$

All these reactions involve a parity non-conserving vertex, so that these decays belong to class I, with a rather large asymmetry parameter, in disagreement with Tati's results. The situation is not improved by the application of T3, which eliminates reactions (8), (9), and (11). It is because there is no place within the E. P. formalism for the reactions $\Lambda \to n+n+\bar{n}$ and $\Sigma^+ \to p+p+\bar{p}$ that these decays may not be included in class II, as Tati did.

4. Fourth Order Effects

For the purpose of the present discussion, the only corrections of interest are those due to the emission of a charged pion before the decay and absorption of this pion after the decay, because only these processes may change the type of particles involved in the weak decay vertex †. It may be shown that for the Λ decay into a neutral pion and for Σ^+ decays, the classification found to the second order does not change, but the situation is completely different for the Λ and Σ^- decay into a charged pion.

Among other possibilities, the decay $\Lambda \to p+\pi^-$ may go via the process $\Lambda \to \pi^+ + \Sigma^-$ followed by the Σ^- decay $\Sigma^- \to n+n+\bar{p} \to n+\pi^-$ and $n+\pi^+ \to p$, but in this case, the weak vertex responsible for the Λ decay is a parity conserving vertex, so that this decay may now occur either through a parity conserving or a parity non-conserving vertex, and should be included in class II, in contradiction with the experimental results.

Something similar happens for the $\Sigma^- \to n+\pi^-$ decay, which may go via the process $\Sigma^- \to \pi^- + \Lambda$ followed by $\Lambda \to p+\bar{p}+n \to p+\pi^-$ and $p+\pi^- \to n$, put the weak vertex responsible for the decay is now a parity non-conserving vertex: therefore, this decay may also occur either through a parity conserving or a parity non-conserving vertex, and should be included in class II, in contradiction with the experimental data.

5. Concluding Remarks

It has been shown that in the framework of the E.P. formalism for strong and weak interactions, reasonable agreement is found with both Tati's results and experimental data, as long as one considers only second-order effects in the decay of hyperons; the discrepancies found in the Λ and Σ^+ decays into a neutral pion are not too serious because there are not yet enough experimental data on parity non-conservation for these decays. This situation is, however, completely reversed if one includes higher order corrections, because then the Λ and Σ^- decays into a charged pion should belong to the same class, with a relatively small value of the asymmetry

† The effects of multiple dispersion after the decay have been recently considered for the case of Λ hyperons by Okubo *et al.*[6]).

parameter, whereas the experimental results give a high degree of parity non-conservation for the decay $\Lambda \to p+\pi^-$, and an extremely low degree of parity non-conservation for the decay $\Sigma^- \to n+\pi^-$. This might be considered to be an objection to the E.P. formalism; however, since this formalism is in many other points in agreement with the experimental results, it seems better to look for the causes of the different behaviour of Λ and Σ hyperons with respect to parity non-conservation along other lines [7]).

The author wishes to acknowledge the kind hospitality extended to him by the late Professor W. Pauli in Zürich and by Professors Niels Bohr and Aage Bohr in Copenhagen. He is also indebted to Drs. Ch. Enz, H. P. Stapp, A. Bohr, L. Rosenfeld, and S. Barshay for many helpful discussions, and to the United Nations Technical Assistance Administration and the Mexican National Nuclear Energy Commission, for financial support.

References

1) T. Tati, Progr. Theoret. Phys. **20** (1958) 398
2) B. d'Espagnat and J. Prentki, Nuclear Physics **6** (1958) 596
3) F. S. Crawford *et al.*, Phys. Rev. **108** (1957) 1102
4) F. Eisler *et al.*, Phys. Rev. **108** (1957) 1353
5) R. L. Cool *et al.*, Phys. Rev. Letters **2** (1959) 378
6) Okubo, Marshak and Sudarshan, Phys. Rev. **113** (1959) 944
7) See, for instance, M. Sugawara, Phys. Rev. **113** (1959) 1361

NORTH-HOLLAND BOOKS

ANALYTICAL and CANONICAL FORMALISM in PHYSICS

by ANDRÉ MERCIER

Head of the Department of Theoretical Physics University of Berne

6×9″ VIII + 222 pp. Guilders 20.00 (40s.)

CONTENTS

i. LAGRANGIAN FORMALISM
ii. LAGRANGIAN DENSITY
iii. CANONICAL FORMALISM
iv. CANONICAL FORM OF ELECTRODYNAMICS
v. HAMILTONIAN DENSITIES
vi. TRANSFORMATIONS
vii. CANONICAL FORMALISM WITH VANISHING JACOBIAN DETERMINANT

Those who are not highly specialized in these matters but do want to get a fairly broad knowledge of the subject are not aware of the fact that the greater parts of this formalism, including many specific conclusions of physical concern, do not involve in the least quantum theory, i.e. "quantization" of the fields. To show this and to provide the reader with a fairly complete presentation of the *classical* (i.e. not yet quantized) theory of fields is one of the main aims of the book.

This formalism is presented with great generality. Some special topics have also been included when they are found to be of importance in connection with the problems raised; however, they are not elaborated with the same generality, but just formulated as far as is found necessary for the understanding of these connections; for instance we can name: tensorial formalism and spinorial formalism.

A special chapter has been devoted to transformations of several kinds including canonical transformations, reversibility and the like as well as their interrelations, so that the ground is prepared for an understanding of the CPT-Theorems.

A short chapter on Dirac's dynamics with vanishing Jacobian closes the book.

The work builds upon the well-known *Principles of Analytical Dynamics* by the same author (in French), where particular weight is laid upon the homogeneous formalism, but it can easily be read with profit without knowledge of the latter by any advanced students in physics, astronomy or mathematics as well as by research workers who want to get a thorough practice in the use of these methods.

Many examples and as many as 124 problems illustrate the formalism exposed.

Sole Agency for U.S.A.: Interscience Publishers Inc. - New York

NORTH-HOLLAND PUBLISHING COMPANY - AMSTERDAM

NORTH-HOLLAND BOOKS

ASYMPTOTIC METHODS in ANALYSIS

by **N. G. DE BRUIJN** *Professor of Mathematics at the University of Amsterdam*

Asymptotics is that part of analysis which considers problems of the type dealt with in this book

Contents

Ch. I. Introduction
Ch. II. Implicit Functions
Ch. III. Summation
Ch. IV. The Laplace Method for Integrals
Ch. V. The Saddle Point Method
Ch. VI. Applications of the Saddle Point Method
Ch. VII. Indirect Asymptotics
Ch. VIII. Iterated Functions
Ch. IX. Differential Equations

6×9" XII+200 pages Guilders 20.00 (40s.)